UNIVERSITY OF ST. ANDREWS

Thesis Copyright Declaration Form.

A UNRESTRICTED

"In submitting this thesis to the University of St. Andrews I understand that I am giving permission for it to be made available for public use in accordance with the regulations of the University Library for the time being in force, subject to any copyright vested in the work not being affected thereby. I also understand that the title and abstract will be published, and that a copy of the work may be made and supplied to any bona fide library or research worker."

Declaration

I wish to exercise option A [i.e. A, Ba or Bb] of the above options.

Signature

Date 6th July 1988

A STUDY OF ION-MOLECULE REACTIONS IN THE GAS PHASE USING A TRIPLE QUADRUPOLE MASS SPECTROMETER

being a thesis presented by

Alan Lyall Mitchell, B.Sc.

to the

University of St. Andrews

in application for

the Degree of Doctor of Philosophy

May 1988

DECLARATION

I declare that this thesis is based on the results of experiments carried out by myself, that it is of my own composition, and that it has not been submitted previously in application for a higher degree.

May 1988 Alan L. Mitchell

CERTIFICATE

I hereby certify that Alan Lyall Mitchell, B.Sc., has spent ten terms at research work under my supervision, has fulfilled the conditions of the Resolution of the University Court, 1967 No 1, and is qualified to submit the accompanying thesis in application for the Degree of Doctor of Philosophy.

Director of Research

UNIVERSITY CAREER

I entered the University of St Andrews in October 1977, and subsequently graduated with Upper Second Class Honours in Chemistry in July 1982.

In October 1982 I was awarded a St Andrews University Research Bursary, and from then until July 1985 I carried out the work which is embodied in this thesis. This work was undertaken in the Department of Chemistry, University of St Andrews, under the supervision of Professor J.M. Tedder. There then followed an interval of several years before the presentation of this thesis in May 1988.

ACKNOWLEDGEMENTS

I would like to express my gratitude to Professor J.M. Tedder for his advice, guidance and continued interest in my work, and also his extreme patience and understanding with me while I prepared this thesis.

I would like to thank Professor Tedder and Professor Wyatt for making available the excellent laboratory facilities in the Department of Chemistry at the University of St Andrews.

I am very grateful to the technical staff of the Department of Chemistry, University of St Andrews, especially Mr J. Ward of the electronics workshop. Also, I am indebted to Mrs D.A. Elliott who prepared the typescript for this thesis.

Finally I would like to thank the University of St Andrews for making available the funds for me to undertake this research.

EXPLANATORY NOTE

This thesis is divided into four sections, Parts 1, 2, 3 and 4.

Part 1 consists of a review of the relevant background literature.

Part 2 consists of a description of the apparatus used for this research, and also contains an investigation of the effects of the various instrumental parameters.

Part 3 consists of a discussion of the results obtained.

Part 4 consists of the experimental results tabulated, and is complementary to Part 3.

Where reference is made to the chemical literature, this is indicated by a number in the superscript, a key to which can be found at the end of this thesis. The structural formulae which have been reproduced for illustrative purposes have been assigned alphabetical labels.

CONTENTS

Page

TABULATED RESULTS

SUMMARY

A triple quadrupole mass spectrometer was used to study a number of different ion-molecule reactions. The TQMS is a relatively new device, and is ideally suited to the study of gaseous ion-molecule reactions. It avoids the major complication inherent in other techniques - namely, only one primary ion is ever present in the collision chamber. Consequently, the spectra which were obtained were much easier to interpret than before.

The initial experiments undertaken involved the use of two previously rarely used cationic species, CH_3^+ and $CH_4^{+\cdot}$. These were reacted with n-, iso- and cyclo-alkanes, and the results showed that the two primary ionic species brought about ionisation of the collision molecules in different ways.

Methane radical cation ($CH_4^{+\cdot}$) effected ionisation by charge-transfer, whilst methyl cation (CH_3^+) reacted via a hydride transfer, giving $(M-1)^+$ ions. Thus ionised, we were then able to follow the breakdown of the collision molecules, producing fragmentation schemes for these species. Comparisons between the spectra for n- and iso- alkanes (using both primary ionic species), revealed that the $(M-1)^+$ ions produced in the reactions with CH_3^+ were in fact the same species. In other words, there is a structural rearrangement of the carbon skeleton before fragmentation. (No such rearrangement was observed for the M^+ ions produced in $CH_4^{+\cdot}$ ionisation).

The reaction of methyl and trideuteromethyl cations with ethyne produced an excess of the $C_3H_3^+$ ion, which was shown to have the cyclopropenyl structure, rather than the propargyl structure.

The reactions of the fluoromethyl cations (CH_2F^+, CHF_2^+ and CF_3^+) with the simple alkenes displayed a number of interesting reactions. In particular a "knock-on" elimination of $:CF_2$, and a concerted addition-elimination of fluoromethyl cation. They also gave important clues as to the actual mechanisms involved in these reactions and those of methyl cation with the simple alkenes.

The remaining investigations all involved the reactions of unsaturated species, mainly the simple alkenes and conjugated dienes. The design of the TQMS also allowed the cross reactions between the various species to be very easily studied.

The spectra for the ethene and propene ion-molecule reactions confirmed the reaction sequences put forward in previous studies of these systems. The butenes on the other hand produced significant differences dependent on both collision gas structure and primary ion source structure, and a change in mechanism was observed as the collision gas pressure was increased, in both the cis but-2-ene and isobutene ion-molecule reactions. (At low pressure the major reaction was collision induced dissociation, which gave way to complex formation/breakdown at higher pressures.)

The fluorinated ethenes gave very interesting results when reacted with both themselves and ethene. In particular, we were able to show that reaction between the various fluorinated ethene radical cations and ethene proceeded via a loosely-bound cyclobutane transition state.

Our investigations of the two C_4H_6 isomers (1,3-butadiene and but-2-yne) produced results which were at variance with the

results obtained in previous studies. We showed that but-2-yne radical cation does not undergo isomerisation prior to fragmentation/reaction, whereas 1,3-butadiene radical cation does. The analogous C_5H_8 isomers (isoprene and pent-1-yne)were also investigated, and again differences were observed in the "low mass" area of the spectra, indicative of the different structures of the two primary ions. We suggest that like the 1,3-butadiene radical cation, the isoprene radical cation isomerises before reaction to the cyclopentene structure.

INTRODUCTION

INTRODUCTION

The studies of gas phase ion-molecule reactions and mass spectrometry are very closely related. Indeed, even in the very earliest experiments in mass spectrometry, both Thomson[1,2] and Aston[3,4] observed spurious signals due to ion-molecule reactions.

The "Aston bands" were caused by the fragmentation of primary ions, resulting from high-energy collisions between these primary ions and the background gas within the analyser of the mass spectrometer. (This process, termed "collisionally activated dissociation" (CAD), is now a widely used technique for determining structural data and its increasing importance will be discussed later in the text.)

Thomson also observed several ions which could not be accounted for by direct ionisation of any species known to be present in the sample, and these ions, including m/z = 3 and 19, could only be explained by postulating the ion-molecule reactions indicated below:-

$$H_2^{+\cdot} + H_2 \rightarrow H_3^+ + H\cdot$$

and

$$H_2O^{+\cdot} + H_2O \rightarrow H_3O^+ + OH\cdot$$

or

$$H_2^{+\cdot} + H_2O \rightarrow H_3O^+ + H\cdot$$

Indeed, these reactions occurred so readily, that H_3O^+ could not be eliminated from any such experiments until considerable improvements in vacuum pumps and techniques had been achieved. With the elimination

of these "complications", mass spectrometry became established as an important analytical tool (rather than purely being a means of studying gaseous ions), especially when its applicability to structure elucidation in organic compounds became apparent. Its use in this way has grown rapidly in the last three decades, and it is now recognised as one of the standard analytical techniques for the detection, identification and quantification of organic compounds, available in most laboratories worldwide.

Mass spectrometry has also been combined with separation techniques such as gas (and liquid)chromatography, which greatly enhances its specifity, and the combined GC/MS technique is now the most commonly used method of analysis for complex organic mixtures.

The success of GC/MS, has led to an upsurge of interest in the coupling of two (or more) mass analysers, and the resulting tandem mass spectrometers (or MS/MS) effect a substantial increase in the amount of mass spectral data generated, whilst retaining the sensitivity, speed and accuracy of "single" mass spectrometry. MS/MS has an obvious speed advantage over GC/MS,but it also offers greatly increased structural information, through the capability to fragment the ions generated in the first mass spectrometer, to give characteristic product ions, detected and separated in the second mass spectrometer - CAD, as first observed by Aston.

MS/MS has three major applications; mixture analysis, structure elucidation and the study of basic gaseous ion chemistry.

The pioneers of the MS/MS technique in its use as a means of analysing complex mixtures and for structural characterisation, could be said to be Professor Fred McLafferty and his many co-workers at Cornell University. In particular, the possibilities for CAD in such MS/MS applications were noted by Haddon and McLafferty[5,6] and by Jennings[7] - with structural elucidation through CAD being set out in the two general papers of McLafferty et al[8,9], and the advantages of CAD to mixture analysis best demonstrated by Levsen and Beckey[10].

It is not really possible to single out any one person as pioneering the use of MS/MS to study basic ion chemistry and physics - the instrument types and applications are so varied - but among those who have had a profound influence on the research conducted for this thesis are Lindholm, Schwarz, Levsen, Bowers, Futrell, Holmes, Gaumann and Jennings.

There have been a great number of different types and configurations of mass spectrometer used in the development of MS/MS over the past 20 years. The first real breakthrough was achieved in 1964, when Barber and Elliot[11] reversed the geometry of their "normal" double-focussing mass spectrometer, giving rise to a method which they termed "direct analysis of daughter ions" (DADI). As a result of this work "mass-analysed ion kinetic energy spectra" (MIKES) became the standard method for MS/MS research, and from these reversed geometry instruments, were developed three and four sector machines[12,13], with greatly enhanced resolution. Other configurations used include the "right-angled" tandem magnetic sector device, used by Lindholm[14] and this laboratory[15]; modified time-of-flight MS/MS[5,16,17] and ion-cyclotron resonance MS/MS[18] - from which Comisarow and Marshall[19] developed the very versatile and

promising FT-ICR instrument. (Single MS devices, with a variety of different sources - high pressure[20], photoionisation[21] and alpha -particle radiolysis[22] - were also used to study ion-molecule reactions).

The most revolutionary recent development in MS/MS instrumentation - and that employed in the research undertaken here - is the tandem or triple quadrupole (TQMS), which uses an RF-only quadrupole as a fragmentation chamber between two quadrupole mass filters*. This concept was first suggested by Morrison and McGilvery[23] of LaTrobe University, Melbourne and Vestal and Futrell[24] of the University of Utah, in 1978. (Lampe[25] having previously demonstrated a tandem quadrupole device, employing a field-free collision cell in 1972). Both instruments were originally designed for studies of the photodissociation of ions; the former using a pulsed, tunable dye laser, and the latter a chopped monochromatic beam from a mercury lamp; unfortunately, the yield of ions from photodissociation was greatly exceeded by those generated by CAD. The analytical importance of this CAD "interference" was recognised by Yost and Enke, who, in collaboration with Morrison and McGilvery produced papers[26, 27, 28] showing just how useful the TQMS could be in the fields of mixture analysis and structure elucidation. Since the publication of these papers, many other laboratories have put together their own TQMS's[29,30,31], and commercial instruments are now offered by most of the leading mass spectrometer manufacturers.

---

*The operation of both the quadrupole mass filter and the TQMS, are described on pages 8 and 13 respectively.

The TQMS differs from other (sector) MS/MS instruments, in that it uses true mass analysis, rather than momentum or energy analysis, and this, along with the relatively low kinetic energies involved (2-20 eV), gives the TQMS technique several advantages over these other devices; advantages which can be utilised in all three main areas of MS/MS application.

The most widespread use of TQMS is in the analysis of complex mixtures, and it is in this application where the advantages (and limitations) of TQMS are probably best illustrated.

TQMS offers unit mass resolution of both parent and daughter ions, permitting specific detection of particular sample compounds[26,29,32]. This unit mass resolution is not possible with the usual two-sector MS/MS devices, because the kinetic energy released in the collision process, leads to a spread in daughter ion velocities. This spread in velocities (v) has no effect on mass resolution in a quadrupole, where mass selection is by mass-to-charge ratio (m/z); but in sector devices, where mass selection is dependent on momentum-to-charge ratio (mv/z - magnetic sector) or kinetic energy-to-charge ratio (mv^2/z - electric sector), this leads to a broadening of the peaks - a loss of resolution.

High sensitivity is another advantage of the TQMS. This results from the high efficiency of the low-energy CAD process, brought about by the focussing action of the RF-only quadrupole (whereby the ions scattered by the collision process are held in stable trajectories by the strong RF-only field in Q2). This CAD efficiency (fraction of the incident parent ions that are collected as daughter ions) is typically 10-50%[26], which compares very favourably with that for most multi-sector instruments, where an efficiency of ca. 1% is normal.

The third advantage of TQMS is in the degree of control available. Each quadrupole can be scanned independently, without affecting the mass selected in the other, unlike the multiple sector case where there is an interdependence between the two sectors. This means that linked scans can be easily operated on the TQMS, where constant daughter ion or neutral losses can be followed, providing the capability to select specific compounds from a mixture by compound class (ie looking for a particular functional group, characteristic of a class of compounds). Rapid scanning and the ability to switch quickly from mass to mass, is another of the control advantages which the TQMS has over sector instruments, since the latter are restricted in the speed of their scan by the response of the magnet. TQMS are also very readily and easily controlled by computer, - all commercial instruments are available with computerised control and dedicated data systems.

These advantages outweigh the few disadvantages of the TQMS, which include; low resolution, which does not allow the separation of isobaric ions from a mixture; limited mass range, which restricts the use of TQMS in analyses of large biomolecules and polymers; and the low ion kinetic energies involved, which do not permit the analytically useful charge-inversion and charge-stripping reactions to be performed. However, this last disadvantage can also be classed as an advantage, in that the TQMS permits the study of basic ionic processes at much lower kinetic energies than before, and the resultant "collisionally activated associative reactions" form the bulk of this thesis. (Note that all of the above processes can still be undertaken using conventional sector devices.)

Looking to the future, the field of MS/MS is still relatively young and of the instrumentation used, the tandem quadrupole mass spectrometer is still in its infancy. Consequently we can expect further development to be fairly rapid in all areas of application of MS/MS.

Advances in the interfacing of the quadrupoles, including the "tailoring" of individual instruments, should ensure a great deal of interest in the analytical applications of TQMS. The promise for structure elucidation has been demonstrated in several papers[33,34,35] which have shown that MS/MS can provide structural and even stereochemical information on parts of a molecule, from which its total structure can be deduced. In its third application - the investigation of the chemistry of ions in the absence of solvents - MS/MS studies will provide results important both for the understanding of chemical reactions in solution, and for theoretical studies. In the latter case, fundamental studies on the behaviour of ions within a quadrupole field and within the fringing fields between quadrupoles should allow much greater correlation between theory and practice, whereas, the way forward for the former appears to lie with the advent of multiple quadrupole mass spectrometry[36] (and also FT-ICR[19] and triple sector instruments[37]). This we can term MS/MS/MS or $(MS)^{(n)}$, and the possibilities for this seem bright, whereby we can investigate directly the CAD of ion-molecule reaction products, showing unequivocally how and from where these reaction products arise. Thus eliminating the uncertainties involved when using "model" ions in CAD studies, from which structural information can only be implied (ie the method used throughout the research for this thesis).

Having briefly discussed the development of MS/MS, and TQMS in particular, all that remains here is to give a description of how the quadrupole mass filter operates and also to outline the theoretical approach to ion-molecule reactions.

Looking first at the operation of the quadrupole mass spectrometer; this has a very simple construction, but a rather complicated analysis of operation. Four precisely parallel rods are arranged as shown in Figure 1, below. Between each pair of opposite and electrically connected rods is applied a dc voltage and a superimposed radio-frequency (RF) potential. Under the influence of this combination of fields, ions in the analyser undergo complex trajectories[38,39]. Mass separation is effected by varying the voltages, either by altering the RF/dc ratio, or more normally, by keeping this ratio constant and varying both RF and dc voltages equally. As these voltages are varied, only one mass is held in a stable trajectory at any one time, the others colliding with the rods (hence the more accurate term of quadrupole mass filter). This is a very simple explanation of the operation of the quadrupole mass spectrometer; for a complete review of this subject, Dawson's book - Quadrupole Mass Spectrometry and its Applications[40] - is recommended.

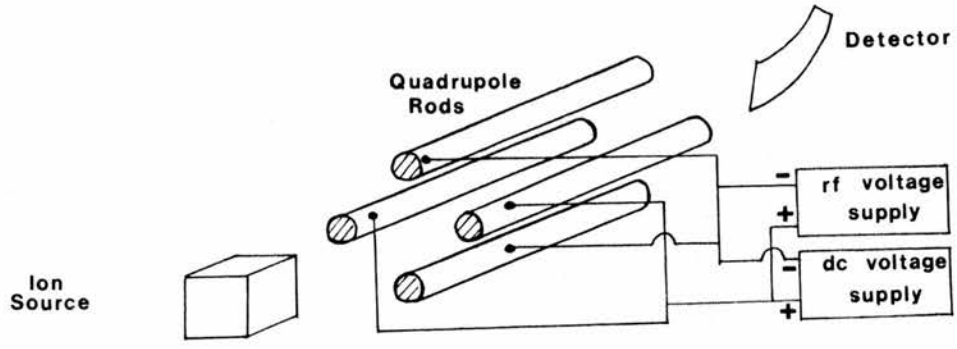

FIGURE 1: The Quadrupole Mass Filter

Gaseous ion-molecule reactions are generally discussed in terms of "reaction cross-sections" rather than rate constants. This is how physicists perceive these reactions, with the neutral molecule presenting a target area to the approaching ion, reaction occurring if the ion hits this target. These values may be compared directly using absolute cross-sections, however, in most cases relative cross-sections (as used here) are sufficient. (Note; the absolute cross-section for any given reaction can be determined by comparing the relative cross-section for this reaction, with that for a known reaction - such as $Ar^{+\cdot} + H_2 \rightarrow ArH^+ + H$ - performed under identical conditions.)

This perception of an ion-molecule reaction also forms the basis for the first detailed quantitative mathematical treatment for ion-molecule collisions (that of Langevin, who was interested in the mobility of ions in gaseous media). This theory isnow recognised as the starting-point in the understanding of such reactions.

Put very simply, the Langevin theory is based on the long-range attractive forces produced if the approaching ion is able to induce appreciable polarisation of the target molecule. If these

forces are sufficiently strong, and the relative velocities of the ion and the target molecule are not too great, the attraction will cause the closest approach of the two particles (r_a) to be considerably smaller than the impact parameter (b), which would be the closest approach of the particles in the absence of any interaction between them (see Figure 2a).

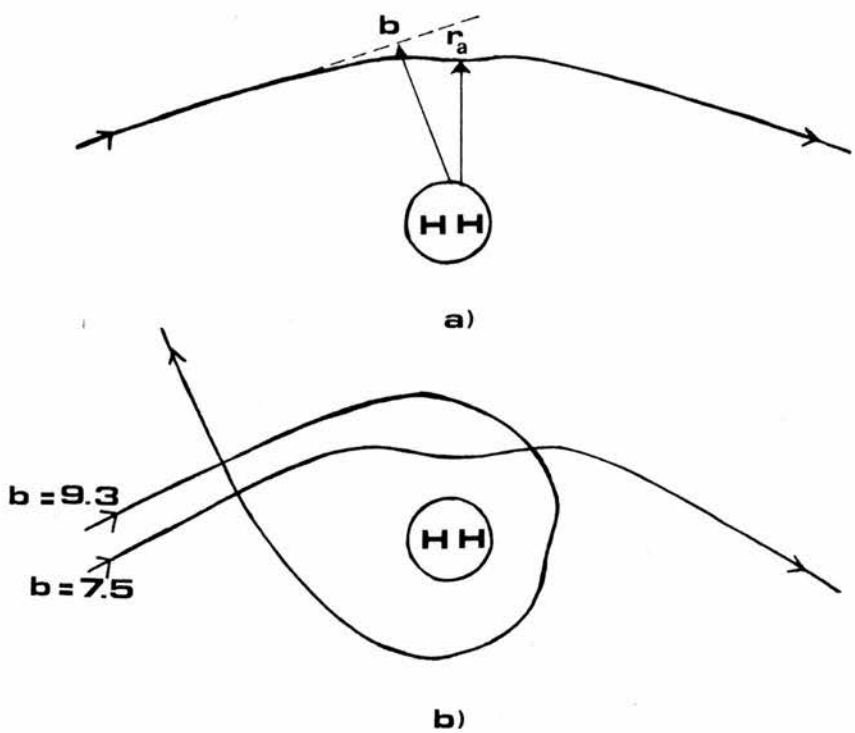

FIGURE 2: (a) Example of a "Distant" collision; b = 10 a.m.u.
(b) Examples of "Close" collision; b = 9.3 and 7.5 a.m.u. (where critical value b_o = 9.4 a.m.u. - calculated for $H_2^+ + H_2$ interaction).

Development of the mathematics involved, enables the calculation of a critical value of the impact parameter (b_o), below which the distance of closest approach, r_a, changes discontinuously to a much smaller value. For values of b, close to b_o, the trajectory of the ion around the molecule takes on a spiral or orbiting nature, which greatly increases the time of the collision (see Figure 2b). In applying

Langevin's theory to ion-molecule reactions, there is one very important assumption made - namely that reaction only occurs for "close" collisions (ie where $b \leq b_o$), "distant" collisions do not produce reaction. This is now regarded as a somewhat arbitrary condition (but undoubtedly true for some ion-molecule interactions), and attempts have been made to modify the Langevin Theory[41,42] but although there have been successes reported for these modified theories, there is no evidence to support the belief that these will prove generally applicable.

An alternative theory for ion-molecule reactions was put forward by J.C. Light[43] - the "phase-space" theory. Based as this is on the principles of statistical thermodynamics, this is too complex and abstract to be described in simple terms. However, in comparison with experimental data[44], this does give better agreement than the Langevin Theory, but it is perhaps fairest to say that these are two opposite extremes, and that the true situation lies somewhere between the two.

With regard to the following discussion of the experiments undertaken for this thesis, all the reactions are assumed to occur as a result of "close" collisions.

EXPERIMENTAL

EXPERIMENTAL

APPARATUS/INSTRUMENTAL PARAMETERS

The triple quadrupole mass spectrometer used throughout this series of experiments was built by VG Gas Analysis Limited, Aston Way, Middlewich, Cheshire; and is based on the design of Yost, Enke, McGilvery and Morrison[45]. It is shown in schematic form in Figure 3.

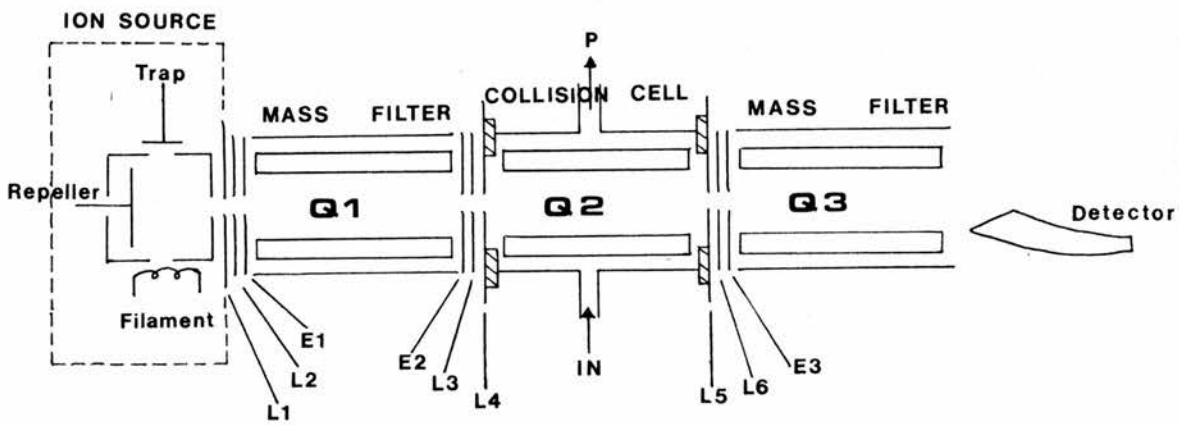

FIGURE 3: Schematic Diagram of the TQMS used Throughout this Research

The three quadrupoles, Q1, Q2 and Q3, were standard VG QXK300 units, each with rods of length 125 mm and diameter 6.32 mm. The radio-frequency supply was 0 to 1320V; 2 MHz, giving a total mass range of 0-300 amu.

The sample to be ionised was introduced into the conventional electron impact source from a small vacuum line (all the samples used were gases or volatile liquids). The primary ions thus generated (using 70V electrons) were then selected in Q1 according to their mass-to-charge ratio, and passed into Q2 which was pressurised with the collision gas (again introduced from a small vacuum line via the side-tube (IN) shown in Figure 3), wherein the ion-molecule reactions occurred. The ions resulting from these collisions were held in stable trajectories by the focussing action of Q2, which was operated with a fixed RF potential only applied to the rods. An adjustable bias potential could be applied to all four rods in Q2, allowing the incident ions to be accelerated or decelerated, thus altering the collision energy. The ions then passed into Q3, where they were mass analysed and detected by a channeltron electron multiplier. The ions were focussed into Q1, and between the quadrupole sections, by the apertures L1 to L6 (see Figure 3), to which adjustable focus potentials could be applied, and also by the apertures E1 to E3, which were earthed.

The pressure inside the collision chamber was measured directly using a Penning head (capacitance manometer), connected to the side-tube (P in Figure 3) situated within the collision chamber. The pressure inside the apparatus as a whole could also be measured using an ionisation gauge (VG VIG23) situated in the main vacuum chamber, above the diffusion pump. The differential pumping factor was 100[46].

The system was pumped by an Edwards oil vapour diffusion pump, fitted with a VG NCT4 cold trap, and backed by an Edwards E2M8 rotary pump.

All data were recorded on a Kipp and Zonen BD8 single-channel chart recorder, and additionally displayed on a CRO.

From the outset, the object of this work was to investigate qualitatively a number of interesting ion-molecule reactions (both previously studied and unstudied). Therefore we have not gone into the instrumental design in any great detail. However, during the course of our initial experiments, we did investigate how the following instrumental variables affected the specta produced:-

(1) Focus potentials L1 - L6

(2) Q2 bias viariation (ie primary ion translational energy)

(3) Source pressure

(4) Collision cell pressure

We will deal with each of these in turn:-

(1) Adjusting the focus potentials (L1 - L6 in Figure 3), surprisingly produced very little difference in the spectra observed, over the range of m/z values used throughout these experiments (m/z = 15 - 140). We therefore left these set at the values used by the installation engineer (Mr J.H. Batey). However, when each new set of experiments was commenced, these potentials were again adjusted, but in all cases the effects were negligible (the results of these variations were not recorded).

(2) The effect of varying the bias voltage on Q2 had been adequately investigated in the series of results taken by Jonathan Batey[46]. Our results, using the systems, CH_4^+/isopentane; CH_3^+/isopentane; and ethene$^{+\cdot}$/ethene (shown in Tables 1, 2 and 3 below confirm the earlier results.

		Normalised secondary ion signal										
Bias Voltage (ev)	m/z ion	29 $C_2H_5^+$	41 $C_3H_5^+$	42 $C_3H_6^{+\cdot}$	43 $C_3H_7^+$	44 $C_3H_8^{+\cdot}$	56 $C_4H_8^{+\cdot}$	57 $C_4H_9^+$	58 $C_4H_{10}^{+\cdot}$	70 $C_5H_{10}^+$	71 $C_5H_{11}^+$	72 $C_5H_{12}^{+\cdot}$
+0·94		16	10	32	100	8	12	63	-	-	-	7
0		3	5	100	75	-	31	54	2	7	13	15
-0·94		2	2	100	59	1	41	52	-	12	20	33
-1·88		2	2	100	59	1	43	54	1	15	21	39
-2·81		3	4	100	62	1	44	53	1	12	19	33
-3·75		4	4	100	68	1	46	57	2	17	21	30
-4·69		5	5	100	70	3	44	52	2	11	25	33

TABLE 1: The Effect of Primary-Ion Energy on the Reaction of $CH_4^{+\cdot}$ with 2-methylbutane at Constant Pressure

		Normalised secondary ion signal									
Bias Voltage (ev)	m/z ion	27 $C_2H_3^+$	29 $C_2H_5^+$	41 $C_3H_5^+$	42 $C_3H_6^{+\cdot}$	43 $C_3H_7^+$	55 $C_4H_7^+$	56 $C_4H_8^{+\cdot}$	57 $C_4H_9^+$	71 $C_5H_{11}^+$	72 $C_5H_{12}^{+\cdot}$
+0·94		11	36	24	-	100	-	-	23	-	-
0		1	10	6	2	100	3	-	9	14	1
-0·94		1	6	3	1	100	3	1	10	27	1
-1·88		1	5	5	2	100	3	1	9	23	2
-3·75		2	10	5	4	100	3	1	13	21	4

TABLE 2: The Effect of Primary-Ion Energy on the Reaction of CH_3^+ with 2-methylbutane at Constant Pressure

		Normalised secondary ion signal							
Bias Voltage (ev)	m/z ion	26 $C_2H_2^{+\cdot}$	27 $C_2H_3^+$	39 $C_3H_3^+$	40 $C_3H_4^{+\cdot}$	41 $C_3H_5^+$	53 $C_4H_5^+$	54 $C_4H_6^{+\cdot}$	55 $C_4H_7^+$
+0·94		100	21	22	3	63	3	2	8
+0·38		89	21	29	4	100	4	1	11
0		51	17	19	2	100	1	1	10
-0·38		31	9	11	3	100	1	1	10
-0·94		11	5	5	3	100	1	1	11
-1·88		9	5	4	2	100	1	1	9
-3·75		7	6	4	2	100	-	1	8
-5·63		7	10	4	3	100	-	-	9

TABLE 3: The Effect of Primary-Ion Energy on the Ethene Ion-Molecule Reaction at Constant Pressure

The first feature to note, is that there is still an appreciable yield of secondary ions even though the bias voltage (ie the potential difference between source and the second quadrupole) is positive. The relative voltage has to exceed +2·5V before all ions are cut off. This is probably due to the build-up of positive charge in the centre of the source. Overall however, the results indicate that there was very little change in the fragmentation pattern when the primary ions translational energy was varied between 0 and 3.75 eV. (This does not hold true for values in excess of 10 eV[46], but these values were outwith the scope of our investigations).

(3) Variation of the source pressure similarly did not adversely affect the results - increasing the source pressure, increased the strength of the primary ion signal, which in turn gave a stronger total ion spectrum than before. For this reason the size of the primary ion signal was always kept at approximately the same level (±5%) throughout a series of experiments. (This was easily checked using the CRO and/or chart recorder connected to Q1). We chose to keep the primary signal strength the same, rather than the source pressure because as the source/filament became dirty, the pressure had to be slightly increased to maintain the signal level.

(4) The variation in collision cell pressure produced the expected results (See Tables 4 and 5 below). Namely, the proportions of some ions increased with pressure, whilst others remained static or decreased.

		Normalised secondary ion signal								
Collision cell	m/z	29	41	42	43	56	57	70	71	72
Pressure (Torr)	ion	$C_2H_5^+$	$C_3H_5^+$	$C_3H_6^{+\cdot}$	$C_3H_7^+$	$C_4H_8^{+\cdot}$	$C_4H_9^+$	$C_5H_{10}^+$	$C_5H_{11}^+$	$C_5H_{12}^{+\cdot}$
6×10^{-5}		-	-	100	53	39	54	-	13	43
4×10^{-4}		2	2	100	59	41	52	12	20	33
3×10^{-3}		2	3	52	65	52	62	48	100	39

TABLE 4: The Effect of Collision Cell Pressure on the Reaction of CH_4^+ with 2-methylbutane

		Normalised secondary ion signal									
Collision cell	m/z	27	29	41	42	43	55	56	57	71	72
Pressure (Torr)	ion	$C_2H_3^+$	$C_2H_5^+$	$C_3H_5^+$	$C_3H_6^+$	$C_3H_7^+$	$C_4H_7^+$	$C_4H_8^{+\cdot}$	$C_4H_9^+$	$C_5H_{11}^+$	$C_5H_{12}^{+\cdot}$
7×10^{-5}		-	9	4	3	100	3	-	9	15	2
4×10^{-4}		1	6	3	1	100	3	1	10	23	1
5×10^{-3}		1	3	3	-	44	2	1	11	100	2

TABLE 5: The Effect of Collision Cell Pressure on the Reaction of CH_3^+ with 2-methylbutane

Looking at the above tables, we see that at the highest pressures used, the base peak has altered in each case. This we can explain in terms of multiple collisions and further ion-molecule reactions. Taking the example shown in Table 5 (CH_3^+/methylbutane); the secondary ion at m/z = 43 is reacting with a further molecule of 2-methylbutane by hydride abstraction to give the ion at m/z = 71, hence their relative decrease/increase. Thus for comparative purposes in the reactions of CH_3^+ and $CH_4^{+\cdot}$ with the various alkanes, all spectra were taken at approximately the same collision cell pressure. (The value actually used was ca 4 x 10^{-4} Torr, chosen because it produced spectra of reasonable size, but without the complication of major tertiary reactions occurring.) In the remaining systems studied however, the results of the pressure variation were the most valuable, and in these cases it is this pressure variation which is discussed.

The one remaining instrumental factor that was briefly investigated, was to see what the ion losses were through the machine. To do this, we selected an ion in Q1 and recorded the peak height of this ion with the chart recorder connected to Q1. The chart recorder was then connected to Q3 and the spectrum swept, with no collision gas present. (A repeat sweep was made after optimisation of the focussing potentials, but as previously mentioned this produced only a negligible change. The primary signal was also rechecked at the end of the run, as a precaution in case of surging in the primary source pressure.) Comparison of the two peak heights gave an ion transmission efficiency of 70%. The ion used for this investigation was CH_3^+,

which effectively eliminated the possibility of metastable decomposition occurring due to the relatively long time between ion production and detection. (Note however, that due to the use of a fixed RF voltage in Q2, ions with different masses will be focussed with different degrees of efficiency in Q2[31].)

The operation of the TQMS has been outlined in the preceding paragraphs, and only the sample handling remains to be discussed.

As previously stated, the samples used were all either volatile liquids or gases at s.t.p., and so the treatment of these before leaking them into the TQMS via needle valves was identical:-

A small amount of the chosen compound was taken in a B19 Quickfit test tube (condensed using liquid nitrogen if gaseous) and attached to the vacuum line. This was then subjected to a freeze-thaw cycle using liquid nitrogen until all the air present had been removed (usually a minimum of three freeze-thaw cycles, checked using the Pirani heads on the line). This was normally considered adequate purification for our purposes, and certainly in the case of the primary ion source compounds this was more than adequate - any trace impurities being filtered out when the primary ion was mass selected in Q1. In all cases the mass spectrum of the sample was taken after de-gassing, and checked for any obviously spurious peaks indicative of impurities. All the samples used were commercial products (99% pure or better).

In cases where the gaseous sample could not be condensed in liquid nitrogen, an alternative procedure was used. This consisted of filling a gas sample tube (Figure 4), by blowing through the tube with the sample gas to expel air, before closing the taps at either end to trap a sample inside. This was then attached to the vacuum line and evacuated as far as Tap 1, before the sample was allowed to expand into the now isolated vacuum line, and treated as before. No problems were encountered with air contamination using this method.

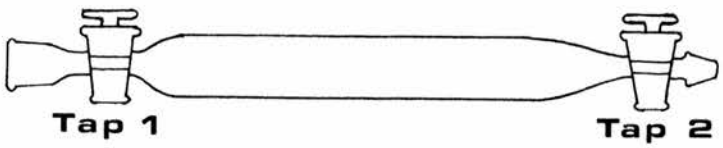

FIGURE 4: Gas Sample Tube used for Non-condensable Samples

In only one case did we require to modify this procedure; this was for the alkynes, and ethyne in particular, where the risks of explosion in the condensed phase were thought to be too high[47,48]. Initially, we used the normal non-condensing technique described immediately above, however, it soon became clear that something else was present in the sample. The mass spectrum of the sample showed peaks at m/z = 43, 58 and 59, thought to be due to acetone, which is normally present in commercial acetylene cylinders. After checking the literature[49], the following procedure was adopted:-

Before collecting the ethyne in the gas sample tube, it was first bubbled through concentrated sulphuric acid, passed through two cold-traps made from acetone/solid carbon dioxide, and finally passed over calcium chloride in a drying tube. This was successful in removing all the acetone impurities.

The spectra recorded on the chart recorder were all run at high gain (3×10^{-9}A and 1V normally), so that even the most minor products could be seen. This required the calibration of the height of the primary ion signal (and occasionally of strong secondary ion signals), which were off scale due to their strength. This was easily accomplished by altering the gain on the recorder and then applying the appropriate multiplication factor to put it on the same scale as the rest of the spectrum.

The spectra were all mass calibrated by reducing both primary and collision gas pressures, and then recording a further spectrum with Q3 in the "total-ion" mode. The resultant spectrum usually had peaks at 90% of the integral mass values, and any gaps were filled by extrapolation onto a "mass calibration scale" taken from this. The peaks were then assigned using this calibration scale, counting from the primary ion, which was of known m/z value and normally the largest peak in the total ion spectrum. Different calibrations were required, as the mass span was varied according to the size of the molecules involved. (This means of mass calibration was used, because although

quadrupoles give a linear scale, we did in fact find some compression of this at higher masses.) The relative heights of all peaks were then measured by hand to the nearest 0·5 mm, and these values noted down. The error correction for naturally occurring ^{13}C contributions were then worked out using the formula:-

$$^{13}C \text{ correction (for } m/z = m+1) = 0{\cdot}011n \times Pm$$

where Pm is the peak height of m/z = m,
n is the number of carbon atoms in m,
and 0·011 is the natural abundance of ^{13}C.

The error-corrected values for each spectrum were then treated in two ways - total ion and normalised. In the first of these, the values for all the ions in the spectrum, including the primary ion, were summed and each ion's value expressed as a fraction of the total. In the second, only the daughter and higher product peaks were taken (P^+ not included). These were then expressed as a normalised figure - the highest secondary signal was taken as the base peak and given the value 100. All other values were then adjusted to scale.

Both of the above treatments were used in the following discussion. The former is used in the majority of systems where we are concerned with watching the effect of pressure on the total system. (Diagrams and tables using this treatment are labelled "% of total ion current"). The latter is used in the first series of experiments, where we are concerned with comparing the reaction of the same primary ion with different collision molecules at constant pressure (these cases are labelled "normalised secondary spectrum").

CAD spectra were obtained and treated in a similar fashion to the ordinary spectra, but using N_2 as the collision gas. Nitrogen was chosen as the target gas, rather than Argon or Helium, because it was literally "on tap" and gave very similar results to Argon. (Helium having been shown[50] to be less suitable for CAD in quadrupoles than in sector instruments). No standard conditions were established for these CAD spectra, although most were taken at very similar values of primary ion current and target thickness (N_2 pressure) because the results were not being used quantitatively. (The setting-up of standardised conditions for the generation of library spectra has yet to be established due to instrumental variations[51].

DISCUSSION

DISCUSSION

The chemical ionisation of alkanes using methane at high pressures has been the subject of numerous studies[52,53,54,55]. In all these cases, the species actually producing the initial charge-exchange reaction is CH_5^+ (and/or $C_2H_5^+$). Thus, in the initial series of reactions undertaken here, it was decided to investigate the behaviour of the previously little studied methane radical cation ($CH_4^{+\cdot}$) & methyl cation (CH_3^+) with the alkanes. Neither of these species had been properly investigated in isolation before, although $CH_4^{+\cdot}$ had been shown to be an important intermediate in chemical[54] and field[56] ionisation studies, and CH_3^+ had received only cursory examination[57]. These experiments would enable the chemistry of these two ions to be compared with one another and with the earlier results using CH_5^+. They would also allow the various instrumental parameters to be investigated thoroughly before moving on to further reactions (see previous section and below).

Our preliminary experiments with methane and methyl cations brought another possible complication to light - that of the source compound for the primary ions.

Tables 6, 7 and 8 below, show the results obtained when the methyl cation is reacted with ethene, propene and 1-butene respectively; and derived from each of three sources - methane, chloromethane and nitromethane.

As can be seen, these results differ significantly for certain collision ions in <u>all</u> cases - ie. m/z = 28 & 39 in the ethene series; m/z = 29 in propene; and m/z = 29, 41 and 42 in 1-butene. The behaviour of CH_3^+ derived from both methane and

Source of CH_3^+	m/z ion	27 $C_2H_3^+$	28 $C_2H_4^{+\cdot}$	29 $C_2H_5^+$	30 $C_2H_6^{+\cdot}$	39 $C_3H_3^+$	40 $C_2H_4^{+\cdot}$	41 $C_3H_5^+$	53 $C_4H_5^+$	55 $C_4H_7^+$	67 $C_5H_9^+$	69 $C_5H_9^+$
		Normalised secondary ion signal										
CH_4		100	6	37	1	14	-	37	2	1	-	1
CH_3Cl		100	11	34	1	25	-	43	2	1	1	1
CH_3NO_2		100	27	38	-	32	2	44	2	3	-	-

TABLE 6: The Effect of Primary-Ion Source on the Reaction of CH_3^+ with Ethene at a Constant Pressure of ca. 5 x 10^{-4} Torr

Source of CH_3^+	m/z ion	27 $C_2H_3^+$	29 $C_2H_5^+$	39 $C_3H_3^+$	40 $C_3H_4^{+\cdot}$	41 $C_3H_5^+$	42 $C_3H_6^{+\cdot}$	43 $C_3H_7^+$	53 $C_4H_5^+$	54 $C_4H_6^{+\cdot}$	55 $C_4H_7^+$	56 $C_4H_8^{+\cdot}$	57 $C_4H_9^+$	69 $C_5H_9^+$	70 $C_5H_{10}^{+\cdot}$
		Normalised secondary ion signal													
CH_4		17	59	19	1	76	100	43	3	1	28	33	9	14	1
CH_3Cl		20	42	20	1	57	100	35	2	1	20	29	8	17	1
CH_3NO_2		20	24	19	2	54	100	38	3	2	26	25	8	17	1

TABLE 7: The Effect of Primary-Ion Source on the Reaction of CH_3^+ with Propene at ca. 5 x 10^{-4} Torr

Source of CH_3^+	m/z ion	27 $C_2H_3^+$	28 $C_2H_4^{+\cdot}$	29 $C_2H_5^+$	39 $C_3H_3^+$	41 $C_3H_5^+$	42 $C_3H_6^{+\cdot}$	43 $C_3H_7^+$	53 $C_4H_5^+$	54 $C_4H_6^{+\cdot}$	55 $C_4H_7^+$	56 $C_4H_8^{+\cdot}$	57 $C_4H_9^+$	69 $C_5H_9^+$	70 $C_5H_{10}^{+\cdot}$	71 $C_5H_{11}^+$
		Normalised secondary ion signal														
CH_4		20	1	72	14	59	50	23	3	2	42	100	20	10	8	2
CH_3Cl		36	-	57	16	49	49	17	4	2	38	100	18	9	8	3
CH_3NO_2		17	2	31	9	29	6	10	2	2	40	100	19	6	10	3

TABLE 8: The Effect of Primary-Ion Source on the Reaction of CH_3^+ with but-1-ene at ca. 5 x 10^{-4} Torr

chloromethane is very similar, whereas the nitromethane derived ion is generally the "odd man out". This suggests that we are dealing with two different methyl cations, although why nitromethane should produce what is presumably a different electronic state, and why these specific secondary ions are affected, we have been unable to discover.

The outcome of this series of experiments was that, where possible, we used the same source for all experiments involving one ion or type of ion. For example; CH_3^+ was always derived from methane, and similarly CD_3^+ from deuteromethane; and the fluoromethyl cations (CH_2F^+, CHF_2^+ and CF_3^+) were derived from either difluoromethane or trifluoromethane. In the majority of cases however, this complication did not arise since we were using radical cations which were all derived directly from the corresponding neutral species.

The initial reaction of the methane radical cation ($CH_4^{+\cdot}$) with linear alkanes (C_nH_{2n+2}) is electron transfer, yielding a neutral methane molecule and an excited alkane radical cation. The product ion thus obtained can then fragment to give a number of daughter ions. The fragmentation patterns obtained using $CH_4^{+\cdot}$ are very similar to those reported in electron impact studies[58], but bear little resemblance to those produced in methane chemical ionisation studies[53,54], where the initial reaction is a proton transfer from the CH_5^+ ionising species, thus - $CH_5^+ + RH \rightarrow RH_2^+ + CH_4$.

The fragmentation using $CH_4^{+\cdot}$ can be depicted in general terms as shown in Scheme 1 below:-

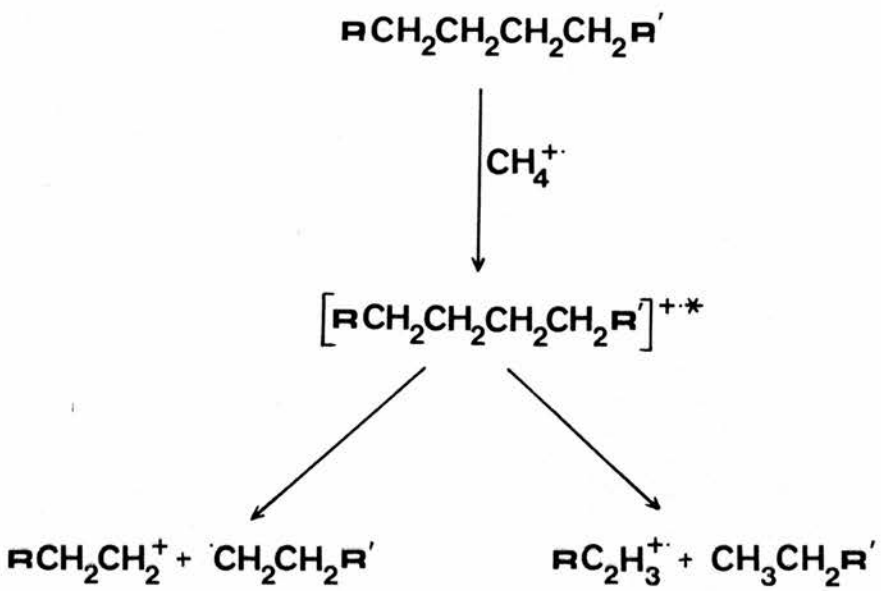

Scheme 1 (where R and R' are saturated alkyl chains; and $R \geqslant R'$).

From the above we see that there are two major fragmentation pathways. In the first of these, the fragments produced are an alkyl cation and an alkyl radical, with the cation able to undergo further fragmentation. Indeed, when we look at the total spectra produced in this series of experiments (See Figure 5(a)), we can see evidence of step-wise degradation of these alkyl cations, yielding ethene and a new carbocation of 28 mass units less.

ie $R - CH_2 - CH_2^+ \longrightarrow R^+ + CH_2 = CH_2$

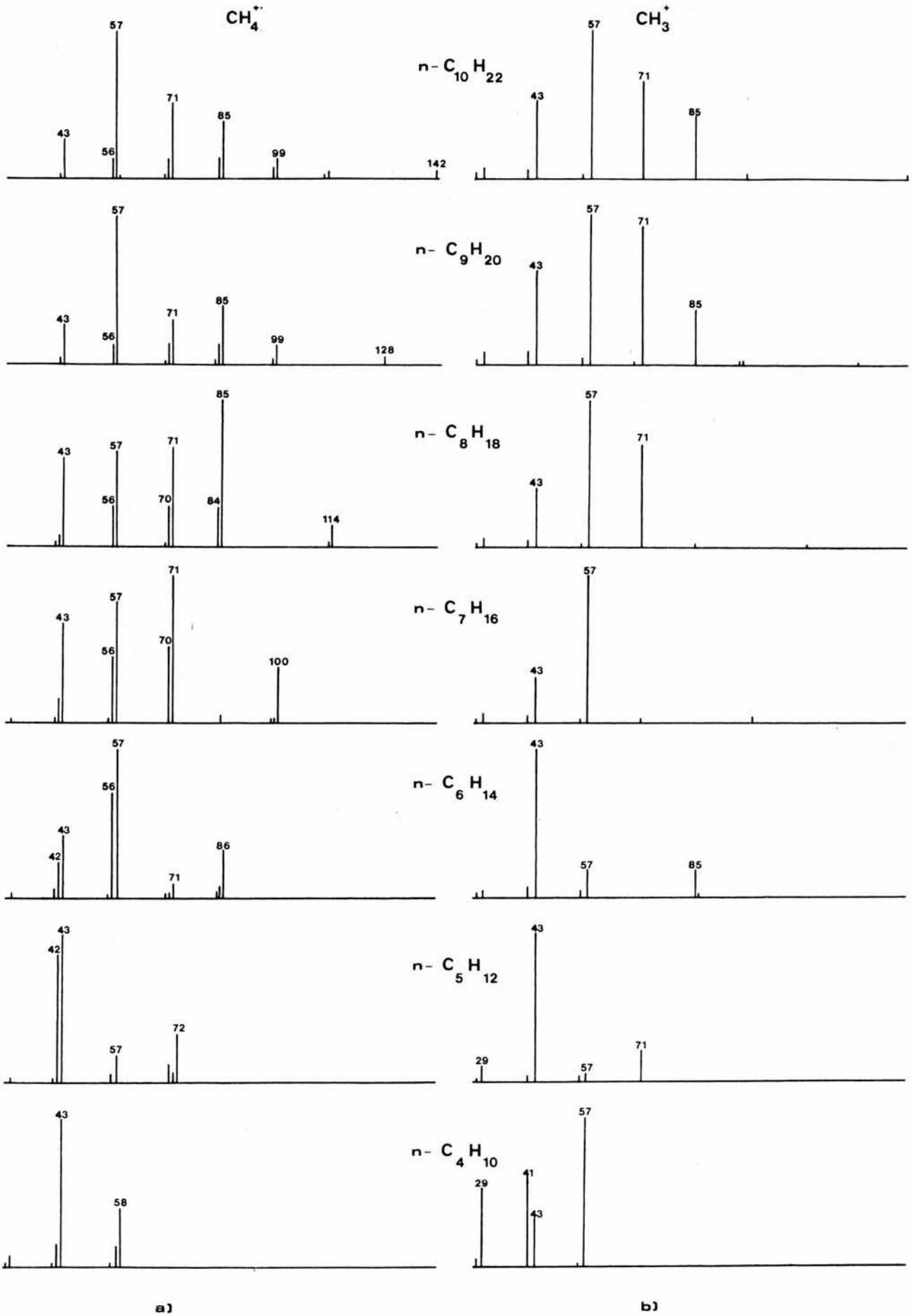

FIGURE 5 The fragmentation spectra of the n-alkanes, produced by ionisation with a) $CH_4^{+\cdot}$ & b) CH_3^+ .

This sequential fragmentation terminates as one of two species; $C_3H_7^+$ or $C_2H_5^+$, with CH_3^+ and H^+ less likely and little seen alternatives. (CH_3^+ may indeed be one of the fragment ions produced in the spectra under discussion here, but due to the strength of the primary ion signal (at m/z = 16), this ion (m/z = 15) is impossible to discern with any clarity. For this reason and for energetic considerations[59,60], CH_3^+ is not considered to be a product of this reaction. H^+ is never observed). The presence of ions separated by 28 a.m.u. in the mass spectrum could also be attributed to cleavage at different C-C bonds in the alkene radical cations, as observed in electron impact mass spectra[61]. However, CAD evidence and studies by other groups[62,63] show that we do infact get this step-wise elimination of ethene.

The second fragmentation pathway shown in Scheme 1, involves the formation of short chain alkanes (C_1H_{21+2}) and the simultaneous formation of alkene radical cations ($C_mH_{2m}^{+\cdot}$) - where 1 + m = n - with these alkene radical cations undergoing further fragmentation with the loss of methyl and/or ethene.

Combining the results from the $CH_4^{+\cdot}$ spectra with the results of the numerous CAD studies performed on the alkane radical cations and their fragments (see Results section), we were able to construct complete degradation schemes for the alkane radical cations, as shown in Scheme 2 below. (Similar schemes for all the n-alkanes studied - C_nH_{2n+2} ; $4 \leqslant n \leqslant 10$ - are given in Appendix 1.)

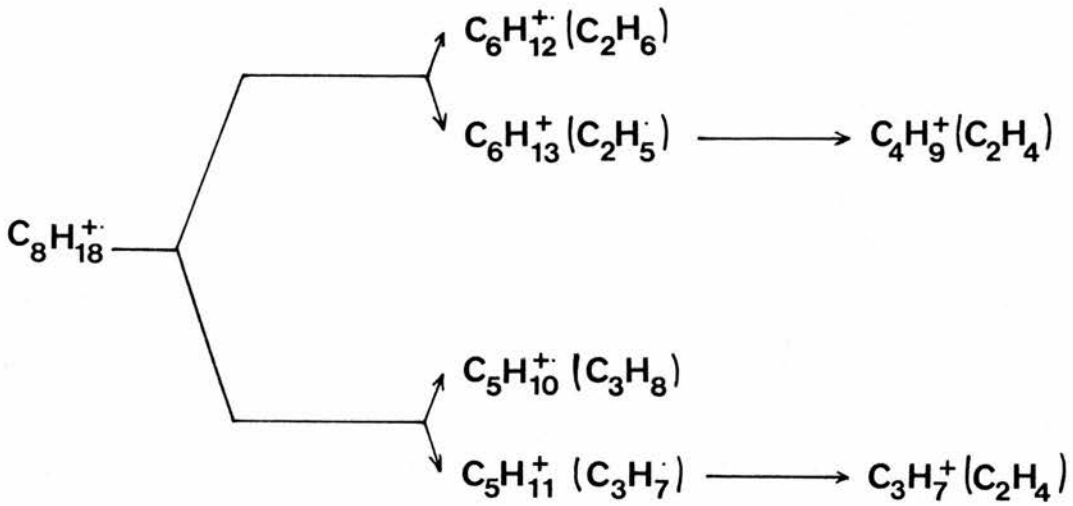

Scheme 2 - The successive CAD spectra of the ionic fragments occuring in the reaction between $CH_4^{+\cdot}$ and C_8H_{18}.

The initial reaction of CH_3^+ with the same linear alkanes is hydride transfer, yielding an excited carbocation and a neutral methane molecule. This cation can then fragment as shown in Scheme 3.

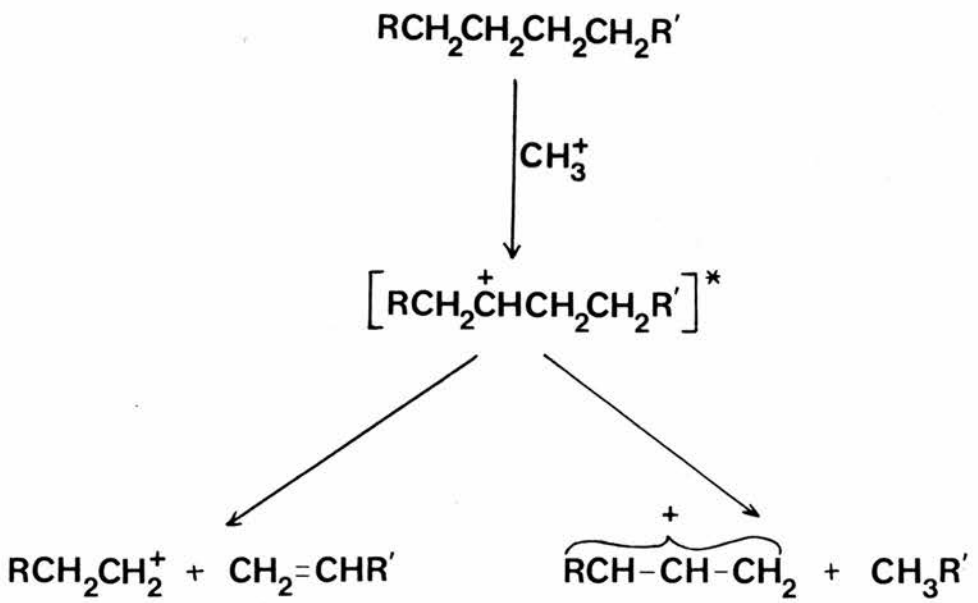

Scheme 3 - (where R and R' are saturated alkyl chains; and $R \geq R'$)

In this case, the principal fragmentation pathway involves the formation of an alkene and an alkyl cation, which in turn undergoes the stepwise elimination of ethene. The total spectrum obtained (See Figure 5(b)) is much simpler than is the case with $CH_4^{+\cdot}$. Infact, after the initial fragmentation observed in the case of $CH_4^{+\cdot}$, we are observing the same step-wise elimination of ethene from the same alkyl cations in both sets of spectra. There is also some evidence that a second minor fragmentation process occurs, producing allylic cations and an alkane. (See Scheme 3). Again we were able to construct degradation schemes in this case for the alkyl cations, with the octyl ion shown as an example in Scheme 4. Similar degradation schemes for all the alkyl cations ($C_nH_{2n+1}^+$; $4 \leq n \leq 10$) are also given in Appendix 1.

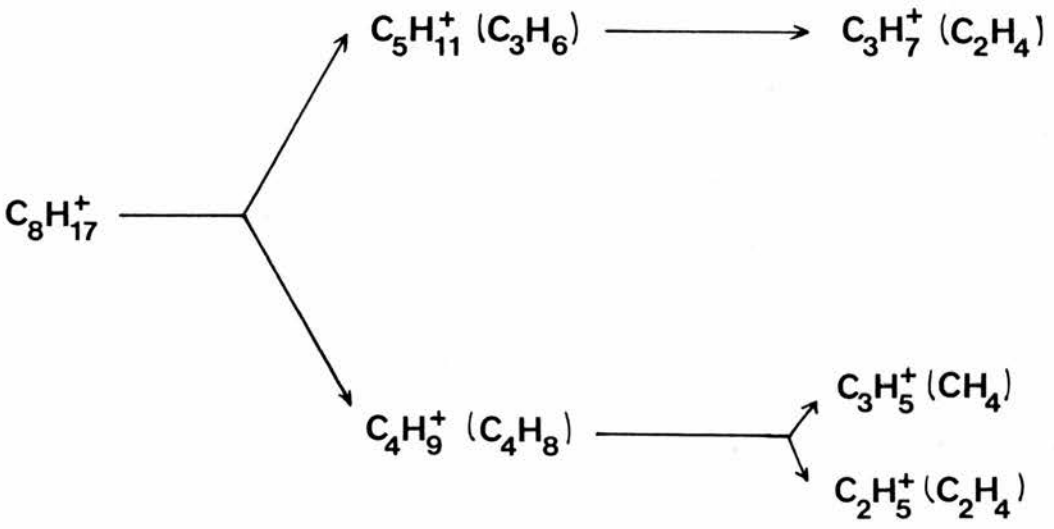

Scheme 4: The Fragmentation of $C_8H_{17}^+$

Moving on to the iso-alkanes, Tables 9 and 10 show the total secondary spectra obtained when $CH_4^{+\cdot}$ and CH_3^+ react with 2-methyl propane and 2-methylbutane respectively (the results for n-butane and n-pentane are included for comparison).

	m/z	27	28	29	41	42	43	55	56	57	58
	ion	$C_2H_3^+$	$C_2H_4^{+\cdot}$	$C_2H_5^+$	$C_3H_5^+$	$C_3H_6^{+\cdot}$	$C_3H_7^+$	$C_4H_7^+$	$C_4H_8^{+\cdot}$	$C_4H_9^+$	$C_4H_{10}^{+\cdot}$
$CH_4^{+\cdot}$	n-C_4	-	6	9	2	15	100	-	4	11	40
	iso-C_4	-	-	-	2	63	100	-	4	12	16
CH_3^+	n-C_4	13	-	54	69	-	35	3	-	100	-
	iso-C_4	2	-	52	70	2	51	2	-	100	4

TABLE 9: The Ions Formed in the Reaction of $CH_4^{+\cdot}$ and CH_3^+ with n-butane and 2-methylpropane (Normalised secondary ion signal)

	m/z	27	29	41	42	43	55	56	57	70	71	72
	ion	$C_2H_3^+$	$C_2H_5^+$	$C_3H_5^+$	$C_3H_6^{+\cdot}$	$C_3H_7^+$	$C_4H_7^+$	$C_4H_8^{+\cdot}$	$C_4H_9^+$	$C_5H_{10}^{+\cdot}$	$C_5H_{11}^+$	$C_5H_{12}^{+\cdot}$
$CH_4^{+\cdot}$	n-C_5	-	3	3	86	100	-	5	19	14	8	32
	iso-C_5	-	3	3	100	58	-	42	52	13	19	32
CH_3^+	n-C_5	1	9	4	1	100	1	-	3	-	20	1
	iso-C_5	1	6	3	1	100	3	1	9	-	22	1

TABLE 10: The Ions Formed in the Reaction of $CH_4^{+\cdot}$ and CH_3^+ with n-pentane and 2-methylbutane (Normalised secondary ion signal)

From these we can see that, in the case of CH_3^+, the spectra are very similar for both straight chain and branched molecules; whereas, with $CH_4^{+\cdot}$ the ions observed occur at the same masses, but the relative proportions of certain ions differ considerably.

To explain this difference in behaviour between CH_3^+ ionisation and $CH_4^{+\cdot}$ ionisation, we must consider how these two primary ions bring about reaction; hydride transfer or electron transfer.

Comparing the results obtained using CH_3^+ first, we must assume from the similarity of the two spectra that in both cases the precursor to the daughter ions is the same. In other words, the carbonium ion formed in the initial hydride abstraction reaction between CH_3^+ and an n-alkane must undergo a structural rearrangement of the carbon skeleton before it fragments. This conclusion is in agreement with Davis, Williams and Yeo[64] who showed that the $C_4H_9^+$ ions generated from n-, iso-, s- and t-butyl structures isomerised to the same structure or mixture of structures before loss of ethene or methane (they include in this the methylated cyclopropane proposed by Mayerson and Rylander[65]). The actual structure taken by the $C_4H_9^+$ ion is open to question, but Liardon and Gaumann[66] (who investigated isotopically labelled butyl ions produced from the corresponding butyl halides by electron impact) suggested the mechanism shown in Scheme 5, involving protonated cyclobutane, which eloquently explains the complete hydrogen and carbon scrambling which they observed, and provides a simple mechanism for the loss of both CH_4 and C_2H_4. A similar mechanism involving cyclisation (4, 5 and 6 - membered rings) was envisaged for the higher alkyl cations[67,68].

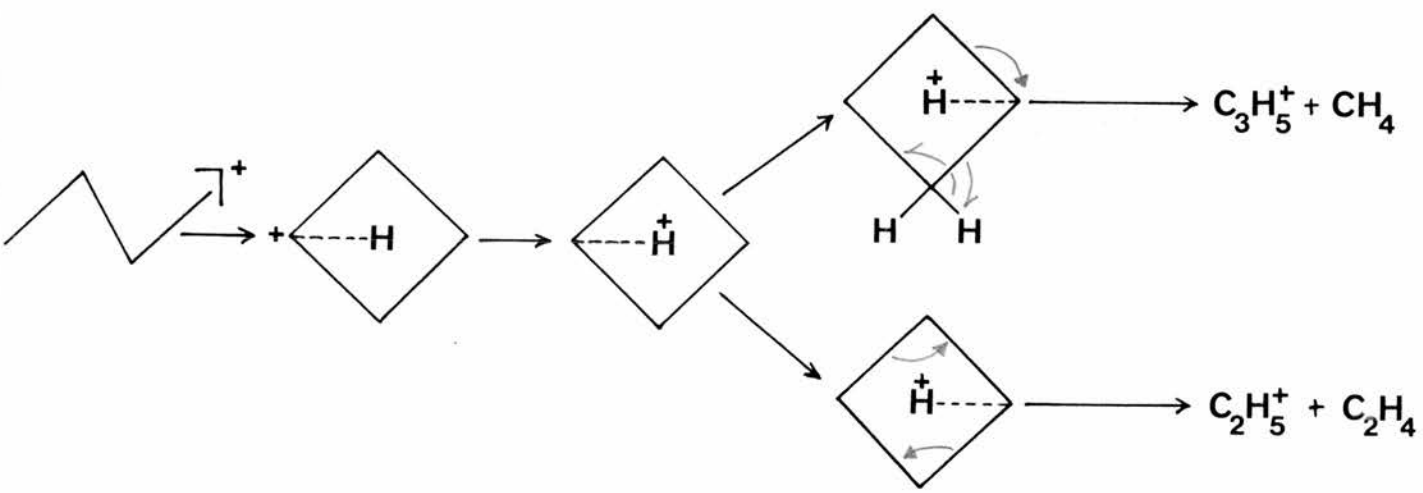

Scheme 5: A Possible Mechanism for the loss of CH_4 & C_2H_4 from the $C_4H_9^+$ ion.

In contrast to the butyl cation discussed above, the butane radical cation $C_4H_{10}^{+\cdot}$, formed by electron transfer to $CH_4^{+\cdot}$, must rearrange as it fragments (if indeed rearrangement occurs). This would explain why the fragmentation patterns of the n-alkanes differ from those of the iso-alkanes when using $CH_4^{+\cdot}$ as the primary ion. Again this conclusion is consistent with the results reported by Liardon and Gaumann[69] and Wolkoff and co-workers[63,70] for the fragmentation of alkane molecular ions formed by electron impact. In particular we see an enhancement in both branched species (see Tables 9 and 10) of the process which eliminates a neutral methane molecule. This can be simply explained by using 1,2-elimination as proposed by Wolkoff et al.

ie. for 2-methylpropane

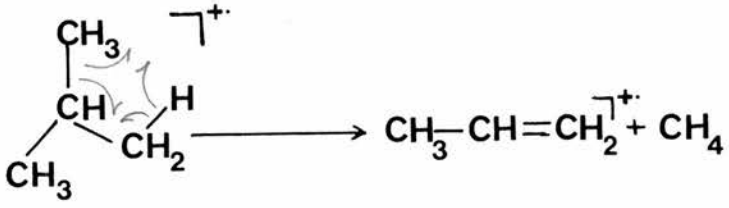

If no isomerisation takes place, then in n-butane the probability of this 1,2 - elimination occurring is reduced, and the much smaller peak seen at m/z = 42 (see Table 9) confirms that this ion does not rearrange before fragmentation. However, we cannot comment as to the structure of the $C_3H_6^+$ ion thus formed*, although when the pentaquadrupole

---

*Wolkoff and co-workers[63] initially favoured the cyclopropane structure here, but later work[71] has shown this ion to have the propene structure.

device currently under development in this laboratory is operational, direct CAD studies on this ion should be possible and its structure determined explicitly.

Looking at the case of 2-methylbutane (see Table 10), we see a similar enhancement of the $(M-16)^{+\cdot}$ ion, accompanied by an enhanced $(M-15)^{+}$ ion. The former we can again explain in terms of the 1,2-elimination illustrated above; whilst the latter can be attributed to an increased probability of terminal methyl loss. (The "Internal" mechanism for CH_3/CH_4 loss found in the labelling experiments of Gaumann[66], Holmes[70] and Wendelboe[72], no doubt occurs in our series of experiments, but without access to selectively labelled molecules we cannot comment on this). In conjunction with these enhanced peaks we also see a decline in the size of the peak at m/z = 43 (as compared with n-pentane). This can be attributed to the reduction in suitable points for C-C bond scission - whereas in n-pentane bond scission between C^2-C^3 and C^3-C^4 produces the same products (namely $C_3H_7^+$ and C_2H_5), in 2-methylbutane there is only one point at which this process can occur.

These results indicate that as in the case of $CH_4^{+\cdot}$ reacting with n- and iso-butane, the alkane radical cation formed in the reaction of $CH_4^{+\cdot}$ and n-pentane <u>does not</u> rearrange before fragmentation. This conclusion is at variance with the mechanism proposed by Wendelboe et al[72] and also with the conclusions drawn by Wolkoff et al[73]. Although the latter states a preference for isomerisation before fragmentation, he does not discount the possibility that the fragmentations are concerted reactions, analogous to those which he proposed for butane[63,70].

m/z	28	29	42	43	57
ion	$C_2H_4^{+\cdot}$	$C_2H_5^+$	$C_3H_6^{+\cdot}$	$C_3H_7^+$	$C_4H_9^+$
n-butane	1	2	26	72	-
iso-butane	-	-	84	13	3

TABLE 11: The CAD Spectra of n-butane and 2-methylpropane (% of Total CAD Spectrum)

m/z	42	43	56	57	70
ion	$C_3H_6^{+\cdot}$	$C_3H_7^+$	$C_4H_8^{+\cdot}$	$C_4H_9^+$	$C_5H_{10}^{+\cdot}$
n-pentane	68	22	4	4	3
iso-pentane	49	8	37	5	-

TABLE 12: The CAD Spectra of n-pentane and 2-methylbutane (% of Total CAD Spectrum)

Further confirmation of our conclusions came when the CAD spectra of the four molecules in question were investigated. (Although the ions used in this experiment were produced by electron impact, they were taken to be valid models for our "chemical ionisation" processes using CH_3^+ and $CH_4^{+\cdot}$). The results are given in Tables 11 and 12, and again show the marked differences between the isomers as discussed above.

Looking at the behaviour of the cycloalkanes (Figure 6), we see that for both CH_3^+ and $CH_4^{+\cdot}$ initiated reactions, the results bear little relationship to those described above for the linear and branched alkanes. The molecular ion ($M^{+\cdot}$) from the $CH_4^{+\cdot}$ series and the molecular ion less one mass unit, $(M-1)^+$, from the CH_3^+ series are relatively much more important in the cyclic molecules. The fragmentation patterns which emerge from these results show the major processes occurring to be loss of methyl radical, loss of ethene and loss of propene from the charge-exchange products. (A number of unexpected ions were detected using CH_3^+, and overall it proved difficult to justify any mechanistic inferences from these results.)

$CH_4^{+\cdot}$ again brings about reaction by electron transfer to give methane and an excited state radical cation. This radical cation then undergoes two main types of fragmentation:-

(1) loss of methyl radical

(2) loss of olefin(s)

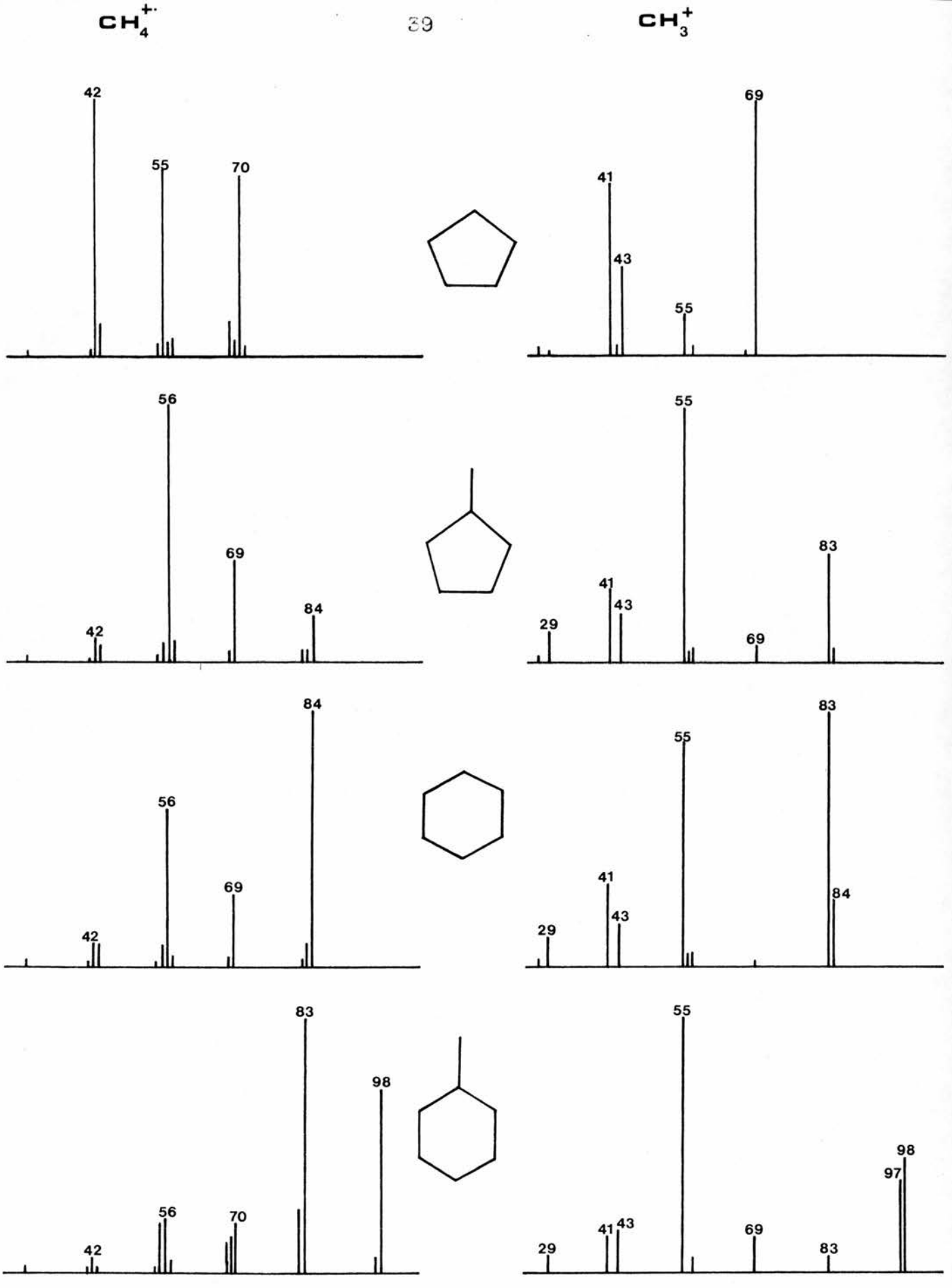

FIGURE 6 The fragmentation patterns for the cyclo-alkanes, produced on collision with $CH_4^{+\cdot}$ & CH_3^+.

Using the combined results from the spectra and CAD experiments (results in Appendix 2), we can attempt to explain the differences found in the spectra of the four molecules under investigation. The best example to take is that of methylcyclopentane and cyclohexane, which both have the same empirical formula.

Rather like the case of the n- and iso-alkanes, there are marked differences between the spectra for methylcyclopentane and cyclohexane, implying that structural integrity is retained by the molecular ions. In cyclohexane, the $M^{+\cdot}$ ion (m/z = 84) is very much larger than that in methylcyclopentane, whilst the ion at m/z = 56, corresponding to loss of ethene is much smaller. Rather surprisingly, the peak at m/z = 69 ($CH_3^{\cdot}$ loss) is very similar in both cases. If the neutral structures are retained in these ions, we could have expected this latter peak to be larger in the case of methylcyclopentane, due to the increased likelyhood of terminal methyl loss. The CAD for both molecules (Table 13) are very similar.

m/z	42	43	55	56	68	69
ion	$C_3H_6^{+\cdot}$	$C_3H_9^{+}$	$C_4H_7^{+}$	$C_4H_8^{+\cdot}$	$C_5H_8^{+\cdot}$	$C_5H_9^{+}$
methylcyclopentane	1	-	1	65	1	33
cyclohexane	1	1	1	59	5	32

TABLE 13: The CAD Spectra of Methylcyclopentane and Cyclohexane (% of Total CAD Spectrum)

It may be that the two different structures give very similar CAD results, but the differences observed are too small to be sure. With these two pieces of evidence apparently contradicting each other,

it was decided to look at the CAD spectra for the major fragment ion, $C_4H_8^{+\cdot}$ (m/z = 56), derived from a number of sources. The results are shown in Table 14 below.

m/z	28	29	40	41	55
ion	$C_2H_4^{+\cdot}$	$C_2H_5^+$	$C_3H_4^{+\cdot}$	$C_3H_5^+$	$C_4H_7^+$
methylcyclopentane	2	-	21	42	36
cyclohexane	1	-	21	36	42
methylcyclohexane	-	-	24	33	43
n-nonane	1	2	22	75	-
n-decane	-	-	17	75	-
but-1-ene	3	3	7	67	11

TABLE 14: The CAD Spectra of the $C_4H_8^{+\cdot}$ ion Derived From 6 Sources (% of Total CAD Spectrum)

From this we see that there appear to be three distinct ions of formula $C_4H_8^{+\cdot}$ present - one derived from but-1-ene, one from the n-alkanes, and one from the cycloalkanes - but again this does not clarify if methylcyclopentane and cyclohexane isomerise to a common structure before fragmentation (yet again there are noticeable differences between the two CAD spectra). In conclusion, we cannot state whether or not the odd-electron c-$C_nH_{2n}^{+\cdot}$ ions behave in a similar fashion to the previously discussed n- and iso-$C_nH_{2n+2}^{+\cdot}$ ions, where there is no isomerisation before fragmentation, but we suspect that this may indeed be the case here. (The use of ^{13}C labelling, not available to us, could help solve this problem, and perhaps help determine how the observed elimination reactions arise - via ring-opening, ring-contraction or otherwise.)

Turning to the series of reactions initiated by CH_3^+, we find that as in the previous experiments using this ion, the major process involved is hydride transfer, followed by olefin elimination. However, these spectra (especially those of cyclohexane and methylcyclohexane) are complicated by the presence of significant amounts of the molecular ion ($M^{+\cdot}$). This can only be the result of a second type of initial reaction (ie. charge transfer rather than hydride abstraction), but quite why this should occur to such a significant extent with this series of compounds we are at a loss to explain. (Nb. This process is observed with the n- and iso-alkanes, but only to a very limited extent; 1% of the total secondary signal.) However, their presence does explain why we see peaks at 14 mass units below the hydride transfer product - these peaks corresponding to the loss of $CH_3^{\cdot}$ from $M^{+\cdot}$, and not the loss of $CH_2^{\cdot}$ from $(M-1)^+$.

Comparison of the results for the two isomeric species, methyl-cyclopentane and cyclohexane, this time shows them to be very similar (excluding the anomalous $M^{+\cdot}$ presence), which is in agreement with previous studies of these ions[74,75], which had shown that cyclohexyl ions isomerise to tertiary methylcyclopentyl ions. (Unfortunately our attempts to perform CAD studies on these ions proved unsuccessful, in that we could not generate a signal (at m/z = 83) strong enough for collisional dissociation, and so we could not use this to confirm the results.) We did study the CAD of the homologous cyclopentyl ion, and the results (see Table 15) indicate that the $C_5H_9^+$ ions derived from the three cyclic precursors have the same structure (which has been suggested[76] to be the tertiary ethylcyclopropyl ion, ).

m/z	41	55	67
ion	$C_3H_5^+$	$C_4H_7^+$	$C_5H_7^+$
methylcyclopentane	75	-	25
cyclohexane	72	-	28
methylcyclohexane	76	-	24
n-decane	77	12	11

TABLE 15: The CAD Spectra of the $C_5H_9^+$ ion Derived from 4 Sources (% of Total CAD Spectrum)

The mechanism for the major elimination reactions which we have observed from the c - $C_nH_{2n-1}^+$ ions (elimination of olefin) is difficult to ascertain from our results, but one possible pathway involves the pyramidal cation suggested by Schwarz[77,78] and shown in Scheme 6.

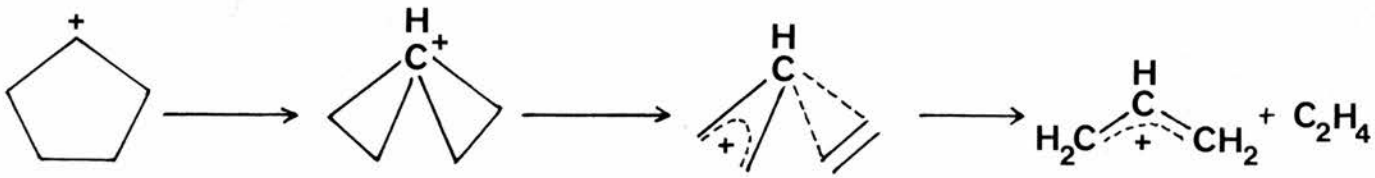

Scheme 6:

This scheme also holds true for the cyclohexyl/methylcyclopentyl isomerisation, and ethene loss[78,79] can be modified (using 1,2 - Me shifts) to account for the loss of propene from these same molecules. Furthermore, if we assume that methylcyclohexyl ions also isomerise to a substituted cyclopentyl structure(s), the same mechanism can be used to account for the loss of ethene, propene and butene from this molecule.

Although we did not have access to iostopically labelled alkanes, we did investigate what happened when $CD_4^{+\cdot}$ and CD_3^+ were used as primary ions in place of $CH_4^{+\cdot}$ and CH_3^+ in the reaction with n-decane. The results are shown in Tables 16 and 17 (below), along with the results for $CH_4^{+\cdot}$ and CH_3^+ for comparison.

m/z	42	43	55	56	57	58	69	70	71	83	84	85	98	99	100	112	113
CH_4	2	25	1	11	100	3	2	11	50	1	13	33	7	10	-	3	4
$CD_4^{+\cdot}$	6	23	4	25	100	5	3	24	69	2	16	33	11	10	7	4	4

TABLE 16: The Ions Formed in the Reaction of $CH_4^{+\cdot}$ and $CD_4^{+\cdot}$ with n-decane (Normalised Secondary Ion Signal)

m/z	29	32	41	43	44	45	46	55	56	57	58	59	60	71	85	99
CH_3^+	6	-	5	51	-	-	-	2	-	100	-	-	-	65	43	6
CD_3^+	1	3	1	24	3	2	3	2	2	100	2	1	3	48	29	3

TABLE 17: The Ions Formed in the Reaction of CH_3^+ and CD_3^+ with n-decane (Normalised Secondary Ion Signal)

From the above we can see that when we use $CD_4^{+\cdot}$ in place of $CH_4^{+\cdot}$, there is very little variation in the fragmentation pattern - there being no peaks that we can definitely assign as being due to the presence of ^2H. However, when we look at the reaction of CD_3^+ with decane we see noticable (though small) effects on certain daughter ions (at m/z = 29, 43 and 57). In each of these cases up to three ^2H atoms are involved, which suggests that during the

course of the initial hydride abstraction, there occurs some H-scrambling or perhaps that the CD_3^+ remains attached to the n-decane and a $CH_3^\cdot$ radical is eliminated. (Again ^{13}C labelling could furnish further information on the exact nature of this process.

The final experiment undertaken involving the ions/neutrals used so far, was to compare the reaction of $CH_4^{+\cdot}$ with n-heptane in the TQMS and in the tandem magnetic sector mass spectrometer previously used in this lab[15]. (In the case of the latter, the primary ions were injected into the collision chamber with ca 8V.)

The major difference between the two spectra (see Table 18), is in the size of the parent ion at m/z = 100. This is much greater in the case of the older machine and illustrates the different discrimination of the two instruments. The tandem sector device has the two mass detectors set at right angles hence it preferentially selects ions formed by "long-range" interactions, with the ions formed by actual collision tending to be swept clear of the extraction zone, along the axis of collision. These ions are the ones detected by the TQMS, where the second quadrupole mass filter is arranged along this axis.

m/z	43	56	57	70	71	100
ion	$C_3H_7^+$	$C_4H_8^+$	$C_4H_9^+$	$C_5H_{10}^+$	$C_5H_{11}^+$	$C_7H_{16}^+$
Triple quadrupole	67	46	83	54	100	38
Tandem Sector	50	25	86	43	54	100

TABLE 18: Ions Formed by the Reaction of $CH_4^{+\cdot}$ with n-heptane in the Triple Quadrupole and Tandem Sector Mass Spectrometers (Normalised Secondary Ion Signal)

The second series of experiments undertaken again involved the use of the methyl cation as the primary ion. This work, using CH_3^+ and the three fluoromethyl cations in reaction with ethyne and the simple alkenes, was done in conjunction with a number of co-workers, and reference will be made to their results in this discussion, but these results are not included in this thesis.

The reaction of methyl cations with ethyne produces a spectrum which effectively contains only one secondary ion, $C_3H_3^+$ (m/z = 39); but before discussing this ion and its structure in detail, we will first look at the minor products (see Table 19).

m/z	26	27	38	39	51	63	65
ion	$C_2H_2^+$	$C_2H_3^+$	$C_3H_2^+$	$C_3H_3^+$	$C_4H_3^+$	$C_5H_3^+$	$C_5H_5^+$
% secondary ion signal	0.4	1.3	1.0	95.1	0.8	0.5	1.0

TABLE 19: The Ions Formed in the Reaction Between CH_3^+ and Ethyne

Two other secondary ions are observed, at m/z = 26 and 27. The first of these is the charge-exchange product ($C_2H_2^{+\cdot}$) and the second ($C_2H_3^+$) is the proton transfer product, thought to occur via the loosely-bound transition state (A).

$$H_2C\text{----}\overset{+}{H}\text{----}C_2H_2$$

A

The remaining ions are all tertiary, products of the further reactions of $C_2H_2^{+\cdot}$ and $C_3H_3^+$, as shown in Scheme 7, below. These reactions were verified by studying each individual step in isolation (see Results and Discussion on the ethyne ion-molecule reaction).

$$C_2H_2^{+\cdot} + C_2H_2 \longrightarrow C_4H_3^+ + H^\cdot \qquad m/z = 51$$

$$C_3H_3^+ + C_2H_2 \longrightarrow \begin{cases} C_3H_2^+ + C_2H_3^\cdot & m/z = 38 \\ C_5H_3^+ + H_2 & m/z = 63 \\ C_5H_5^+ & m/z = 65 \end{cases}$$

SCHEME 7

The most interesting ion observed here however, is the major product, $C_3H_3^+$; the structure of which is taken to be that of the cyclo-propenium cation (B), produced when molecular hydrogen is eliminated from the thermally excited reaction complex $(C_3H_5)^{*+}$. There is both theoretical and experimental evidence to support this conclusion.

Several ab initio calculations have been performed on the $C_3H_3^+$ ion[80,81], which predict that the propargyl ion (C) and the cyclopropenyl ion (B) are the two most stable isomers; with the latter more stable by approximately 130 kJ mol^{-1}. (The experimental difference[82] has been measured at 105 kJ mol^{-1}.)

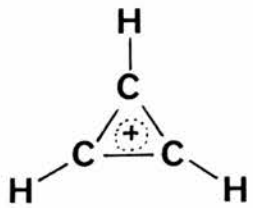

B

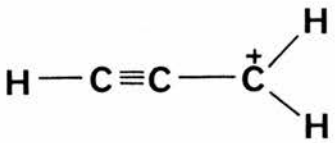

C

These relative heats of formation are convincing enough, but when one considers the calculated barrier for interconversion between B and C, which is very high at 348 kJ mol^{-1}, it seems even more probable that B is the structure involved here.

Experimentally, our results using CD_3^+ confirm this result. At the lowest pressure used, the experimental ratios of the three possible $C_3X_3^+$ isomers, are close to the theoretical ratios obtained if the $(C_3X_5)^{*+}$ reaction complex is symmetrical (see Table 20), and the final product too is symmetrical.

Ion	Experimental	Theoretical
$C_3H_2D^+$ (m/z = 40)	2·5	3
$C_3HD_2^+$ (m/z = 41)	4·6	6
$C_3D_3^+$ (m/z = 42)	1·0	1

TABLE 20: The Theoretical and Experimental Isomer Ratios for $C_3X_3^+$ Formed from Symmetrical $C_3H_2D_3^{*+}$.

That these ratios are not exactly those predicted, could be due to H/D scrambling (which would make any structural inferences dubious), but closer inspection of the spectra as the pressure is varied reveals another reason for this. Table 21 shows how the four possible $C_3X_3^+$ ions' abundances change with pressure.

m/z	39	40	41	42	
ion	$C_3H_3^+$	$C_3H_2D^+$	$C_3HD_2^+$	$C_3D_3^+$	Total
$1{\cdot}2 \times 10^{-4}$	2	14	25	5	46
$6{\cdot}0 \times 10^{-4}$	40	90	100	14	244
$1{\cdot}6 \times 10^{-3}$	184	164	123	26	497
$4{\cdot}1 \times 10^{-3}$	392	221	126	22	761

Table 21: The Effect of Increasing Pressure on the Four Possible $C_3X_3^+$ Ions in the Reaction of CD_3^+ with Ethyne (Fraction of total ion signal 1000)

From this we see that even at the lowest pressure $C_3H_3^+$ is present and goes on to be the most abundant ion at high pressures. This ion cannot be a secondary product of the breakdown of the $(C_3H_2D_3)^{*+}$ reaction complex, and so it must be a tertiary ion produced by H/D exchange when the deuterated $C_3X_3^+$ secondary ions collide with the excess neutral ethyne (Scheme 8).

$$C_3D_3^+ + C_2H_2 \longrightarrow C_3HD_2^+ + C_2HD$$

$$C_3HD_2^+ + C_2H_2 \longrightarrow C_3H_2D^+ + C_2HD$$

$$C_3H_2D^+ + C_2H_2 \longrightarrow C_3H_3^+ + C_2HD$$

SCHEME 8

This H/D exchange is in itself an indication of the structure of the $C_3H_3^+$ ion; the low reactivity of cyclopropenyl ion towards C_2H_2, in comparison with the propargyl ion, having been demonstrated by Fetterolf et al[83]. (ie. the $C_3X_3^+$ ions observed here undergoing non-reactive collisions with C_2H_2, again implying that these are cyclopropenyl).

The reaction between CH_2F^+ and ethyne was also investigated (Table 22) and again the $C_3H_3^+$ ion is the most abundant ion. A second $C_3X_3^+$ is also possible, and this ion ($C_3H_2F^+$; m/z = 57), along with

m/z	27	31	39	41	51	57	65
ion	$C_2H_3^+$	?	C_3H_3	$C_3H_5^+$	CHF_2^+	$C_3H_2F^+$	$C_5H_5^+$
	18	15	100	2	2	16	6

TABLE 22: The Ions Formed in the Reaction Between CH_2F^+ and Ethyne (Normalised Secondary Ion Signal)

the proton transfer product $C_2H_3^+$ (m/z = 27) and the ion at m/z = 31 (CF^+ or $C_2F_2^{2+}$?), are the only secondary ions of any consequence. The $C_5H_5^+$ tertiary product ion is also found in this system, but unlike the methyl initiated reaction, this ion appears in appreciable quantities (up to 13% of the total secondary ion signal cf. 2% using CH_3^+). As mentioned in the preceding discussion of the $C_3H_3^+$ ion structure, the two isomeric forms of this ion have been shown[83,84] to have different reactivities. This same behaviour is displayed by the $C_3H_3^+$ ions under discussion here, which leads us to the conclusion that these $C_3H_3^+$ ions, derived from the reaction of CH_2F^+ cations with ethyne, have the propargyl structure (C) - or possibly a mixture of the propargyl and cyclopropenyl structures.

In view of the above results, which must be a consequence of the fluorine substituent on the methyl primary ion, the reactions of both CHF_2^+ and CF_3^+ with ethyne were performed by Iain Conner, as part of his honours project[85]. Tables 23 and 24 show the results of these experiments.

m/z	27	31	57	59	77
ion	$C_2H_3^+$	?	$C_3H_2F^+$	$C_3H_4F^+$	$C_3H_3F_2^+$
	78	22	11	100	56

TABLE 23: The Ions Formed in the Reaction Between CHF_2^+ and Ethyne (Normalised Secondary Ion Signal). Experiment Conducted by Iain Conner.

m/z	43	45	51	61	75
ion	$C_3H_7^+$	$C_2H_2F^+$	CHF_2^+	$C_3H_6F^+$	$C_3HF_2^+$
	17	17	100	33	17

TABLE 24: The Ions Formed in the Reaction Between CF_3^+ and Ethyne (Normalised Secondary Ion Signal). Experiment Conducted by Iain Conner.

CHF_2^+ produces very little reaction when collided with ethyne, the major secondary ion being the proton transfer product $C_2H_3^+$. The sole $C_3X_3^+$ ion observed is $C_3H_2F^+$ (m/z = 57), which is only seen at high pressures, along with the collisionally stabilised reaction complex $(C_3H_3F_2)^{*+}$ at m/z = 77, and the tertiary species $C_3H_4F^+$ (m/z = 59).

CF_3^+ also produces very little reaction with ethyne. Only two secondary ions are observed; $C_2H_2F^+$ (m/z = 45) and CHF_2^+ (m/z = 51),

formed as shown in Scheme 9. The $C_3X_3^+$ ion, $C_3HF_2^+$ (m/z = 75) is also observed at high ethyne pressures, and the fact that only this ion of the 3 possible $C_3X_3^+$ is produced, may be a function of the reaction complex's structure or it may be that elimination of the HF molecule is energetically more favourable than that of H_2 or F_2.

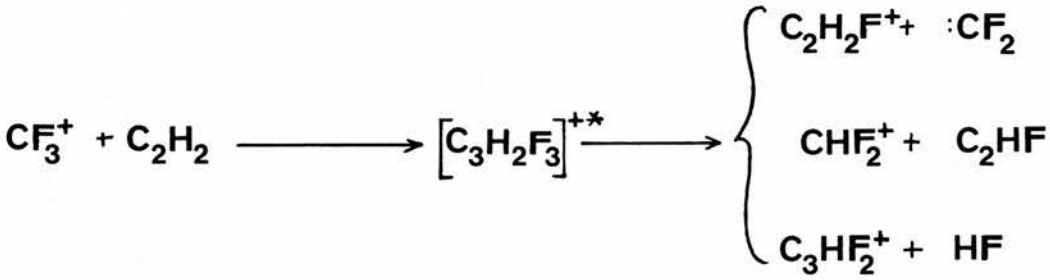

Scheme 9

The reactions of methyl cations with the simple olefins were the first experiments to be undertaken on the TQMS instrument used throughout the research in this thesis[46]. The individual experiments were repeated here, to facilitate a comparison with the reactions of the fluoromethyl cations under identical conditions, and where appropriate reference will be made to these results. Mention will also be given to the reactions of the same four primary ions with three fluoroethene molecules, this work having been done by Keith Stanney during an exchange visit from LaTrobe University, Melbourne, Australia.

Looking first at the reaction between methyl cation and ethene, our results are no different from those of Batey and Tedder[46], but at higher pressures this reaction is more complicated than their simple schematic (Scheme 10).

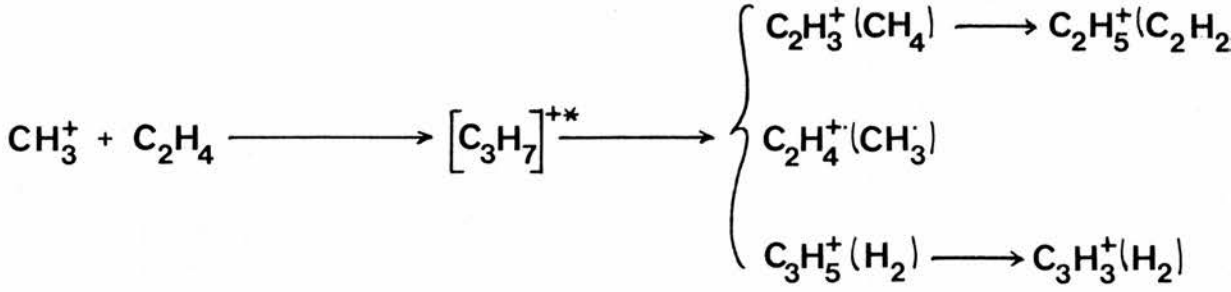

SCHEME 10

From Table 25 below, which shows the low-to-high pressure abundance ratios for the major products in this series of reactions, we can see that the inter-relationship of the $C_2H_3^+$ and $C_2H_5^+$ ions is confirmed. However, the abundance of $C_3H_5^+$ is seen to increase

dramatically with pressure, which we would not expect from the above scheme. The reason for this behaviour was discovered when the "characterising" reactions for the main secondary ions in the ethene ion-molecule reaction were investigated. These reactions (see later in discussion) show that $C_2H_3^+$, $C_2H_4^+$ and $C_2H_5^+$ all produce $C_3H_5^+$ preferentially in an atmosphere of ethene. Thus $C_3H_5^+$ is a product of both secondary and tertiary reactions, hence its build-up with pressure.

Primary m/z	27	29	33	39	41	47	57	59	77
Ion Ion	$C_2H_3^+$	$C_2H_5^+$	CH_2F^+	$C_3H_3^+$	$C_3H_5^+$	$C_2H_4F^+$	CHF_2^+	$C_3H_4F^+$	$C_3H_3F_2^+$
CH_3^+	55/24	8/20	-	13/8	11/35	-	-	-	-
CH_2F^+	18/22	13/12	-	6/5	26/39	-	-	11/11	-
CHF_2^+	20/10	23/19	21/11	2/1	4/15	-	-	26/37	0/1
CF_3^+	13/6	1/6	20/11	-	4/16	22/14	19/14	0/4	5/8

TABLE 25: The Low:High Pressure Abundance Ratios for the Major Products in the Reaction of CX_3^+ with Ethene. (% of Total Secondary Ion Signal)

The same reaction sequence can be used to explain the presence of these same ions in the CH_2F^+ initiated system (Table 25). This system additionally contains a second allylic ion ($C_3H_4F^+$, m/z = 59), and both this and $C_3H_5^+$ are thought to be produced in the manner shown in Scheme 11.

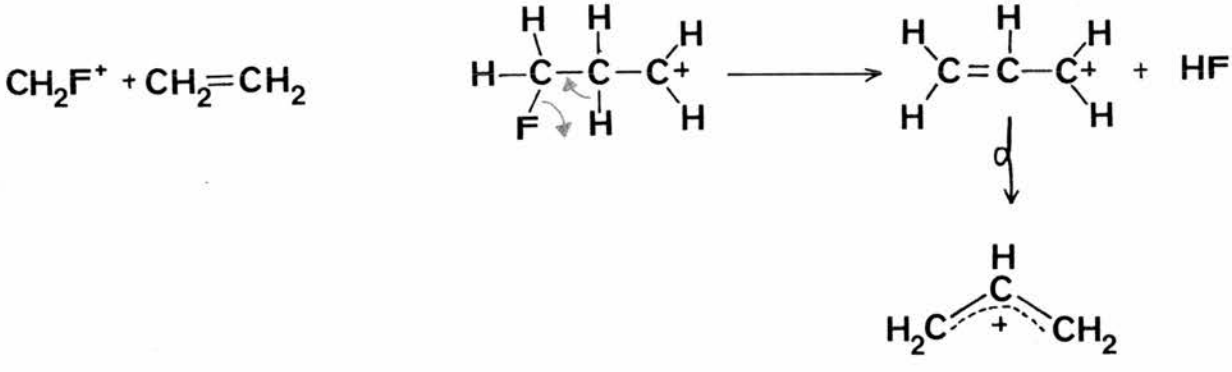

SCHEME 11

When we look at the ion abundances in the CHF_2^+ reaction (Table 25) however, the sequence shown in Scheme 10 no longer holds true. In this case $C_2H_5^+$ is obviously a secondary ion (notice its high abundance at low pressures), involving the co-production of the difluorocarbene species as shown below:-

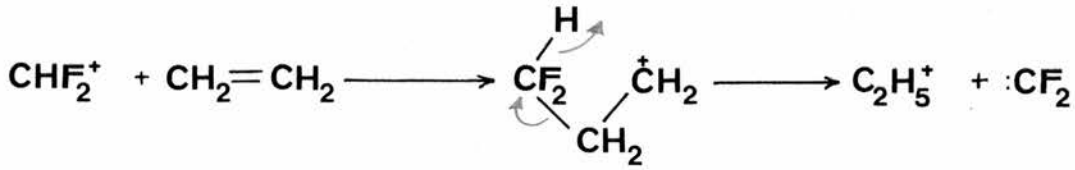

SCHEME 12

The type of elimination reaction shown above is actually observed in all the systems under investigation here (hence $C_2H_5^+$ is also observed as a secondary ion in the two previous systems), but generally $:CF_2$ elimination is favoured over :CHF and $:CH_2$. Keith Stanney's results with the fluoroethenes (Scheme 13) also show that if the collision molecule contains the CF_2 group, this is preferentially eliminated by a "knock-on" process.

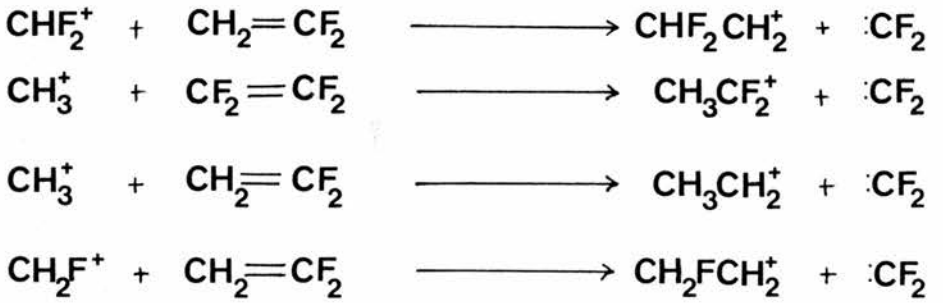

SCHEME 13

The remaining 4 ions in this system are $C_2H_3^+$, $C_3H_5^+$, $C_3H_4F^+$ and CH_2F^+. $C_2H_3^+$ (which is produced as a secondary ion in all these systems) is the result of hydride abstraction by CHF_2^+;

$C_3H_5^+$ is a tertiary ion; $C_3H_4F^+$ is produced by an HF elimination, similar to that in Scheme 11; and CH_2F^+ is the product of the concerted addition - elimination reaction (Scheme 14) involving fluorine transfer. (The closely related hydrogen transfer is

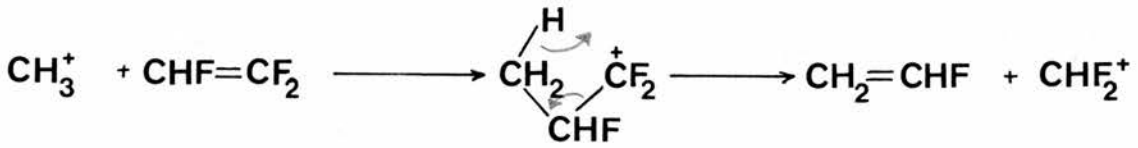

SCHEME 15

observed in the reactions of the fluoroethenes[86], where CHF_2^+ is the predominant ionic product (Scheme 15)).

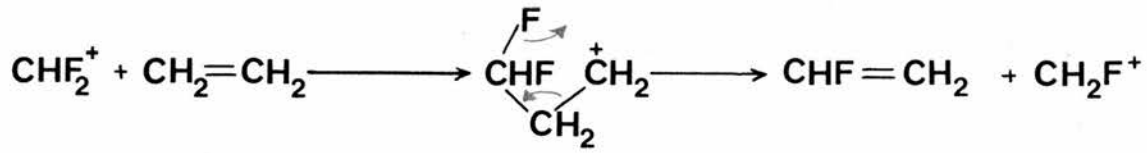

SCHEME 14

The same ions are observed in the reaction of the CF_3^+ cation (Table 25), along with the additional ions at m/z = 47 ($C_2H_4F^+$), m/z = 51 (CHF_2^+) and m/z = 77 ($C_3H_3F_2^+$). $C_2H_4F^+$ is the difluorocarbene elimination similar to Scheme 12; CHF_2^+ is the fluorine transfer reaction like Scheme 14; and $C_3H_3F_2^+$ is a Scheme 11 type HF elimination. We also observe a tertiary ion ($C_3H_4F^+$; m/z = 59) in this case, which arises from the further reaction of the fluorine transfer product, CH_2F^+ (see Scheme 16).

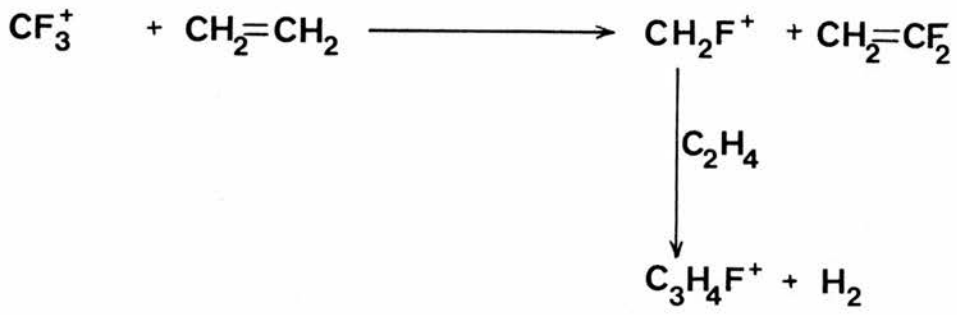

SCHEME 16

The reaction of CH_3^+ with propene (Table 26) produces four main secondary ions as shown in Scheme 17. These include the

m/z	27	29	39	41	42	43	55	56	57	69
ion	$C_2H_3^+$	$C_2H_5^+$	$C_3H_3^+$	$C_3H_5^+$	$C_3H_6^{+\cdot}$	$C_3H_7^+$	$C_4H_7^+$	$C_4H_8^{+\cdot}$	$C_4H_9^+$	$C_5H_9^+$
	21	26	21	67	100	59	39	40	20	26

TABLE 26: The Ions Formed in the Reaction Between CH_3^+ and Propene (Normalised Secondary Ion Signal)

charge exchange product $C_3H_6^{+\cdot}$, and it is this in turn which reacts further with propene to give the tertiary ions ($C_3H_7^+$; $C_4H_7^+$ and $C_5H_9^+$) which predominate at high pressure. (The results for the propene ion-molecule reaction, confirm the derivation of the latter three ions.)

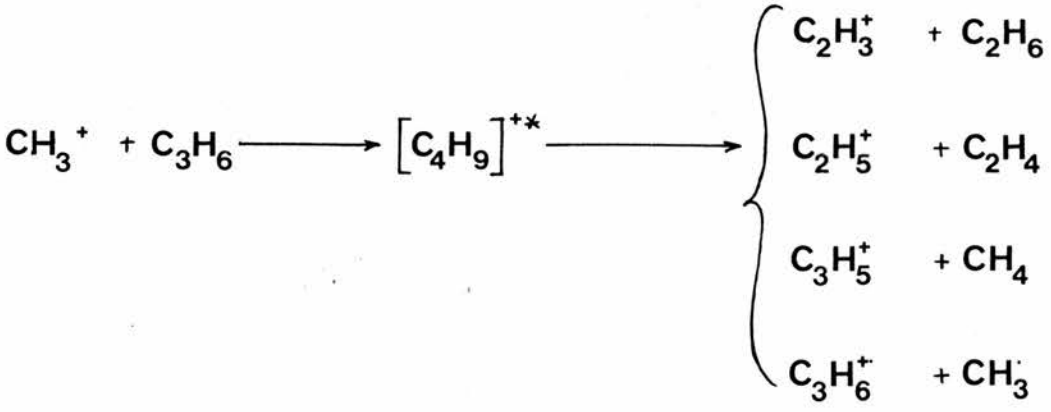

SCHEME 17

When fluoromethyl cations replace the methyl ions in the reaction with propene, we again observe the ions shown in Scheme 17 above, plus in all cases the $C_2H_4F^+$ ion (m/z = 47), which results from the ethene elimination shown in Scheme 18.

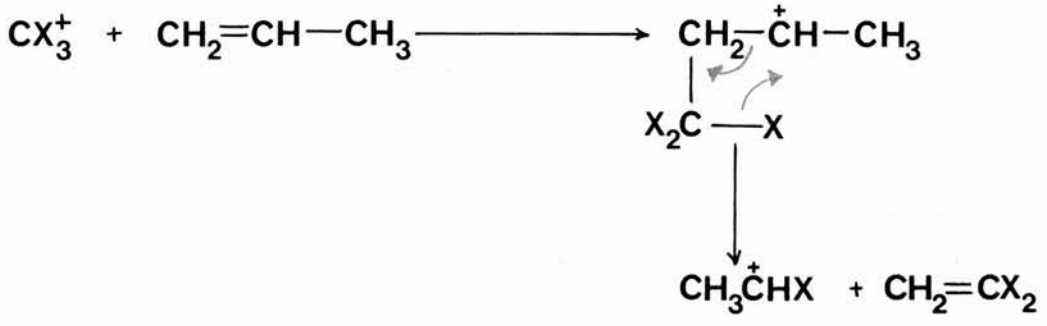

SCHEME 18

The m/z = 43 ($C_3H_7^+$) ion is also observed in these reactions (Table 27); as a secondary product (present at low pressures) with CHF_2^+ - associated with the co-production of difluoro-carbene ($:CF_2$); and as a tertiary product in the case of CF_3^+, where this ion is due to the further reaction of the charge-exchange product.

Primary m/z ion	27	29	33	39	41	42	43	47	51	55	56	57	61	65	69	73
CH_2F^+	17	100	*	5	49	31	53	21	-	24	9	6	-	-	5	-
CHF_2^+	5	22	1	-	36	5	43	100	*	18	1	5	1	15	6	6
CF_3^+	7	4	5	2	33	87	39	100	16	24	24	10	4	5	*	1

TABLE 27: The Ions Produced in the Reaction of CX_3^+ with Propene (Normalised Secondary Ion Signal)

*Primary ion

The CF_3^+/propene reaction also shows similarities with the ethene case, in that we observe H/F transfer reactions, giving rise to CHF_2^+ (m/z = 33) and CH_2F^+ (m/z = 51). This system also produces the $C_3H_3F_2^+$ ion (m/z = 73) which we can envisage as occurring in a manner similar to that in the ethene case (see Scheme 19 - NB. CH_2F^+ and CHF_2^+ preferentially produce $C_3H_5^+$ from this reaction, $C_3H_3F^+$ and $C_3H_3F_2^+$ are not observed).

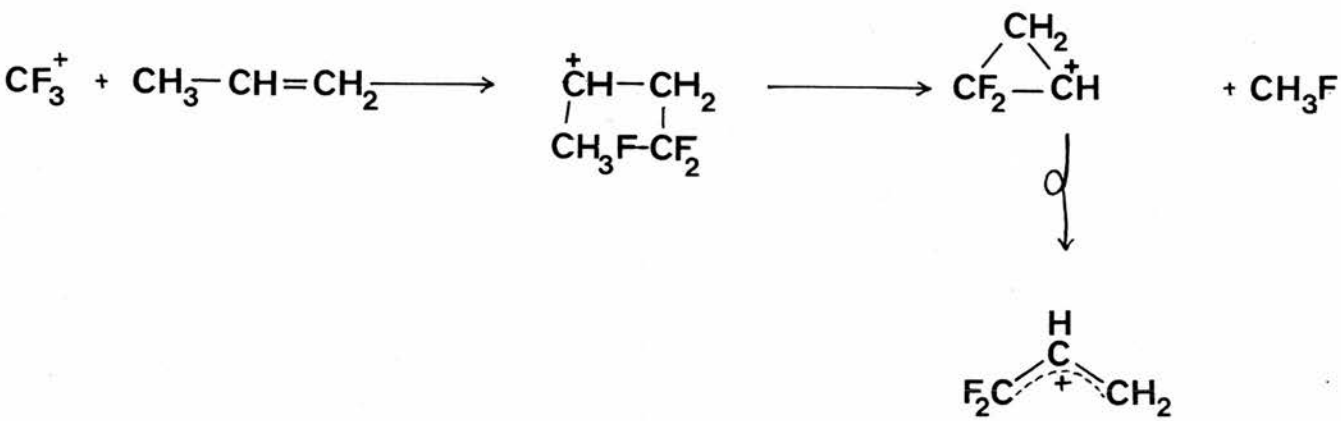

SCHEME 19

The reactions of the methyl cation with the three butene isomers available produce similar products, but in varying abundances depending on the isomer involved (Table 28). The major secondary ions from this reaction are shown in Scheme 20 below.

Collision m/z	27	29	39	41	43	55	56	57	69	70	71	83	84
Gas ion	$C_2H_3^+$	$C_2H_5^+$	$C_3H_3^+$	$C_3H_5^+$	$C_3H_7^+$	$C_4H_7^+$	$C_4H_8^{+\cdot}$	$C_4H_9^+$	$C_5H_9^+$	$C_5H_{10}^{+\cdot}$	$C_5H_{11}^+$	$C_6H_{11}^+$	$C_6H_{12}^{+\cdot}$
but-1-ene	12	30	5	22	8	36	100	22	8	8	5	5	3
cis but-2-ene	16	14	2	10	4	28	100	6	5	-	1	1	-
2 methyl-propene	13	33	5	24	9	35	100	88	8	2	1	1	1

TABLE 28: The Normalised Secondary Ion Spectra Produced in the Reactions of CH_3^+ with the Butenes

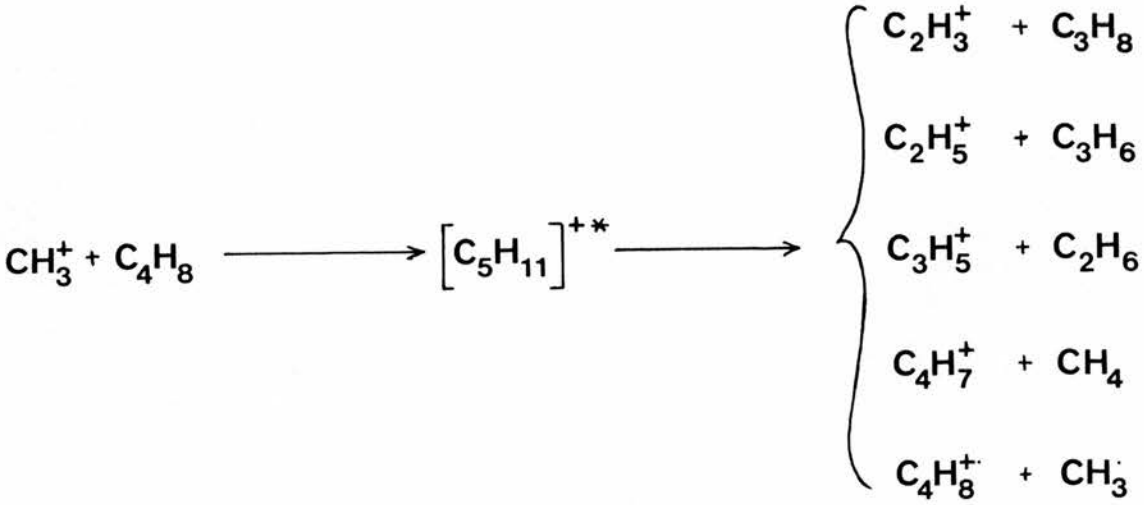

SCHEME 20

Of these ions, the most abundant at low pressures is the charge-exchange product $C_4H_8^{+\cdot}$ (m/z = 56); and like the propene case just discussed, this ion reacts further, producing tertiary ions which complicate the spectra. In particular, there is a build-up of the $C_4H_9^+$ ion (m/z = 57) with pressure in the case of isobutene, which can be directly attributed to the isobutene ion-molecule reaction, below. (This reaction will be discussed fully later

$$i\text{-}C_4H_8^{+\cdot} + i\text{-}C_4H_8 \rightarrow (C_8H_{12})^{*+\cdot} \rightarrow t\text{-}C_4H_9^+ + C_4H_7^{\cdot}$$

in the text.)

The same behaviour is seen with the fluoromethyl cations, where charge-exchange again dominates (Table 29), although CHF_2^+ favours hydride abstration over charge-exchange.

m/z	29	41	43	47	55	56	57	58	61	65	69	77
ion	$C_2H_5^+$	$C_3H_5^+$	$C_3H_7^+$	$C_2H_4F^+$	$C_4H_7^+$	$C_4H_8^+$	$C_4H_9^+$	$C_3H_4F^+$	$C_3H_6F^+$	$C_2H_3F^+$	$C_5H_9^+$	$C_3H_3F_2^+$
But-1-ene												
CH_3^+	30	22	8	-	36	100	22	-	-	-	8	-
CH_2F^+	64	86	43	23	100	60	37	3	4	-	14	-
CHF_2^+	45	71	19	46	100	14	34	56	28	16	18	-
CF_3^+	27	26	6	6	34	100	16	7	10	2	*	7
But-2-ene												
CH_3^+	14	10	4	-	28	100	6	-	-	-	5	-
CH_2F^+	19	18	10	9	36	100	9	1	2	-	7	-
CHF_2^+	40	40	15	57	100	74	27	35	21	23	18	1
CF_3^+	9	4	2	7	12	100	3	2	2	1	*	-
2-methylpropene												
CH_3^+	33	24	9	-	35	100	88	-	-	-	8	-
CH_2F^+	36	51	33	17	63	96	100	2	2	-	16	-
CHF_2^+	42	66	19	40	100	38	96	55	73	14	24	1
CF_3^+	14	18	4	8	21	100	75	7	15	2	*	6

TABLE 29: The Normalised Secondary Ion Spectra Produced in the Reactions of CX_3^+ with the Butenes

The incorporation of fluorine into the secondary ions is widespread, although even when CF_3^+ is the primary ion we do not see any secondary ions which incorporate all three fluorine atom s. This behaviour is not consistent with H/F scrambling, and we can explain many of these ions and their relative abundances by drawing elimination reaction schemes of the type used when we considered the reactions of the fluoromethyl cations with ethene (Schemes 11 - 14).

Using the reactions of CHF_2^+ as an example, we see from Table 30, that a different fluorine-containing ion is favoured by each of the butenes; $C_3H_4F^+$ with but-1-ene; $C_2H_4F^+$ with but-2-ene; and $C_3H_6F^+$ with 2-methylpropene.

m/z	47	59	61	65
ion	$C_2H_4F^+$	$C_3H_4F^+$	$C_3H_6F^+$	$C_2H_3F^+$
but-1-ene	7	10	6	3
cis but-2-ene	10	6	4	4
2-methylpropene	5	8	12	2

TABLE 30: The Relative Abundances for the Fluorine-Containing Ions in the Reactions of CHF_2^+ with the Butenes

This behaviour can be related to the neutral butene structures involved, as shown in reaction Schemes 21, 22 and 23 below; relating to but-1-ene, but-2-ene and isobutene respectively.

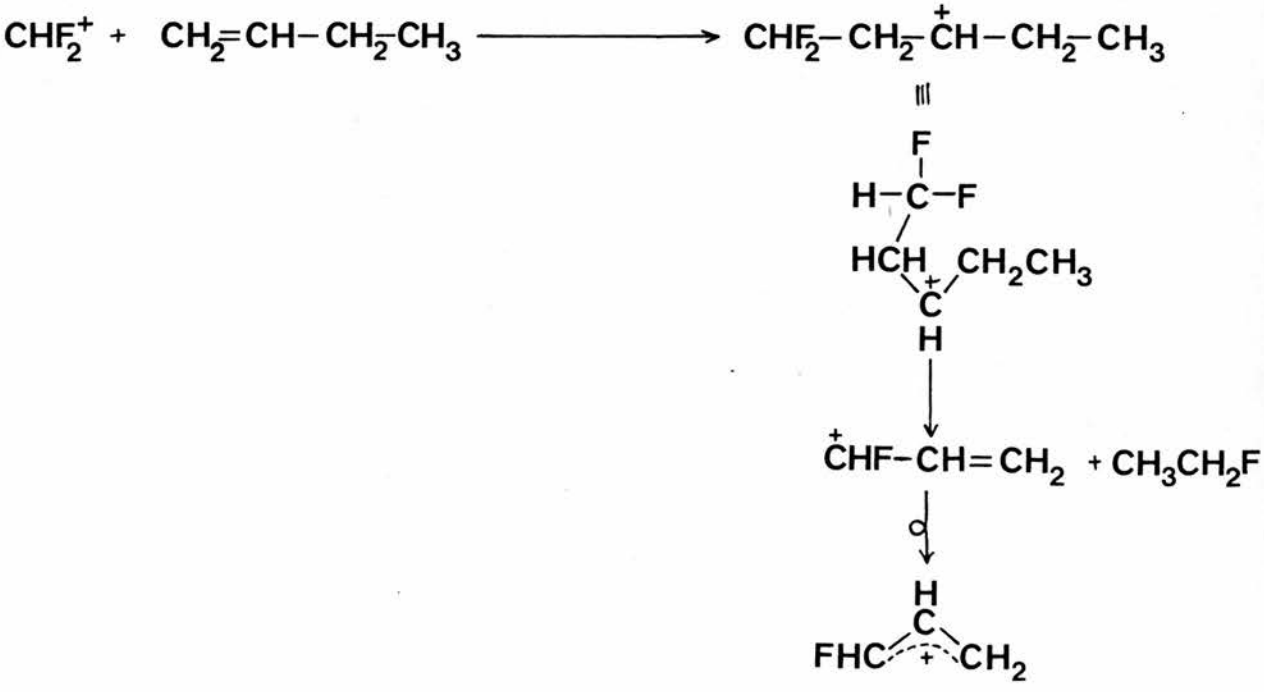

SCHEME 21

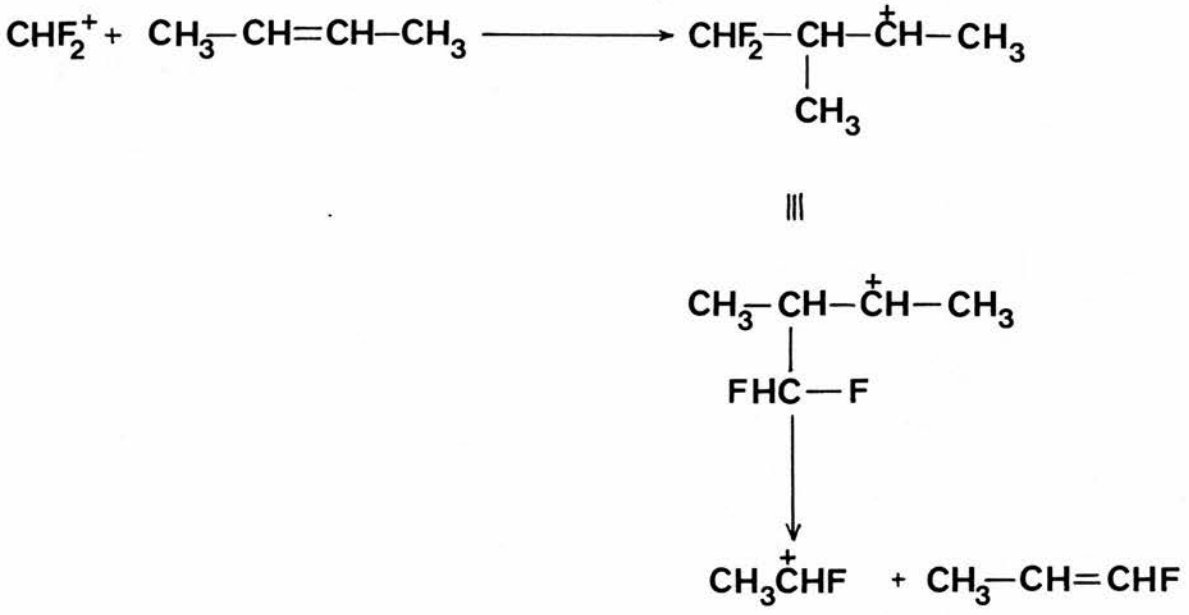

SCHEME 22

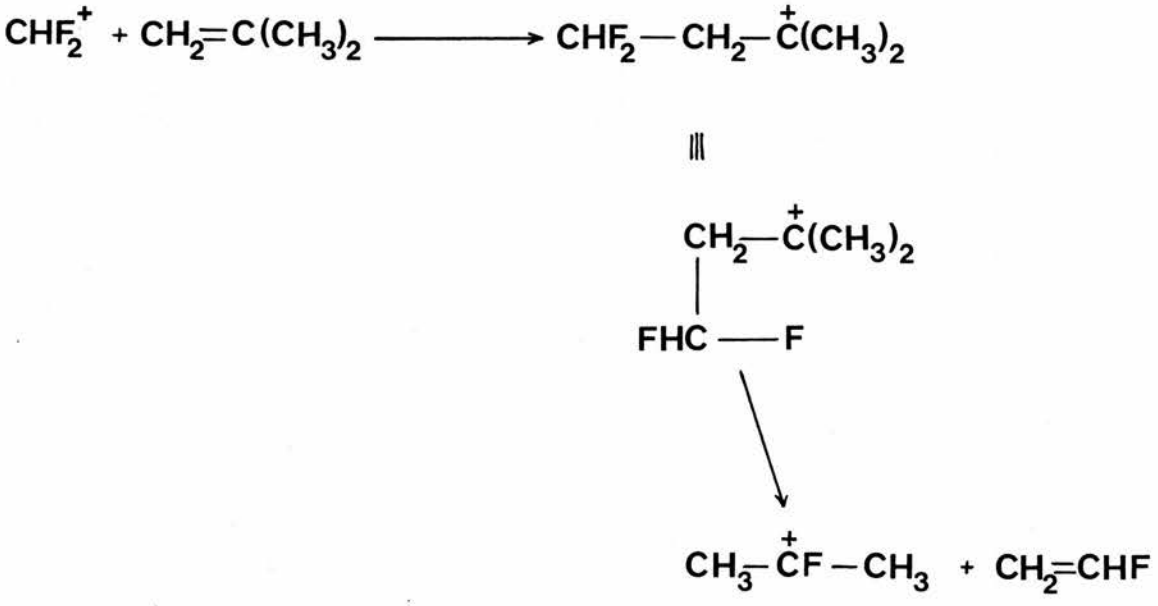

SCHEME 23

The reactions of alkene radical cations (particularly $C_2H_4^{+\cdot}$) have been studied extensively, using a number of different techniques[18,20,22,87]. However, it was felt that a further investigation using the TQMS would be useful - an instrument of this type had never previously been used to study these systems, and it was operated at pressures (10^{-5} - 10^{-3} Torr) between those previously used (>1 Torr[20,22]; 10^{-6} Torr[87]). The TQMS also allowed the crossreaction between one alkene radical cation and a different alkene molecule to be studied very much easier than previously, and also permitted the investigation of individual reaction steps.

The reactions investigated were all studied over a range of secondary reactant pressures. These results are fully tabulated in the "Results" section of this thesis, but where necessary, these are displayed graphically at appropriate points in the text.

The first system to be studied was that of the ethenyl radical cation ($C_2H_4^{+\cdot}$) interacting with ethene. In discussing this system we will concentrate on the variation with pressure. However, the effect of varying the pole bias (collision energy) was also recorded, and Table 31 below shows the behaviour of the major peaks under these conditions.

Bias setting	m/z ion	26 $C_2H_2^{+\cdot}$	27 $C_2H_3^+$	39 $C_3H_3^+$	40 $C_3H_4^{+\cdot}$	41 $C_3H_5^+$	55 $C_4H_5^+$
+1·50		7	10	6	3	100	9
+1·25		10	6	5	2	100	8
+1·00		7	6	4	2	100	8
+0·75		7	3	4	2	100	8
+0·50		9	5	4	2	100	9
+0·25		11	5	5	3	100	11
+0·00		51	17	19	2	100	10
-0·25		100	21	22	2	63	8

TABLE 31: The Effect of Varying Pole Bias on the Major Ions Produced in the Ion-Molecule Reaction (Normalised Secondary Ion Signal)

This behaviour is as we would expect from the preliminary investigations conducted into this parameter (page 15); with minor variations over the range +1·5 to +0·25 units (5·6 to 0·9 eV), and very noticeable changes in the range 0 to -0·4 units. This latter range in fact represents a retarding voltage, and the base peak changes from m/z = 41 to m/z = 26, which shows that the dissociation process (1·1) is enhanced at these very low collision energies.

$$C_2H_4^{+\cdot} \xrightarrow{M} C_2H_2^{+\cdot} + H_2 \qquad 1.1$$

Looking at the ion abundance v pressure plot for the major ions (Figure 7) we can see that the principal reaction between

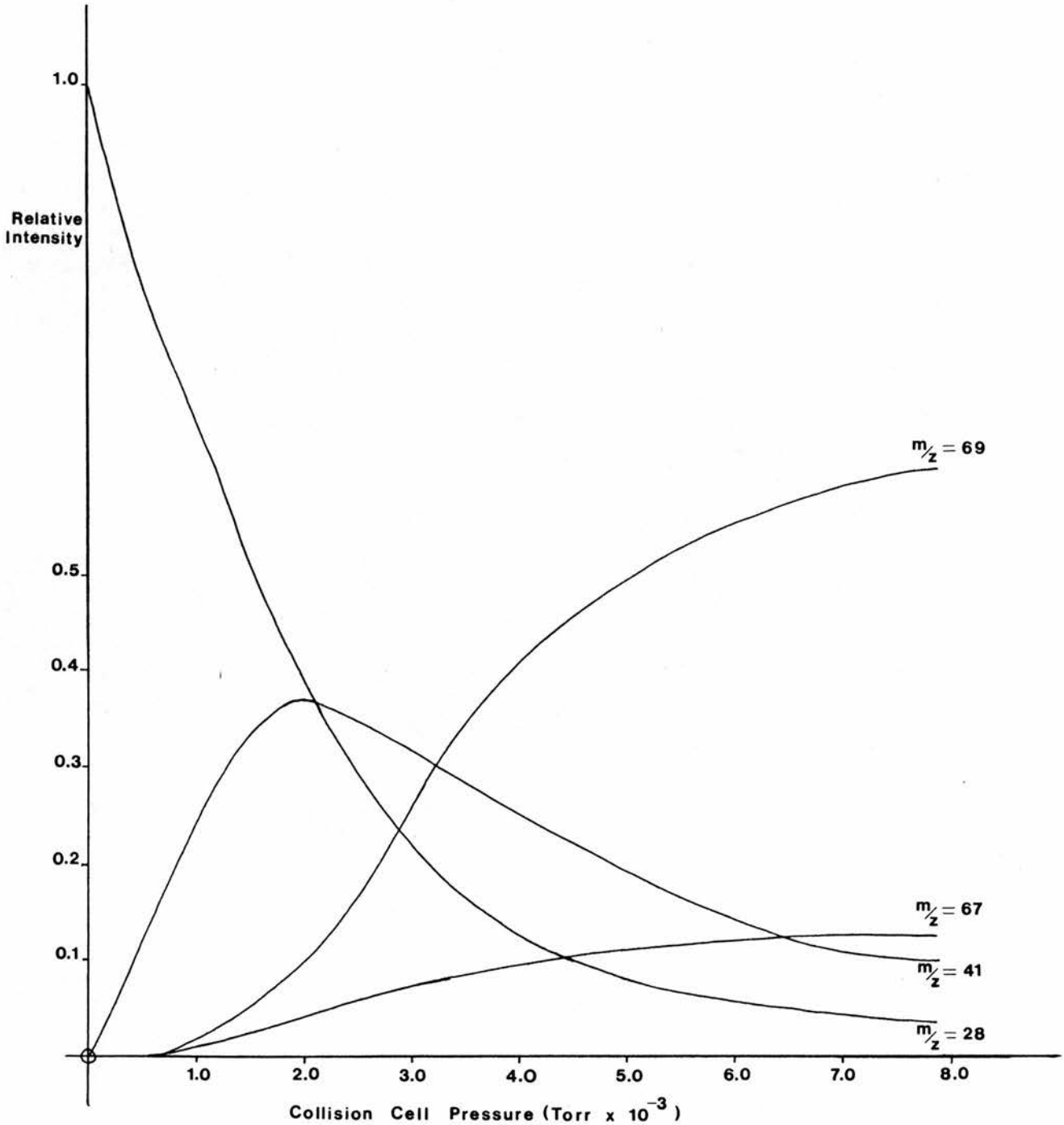

FIGURE 7: The Pressure Variation of the 4 Major Ions in the Ethene Ion-Molecule Reaction

the ethenyl radical cation and ethene is disproportionation of the adduct, to yield allyl cation (m/z = 41) and methyl radical (1·2).

$$C_2H_4^{+\cdot} + C_2H_4 \longrightarrow \left[C_4H_8\right]^{+\cdot *} \longrightarrow C_3H_5^{+} + CH_3^{\cdot} \qquad 1.2$$

As the pressure is increased, this ion reacts with a further molecule of ethene to produce the two major tertiary ions $C_5H_9^+$ (m/z = 69) and $C_5H_7^+$ (M/z = 67) - Scheme 24.

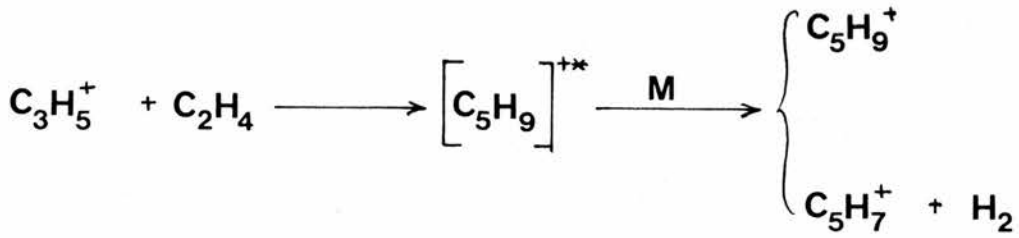

SCHEME 24

Confirmation of this sequence of events was obtained when we studied the reaction of $C_3H_5^+$ (prepared by electron impact on a number of different molecules) with ethene. (Pressure limitations prevented the direct production of this species as a secondary ion in the source.) This reaction produced $C_5H_9^+$ in high yield (Table 32), with lower yields of $C_5H_7^+$. The CAD of $C_5H_9^+$ (Scheme 25) below also indicated that $C_5H_7^+$ was derived from $C_5H_9^+$.

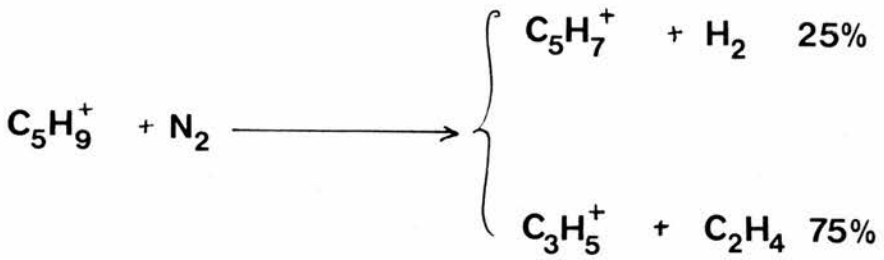

SCHEME 25

This is in agreement with the reaction sequence suggested in the previous studies of this system, and in common with both Tiernan and Futrell[87] and Wesler and Marshall[20] we appear to have an apparent

m/z	29	39	41	43	53	67	69
ion	$C_2H_5^+$	$C_3H_3^+$	$C_3H_5^+$	$C_3H_7^+$	$C_4H_5^+$	$C_3H_7^+$	$C_5H_9^+$
	1	3	38	1	1	8	46

TABLE 32: The Ions Formed in the Reaction Between $C_3H_5^+$ and C_2H_4 (% Total Secondary Ion Signal)

excess of $C_5H_9^+$. Unlike those two studies, we cannot attribute this to the production of $C_2H_4^{+\cdot}$ from a charge transfer reaction between primary ionic $C_2H_2^{+\cdot}$ and neutral ethene, since there is no primary $C_2H_2^{+\cdot}$ present in our investigations. Therefore we must assume that this ion is also produced by one or more higher order processes.

Field[88] attributed the high pressure production of this ion to the reaction sequence shown in Scheme 26.

$$C_2H_4^{+\cdot} + C_2H_4 \longrightarrow [C_4H_8]^{+\cdot *}$$
$$[C_4H_8]^{+\cdot *} + C_2H_4 \longrightarrow [C_6H_{12}]^{+\cdot *}$$
$$[C_6H_{12}]^{+\cdot *} \longrightarrow C_5H_9^+ + CH_3^{\cdot}$$

SCHEME 26

However, our investigations of the reactions of secondary and higher order ions with ethene (using appropriate model precursors) and also CAD data, lead us to believe that this ion and many of the other ions observed in this system result from a number of different precursors, thus making the kinetics and overall reaction dynamics very complex. In our series of confirmatory reactions (Table 33), in every case, the ions $C_3H_5^+$ and $C_5H_9^+$ are observed to be major products. The fact that the ratio of m/z 69:67 increases with pressure also

indicates the main reason for the accumulation of the $C_5H_9^+$ at high pressures - namely increasing collisional stabilization of the $(C_5H_9)^{*+}$ adduct, rather than dissociation (see Scheme 24).

Primary ion	ion $C_2H_2^{+\cdot}$	$C_2H_3^+$	$C_2H_4^{++}$	$C_2H_5^+$	$C_3H_3^+$	$C_3H_5^+$	$C_4H_7^+$	$C_5H_7^+$	$C_5H_9^+$	$C_6H_{11}^+$
$C_2H_2^{+\cdot}$	*	6	31	6	16	100	19	27	91	-
$C_2H_3^+$	-	*	-	98	7	100	4	9	26	-
$C_2H_5^+$	-	14	8	*	3	100	9	17	71	-
$C_3H_3^+$	-	2	4	2	*	100	-	16	79	2
$C_4H_7^+$	-	3	-	100	17	98	*	13	28	86

TABLE 33: The Ions Observed in the Reactions of Various Primary Species with Ethene (Normalised Secondary Signal)

The only other secondary ion formed in appreciable yield is $C_4H_7^+$ (m/z = 55), produced by the loss of a hydrogen atom from $(C_4H_8)^{*\cdot+}$ ie. $C_2H_4^{+\cdot} + C_2H_4 \longrightarrow (C_4H_8)^{*\cdot+} \longrightarrow C_4H_7^+ + H^\cdot$. The corresponding tertiary ion $C_6H_{11}^+$ (m/z = 83) is also observed, a product of the further reaction of $C_4H_7^+$ (see Table 33).

The alternative fate for the two secondary ions is fragmentation and this was studied using the CAD spectra for these ions. The results shown in Scheme 27 below indicate the likely parentage of the ions $C_4H_5^+$ (m/z = 53), $C_3H_3^+$ (m/z = 39) and $C_2H_5^+$ (m/z = 29). These and other minor ions are shown in Figure 8.

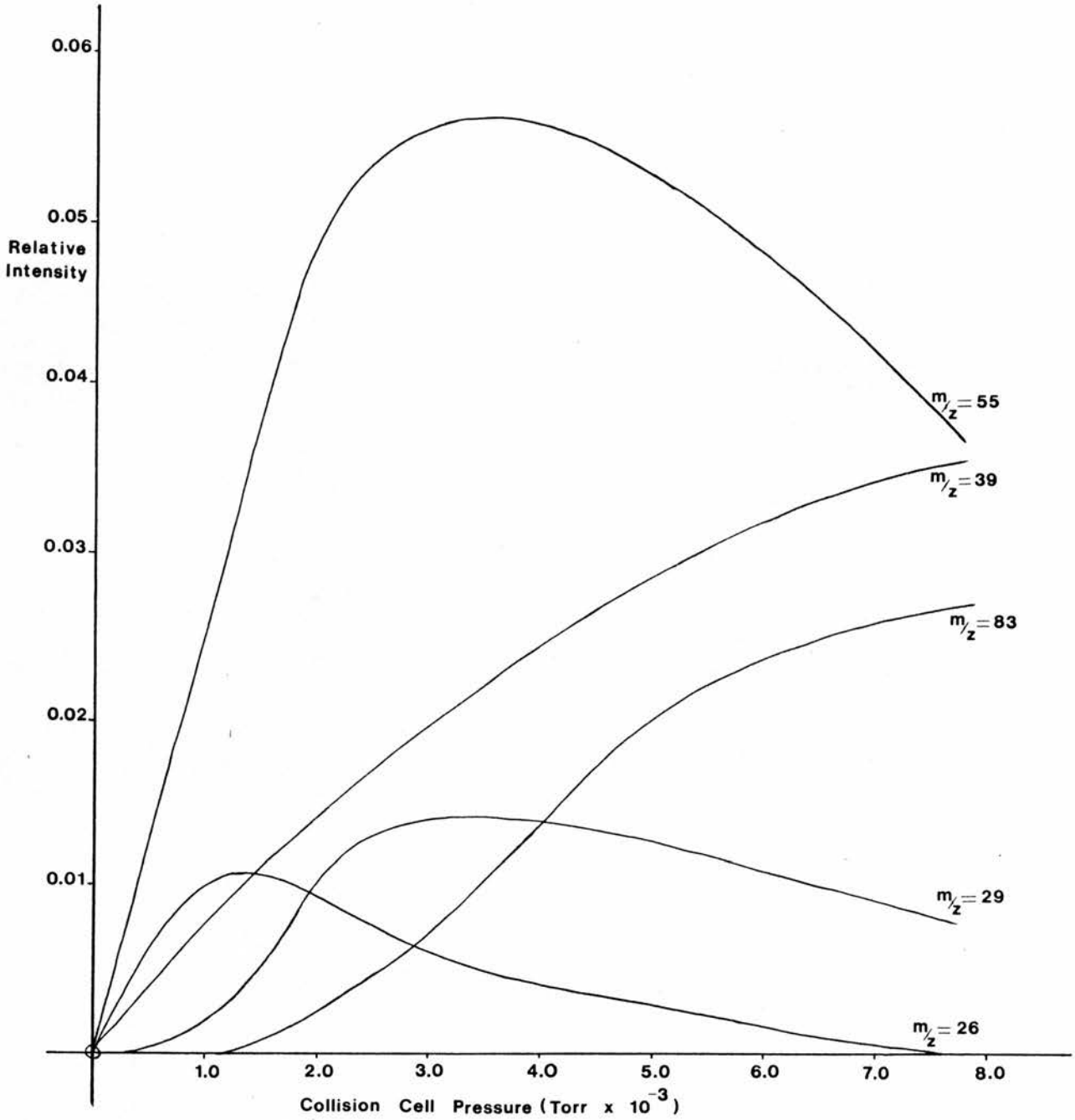

FIGURE 8 The pressure variation of the minor ions in the ethene ion-molecule reaction.

$$C_3H_5^+ + N_2 \longrightarrow C_3H_3^+ + H_2$$

$$C_4H_7^+ + N_2 \longrightarrow \begin{cases} C_4H_5^+ + H_2 \\ C_3H_3^+ + CH_4 \\ C_2H_5^+ + C_2H_2 \end{cases}$$

SCHEME 27

The remaining ions found in this system are of very low concentration and are listed below, along with their likely origin.

$C_2H_2^{+\cdot}$ (m/z = 26) - the appearance of this ion at even the lowest pressure indicates that it is a secondary ion derived directly from $(C_4H_8)^{*\cdot+}$.

$C_2H_3^+$ (m/z = 27 - derived from several sources; $(C_4H_8)^{*\cdot+}$ at low pressures and $C_2H_5^+$ at higher pressures.

$C_3H_4^{+\cdot}$ (m/z = 40) - again derived from $(C_4H_8)^{*\cdot+}$.

$C_4H_6^{+\cdot}$ (m/z = 54) - probably derived from the reaction of $C_2H_2^{+\cdot}$ with C_2H_4.

$C_4H_8^{+\cdot}$ (m/z = 56) - this ion is due to collisional stabilisation of the $(C_4H_8)^{*\cdot+}$ adduct by third body collisions at higher pressures.

$C_7H_{13}^+$ (m/z = 97) - a quaternary ion formed by the reaction of $C_5H_9^+$ with C_2H_4.

We can now draw Scheme 28 (below) which shows the forward interactions occurring in the reaction of ethene radical cation with ethene (many of these steps will be reversible and many minor pathways are not included).

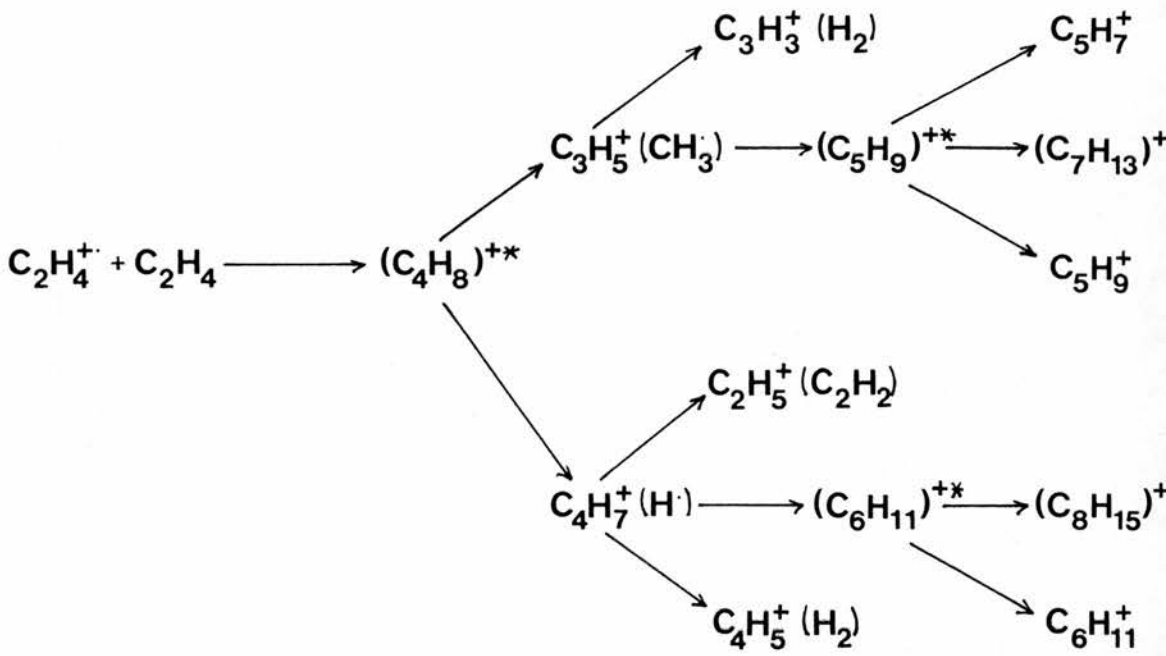

SCHEME 28 The Forward Reaction Sequences in the Ethene Ion-Molecule Reaction

A comparison of our results with three of the previous studies is shown in Table 34, and the results, arranged in order of increasing pressure, show a concordant picture. The only anomaly being the large cross section for m/z = 29 reported by Field[88], which in view of the other reported data, must be an instrumental artefact.

The most interesting feature of the interaction between propenyl radical cations ($C_3H_6^{+\cdot}$) and propene is the occurrence of two distinct reaction sequences; one involving even electron ions and the other involving odd electron ions; contrasting with the previously discussed ethene ion-molecule reaction, where all the major ions were even electron species. Also unlike this system,

	Tiernan & Futrell[87]		Field[88]	Present Work			Wexler[20]
m/z	5×10^{-6}	6×10^{-5}	2×10^{-4}	4×10^{-4}	3×10^{-3}	8×10^{-3}	2×10^{-2}
26	-	-	0.9	4.5	1.1	-	0.1
27	-	-	7.7	1.8	0.6	0.5	0.2
29	2.3	1.9	19.3	-	1.7	0.6	0.7
39	0.6	0.7	4.2	2.8	2.3	3.6	5.2
40	0.9	1.1	1.2	2.2	0.7	0.1	0.1
41	84	80	52	77	49	11	5
53	-	0.2	3.0	0.5	0.8	1.4	3.1
54	0.4	0.4	0.3	0.3	0.5	0.4	0.2
55	10.0	9.4	4.2	7.0	7.4	3.7	2.0
56	0.2	0.5	1.5	0.2	0.2	0.7	6.0
57	-	-	0.2	-	0.1	0.4	5.5
67	-	0.5	0.6	1.5	8.1	12.0	2.8
69	0.1	3.1	2.1	1.8	27	62	60
79	-	-	0.2	-	-	0.3	1.2
81	-	-	0.01	-	-	-	1.3
83	-	-	0.05	-	0.6	2.7	3.4
97	-	-	-	-	-	0.3	1.0

TABLE 34 The Reaction of Ethenyl Radical Cations with Ethene (Expressed as % of Total Secondary Ion Current)

which had only one predominant secondary ion, there are four significant secondary ions here, all formed in roughly equal yield. These ions consist of three even electron species ($C_3H_7^+$, C_4H_7 and $C_5H_9^+$) and one odd electron cation ($C_4H_8^{+\cdot}$) and are the principal ions observed in previous studies of this system. Table 35 compares our results with these previous results.

ion	m/z	Abramason & Futrell[89]	Koyano et al[90]	Harrison (91)	MacKenzie -Peers[92]	Herod & Harrison[93]	Present Work low P.	Work High P	Bowers et al[94]
$C_3H_7^+$	43	27	32	27	26	21	24	23	24
$C_4H_7^+$	55	18	28	21	19	11	20	16	13
$C_4H_8^{+\cdot}$	56	34	24	29	33	42	33	23	43
$C_5H_9^+$	69	21	16	23	22	26	23	39	24

TABLE 35: The Reaction of Propenyl Radical Cations with Propene (Expressed as % of Principal Secondary Ions)

As this table shows, these results are all very similar, considering the many different techniques and pressures involved. The only noticeable differences being the increased yields of $C_4H_8^+$ observed by Herod and Harrison and Bowers et al and our high yield of $C_5H_9^+$ at high pressure. In the former case this seems likely to be due to the different discrimination of the instruments involved and/or the pressures involved; and our high yield of $C_5H_9^+$ is due to increasing collisional stabilisation and a quaternary source of this ion. What is not shown in Table 35 are the significant quantities of tertiary and higher order ions which we observe at elevated pressures.

If we turn our attention to the even electron species first, the three principal secondary ions are shown in Scheme 29 below.

$$C_3H_6^{+\cdot} + C_3H_6 \longrightarrow [C_6H_{12}]^{+\cdot *} \longrightarrow \begin{cases} C_3H_7^+ + C_3H_5^{\cdot} \\ C_4H_7^+ + C_2H_5^{\cdot} \\ C_5H_9^+ + CH_3^{\cdot} \end{cases}$$

SCHEME 29

As the pressure of propene increases, so the yield of the tertiary ion $C_4H_9^+$ (m/z = 57) increases, until at the highest pressures it becomes the major product ion (see pressure v ion abundance plot shown in Figure 9). The precursor to this ion could not be readily determined from Figure 9, and so it was decided to investigate the reactions of each of the secondary ions with propene in isolation, using the "model ion" technique described earlier in the text. From the resultant data (Tables 24, 25 and 28 in the Results section), it was ascertained that at relatively high pressures, $C_4H_9^+$ was the major product in the reaction between $C_3H_7^+$ and propene (1·3), as well as being a significant product in the reactions of $C_4H_7^+$ and $C_4H_8^+$ with propene.

$$C_3H_7^+ + C_3H_6 \longrightarrow C_4H_9^+ + C_2H_4 \qquad 1.3$$

Using the complete series of model reactions for this system, the formation and behaviour of the remaining tertiary ions was elucidated, enabling the reaction sequences (Scheme 30) for the principal forward reactions of the propene ion-molecule reaction to be drawn.

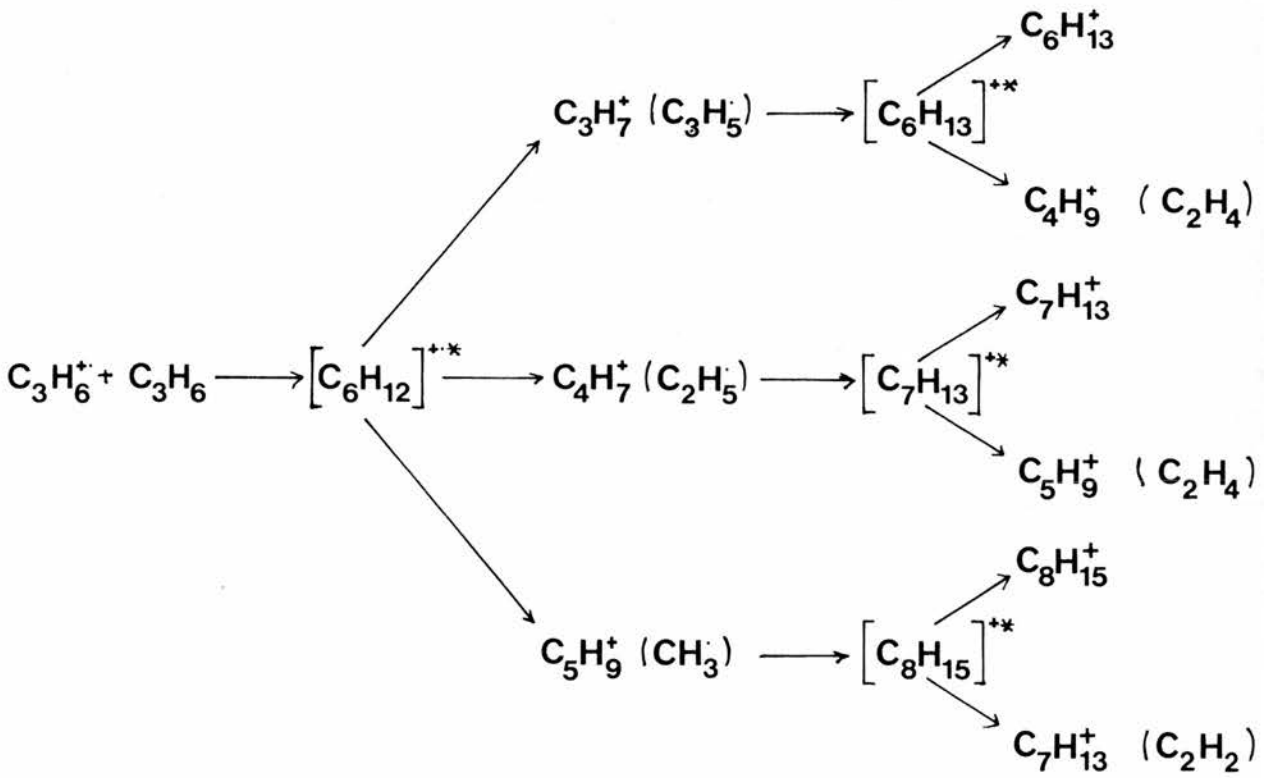

SCHEME 30: The Forward Reaction Sequences of the Even Electron Ions in the Propene Ion-molecule Reaction

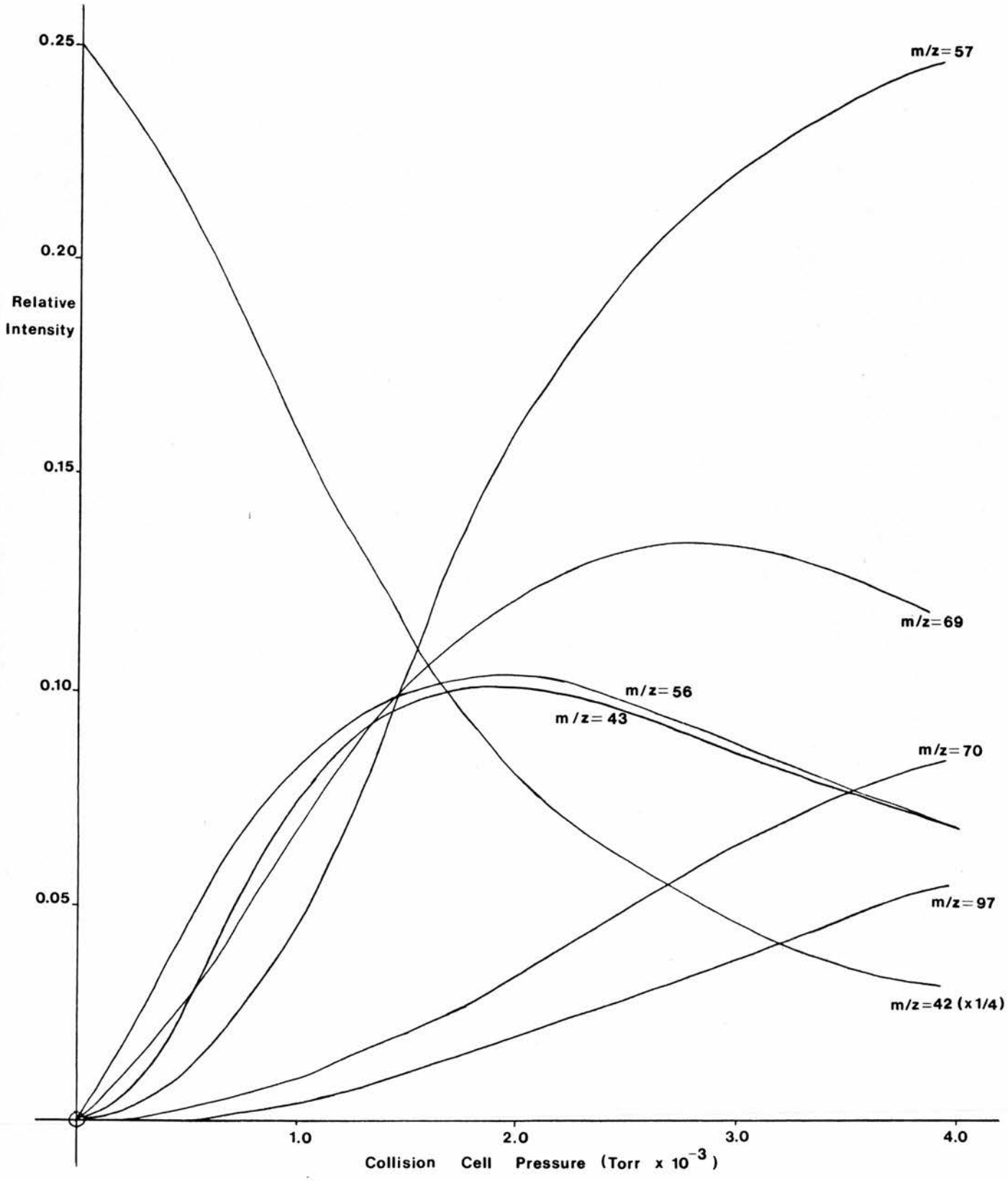

FIGURE 9 The intensity v. pressure plot for the propene ion-molecule reaction.

From this we can see that there are three series of even electron ions; two of the form $C_nH^+_{2n-1}$ ($C_4H_7^+$ and sequence and $C_5H_9^+$ and sequence) producing a number of common ions; and one of the form $C_nH^+_{2n+1}$ ($C_3H_7^+$ and sequence). Compare this with the ethene ion-molecule reaction, where only C_nH_{2n-1} series are observed.

Turning now to the odd-electron sequence; $C_4H_8^{+\cdot}$ is the only significant odd-electron secondary ion, and derived from this is the $C_5H_{10}^{+\cdot}$ ion which is an important tertiary ion. This relationship can be inferred from the relative behaviour of the pressure dependence curves (Figure 9), but the model reaction for $C_4H_8^+/C_3H_6$ was used to confirm this, and in addition showed that $C_4H_9^+$ was also a significant product of this reaction. The higher odd electron homologues in this series ($C_6H_{12}^{+\cdot}$ and $C_7H_{14}^{+\cdot}$) are also seen in small concentrations at higher pressures, but the principal reaction sequence is given in Scheme 31 below.

$$C_3H_6^{+\cdot} + C_3H_6 \longrightarrow \left[C_6H_{12}\right]^{+\cdot *} \longrightarrow C_4H_8^{+\cdot}\ (C_2H_4) \longrightarrow C_5H_{10}^{+\cdot}\ (C_2H_4)$$

SCHEME 31: The Forward Reaction Sequence of the Odd Electron Ions in the Propene Ion-Molecule Reaction

Looking again at Figure 9, the most striking feature of this is the closeness of the curves for $C_3H_7^+$ (m/z = 43) and $C_4H_8^{+\cdot}$ (m/z = 56). We could infer from this that the two ions are derived from a common precursor (see Scheme 32) with roughly equal probability.

$$C_3H_6^{+\cdot} + C_3H_6 \longrightarrow \left[C_6H_{12}\right]^{+\cdot *} \begin{cases} \nearrow\ C_3H_7^+ + C_3H_5 \\ \searrow\ C_4H_8^{+\cdot} + C_2H_4 \end{cases}$$

SCHEME 32:

In order to try and confirm this, a number of further reactions were considered. The model reactions $C_3H_7^+/C_3H_6$ and $C_4H_8^{+\cdot}/C_3H_6$ (see Results section) give little useful evidence, other than that each ion appears in the spectrum of the other. More informative is the reaction between $C_6H_{12}^+$ and C_3H_6 at low pressure (with $C_6H_{12}^{+\cdot}$ derived from trans-3-hexene). The results at higher pressures are complicated by the charge-transfer product reacting with neutral propene, making interpretation of the spectrum difficult. In this case, $C_4H_8^{+\cdot}$ is one of three predominant secondary ions - along with the charge-transfer product ($C_3H_6^{+\cdot}$) and the hydrogen transfer product ($C_6H_{11}^+$) - with $C_3H_7^+$ only occurring as a minor product. A similar result is also observed in the CAD spectra of $C_6H_{12}^{+\cdot}$ ions derived from both cyclic and linear compounds, as shown in Table 36 below.

m/z	42	43	55	56	68	69
Source Molecule ion	$C_3H_6^{+\cdot}$	$C_3H_7^+$	$C_4H_7^+$	$C_4H_8^{+\cdot}$	$C_5H_8^{+\cdot}$	$C_5H_9^+$
cyclohexane	1	1	1	59	5	32
n-decane	4	1	3	61	-	30
trans-3-hexene	-	3	3	64	-	30

TABLE 36: The CAD Spectra of the $C_6H_{12}^{+\cdot}$ Ion Derived from 3 Sources

These results lead us to the conclusion that the coincidence of the pressure dependent curves for $C_3H_7^+$ and $C_4H_8^{+\cdot}$ is just that, and that there is no mechanistic reason for their very similar behaviour.

It has been suggested in previous studies[95,96] of the propene ion-molecule reaction, that the intermediate ion complex $C_6H_{12}^{+\cdot}$ has a linear structure, a conclusion which we agree with; but whether this takes the form suggested by MacKenzie Peers (D) or that favoured by Abramson and Futrell (E) we cannot say.

$CH_3\dot{C}HCH_2CH_2\overset{+}{C}H\,CH_3$ **D**

$CH_3CH_2\dot{C}H\overset{+}{C}HCH_2CH_3$ **E**

We can depict the formation and structures of the major secondary ions as being those shown in Scheme 33.

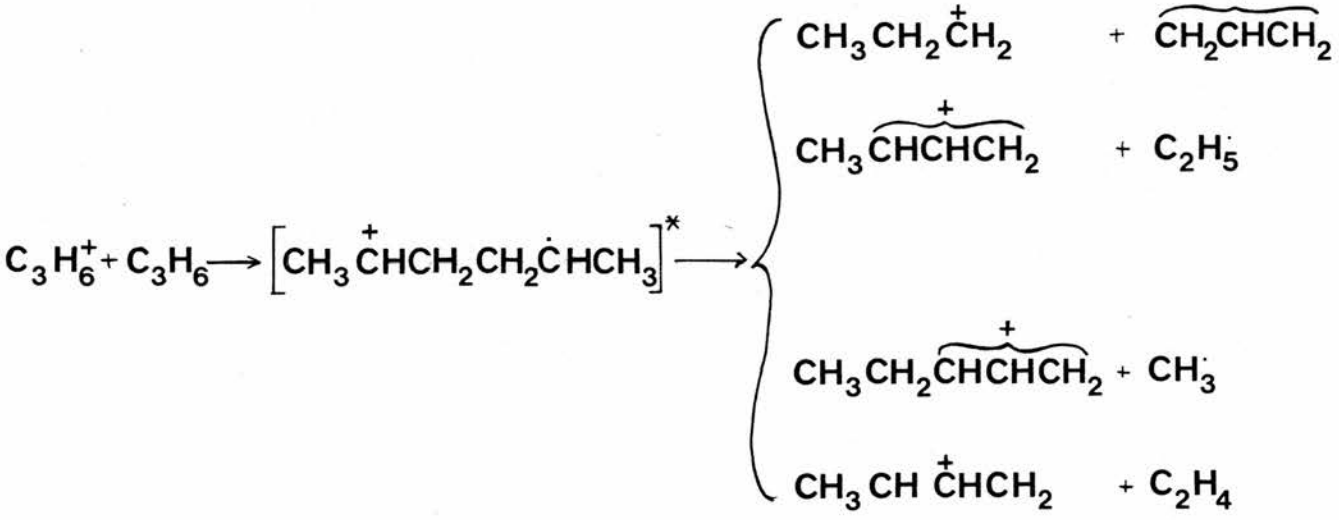

SCHEME 33

When we consider the major tertiary ion $C_4H_9^+$, it seems likely that this ion will have a branched structure; as evinced by its accumulation at higher pressures, which suggests that it is relatively unreactive. (Steric considerations indicating that reactivity decreases with branching.) This ion may be either the 2-methylpropyl cation (F) or more probably the tertiary butyl cation (G), which is known to be highly stable[97,98].

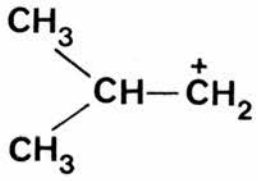

F

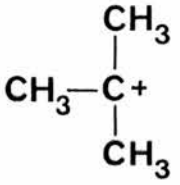

G

The principal product ions from the interaction of the butenyl radical cations with their corresponding butenes are listed in Table 37 below. The most noticeable feature of this table, compared with

m/z	40	41	55	57	69	70	71	82	83	84
Reaction ion	$C_3H_4^+$	$C_3H_5^+$	$C_4H_7^+$	$C_4H_9^+$	$C_5H_9^+$	$C_5H_{10}^{+\cdot}$	$C_5H_{11}^+$	$C_6H_{10}^{+\cdot}$	$C_6H_{11}^+$	$C_6H_{12}^{+\cdot}$
but-1-ene$^{+\cdot}$/ t-1-ene	16	9	35	-	5	19	1	-	8	6
-2-ene$^{+\cdot}$/ -2-ene	29	11	57	-	-	-	-	-	-	-
o butene$^{+\cdot}$/ iso butene	36	15	49	-	-	-	-	-	-	-

TABLE 37: The Ions Formed in the Various Butene Ion-Molecule Reactions at low Pressure (% Total Secondary Ion Signal)

those for the ethene and propene ion-molecule reactions, is that all the product ions can be classed as "fragment" ions (of the transition state $(C_8H_{16})^{*\cdot+}$). There are none of the higher order ions and condensation products observed in those, although these have been shown to exist for the butenes using high pressure photoionisation mass spectrometry[99].

Again, like the propenyl system, there are two distinct types of product ions - one involving even electron ions, the other

odd electron ions. Table 37 also shows that the secondary ions observed are similar for all three butenes (cis and trans isomers of but-2-ene have been previously shown to react in an identical manner[100], although the differences in the relative proportions of these ions appears to indicate that we are dealing with different ionic structures. Table 38 shows the secondary ion proportions at high collision gas pressures, and comparison of this table with the previous table (showing low pressure results) indicates several interesting features.

Reaction ion	$C_3H_5^+$	$C_4H_7^+$	$C_4H_9^+$	$C_5H_9^+$	$C_5H_{10}^{+\cdot}$	$C_5H_{11}^+$	$C_6H_{10}^{+\cdot}$	$C_6H_{11}^+$	$C_6H_{12}^{+\cdot}$
but-1-ene$^{+\cdot}$/ but-1-ene	7	7	16	8	12	17	2	9	10
cis but-2-ene$^{+\cdot}$/ but-2-ene	4	5	8	6	8	5	1	32	25
isobutene$^{+\cdot}$/ isobutene	2	1	87	1	2	5	-	-	-

TABLE 38: The Ions Formed in the Various Butene Ion-Molecule Reaction at High Pressure (% Total Secondary Ion Signal)

At low pressure (in all cases), the principal ions are; $C_3H_4^{+\cdot}$ (m/z = 40); $C_3H_5^+$ (m/z = 41) and $C_4H_7^+$ (m/z = 55); corresponding to the collision induced fragmentation processes shown in Scheme 34.

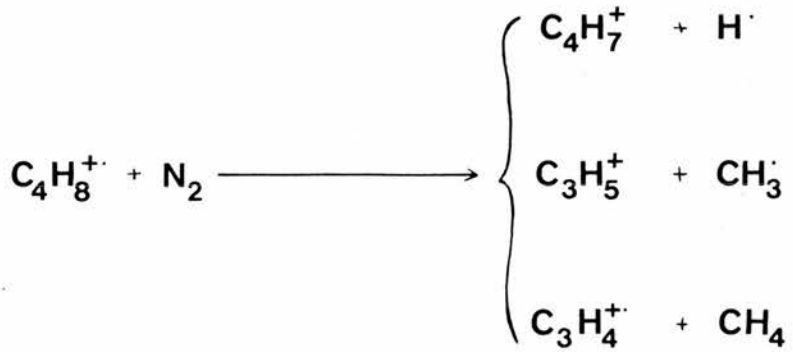

SCHEME 34

However, in the but-1-ene system, it appears as if the above ions are

derived from the activated complex, ($C_8H_{16}^{*\cdot+}$), as shown by the presence of ions containing 5 and 6 carbon atoms.

At higher pressures, one of the principal reactions of all three butenes, is the hydrogen transfer (1·4), but the carbon skeleton of these ions is assumed to vary from butene to butene.

$$C_4H_8^{+\cdot} + C_4H_8 \longrightarrow C_4H_9^+ + C_4H_7^{\cdot} \qquad 1.4$$

With but-1-ene and but-2-ene the butyl cation is likely to be the 2-butyl ion ($CH_3\overset{+}{C}HCH_2CH_3$), but with isobutene (2-methylpropene) the product ion is considered to be the tertiary butyl cation, $(CH_3)_3C^+$; due to the much larger cross-section observed for this ion in the isobutene case. This suggests a highly stable ion, and the high stability of the tertiary butyl cation, due to hyper-conjugation, has been established both experimentally[97] and theoretically[98].

As the collision gas pressure is increased, several other interesting differences between the butenes are observed. With but-1-ene, the principal product ions are $C_4H_9^+$ and $C_5H_{11}^+$. These ions are taken to have a linear structure, arising from the linear transition state shown in Scheme 35. However, at high pressures in cis but-2-ene

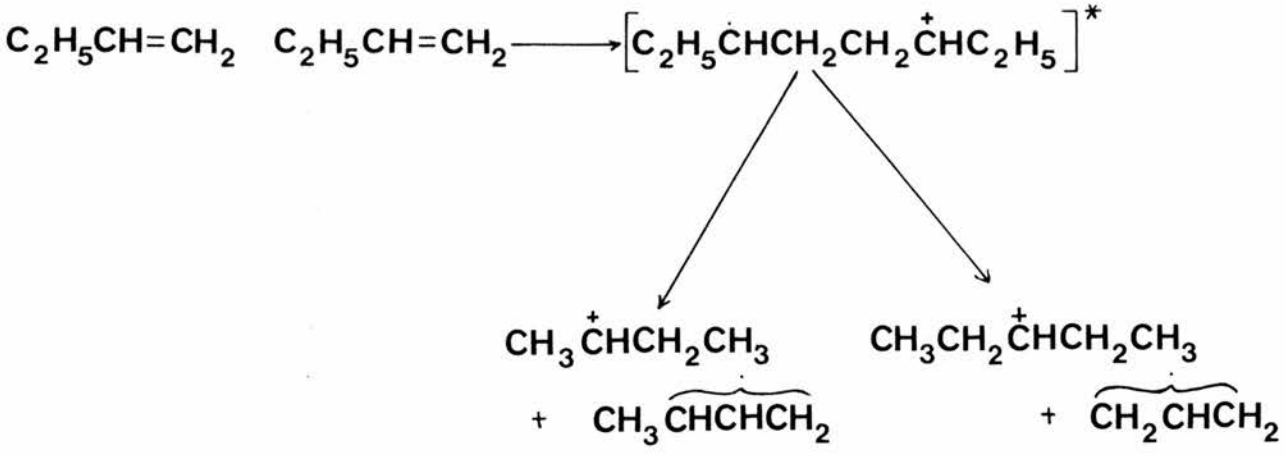

SCHEME 35

the principal ions are $C_6H_{11}^+$ and $C_6H_{12}^+$. This difference we can attribute to steric effects which will prevent the formation of a linear transition state in this latter case. We can therefore depict this reaction occurring as shown in Scheme 36.

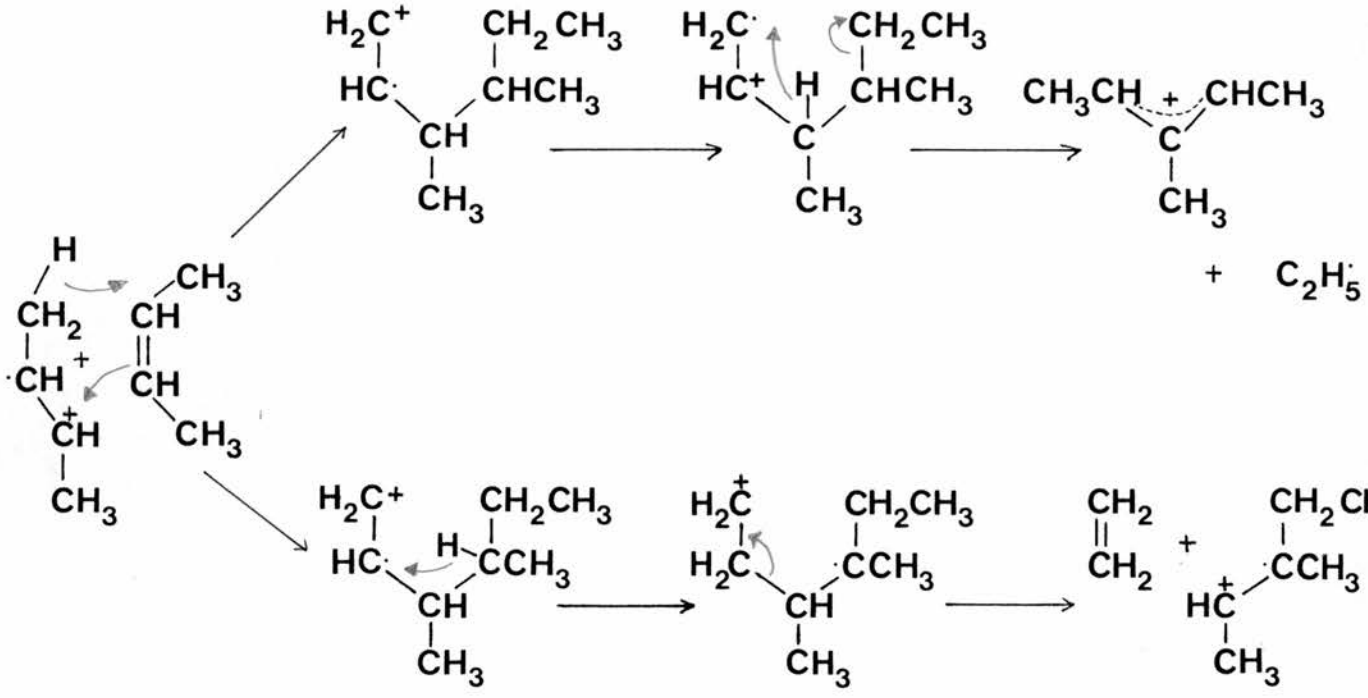

SCHEME 36

The difference between the low and high pressure reactions of but-2-ene (and isobutene) can be attributed to a change in mechanism. At low pressure the major reaction pathway involves collision induced dissociation, whereas at higher pressures the activated complex $(C_8H_{16})^{*\cdot+}$ is formed, which preferentially fragments as shown in Scheme 36. A similar change in mechanism is not observed with but-1-ene, because there is no appreciable steric hind rance in the formation of the linear activated complex.

The reactions between a neutral alkene and a different radical cation can be very easily and effectively studied using a multiple quadrupole mass spectrometer, without the disadvantages of other techniques, such as the need for additional clarifying experiments and the presence of more than one primary ion.

The first of these cross reactions studied, was that between ethenyl radical cations and propene (and the reverse reaction between propene radical cations and ethene), the results for which are shown in Table 39 below; along with the results for the one molecule systems for comparison.

m/z	28	41	42	43	55	56	57	67	69	70	83	111
Reaction ion	$C_2H_4^{+\cdot}$	$C_3H_5^+$	$C_3H_6^{+\cdot}$	$C_3H_7^+$	$C_4H_7^+$	$C_4H_8^{+\cdot}$	$C_4H_9^+$	$C_5H_7^+$	$C_5H_9^+$	$C_5H_{10}^{+\cdot}$	$C_6H_{11}^+$	$C_8H_{15}^+$
$C_2H_4^{+\cdot} + C_2H_4$	P	21	-	-	5	-	-	11	52	-	2	-
$C_3H_6^{+\cdot} + C_2H_4$	-	8	P	-	49	-	-	2	6	12	16	-
$C_2H_4^{+\cdot} + C_3H_6$	P	2	5	9	6	9	29	1	14	8	1	1
$C_3H_6^{+\cdot} + C_3H_6$	-	2	P	8	6	8	28	1	14	10	1	3

TABLE 39: The Ion Formed in the Interactions of Ethene Radical Cations and Propene Radical Cations, with Both Ethene and Propene. (% Total Secondary Ion Signal)

The most noticeable feature of this table is the close similarity between the results for the ethenyl cation/propene and propenyl cation/propene systems, especially at higher pressures. This is due to the principal reaction in the former system being charge exchange, followed by the further reaction of this charge exchange product ($C_3H_6^{+\cdot}$) with propene, a reaction we can depict as shown in Scheme 37.

$$C_2H_4^{+\cdot} + C_3H_6 \longrightarrow C_3H_6^{+\cdot} + C_2H_4 \xrightarrow{C_3H_6} \left[C_6H_{12}\right]^{+\cdot *} \longrightarrow \begin{cases} C_3H_7^+ + C_3H_5^\cdot \\ C_4H_7^+ + C_2H_5^\cdot \\ C_5H_9^+ + CH_3^\cdot \end{cases} \text{ et seq.}$$

SCHEME 37

This behaviour, and that for the second cross reaction, is as expected when considering the relative ionisation potentials of the two radical cations involved ($C_2H_4^{+\cdot}$ = 10·51 eV; $C_3H_6^{+\cdot}$ = 9·73 eV); when the impacting ion has the higher IP it undergoes charge exchange; whereas, when the situation is reversed, an activated complex is formed, which then fragments in a unique way. This latter behaviour is displayed by the propenyl cation/ethene system which produces a spectrum unlike that observed in either the ethenyl cation/ethene or propenyl cation/propene systems. In this case the major reaction sequence is shown below (Scheme 38).

$$C_3H_6^+ + C_2H_4 \longrightarrow \left[C_5H_{10}\right]^{+\cdot *} \longrightarrow C_4H_7^+ + CH_3^\cdot \xrightarrow{C_2H_4} C_6H_{11}^+$$

SCHEME 38

Table 40, shows that the principal reaction of the ethenyl cation with each of the three butene isomers used (as expected), is simply charge exchange (based on IP's for ethene of 10·51 eV; and

for butene (averaged) of 9·31 eV). Each isomer showing the individual behaviour typical of its individual ion-molecule reaction - namely; high yields of $C_6H_{11}^+/C_6H_{12}^{+\cdot}$ in but-2-ene and the large cross-section for $C_4H_9^+$ in 2-methylpropene.

m/z	41	43	55	56	57	67	69	70	71	82	83	84
Reaction ion	$C_3H_5^+$	$C_3H_7^+$	$C_4H_7^+$	$C_4H_8^{+\cdot}$	$C_4H_9^+$	$C_5H_7^+$	$C_5H_9^+$	$C_5H_{10}^{+\cdot}$	$C_5H_{11}^+$	$C_6H_{10}^{+\cdot}$	$C_6H_{11}^+$	$C_6H_{12}^{+\cdot}$
$C_2H_4^{+\cdot}$/ but-1-ene	5	2	9	41	11	1	6	6	7	2	6	4
$C_2H_4^{+\cdot}$/cis but-2-ene	1	1	2	38	10	1	5	3	3	1	18	16
$C_2H_4^{+\cdot}$/2-methyl-propene	2	1	2	8	76	-	2	2	5	1	1	1
but-1-ene$^{+\cdot}$/ ethene	18	4	20	P	-	6	29	4	2	-	9	5
cis but-2-ene$^{+\cdot}$/ ethene	14	1	10	P	-	10	34	1	1	-	3	18
2-methyl-propene$^{+\cdot}$/ ethene	39	4	18	P	-	9	19	2	-	-	-	9

TABLE 40: The Ions Observed in the Cross Reactions Between Ethenyl Cations and Butenyl Cations and the Butenes and Ethene Respectively (% Total Secondary Ion Signal)

The reactions of the three butenyl cations with ethene (Table 40) all show similar behaviour, although the proportions of the products vary from butene to butene. Rather like the individual butene ion-molecule reactions, the principal ions in this case are all fragments derived from the transition complex, $(C_6H_{12})^{*\cdot+}$, as shown in Scheme 39.

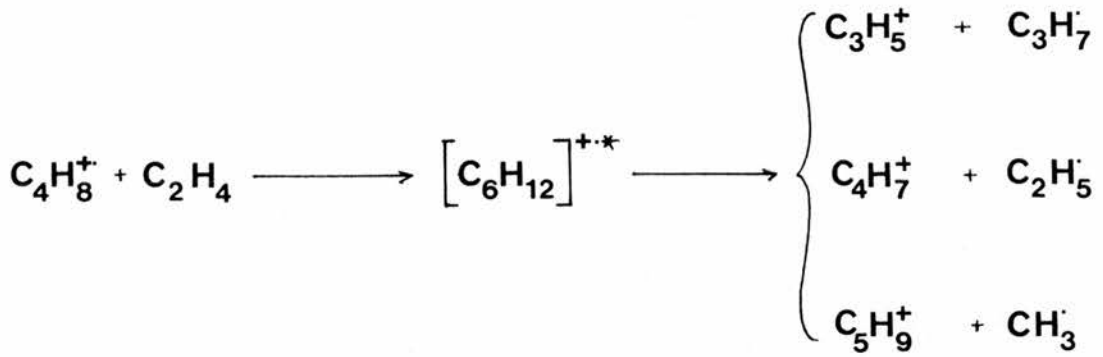

SCHEME 39

The interesting feature of Scheme 39, is the fact that in every case the radical coproduced is an alkyl, with each of the cations potentially having an allylic structure. When we consider the relative proportions of these (and other) ions, the differences observed suggest that like the individual butene ion-molecule reactions, the transition complexes involved retain the structural differences of the primary ions. These variations (See Table 40) may be discussed using simple probability/bond scission arguments; however this may be complicated by the three principal secondary ions reacting further with ethene. In particular, we have already shown the important relationship between $C_3H_5^+$ and $C_5H_9^+$ in an atmosphere of ethene.

In the but-1-enyl cation case, we expect a linear transition complex which will fragment at a number of positions giving the observed spectrum (where losses of methyl, ethyl and propyl radicals are comparable; ie. at m/z = 69, 55 and 41 respectively). However, for both but-2-ene and 2-methylpropene, the transition complexes will be branched, which we would expect to give enhanced fragmentation at the branching point(s). This appears to be the case with but-2-enyl cations, where methyl elimination is slightly enhanced (m/z = 69). We also see an enhancement of the ion at m/z = 41 with 2-methylpropene, again indicative of bond scission at the branching point (ie. between $C_2$and

C_3, assuming the transition complex to have the structure $(CH_3)_2\dot{C}H\overset{+}{C}HCH_3$). There is also an increase in the abundance of the adduct radical cation ($C_6H_{12}^{+\cdot}$) in these cases, which again may be indicative of structural differences between the $(C_6H_{12})^{*\cdot+}$ ions.

The final systems studied in this section involve the cross reactions between the three isomeric forms of butene available. This follows on from the results obtained above, which appear to indicate that the neutral structure of a molecule is retained on ionisation. Table 41 shows the secondary ion yields for the four systems studied, along with the ion-molecule spectra for the three isomers for comparison.

m/z	41	55	56	57	69	70	71	83	84	85	97
Reaction ion	$C_3H_5^+$	$C_4H_7^+$	$C_4H_8^+$	$C_4H_9^+$	$C_5H_9^+$	$C_5H_{10}^+$	$C_5H_{11}^+$	$C_6H_{11}^+$	$C_6H_{12}^+$	$C_6H_{13}^+$	$C_7H_{13}^+$
but-1-ene$^{+\cdot}$/ but-2-ene	3	4	P	8	5	8	5	31	29	-	-
but-2-ene$^{+\cdot}$/ but-1-ene	3	4	P	14	6	12	18	10	13	3	5
2-methyl-propene$^{+\cdot}$/ but-1-ene	5	6	P	40	6	10	17	4	6	2	1
2-methyl-propene$^{+\cdot}$/ but-2-ene	5	5	P	31	5	7	8	20	18	-	-
but-1-ene$^{+\cdot}$/ but-1-ene	7	8	P	16	8	12	17	9	10	1	3
but-2-ene$^{+\cdot}$/ but-2-ene	4	5	P	8	6	8	5	32	25	-	-
2-methyl-propene$^{+\cdot}$/ 2-methyl-propene	2	1	P	87	1	2	5	-	-	-	-

TABLE 41: The Total Secondary Ion Spectra for the Cross Reactions Between the Various C_4H_8 Isomers

These results appear to show that under the conditions used in these experiments, the primary ions do indeed retain the structures of their neutral precursors; and furthermore they also show that both primary ion and collision gas structures have an influence on the resultant spectra.

Taking the reactions between isobutene radical cations and both but-1-ene and cis but-2-ene first, we see the clear influence of both factors. In both cases there is considerable enhancement of the signal at m/z = 57. This is indic ative of the isobutane primary ion, which favours the abstraction of a hydrogen atom from the neutral molecule. Also, we have the enhancement of m/z = 71, (which is typical of the but-1-ene ion-molecule reaction) when we use but-1-ene collision gas; and in the cis but-2-ene case, the signals at both m/z = 83 and 84 are increased (typical of the cis but-2-ene ion-molecule reaction). The other two isomeric cross reactions again show the influence that this latter factor has on the ion-molecule spectra, but the retention of primary ionic structure is less obvious. The only ions showing any indication of this being those at m/z = 83 and 84 in the but-2-ene radical cation/but-1-ene system, which have slightly increased abundances compared with the but-1-ene ion-molecule reaction.

We cannot draw any definite conclusions regarding the retention of structure using 70 eV electrons from the above results. Indeed, the influence attributed to the collision molecule's structure could be due to charge exchange; the extent of which could not be determined since both primary ion and collision molecule were of identical mass. These results were encouraging however, and several other isomeric systems were also studied to this end. (These results will be discussed on subsequent pages). The use of reactive collisions as a means of determining ionic

structures was also investigated by Dr Jorma Jalonen[101], a visiting post-doctoral worker from the University of Turku, Finland, using our TQMS instrument.

Our attention then turned to substituted ethenes, and how the presence of the substitutent(s) would alter the spectra compared with that for the unsubstituted ethene ion-molecule reaction. Also in the absence of both ^{2}H and ^{13}C labelling, we were hoping for some mechanistic clues about the formation/breakdown of the reaction complexes involved.

The compounds chosen for this series of reactions were the fluorinated ethenes. These were considered to be appropriate molecules for a number of reasons; four of the five possible molecules were readily available in the lab; we had already investigated the unsubstituted case; the molecules involved were relatively simple, minimising the chance of over complex reaction pathways; and in the expectation that the electronegativity of the fluorine substituents would create the largest possible effect.

The first molecule to be studied was vinyl fluoride; the reactions of its radical cation with both itself and ethene, and also the reverse reaction between the ethene radical cation and vinyl fluoride are discussed below.

m/z	28	41	46	47	54	55	59	67	69	72	77	85
reaction ion	$C_2H_4^{+\cdot}$	$C_3H_5^+$	$C_2H_3F^{+\cdot}$	$C_2H_4F^+$	$C_4H_6^+$	$C_4H_7^+$	$C_3H_4F^+$	$C_5H_7^+$	$C_5H_9^+$	$C_4H_5F^+$	$C_3H_3F_2^+$	$C_5H_6F^+$
vinyl fluoride$^{+\cdot}$ / vinyl fluoride	-	2	P	-	-	-	6	19	-	3	60	6
vinyl fluoride$^{+\cdot}$ / ethene	P	2	19	3	1	-	7	11	-	1	39	4
ethene$^{+\cdot}$ / vinyl fluoride	2	25	P	-	3	5	11	15	24	-	-	-

TABLE 42: The Ions Produced in the Vinyl Fluoride Ion-Molecule Reaction and the Cross Reactions Between Vinyl Fluoride and Ethene (% Total Secondary Ion Current) @ ca. 3×10^{-3} Torr

In the vinyl fluoride ion-molecule reactions, the initial reactions (at low pressure) involve the elimination of HF neutral and H· transfer, as shown in Scheme 40.

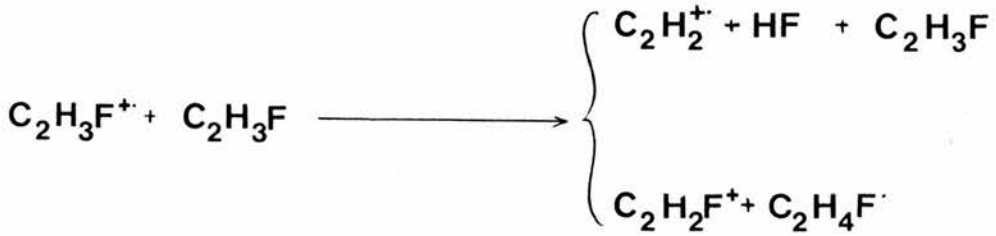

SCHEME 40

As we increase the pressure of collision gas, the above two products importance rapidly diminishes, until at high pressures we observe the products shown in Table 42. The most important series of molecules observed is that of the three possible allylic cations, at m/z = 41, 59 and 77, each associated with the co-production of a methyl or fluoromethyl radical (Scheme 41).

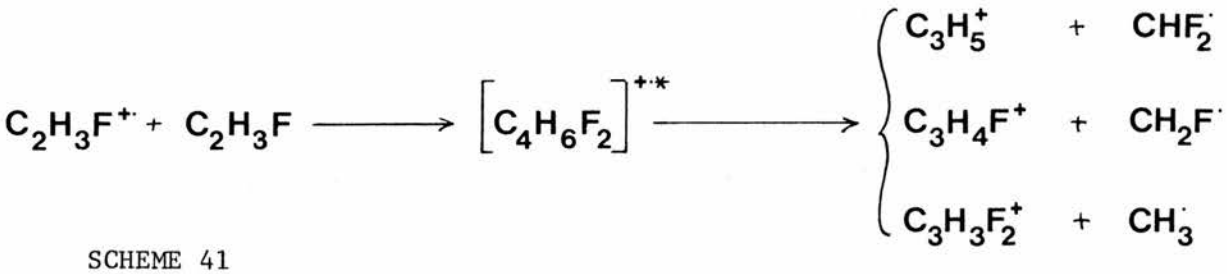

SCHEME 41

This is anal gous t the ethene ion-molecule reaction, where the major secondary ion is $C_3H_5^+$, but unlike that system there appears to be no further reaction producing a tertiary analogue for the $C_5H_9^+$ ion. Rather, one or more of the secondary ions reacts with a further molecule of vinyl fluoride, again eliminating a methyl or fluoromethyl radical. From the appearance of the reaction plot for this system (See Figure 10), it seems probable that the principal tertiary reaction is (1·5), although we cannot rule out there being a contribution from

the other secondary ions, or perhaps the elimination of HF from the initial reaction complex (ie $(C_4H_6F_2)^{*\cdot+} \rightarrow C_4H_5F^{+\cdot} + HF$).

$$C_3H_4F^+ + C_2H_3F \longrightarrow C_4H_5F^{+\cdot} + CH_2F^{\cdot} \qquad 1.5$$

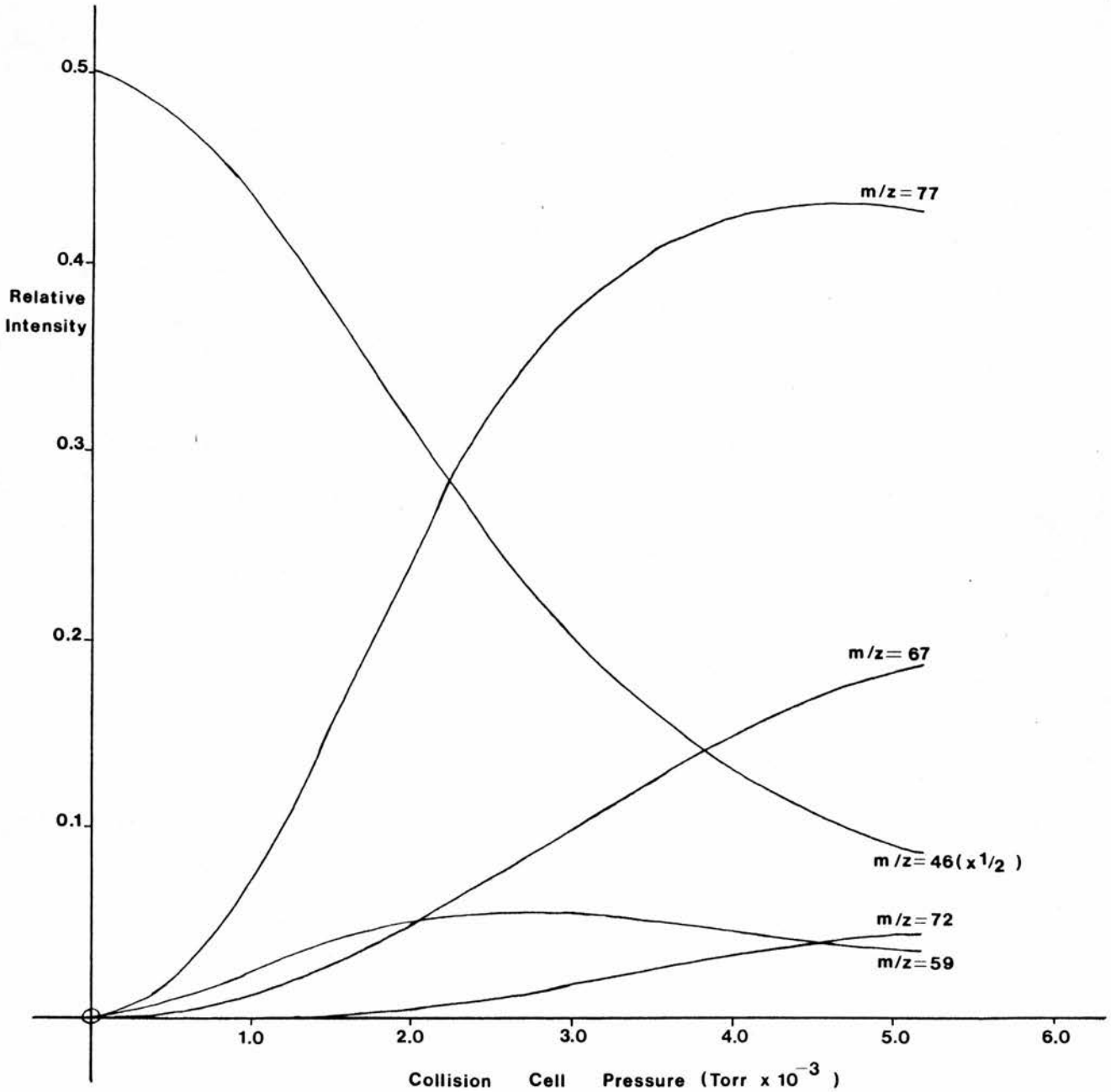

FIGURE 10: The Major Secondary Ions Observed in the Vinyl Fluoride Ion Molecule Reaction

At the higher pressures where the above tertiary ion and others are observed, we also come across a major complication in the

presence of an anomalous ion at m/z = 67, which occurs in increasingly large proportions. This ion, which can only be $C_5H_7^+$, could be construed as arising from the further reaction of $C_3H_5^+$ (m/z = 41) with vinyl fluoride - similar to the production of $C_5H_7^+$ in the ethene ion-molecule reaction - co-producing HF. However, this supposition can be rejected, due to the presence of m/z = 67 at low-to-intermediate pressures, when the concentration of the $C_3H_5^+$ precursor is itself very low. With no other feasible explanation for this ion, it was clear that it could only be due to a contaminant; and after consulting the literature[102] the probable source of this was identified as a terpene polymerisation inhibitor (eg δ-limonene), used in commercial supplies of vinyl fluoride. Unfortunately, when an attempt was made to re-run this experiment with the inhibitor filtered out, the cylinder was found to be virtually empty (hence the apparent high concentration of inhibitor in the available spectra). Even more unfortunate was the subsequent discovery that vinyl fluoride was no longer commercially available in this country. Several methods for producing this compound were found in the literature[103,104,105], but as these involved the reaction of acetylene and hydrogen fluoride (and in one case above atmospheric pressure), it was thought inappropriate to attempt this synthesis in the lab.

A further complication arising from the presence of this inhibitor, is the question of the origin of the one remaining major ion observed in the vinyl fluoride ion-molecule reaction - that at m/z = 85 ($C_5H_6F^+$). There are several routes by which this could be produced from the observed secondary ions, all of which involve the co-production of a diatomic species (ie F_2, HF or H_2), and it seems

much more likely that this ion is derived from the $C_5H_7^+$ "alien" via reaction (1·6).

$$C_5H_7^+ + C_2H_3F \longrightarrow C_5H_6F^+ + C_2H_4 \qquad 1.6$$

The presence of the inhibitor also affects the results when ethene radical cation is reated with vinyl fluoride. In this case the only reaction observed is charge exchange (Table 42), followed by the previously discussed vinyl fluoride ion-molecule reaction (including the two extraneous peaks noted above).

No such problems were encountered when vinyl fluoride radical cation was reacted with ethene, which resulted predominantly in charge-exchange (Table 42). Thus as the pressure is increased we see the by now familiar ethene ion-molecule reaction spectrum (ie m/z = 28 → m/z = 41 → m/z = 67,69). However, we also observe reaction between the two species, producing a three carbon ion and a methyl radical (Scheme 42).

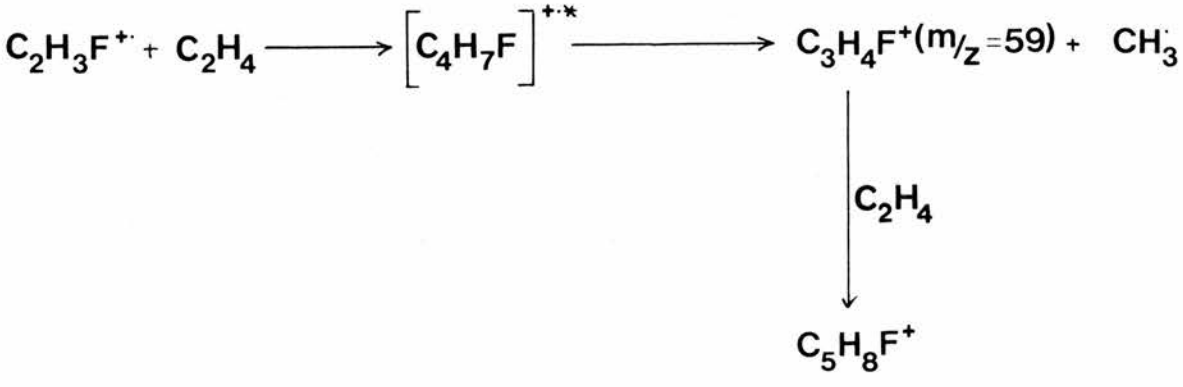

SCHEME 42

At the highest pressure this ion reacts further with ethene to produce the ion $C_5H_8F^+$ (m/z = 87) in an associative collision like that observed for $C_3H_5^+$ in ethene.

The second fluorinated molecule studied was 1,1-difluoroethene which showed very little reaction with itself (possibly due to steric factors to be discussed later). Even at the very highest pressures, over 84% of the total ion signal was due to the primary ion (See Results).

The total secondary ion spectrum for the 1,1-difluoroethene ion-molecule reaction is shown in Table 43. The largest secondary

m/z	28	33	39	40	41	59	64	65	67	69	77	95
Reaction ion	$C_2H_4^{+\cdot}$	CH_2F^+	$C_3H_3^+$	$C_3H_4^{+\cdot}$	$C_3H_5^+$	$C_3H_4F^+$	$C_2H_2F_2^{+\cdot}$	$C_2H_3F_2^+$	$C_5H_7^+$	$C_5H_9^+$	$C_3H_3F_2^+$	$C_3H_2F_3^+$
1,1-difluoro-ethene$^{+\cdot}$ / itself	-	5	3	4	-	4	P	36	-	-	12	14
ethene$^{+\cdot}$ / 1,1-difluoro-ethene	P	-	1	-	1	-	82	7	-	-	1	1
1,1-difluoro-ethene$^{+\cdot}$ / ethene	13	-	-	1	25	1	P	-	5	16	27	-

TABLE 43: The Principal Secondary Ions Observed in the Reactions of the 1,1-difluoroethene Radical Cation and Ethene Radical Cation with 1,1-difluoroethene and Ethene. (% Total Secondary Ion Signal.

ion is that at m/z = 65, arising from hydrogen abstraction from the neutral molecule (1·7).

$$C_2H_2F_2^{+\cdot} + C_2H_2F_2 \longrightarrow C_2H_3F_2^+ + C_2HF_2^{\cdot} \qquad 1.7$$

The remaining ions of any consequence all have (as is the case with vinyl fluoride) the allylic formula, $C_3H_xF_{5-x}^+$, with in this case x = 2,3 and 4 - see Scheme 43.

$$C_2H_2F_2^{+\cdot} + C_2H_2F_2 \longrightarrow \left[C_4H_4F_4\right]^{+\cdot *} \longrightarrow \begin{cases} C_3H_4F^+ + CF_3^{\cdot} \\ C_3H_3F_2^+ + CHF_2^{\cdot} \\ C_3H_2F_3^+ + CH_2F^{\cdot} \end{cases}$$

SCHEME 43

The results obtained when ethene radical cation is reacted with 1,1-difluoroethene are as expected (see Table 43). As in the ethene$^{+\cdot}$/vinyl fluoride case, the only reaction which appears to occur is charge exchange, followed by the 1,1-difluoroethene ion-molecule reaction. However, in this case the icn $C_2H_3F_2^+$ (m/z = 65) is present from the very lowest pressures, and climbs steadily until at ca. 3×10^{-3} Torr it contributes 12% of the total ion signal. This compares with only 7% of the total signal achieved in the preceding reaction. These two factors indicate this ion is derived from two sources; as a tertiary ion derived from $C_2H_2F_2^{+\cdot}$; and as a secondary ion, brought about by the transfer of a proton from the ethene radical cation (1·8).

$$C_2H_4^{+\cdot} + C_2H_2F_2 \longrightarrow \left[C_4H_6F_4\right]^{+\cdot *} \longrightarrow C_2H_3 + C_2H_3F_2^+ \qquad 1.8$$

When the above reaction is reversed, we again observe charge exchange as the dominant reaction, but in addition to this there are also several other important reactions involving the "allylic" cations, $C_3H_xF_{5-x}^+$. The first of these ions is $C_3H_5^+$, which we have already shown to be the major secondary ion in the ethene ion-molecule reaction. However, just like the $C_2H_3F_2^+$ ion discussed immediately above, this ion is observed at even the lowest

pressure, implying that it is a secondary ion (Scheme 44), as well as a tertiary ion derived from the charge-exchange product. Similarly, we also observe the ion m/z = 77 at low pressure, indicating that the $(C_4H_6F_2)^{*\cdot+}$ reaction complex also breaks down to give the alternative $C_3H_3F_2^+$ allylic cation (see Scheme 44 below).

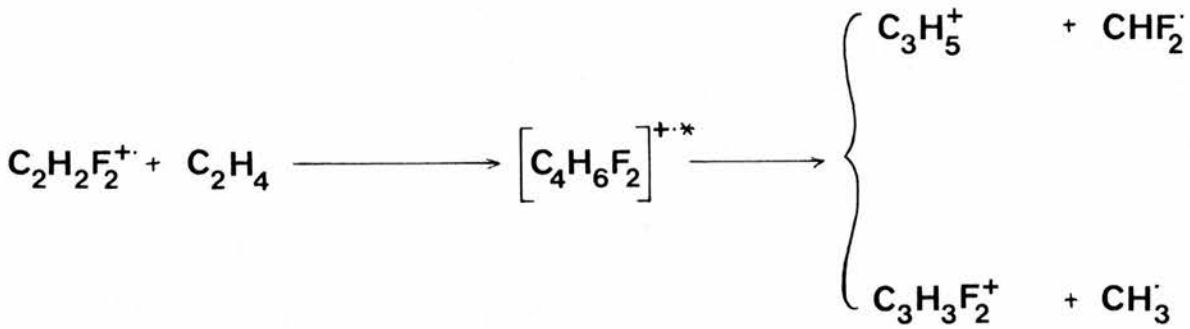

SCHEME 44

However, the other possible allylic ion, $C_3H_4F^+$ - m/z = 59, is observed only as a very minor product in this reaction. This may be a consequence of the way in which the primary ion reacts with the neutral ethene.

There are two possible orientations for the transition complex involved (assuming here, that this is linear); in the first of these (H, below), the two fluorine atoms are carried by a terminal carbon atom; whereas in Structure I, the fluorines appear on a secondary carbon. (Note that although we have assigned the positive charge and unpaired electron to particular sites in these structures,

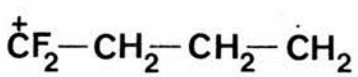

H

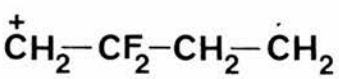

I

Le Breton's[106] discussion of the ethene ion-molecule reaction suggests that the most stable structure will probably take a form similar to that shown in J). If we now assume that the allylic ions

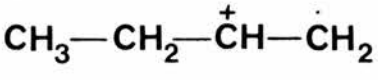

J

$(C_3H_xF^+_{5-x})$ are produced by elimination of the terminal carbon atom(s), following a 1,3-hydrogen shift to this more stable structure, then from structure H we obtain the two products shown in Scheme 45; but from Structure I, the fluorine-containing ion is the only possible

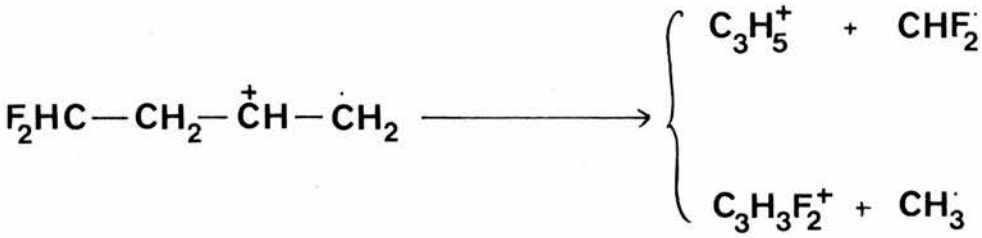

SCHEME 45

product (Scheme 46).

SCHEME 46

These results suggest that the transition complex does infact take structure H, since the two ions in Scheme 45 have been shown to be secondary ions in this case (Scheme 46 does not allow for the production of $C_3H_5^+$ as a secondary ion). As to the appearance of $C_3H_4F^+$ at higher pressures, this we must attribute to an H/F exchange involving $C_3H_3F_2^+$ (1·9).

1.9

Although we have discussed this reaction in terms of linear transition complexes, we have not ruled out the possibility that a cyclic intermediate may be involved, and this will be discussed

fully with reference to the reaction between trifluoroethene radical cation and ethene.

The third molecule to be studied was trifluoroethene, and the product ions observed in the ion-molecule reaction of this compound are listed in Table 44.

pressure	m/z ion	43 $C_3H_7^+$	57 CHF_2^+	58 $C_4H_{10}^+$	77 $C_3H_3F_2^+$	81 $C_2F_3^+$	82 $C_2HF_3^+$	95 $C_3H_2F_3^{+\cdot}$	113 $C_3HF_4^+$	116 $C_9H_8^{+\cdot}$	118 $C_9H_{10}^{+\cdot}$
low - $1x10^{-4}$Torr		-	1	1	-	6	993	-	-	-	-
medium - $1.5x10^{-3}$Torr		1	14	8	3	3	881	55	3	17	5
high - $4.6x10^{-3}$Torr		16	18	50	23	12	351	309	64	73	26

TABLE 44: The Ions Observed in the Trifluoroethene Ion-Molecule Reaction at Low, Medium and High Pressure (Total Ion Signal = 1000).

Of the ions listed above, three are allylic (at m/z = 77, 95 and 113); and of these, the ion at m/z = 77 must be tertiary (since the transition complex contains only two hydrogen atoms), probably derived from the further reaction of the major secondary ion, $C_3H_2F_3^+$, involving an H/F exchange similar to that observed for $C_3H_3F_2^+$ in the 1,1-difluoroethene radical cation/ethene reaction (1·9) - see Scheme 47.

$$C_3H_2F_3^+ + C_2HF_3 \longrightarrow \left[C_5H_3F_6\right]^{+\cdot *} \longrightarrow C_3H_3F_2^+ + C_2F_4$$

SCHEME 47

The ion at m/z = 81, arises from the hydrogen transfer reaction shown below (1·10).

$$C_2HF_3^{+\cdot} + C_2HF_3 \longrightarrow C_2F_3^{+} + C_2H_2F_3^{\cdot} \qquad 1.10$$

The ion at m/z = 51 can only be CHF_2^+; but the remaining four ions cannot be assigned any rational formulae using the atoms known to be present in the system, and thus appear to be due to an unidentified impurity in the trifluoroethene sample (m/z = 43 and 58 are probably acetone derived).

As before, when ethene is used as the primary ion, with trifluoroethene as the collision gas, charge exchange is the sole reaction (see Table 45).

m/z	28	43	51	58	59	69	77	82	95	113	116	118
Reaction ion	$C_2H_4^{+\cdot}$	$C_3H_7^+$	CHF_2^+	$C_4H_{10}^{+\cdot}$	$C_3H_4F^+$	CF_3^+	$C_3H_3F_2^+$	$C_2HF_3^{+\cdot}$	$C_3H_2F_3^+$	$C_3HF_4^+$	$C_9H_8^{+\cdot}$	$C_9H_{10}^{+\cdot}$
trifluoroethene$^{+\cdot}$/ itself	-	1	5	7	1	2	2	P	54	6	13	4
ethene$^{+\cdot}$/ trifluoroethene	P	-	1	1	1	1	2	37	34	4	9	3

TABLE 45 The Products of the Reactions Between Trifluoroethene Radical Cations and Ethene Radical Cations with Trifluoroethene (% Total secondary Ion Signal)

The reverse process (trifluoroethene radical cation/ ethene) gives results similar to those obtained in the reactions for both vinyl fluoride and difluoroethene radical cations with ethene - mainly charge exchange, with some reaction due to the breakdown of the transition complex, resulting in the expected allylic cations $C_3H_xF_{5-x}^+$. Where this reaction differs is in the

production of two ions which appear to involve H/F exchange between the primary ion and the neutral. These ions appear at m/z = 64 and 46 (Table 46). This behaviour cannot easily be explained using

Pressure	m/z ion	28 $C_2H_4^{+\cdot}$	41 $C_3H_5^+$	46 $C_2H_3F^{+\cdot}$	51 CHF_2^+	55 $C_4H_7^+$	59 $C_3H_4F^+$	64 $C_2H_2F_2^+$
low - $1{\cdot}3\times10^{-4}$		8	2	3	1	-	-	8
medium - 1.3×10^{-3}		31	48	10	4	5	12	35
high - $3{\cdot}2\times10^{-3}$		29	68	11	6	15	29	47

Pressure	m/z ion	67 $C_5H_7^+$	69 CF_3^+ &/or $C_5H_9^+$	77 $C_3H_3F_2^+$	82 $C_2HF_3^+$	95 $C_3H_2F_3^+$
low - $1{\cdot}3\times10^{-4}$		-	-	-	974	1
medium - 1.3×10^{-3}		8	13	26	783	6
high - 3.2×10^{-3}		48	113	91	448	18

TABLE 46: The Products of the Reaction Between Trifluoroethene Radical Cation and Ethene at Low, Intermediate and High Pressure (% Total Ion Current)

the linear transition complex used to illustrate the production of allylic cations with 1,1-difluoroethene. However, if we proceed instead via a loosely-bound cyclobutane transition complex, then this provides a very eloquent answer to the method of formation of these two ions (see Scheme 48).

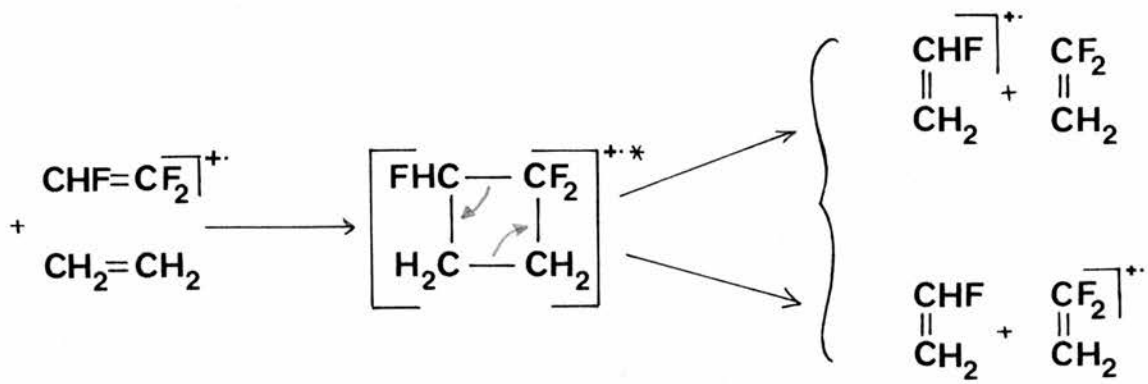

SCHEME 48

As the radical cation and neutral molecule collide, they produce the cyclobutane transition complex, which can then do several things.

It can:-

(a) regenerate the original ion/neutral pair.

(b) produce the reverse ion/neutral pair - effectively charge exchange. This would explain why we observe what appears to be charge exchange in all the cross reactions involving the fluoroethenes and ethene. Normally, from consideration of the ionisation potentials, we would expect charge exchange only to occur when ethene radical cation is used as primary ion.

(c) produce one or other of the new ion/neutral pairs shown in Scheme 48.

or

(d) ring-open, and eliminate a methyl/fluorinated methyl radical and an allylic cation.

All of the above reactions (a-d) are observed in this case, including all four possible allylic ions from (d) - m/z = 41, 59, 77 and 95. If we apply this mechanism to the two previous cases where fluoroethene radical cation is reacted with ethene, it again holds true for all four reactions, although in both cases, reaction (c) produces the same products as reaction (a) - see Scheme 49.

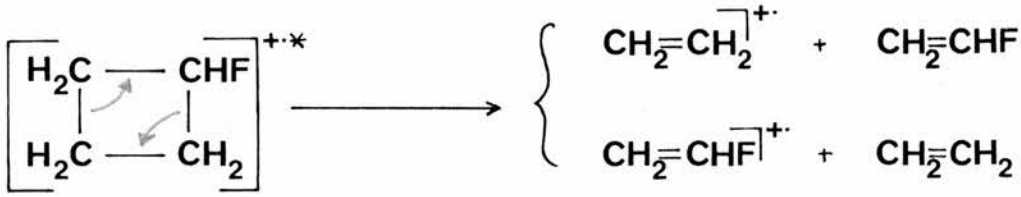

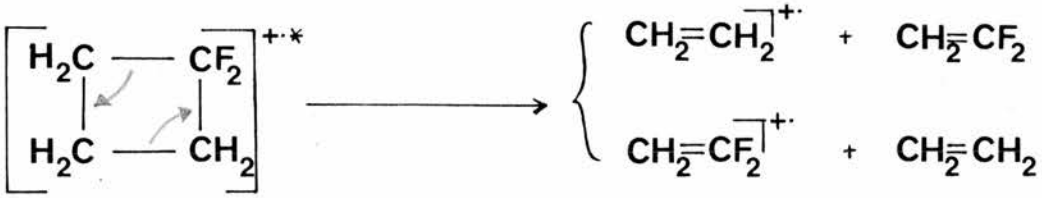

SCHEME 49

Extending the (2+2) cycloaddition mechanism to the fluoroethene ion-molecule reactions, we again achieve very good agreement with the experimental results, although here there are complications; with the orientation of the two molecules - do they combine "head-to-head" or "head-to-tail"?; and with the mechanism of the methyl/fluorinated methyl radical elimination - does this involve a 1,2- or 1,3-migration of hydrogen and/or fluorine or both? If "head-to-head" addition is occurring, then we should see evidence of reaction (c) - the formation of fluoroethene radical cations and neutrals other than those used as reactants. Taking trifluoroethene as an example, we should observe both difluoroethene and tetrafluoroethene radical cations from a "head-to-head" collision (see Scheme 50).

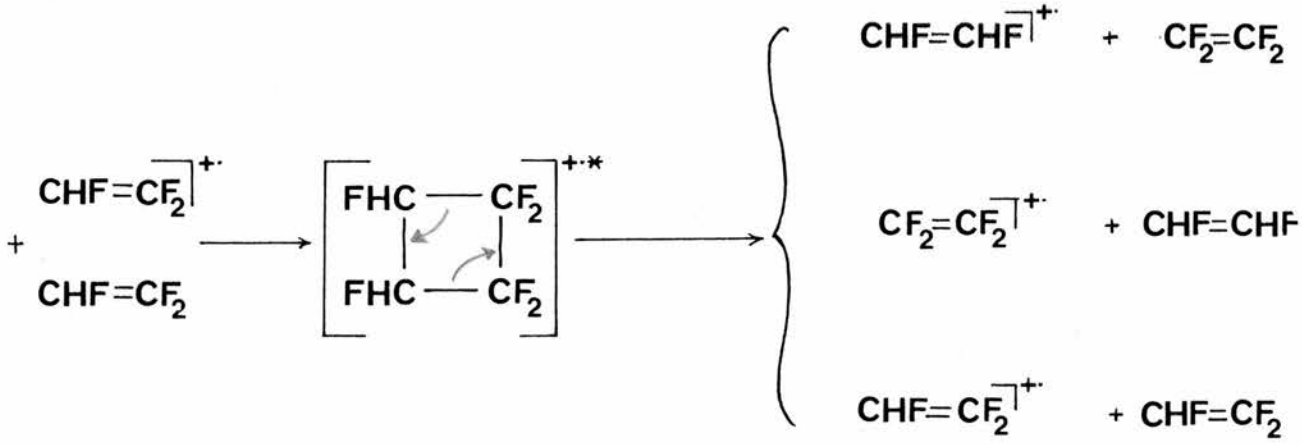

SCHEME 50

These ions are both observed, but in very small proportions, and $C_2F_4^{+\cdot}$ only appears at high pressures. Therefore we must conclude that this "head-to-head" mechanism does occur, but only to a limited extent, and at higher pressures where the probable steric hind rance due to the bulky CF_2 groups can be overcome.

There is one remaining fluoroethene yet to be considered - tetrafluoroethene. When the tetrafluoroethene radical cation is reacted with tetrafluoroethene, we do not get results similar to those of the other fluoroethenes (Table 47).

m/z	31	43	58	69	131
ion	CH_2F^+	$C_3H_7^+$	$C_4H_{10}^{+\cdot}$	CF_3^+	$C_3F_5^+$
tetrafluoroethene$^{+\cdot}$/ itself	11	-	10	70	10

TABLE 47: The Products of the Tetrafluoroethene Ion-Molecule Reaction (% Total Secondary Ion Signal)

In this case the major secondary ion occurs at m/z = 69, which must be the trifluoromethyl cation, with the $C_3F_5^+$ ion the only other secondary ion observed at m/z = 131. The remaining three ions in this spectrum, at m/z = 31,43 and 58, cannot be assigned any rational formulae and would appear to be due to acetone contained in tetrafluoroethene sample. This impurity could not be removed from the sample, due to the small sample volume (1 dm^3) and handling difficulties.

When ethene radical cation is reacted with tetrafluoroethene the results again differ from the previous cases, in that significant reaction between the two is observed. The major peaks are listed in Table 48 below.

Pressure	m/z ion	26 $C_2H_2^{+\cdot}$	27 $C_2H_3^+$	28 $C_2H_4^{+\cdot}$	51 CHF_2^+	58 $C_4H_{10}^{+\cdot}$	64 $C_2H_2F_2^{+\cdot}$	69 CF_3^+	77 $C_3H_3F_2^+$	100 $C_2F_4^{+\cdot}$	131 C_3F
low-6×10^{-5}Torr		2	1	993	-	-	1	-	1	3	-
medium-9×10^{-4}Torr		22	5	881	1	-	1	3	3	82	-
high-2.5×10^{-3}Torr		40	19	569	3	6	-	20	14	310	6

TABLE 48: The Ions Observed in the Reaction Between Ethene Radical Cations and Tetrafluoroethene (% Total Ion Current)

From the above we can see that the major reaction is charge exchange (m/z = 100), which includes the ions at m/z = 69 and 131, due to the further reaction of $C_2F_4^{+\cdot}$. The other significant ions all indicate that reaction occurs between ethene radical cation and tetrafluoroethene. The ion at m/z = 64 in particular can be attributed to the (2+2) cyclisation mechanism (Scheme 51), whilst the ion at

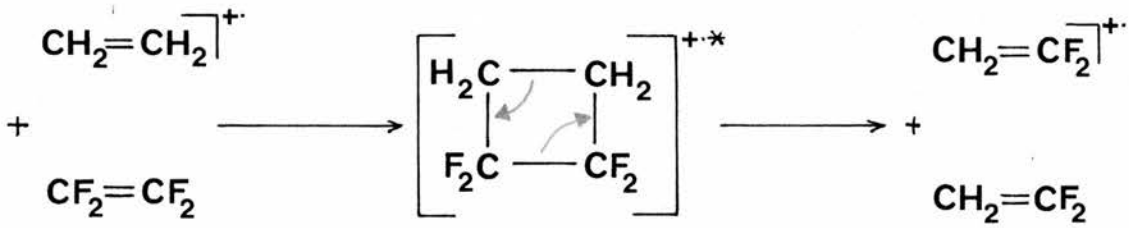

SCHEME 51

m/z = 77 is the only possible allylic ion from this cyclobutane transition complex if H-migration only is allowed. Of the other ions; m/z = 51 is CHF_2^+; m/z = 58 is probably the acetone impurity; and m/z = 26 and 27 are $C_2H_2^{+\cdot}$ and $C_2H_3^+$ respectively. These latter two ions are in fact found in all the systems involving $C_2H_4^{+\cdot}$ as the primary ion.

The reverse cross-reaction between tetrafluoroethene radical cation and ethene could not be performed since our sample of tetrafluoroethene became exhausted, and again this is no longer commercially available.

These results are in very good agreement with the earlier ICR studies of Anicich and Bowers[107-110] and Ferrer-Correia and Jennings[111].

The acetylene (ethyne) ion-molecule reaction has been comprehensively studied[112-117], and has been included here because a number of reactions involving ethyne as primary ion and/or neutral were envisaged, and it was thought better to perform this reaction on the TQMS in case any instrumental artefacts were observed. No such instrumental problems were encountered and the results are in agreement with the previous studies. However, we did have problems in cleaning the ethyne sample used, but these were eliminated using the method outlined on page 21 in the experimental section.

Figure 11 below shows very clearly how the acetylene ion-molecule reaction proceeds.

The initial reaction involves the formation of the two species $C_4H_2^{+\cdot}$ (m/z = 50) and $C_4H_3^+$ (m/z = 51) as shown in Scheme 52.

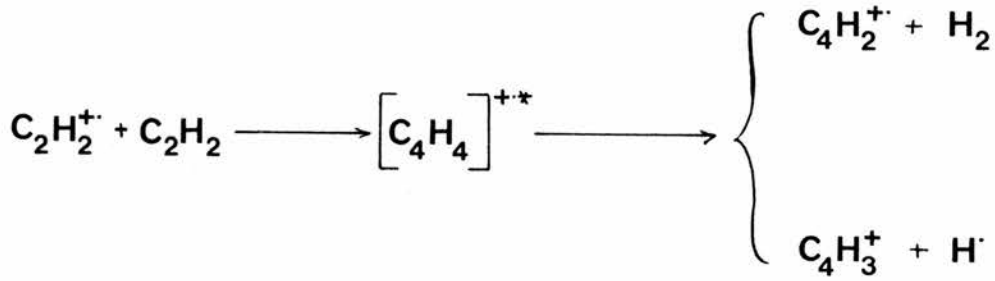

SCHEME 52

These two species then "polymerise" to give the remaining major ions at m/z = 76, 77; 102, 103; and 128. (In each case the ion concerned reacts with the neutral molecule without radical/neutral elimination.)

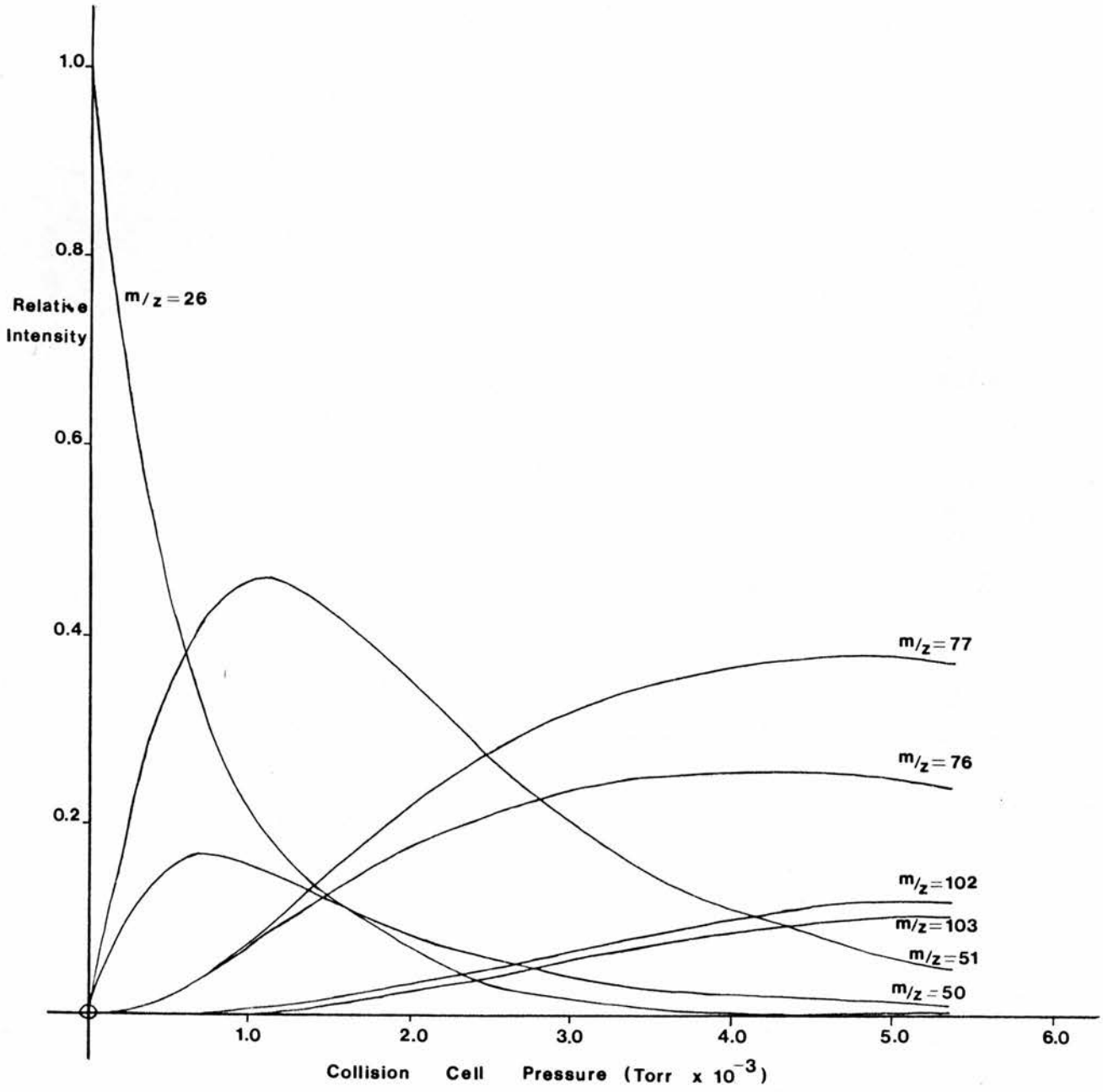

FIGURE 11: The Principal Products in the Ethyne Ion-Molecule Reaction (pressure v intensity plot)

We can thus depict the reaction sequence for the ethyne ion-molecule reaction thus:-

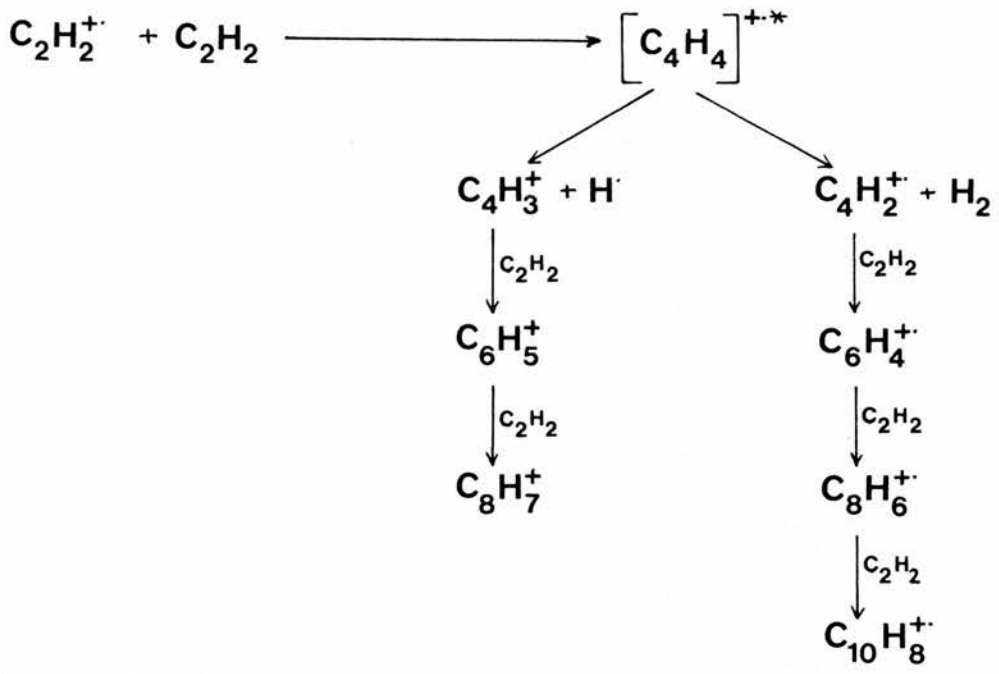

SCHEME 53

The above ions constitute 92% of the secondary ion spectrum, with the remaining 8% arising from reactions akin to those mentioned above.

The first of these minor ions (and the only other secondary ion) is that at m/z = 27. This is formed by the hydrogen transfer observed in all the systems under study here - transfer of H· from the neutral molecule to the primary ion. This ion ($C_2H_3^+$) then appears to behave in a manner similar to the two major secondary ions - it "polymerises" with ethyne, giving rise to the ions at m/z = 53, 79 and 105 (Scheme 54).

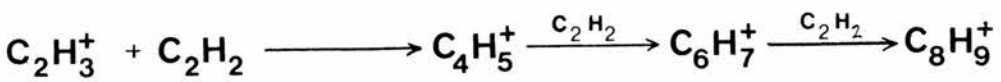

SCHEME 54

The next minor ion, in order of ascending mass number, is that at m/z = 52 ($C_4H_4^{+\cdot}$), which only appears at higher pressures, suggesting that it is the collisionally stabilised transition complex formed in the initial ion-molecule interaction (again a reaction observed in previous systems). This ion may then be responsible for the production of $C_6H_6^{+\cdot}$ (m/z = 78), which is only observed at the highest pressures used.

The ions at m/z = 74 and 75 seem likely to be formed in a reaction analogous to that of $C_2H_2^{+\cdot}$ (Scheme 52), and if we then assume that these two ions behave in a similar manner to $C_4H_2^{+\cdot}$ and $C_4H_3^{+}$, we can account for the four remaining ions in the spectrum (see Scheme 55).

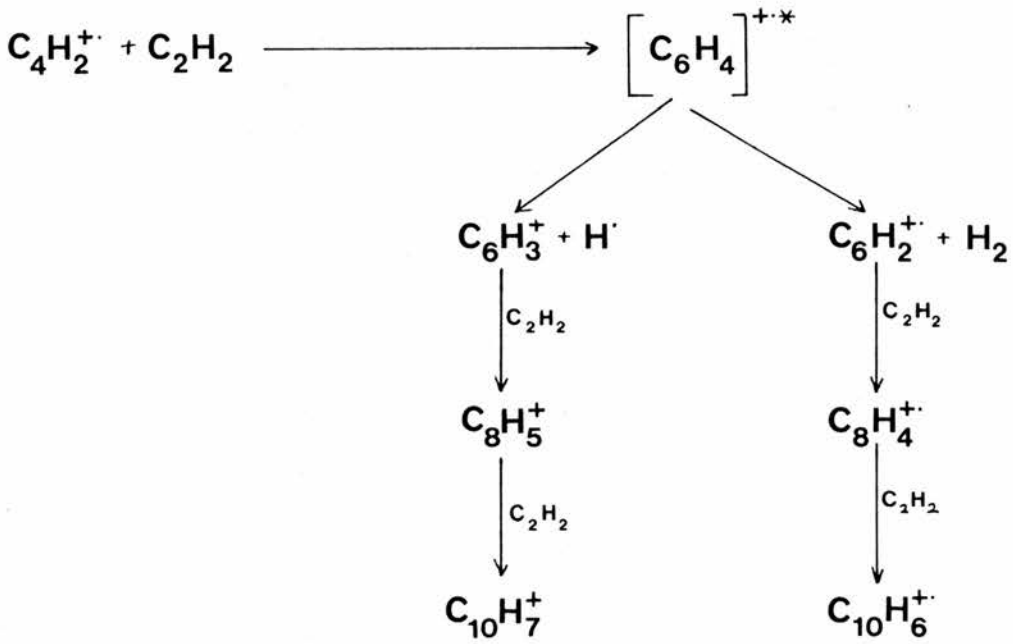

SCHEME 55

We next looked at the cross reactions between ethene and ethyne, which proceed via the much studied $C_4H_6^{+\cdot}$ reaction complex.

Consideration of the ionisation potentials of the two molecules ($C_2H_2^{+\cdot}$ = 11·40 eV; $C_2H_4^{+\cdot}$ = 10·51 eV) indicates that when $C_2H_2^{+\cdot}$ is the primary ion, charge-exchange is likely to be the major reaction observed. This appears to be borne out by the results as shown in Table 49 and Figure 12 below; however the relative proportions of the two ions at m/z = 39 and 53 indicate otherwise.

	m/z	26	27	28	29	39	41	53	55	67	69	79
Pressure	ion	$C_2H_2^{+\cdot}$	$C_2H_3^+$	$C_2H_4^{+\cdot}$	$C_2H_5^+$	$C_3H_3^+$	$C_3H_5^+$	$C_4H_5^+$	$C_4H_7^+$	$C_5H_7^+$	$C_5H_9^+$	$C_6H_7^+$
3×10^{-3}Torr		P	2	11	2	6	38	4	6	7	21	1

TABLE 49: The Ions Observed in the Reaction of Ethyne Radical Cation with Ethene (% Total Secondary Ion Current)

Both $C_3H_3^+$ and $C_4H_5^+$ arise in the ethene ion-molecule reaction, products of the CAD of the two secondary ions $C_3H_5^+$ and $C_4H_7^+$ respectively (page 69). As such these ions are very minor products, but if we look at the results in Table 50, we see that at the lowest pressures used in this experiment, m/z = 39 and 53 are larger than, and appear before, their assumed precursors at m/z = 41 and 55.

m/z		26	28	29	39	41	51	53	55
Pressure	ion	$C_2H_2^{+\cdot}$	$C_2H_4^{+\cdot}$	$C_2H_5^+$	$C_3H_3^+$	$C_3H_5^+$	$C_4H_3^+$	$C_4H_5^+$	$C_4H_7^+$
4×10^{-5} Torr		9715	229	2	24	9	5	14	-
9×10^{-5} Torr		9265	580	13	50	39	8	36	2

TABLE 50: The Ions Observed at low Pressure in the Reaction of Ethyne Radical Cation with Ethene (% Total Ion Current)

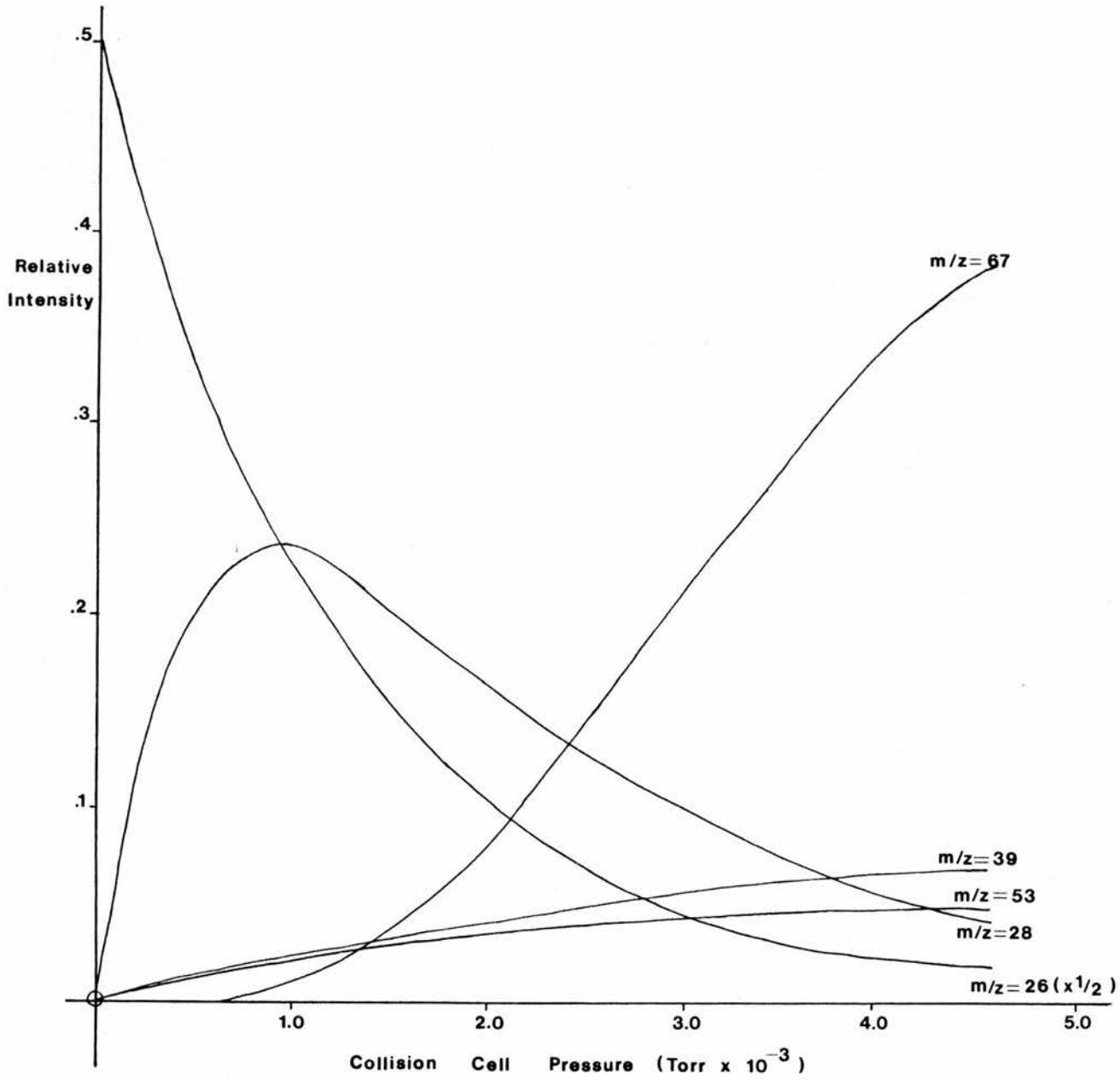

FIGURE 12: The Pressure v Intensity Plot for the Reaction Between Ethyne Radical Cation and Ethene

Thus, in addition to the expected charge-exchange product, we are also observing two additional secondary ions as shown in Scheme 56.

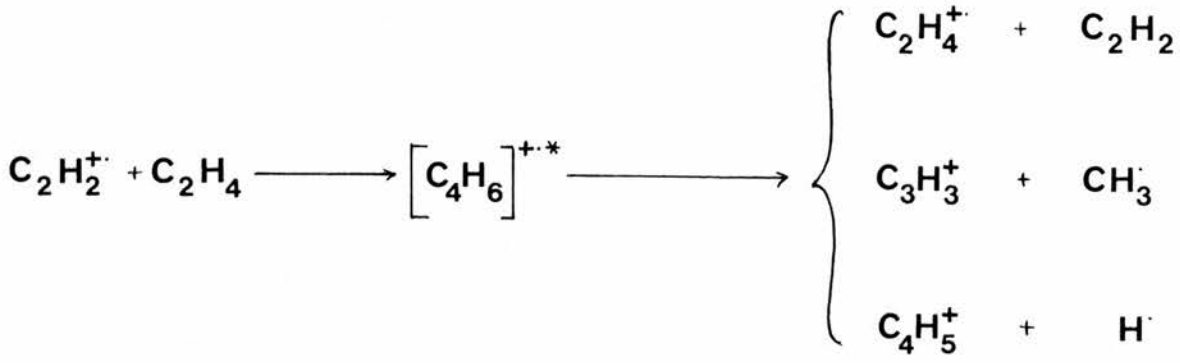

SCHEME 56

The occurrence of $C_3H_3^+$ and $C_4H_5^+$ as secondary ions can be explained using the transition state switching model proposed by Chesnavich et al[118], and fully investigated (experimentally and theoretically) by Jarrold et al[119]. This allows for the existence of at least two transition states along the reaction co-ordinate in each reaction channel; so that in this case we have a tight transition state close to the unimolecular reactant ($[CH_2=CH-CH=CH_2]^{+\cdot}$ in Figure 13) and an orbiting transition state close to the separated products ($[C_2H_2 \cdot C_2H_4]^{+\cdot}$ in Figure 13). Charge-exchange is envisaged as occurring predominantly via the shallow well corresponding to the loosely bound $[C_2H_2 \cdot C_2H_4]^{+\cdot}$ complex.

By extending this experiment to much higher pressures of ethene we are able to follow the tertiary and higher reactions in this system, which in view of the overwhelming proportion of $C_2H_4^{+\cdot}$ formed through the charge-exchange channel, are all attributable to further reaction of this product (Scheme 28). The one exception being the enhanced presence of the ion at m/z = 79, due to the increased proportion of $C_4H_5^+$ present in this system over that in the

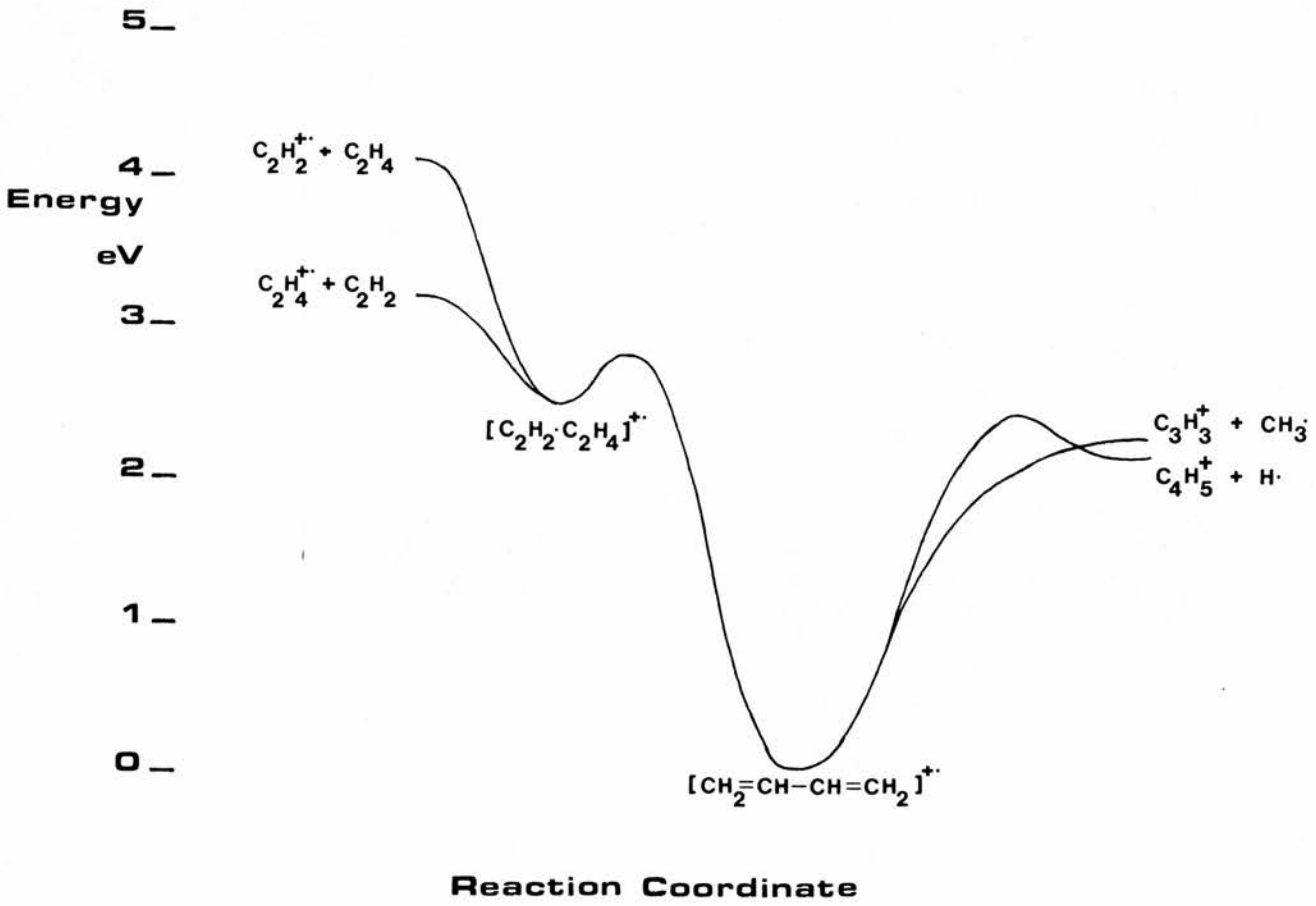

FIGURE 13: The Reaction Coordinate Diagram for the $C_4H_6^{+\cdot}$ System (after Jarrold et al (119))

ethene ion-molecule reaction. This ion results from reaction (1·11).

$$C_4H_5^+ + C_2H_4 \longrightarrow \left[C_6H_9\right]^{+*} \longrightarrow C_6H_7^+ + H_2 \qquad 1.11$$

The reverse cross reaction produces more interesting results. Here the two lesser secondary ions discovered in the

previous reaction are very much the major products of this reaction, where the internal energy of the primary ion is not sufficient to cause the ionisation of the neutral collision molecule - although we do observe the ion $C_2H_2^{+\cdot}$, which corresponds to this charge-exchange process.

At the lowest pressure studied there are in fact four secondary ions observed (Table 51).

	m/z	26	27	28	39	53
Pressure	ion	$C_2H_2^{+\cdot}$	$C_2H_3^{+}$	$C_2H_4^{+\cdot}$	$C_3H_3^{+}$	$C_4H_5^{+}$
4.7×10^{-5}	Torr	48	30	9889	24	9

TABLE 51: The Ions Found at low Pressure in the Reaction Between Ethene Radical Cation and Ethyne (% Total Ion Current)

In addition to the two expected ions (m/z = 39 and 53) observed in all previous studies of this system[119,120,121], we also find ions at m/z = 26 and 27. The ion at m/z = 27 ($C_2H_3^+$) is a product of either proton or hydrogen transfer between the two reactants, but without access to deuterium labelling, we cannot state which of these two processes actually occurs (both are observed in the various systems discussed here). $C_2H_2^{+\cdot}$, at first sight, appears to be the result of a straight forward charge-exchange reaction. However, as this reaction is not thermodynamically favoured (see Figure 13), a more plausible explanation is that this ion is the product of the collisionally activated dissociation of the primary ion (1·12).

$$C_2H_4^{+\cdot} + C_2H_2 \longrightarrow C_2H_2^{+\cdot} + H_2 + C_2H_2 \qquad 1.12$$

As the pressure of ethyne is increased, we observe tertiary and higher products, but unlike the ethyne ion-molecule spectrum or the reverse cross reaction, where these products dominate at higher pressures, here these ions constitute less than 20% of the total ion signal. In fact most of these higher order ions (listed in Table 52 below) can be shown to arise from the further reaction of the $C_2H_2^{+\cdot}$ secondary ion. In particular the ions at m/z = 50 and 51 and m/z = 76 and 77 behave very like the same ion in the ethyne-only system (compare Figure 14 below with Figure 11).

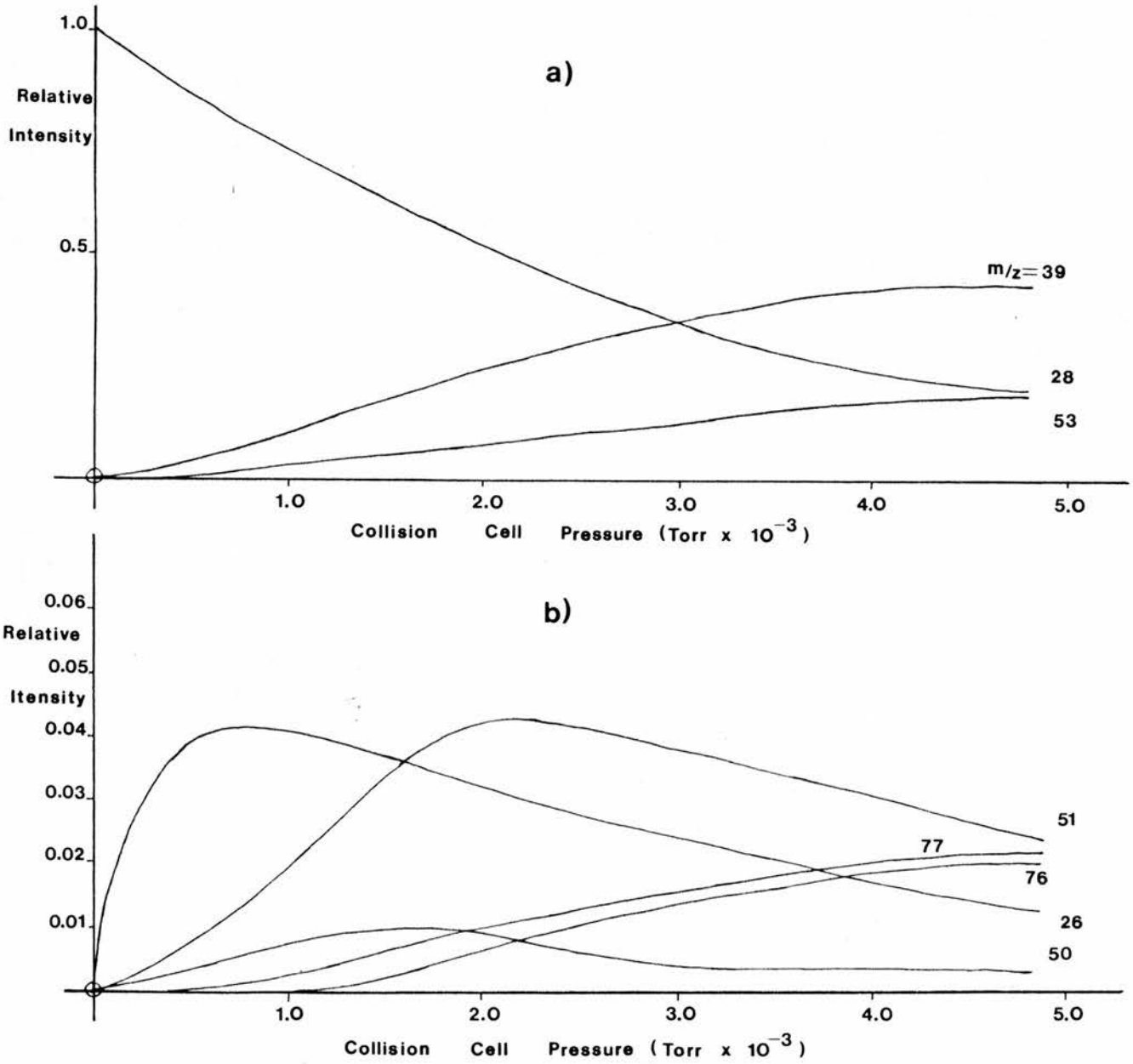

FIGURE 14: The Pressure v Intensity Plots for (a) the Major Secondary Ions and (b) the Major Tertiary Ions in the Reaction Between $C_2H_4^{+\cdot}$ and C_2H_2

Structurally we cannot make any definite assignments, but the build-up of $C_3H_3^+$ with pressure, and the very minor presence of ions directly attributable to the further reaction of this ion (Scheme 57), lead us to believe that this ion has the cyclopropenyl structure (B).

ion	m/z	source
$C_2H_2^{+\cdot}$	26	CAD of $C_2H_4^{+\cdot}$
$C_2H_3^+$	27	H^+ &/or H· transfer
$C_2H_4^{+\cdot}$	28	Primary ion
$C_2H_5^+$	29	H· transfer
$C_3H_3^+$	39	Secondary ion - see text
$C_4H_2^{+\cdot}$	50	$C_2H_2^{+\cdot}$ i-m reaction; $C_2H_2^{+\cdot} + C_2H_2 \longrightarrow C_4H_2^{+\cdot} + H_2$
$C_4H_3^+$	51	$C_2H_2^{+\cdot}$ i-m reaction; $C_2H_2^{+\cdot} + C_2H_2 \longrightarrow C_4H_3^+ + H\cdot$
$C_4H_4^{+\cdot}$	52	minor secondary ion; $C_2H_4^{+\cdot} + C_2H_2 \longrightarrow C_4H_4^{+\cdot} + H_2$
$C_4H_5^+$	53	Secondary ion - see text
$C_4H_6^{+\cdot}$	54	Collisionally stabilised reaction complex
$C_5H_3^+$	63	Further reaction of $C_3H_3^+$; $C_3H_3^+ + C_2H_2 \longrightarrow C_5H_3^+ + H_2$
$C_5H_5^+$	65	Further reaction of $C_3H_3^+$; $C_3H_3^+ + C_2H_2 \longrightarrow C_5H_5^{+\cdot}$
$C_6H_4^{+\cdot}$	76	$C_2H_2^{+\cdot}$ i-m reaction; $C_4H_2^{+\cdot} + C_2H_2 \longrightarrow C_6H_4^{+\cdot}$
$C_6H_5^+$	77	$C_2H_2^{+\cdot}$ i-m reaction; $C_4H_3^+ + C_2H_2 \longrightarrow C_6H_5^+$

TABLE 52: The Ions Found in the Ethene Radical Cation/Ethyne Reaction and Their Probable Sources

We have previously discussed the low reactivity of the cyclopropenyl cation compared with that for the propargyl ion[83] (page 50). $C_4H_5^+$ is thought to have the structure of the methylcyclopropenyl ion[122].

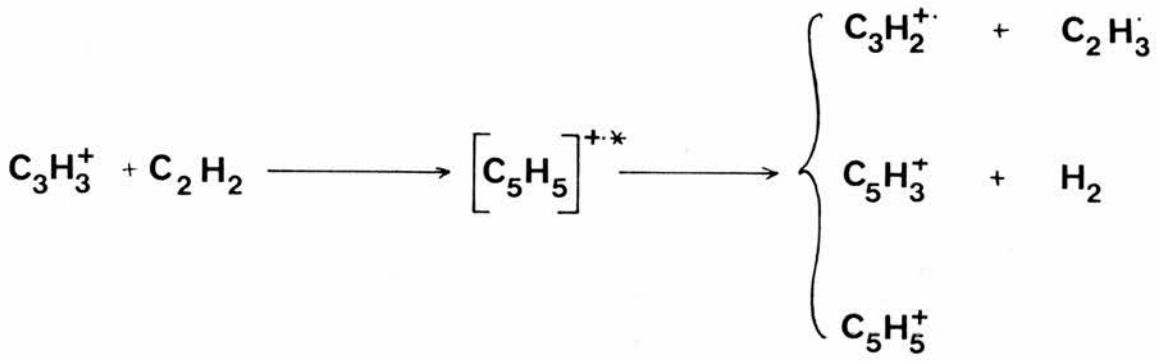

SCHEME 57

Following on from the investigations of the ethene/ethyne cross reactions, a number of reactions involving these molecules and the two conjugated dienes 1,3-butadiene and isoprene were undertaken. (1,3-butadiene being of particular interest, as this corresponds to the reaction complex in the ethene/ethyne reactions).

In the first of the reactions involving butadiene, using ethene radical cations as the primary source, we would expect, by virtue of the higher ionisation potential of ethene, that the predominant reaction between these would be charge-exchange, and this is indeed what is observed. We will therefore consider both this reaction and the butadiene ion-molecule reaction together.

Table 53, shows the results of the two reactions at similar pressures of 1,3-butadiene.

Examination of this table shows that the similarity between the two spectra is striking - there are no peaks which are not common

m/z	28	39	41	53	54	55	66	67	79	80	81	93	109	121
Primary ion	$C_2H_4^{+\cdot}$	$C_3H_3^+$	$C_3H_5^+$	$C_4H_5^+$	$C_4H_6^{+\cdot}$	$C_4H_7^+$	$C_5H_6^{+\cdot}$	$C_5H_7^+$	$C_6H_7^+$	$C_6H_8^{+\cdot}$	$C_6H_9^+$	$C_7H_9^+$	$C_8H_{13}^+$	$C_9H_{13}^+$
$C_4H_6^{+\cdot}$	-	10	-	1	P	2	2	26	6	12	3	24	4	4
$C_2H_4^{+\cdot}$	P	9	1	2	7	4	2	27	6	10	3	16	3	2

TABLE 53: The Ions Observed in the Reaction of Butadiene Radical Cation and Ethene Radical Cation with Butadiene (% Total Secondary Ion Current)

to both spectra, and the ion abundances are remarkably close. (There being a slightly greater proportion of the tertiary ions in the butadiene ion-molecule reaction).

Three ions appear at masses below that of butadiene (m/z = 54). The first of these is $C_3H_3^+$ (m/z = 39), and it, along with the ion at m/z = 53 ($C_4H_5^+$) are products of the collisionally activated dissociation of $C_4H_6^{+\cdot}$. $C_3H_3^+$ is more abundant than $C_4H_5^+$ and this may be due to the saddle point transition state for the latter ion on the $C_4H_6^{+\cdot}$ reaction co-ordinate (Figure 13). The slight increase in abundance of the $C_4H_5^+$ ion in the ethene radical cation initiated reaction is likely to be due to the excess energy imparted to the butadiene molecule during the charge-exchange collision. The third of these "low-mass" ions is $C_3H_5^+$ (m/z = 41), which is found in greater proportion (though still very minor) in the ethene radical cation reaction. This increase is a consequence of

its probable derivation from the reaction complex (1·13). The non-appearance of this ion at low pressures in the butadiene ion-molecule

$$C_2H_4^{+\cdot} + C_4H_6 \longrightarrow \left[C_6H_{10}\right]^{+\cdot *} \longrightarrow C_3H_5^{+} + C_3H_5^{\cdot} \qquad 1.13$$

reaction, indicates that in this case, $C_3H_5^+$ is a tertiary ion; a CAD product of one or more of the major secondary ions (eg $C_5H_7^+ \xrightarrow{m} C_3H_5^+ + C_2H_2$).

There are five secondary ions observed above m/z = 54, the first of which is $C_4H_7^+$ (m/z = 55), corresponding to the ubiquitous proton and/or hydrogen transfer between the two reactants. The remaining four ions are all derived from the $C_8H_{12}^{+\cdot}$ reaction complex, as shown in Scheme 58 below. All eight secondary ions (plus m/z = 66) are observed by Koyano et al[90], in their photoionisation study of

$$C_4H_6^{+\cdot} + C_4H_6 \longrightarrow \left[C_8H_{12}\right]^{+\cdot *} \longrightarrow \begin{cases} C_5H_7^+ + C_3H_5^{\cdot} \\ C_6H_7^+ + C_2H_5^{\cdot} \\ C_6H_8^{+\cdot} + C_2H_4 \\ C_7H_9^+ + CH_3^{\cdot} \end{cases}$$

SCHEME 58

1,3-butadiene, but in addition to these we see three peaks of appreciable size, at m/z = 81, 109 and 121.

m/z = 81 was at first thought to be a secondary ion, but closer inspection of the spectra revealed that it did not appear until mid-range pressures, so it seems likely that this is a tertiary ion arising from the hydrogen transfer reaction (1·14).

$$C_6H_8^{+\cdot} + C_4H_6 \longrightarrow C_6H_9^{+} + C_4H_5^{\cdot} \qquad 1.14$$

The behaviour of these two ions with pressure (See Figures 15 (a) and (b)) endorses this opinion. $C_8H_{13}^{+}$ (m/z = 109) on the other hand has no obvious derivation.

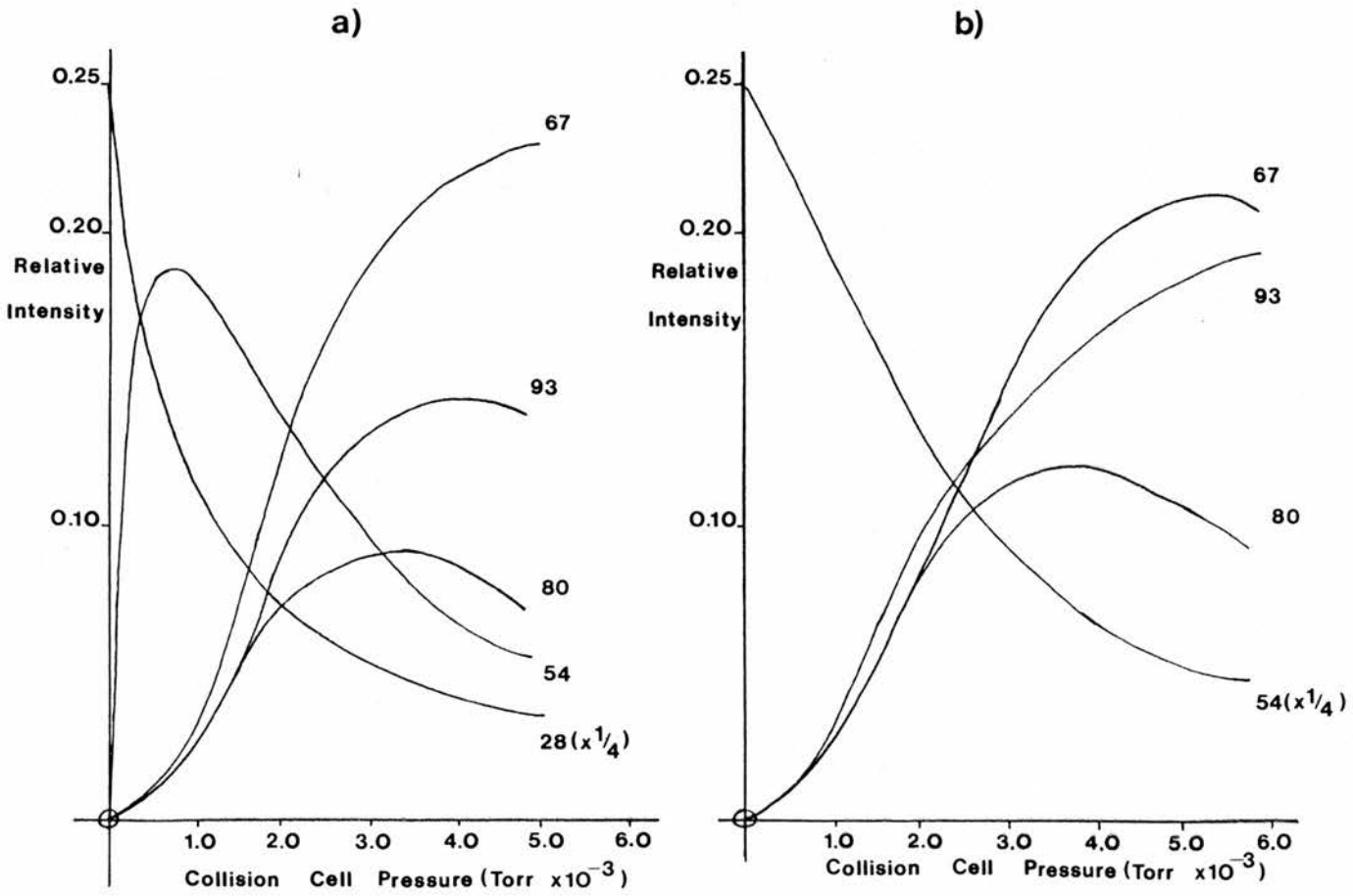

FIGURE 15: The Pressure v Intensity Plot for (a) the Reaction Between $C_2H_4^{+\cdot}$ and 1,3-Butadiene and (b) the Reaction Between 1,3-Butadiene Radical Cation and Ethene

Initially this was also thought to be due to the further reaction of $C_6H_8^{+\cdot}$, but this can be rejected (as can the further reaction of $C_5H_7^+$) since this would require the co-production of CH· (or atomic carbon) as the neutral species. The mass calibration was checked - it was thought that this may in fact have been m/z = 108; the collisionally stabilized dimer, $C_8H_{12}^{+\cdot}$ - but it was found to be accurate, and so the only possible reaction that could produce this ion is (1·15). Reaction (1·16) shows that the $C_5H_7^+$ ion is responsible for the

$$C_7H_9^+ + C_4H_6 \longrightarrow \left[C_{11}H_{15}\right]^{+*} \longrightarrow C_8H_{13}^+ + C_3H_2 \qquad 1.15$$

formation of the final ion observed in this system.

$$C_5H_7^+ + C_4H_6 \longrightarrow C_9H_{13}^+ \qquad 1.16$$

The butadiene radical cation/ethene reaction is contrastingly much simpler, with only two major secondary ions observed at m/z = 39 and 67, the ions we would predict from the just discussed ethene radical cation/butadiene reaction (see Scheme 59 below). Together these two ions constitute over 80% of the secondary ion signal, and if we look at the secondary ion distribution at the highest pressure used (Table 54), we see that only four other ions have an abundance greater than 1%.

m/z	39	41	53	54	65	66	67	69	79	80	81	82	93
Pressure ion	$C_3H_3^+$	$C_3H_5^+$	$C_4H_5^+$	$C_4H_6^{+\cdot}$	$C_5H_5^+$	$C_5H_6^{+\cdot}$	$C_5H_7^+$	$C_5H_9^+$	$C_6H_7^+$	$C_6H_8^+$	$C_6H_9^+$	$C_6H_{10}^{+\cdot}$	$C_7H_9^+$
5×10^{-3} Torr	32.8	1.1	2.6	P	0.5	1.1	53.4	1.4	0.7	0.7	1.0	4.5	0.4

TABLE 54: The Secondary Ion Abundances of the Ions Found in the Reaction Between Butadiene Radical Cation and Ethene

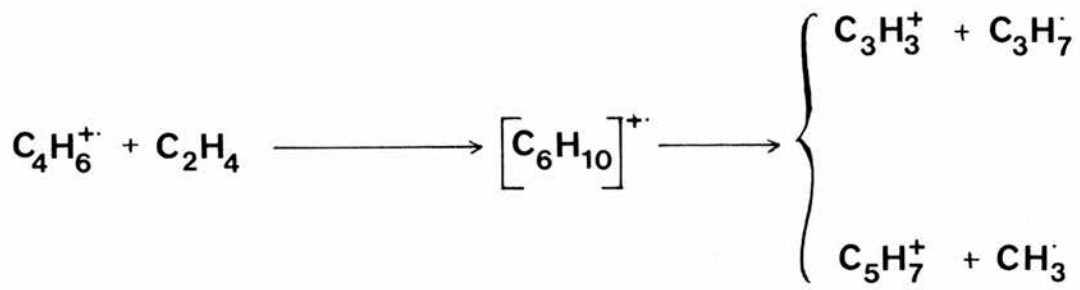

SCHEME 59

The largest of these four ions, is that at m/z = 82, observed at high pressures due to collisional stabilisation of the reaction complex (1·17). We cannot say whether a Diels-Alder type

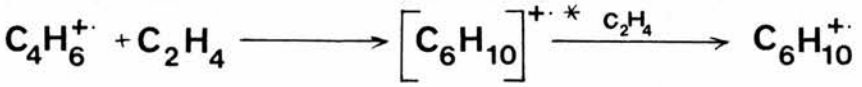

1.17

cycloaddition is involved here, but the recent evidence of Gross et al[123] (using ^{2}H and ^{13}C labelling) suggests that this is not the case. It has been postulated[124] that this reaction proceeds either through an acyclic intermediate, or via a [3+2] cycloaddition as shown below (Scheme 60).

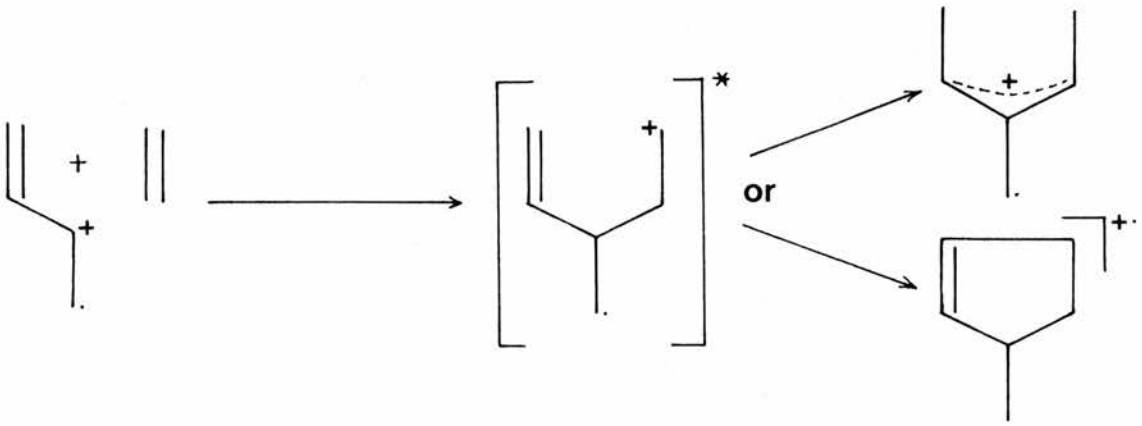

SCHEME 60

Note however, that the reaction between the 1,3-butadiene radical cation and vinyl methyl ether does react via a Diels-Alder type [4+2] cycloaddition[125].

$C_4H_5^+$ is the second largest of these ions and is the product of the familiar hydrogen transfer reaction between the two primary reactants.

The two remaining ions under consideration are m/z = 41 and 69, which we have already shown to be interrelated in an atmosphere of ethene (see page 68). In view of the minor nature of these ions, and the results of several additional reactions involving ethene as collision gas, we can determine their derivation. $C_3H_5^+$ (m/z = 41) could be a product of the breakdown of the transition complex $(C_6H_{10})^{*\cdot+}$, but its non-appearance at the lowest pressures suggests that it is a tertiary ion. $C_3H_3^+$ is the obvious precursor for $C_3H_5^+$, and examination of our earlier results for the reaction of $C_3H_3^+$ with ethene, shows that $C_3H_5^+$ is indeed the major product of this reaction; and yet again the low reactivity of $C_3H_3^+$ suggests that it has the cyclopropenyl structure. $C_3H_5^+$ may then react with ethene in the known reaction to give rise to $C_5H_9^+$ (m/z = 69), but the relative abundances of these two ions suggests differently, and the greatest proportion of $C_5H_9^+$ must arise from the further reaction of the largest secondary ion ($C_5H_7^+$ - Scheme 61). The remaining minor ions are also presumed to be products of the tertiary reactions shown in Scheme 61.

$$C_3H_3^+ + C_2H_4 \longrightarrow \left[C_5H_7\right]^{+*} \longrightarrow C_3H_5^+ + C_2H_2$$

$$C_5H_7^+ + C_2H_4 \longrightarrow \left[C_7H_{11}\right]^{+*} \longrightarrow C_5H_9^+ + C_2H_2$$

SCHEME 61

Having just studied the cross reactions between butadiene and ethene, it is interesting to compare these results with those for the butadiene/ethyne systems.

When ethyne is used as the primary ion, the results (Table 55) are similar to those using ethene or butadiene radical cation (Table 53). The only noticeable difference between the tables being the much greater proportion of $C_3H_3^+$ found in this reaction. This we can put down to the greater ionisation potential of ethyne (11·4 eV for $C_2H_2^{+\cdot}$ cf. 10·5 eV ($C_2H_4^{+\cdot}$) and 9·1 eV ($C_4H_6^{+\cdot}$)), energy which will be transferred as excess internal energy on collision, making the fragmentation of the butadiene charge-exchange product much more likely. Otherwise the reaction sequence is as previously discussed - charge-exchange followed by the butadiene ion-molecule reaction.

m/z	26	39	53	54	55	66	67	79	80	81	91	93	109	121
Pressure ion	$C_2H_2^{+\cdot}$	$C_3H_3^+$	$C_4H_5^+$	$C_4H_6^{+\cdot}$	$C_4H_7^+$	$C_5H_6^{+\cdot}$	$C_5H_7^+$	$C_6H_7^+$	$C_6H_8^{+\cdot}$	$C_6H_9^+$	$C_7H_7^+$	$C_7H_9^+$	$C_8H_{13}^+$	$C_9H_{13}^{+\cdot}$
5×10^{-3} Torr	P	40	7	1	1	1	16	2	5	3	2	10	3	4

TABLE 55: The Ions Observed in the Reaction Between Ethyne Radical Cation and Butadiene (% Total Secondary Ion Current)

When butadiene is the impacting ion, the spectrum is very much simpler, with only five secondary ions observed at the highest pressure (Table 56). These ions are as expected, although the proportions are not. If we compare these results with those for

	m/z	28	39	53	54	65	79
Pressure	ion	$C_2H_4^{+\cdot}$	$C_3H_3^+$	$C_4H_5^+$	$C_4H_6^+$	$C_5H_5^+$	$C_6H_7^+$
5×10^{-3}		1	79	6	P	1	15

TABLE 56: The Ions Observed in the Reaction Between Butadiene Radical Cation and Ethyne (% Total Secondary Ion Current)

butadiene radical cation/ethene (Table 54) and ethene radical cation/ethyne (Table 51), we see that the methyl radical loss process (1·18) is reduced to virtually nil.

$$C_4H_6^{+\cdot} + C_2H_2 \longrightarrow \left[C_6H_8\right]^{+\cdot *} \longrightarrow C_5H_5^+ + CH_3^{\cdot} \qquad 1.18$$

Of the other ions; m/z = 79 is the hydrogen loss product, analogous to $C_4H_5^+$ as observed in the ethene/ethyne systems (Scheme 56); m/z = 53 itself is due to the commonly observed hydrogen transfer between the primary reactants; m/z = 28 may be the result of the breakdown of the transition complex (Scheme 62), or it may be the product of the CAD of the impacting $C_4H_6^{+\cdot}$ species (Scheme 63); and $C_3H_3^+$ may also be the product of the two reactions indicated in Schemes 62 and 63 (the lack of reactivity again indicates that the cyclopropenyl ion is produced).

$$C_4H_6^{+\cdot} + C_2H_2 \longrightarrow \left[C_6H_8\right]^{+\cdot *} \longrightarrow \begin{cases} C_6H_7^+ + H^{\cdot} \\ C_5H_5^+ + CH_3^{\cdot} \\ C_3H_3^+ + C_3H_5^{\cdot} \\ C_2H_4^{+\cdot} + C_4H_4 \end{cases}$$

SCHEME 62

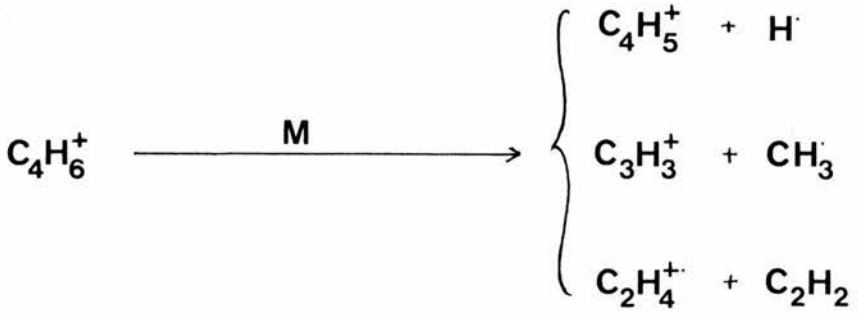

SCHEME 63

Mechanistically this reaction cannot be easily explained using the type of intermediates postulated by Gross et al[123] (see Scheme 60) . Indeed, mechanistically the production of $C_3H_3^+$ from this reaction scheme, especially via the acyclic intermediate, does not appear very obvious. Also, the elimination of CH_3· from these intermediates (structures K and L in this case) looks to be facile, but this process has already been shown to be virtually non-existent. Accordingly, we believe that this reaction must proceed via either a Diels-Alder type [4+2] cycloaddition (structure M) or via a linear transition complex (N), but without access to

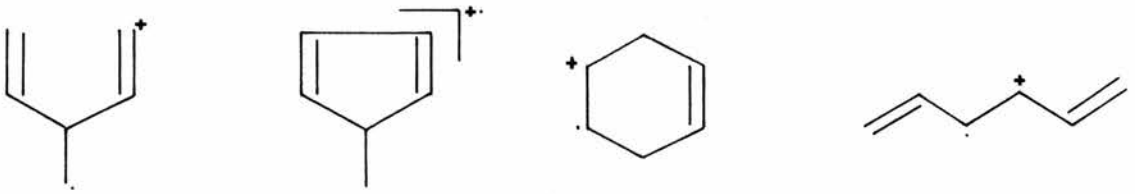

K L M N

labelling experiments we cannot pass any further comments of the structure of this intermediate.

Several other systems involving the $C_4H_6^{+\cdot}$ ion were investigated briefly, concerned mainly with the previously mentioned

use of reactive ion-molecule reactions to determine ion structures (page 92).

The first of these follows on from the cross reactions between the various butene isomers, which indicated that the structure of the collision molecule had a greater influence on the observed spectra than the assumed different structures of the isomeric primary ions. Isobutene was chosen as the cross-reactant with butadiene since it was the only butene radical cation isomer which showed clear evidence of structure retention on ionisation (Table 41).

Table 57, below shows the results obtained for the cross reactions between isobutene and butadiene, and includes the individual ion-molecule reactions for both compounds.

m/z	39	41	54	55	56	57	66	67	69	70	71	79	80	81	93
Reaction ion	$C_3H_3^+$	$C_3H_5^+$	$C_4H_6^{+\cdot}$	$C_4H_7^+$	$C_4H_8^+$	$C_4H_9^+$	$C_5H_6^+$	$C_5H_7^+$	$C_5H_9^+$	$C_5H_{10}^{+\cdot}$	$C_5H_{11}^+$	$C_6H_7^+$	$C_6H_8^{+\cdot}$	$C_6H_9^+$	$C_7H_9^+$
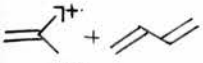	-	3	29	8	P	-	5	17	-	-	-	10	11	2	11
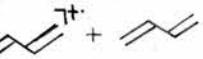	10	-	P	1	-	-	2	26	-	-	-	6	12	3	24
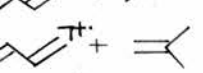	8	-	P	-	20	44	-	2	2	2	4	-	1	4	-
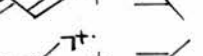	-	2	-	1	P	87	-	-	1	2	5	-	-	-	-

TABLE 57: The Ions Found in the Cross Reactions of Butadiene Radical Cation and Isobutene Radical Cation with Butadiene and Isobutene (% Total Secondary Ion Signal)

In the system initiated by isobutene radical cation, we see that this reaction proceeds via charge-exchange, to give a spectrum very similar to the butadiene ion-molecule raction. Only one additional peak is observed at m/z = 41; the ion $C_3H_5^+$, produced

by the collision induced loss of methyl radical from the primary ion.

The reverse cross reaction shows features common to both the butadiene radical cation and the isobutene neutral molecule. The ion at m/z = 39 is due to methyl radical loss from the butadiene radical cation on collision with isobutene, but this in itself does not prove that $C_4H_6^{+\cdot}$ has retained the 1,3-butadiene structure; and the other secondary ions do not offer any further clues to this. m/z = 56 corresponds to the charge-exchange product, but without ^{13}C labelling this cannot be confirmed. (On all previous evidence this product should not be detected, since the impacting ion has the lower ionisation potential, albeit by only 0·16 eV). $C_4H_9^+$ (m/z = 57) is by far the most abundant ion, and is the product of proton transfer from the primary ion to the isobutene molecule, which has already been shown to have a strong proton affinity.

The remaining ions listed in Table 57 are products of the breakdown of the transition complex, with the exception of m/z = 69, 70 and 71 which can be assigned (at least in part) to the further reaction of the $C_4H_8^{+\cdot}$ ion with isobutene. However, whether this reaction complex is cyclic (O) or acyclic (P or Q) we cannot say with any certainty.

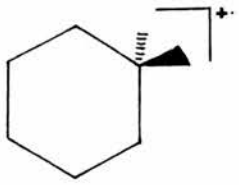

O

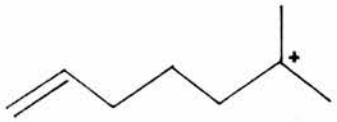

P

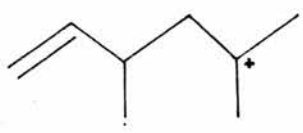

Q

The second of these brief investigations involving the $C_4H_6^{+\cdot}$ ion, is the but-2-yne ion-molecule reaction discussed below. This system shows some interesting differences from the butadiene ion-molecule reaction (Table 58).

m/z	39	53	54	55	67	77	79	80	81	91	93	107	109	121
Reaction ion	$C_3H_3^+$	$C_4H_5^+$	$C_4H_6^{+\cdot}$	$C_4H_7^+$	$C_5H_7^+$	$C_6H_5^+$	$C_6H_7^+$	$C_6H_8^{+\cdot}$	$C_6H_9^+$	$C_7H_7^+$	$C_7H_9^+$	$C_8H_{11}^+$	$C_8H_{13}^+$	$C_9H_{13}^+$
but-2-yne ion-molecule	19	3	P	28	8	4	2	-	4	5	17	3	-	-
1,3-butadiene ion-molecule	7	1	P	3	26	-	11	17	2	1	22	-	2	1

TABLE 58: The Ions Observed in the Isomeric but-2-yne and 1,3-butadiene ion-molecule Reactions (% Total Secondary Ion Current

The ion of lowest mass in the above table is $C_3H_3^+$ (m/z = 39), which is more abundant in the but-2-yne system. This ion arises from the CAD of the primary ion, and the greater proportion of $C_3H_3^+$ with but-2-yne may be due to the neutral structures involved, implying that we are observing the reaction of two different $C_4H_6^{+\cdot}$ ions. This is contrary to the results of Werner and Baer[126], Jarrold et al[119] and Russell et al[127], who suggest that $C_4H_6^{+\cdot}$ radical cations from all seven possible C_4H_6 isomers undergo rapid isomerisation prior to fragmentation (probably to the 3-methylcyclopropene ion); but is in agreement with the results of Preuninger and Farrar[120], who suggest that this isomerisation occurs for all the $C_4H_6^{+\cdot}$ cations except the butynes.

The next significant difference is in the relative abundance of the proton transfer product $C_4H_7^+$ (m/z = 55), which is again favoured by but-2-yne. This could be due to the carbon-carbon triple bond offering a greater proton affinity than the inherently more stable conjugated double bonds in 1,3-butadiene. Butyne also favours the three secondary ions at m/z = 77, 91 and 107. Of these, $C_8H_{11}^+$ (m/z = 107) corresponds to hydrogen loss from the transition complex, but both $C_6H_5^+$ (m/z = 77) and $C_7H_7^+$ (m/z = 91) require the production of two neutral products if they are secondary ions (see Scheme 64); and it could be that these are infact tertiary ions, products of the further reaction of $C_3H_3^+$, (Scheme 65). Assuming our speculation that but-2-yne does not isomerise to the 3-methylcyclopropenyl cation is correct, then $C_3H_3^+$ in this case is almost certainly the more reactive propargyl ion, making Scheme 65 much more likely. (These ions are very

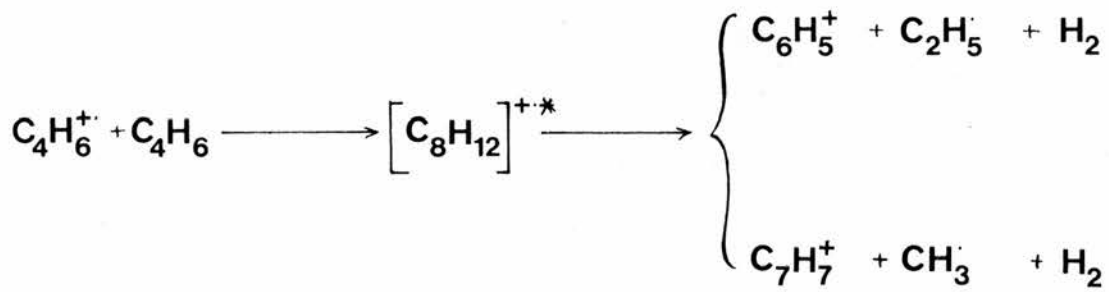

SCHEME 64

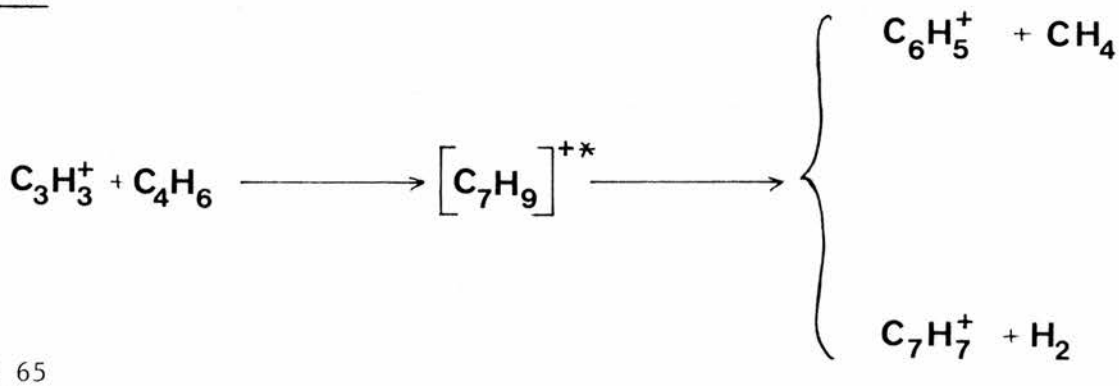

SCHEME 65

definitely tertiary in the butadiene ion-molecule reaction, as evinced by their non-appearance until higher pressures.)

The butadiene ion-molecule reaction on the other hand shows increased abundances of the three ions at m/z = 67, 79 and 80, which we can attribute to the two systems having very different reaction complexes, though we can again only speculate as to the structures involved - see R and S below.

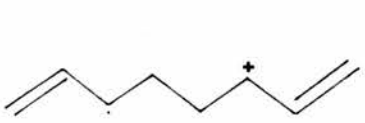

R

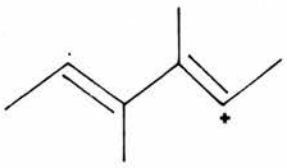

S

The above are possible structures* for the $C_8H_{16}^{+\cdot}$ reaction complex formed in the two $C_4H_6^{+\cdot}/C_4H_6$ systems under discussion - R from 1,3-butadiene and S from but-2-yne - which allow us to explain the increased abundances for $C_5H_7^+$, $C_6H_7^+$ and $C_6H_8^{+\cdot}$ found in the butadiene ion-molecule reaction. Simple bond scission can be applied to R to give the observed ions, but the same is not true of structure S without skeletal rearrangement.

The final ion to be investigated in this series of experiments involving the ion-molecule reactions of unsaturated hydrocarbons is $C_5H_8^{+\cdot}$, in the two isomeric forms; isoprene (2-methyl 1,3-butadiene) and pent-1-yne.

---

*It is not possible to say whether the reaction complex for butadiene is linear, branched or cyclic, but S is the only structure possible assuming that the but-2-yne radical retains its structure on ionisation, as we have already discussed.

The isoprene ion-molecule reaction was first to be studied, and this will be discussed briefly in isolation before we move on to compare it with the isomeric system of pentyne and the homologous system of butadiene.

Table 59 displays the total ion abundances for the isoprene ion-molecule reaction at low, medium and high pressures for the twelve major ions. Two ions are observed at mass lower than that of the primary ion. The first of these at m/z = 67 is formed as a result

m/z	53	67	68	69	80	81	93	94	95	107	108	121
Pressure ion	$C_4H_5^+$	$C_5H_7^+$	$C_5H_8^{+\cdot}$	$C_5H_9^+$	$C_6H_8^{+\cdot}$	$C_6H_9^+$	$C_7H_9^+$	$C_7H_{10}^{+\cdot}$	$C_7H_{11}^+$	$C_8H_{11}^+$	$C_8H_{12}^{+\cdot}$	$C_9H_{13}^+$
low (2×10^{-4} Torr)	-	14	978	-	1	3	2	-	1	-	-	-
medium (1.7×10^{-3}Torr)	2	22	856	-	15	32	48	19	9	15	6	4
high ($6\cdot4\times10^{-3}$Torr)	20	46	314	41	14	315	45	34	57	46	26	13

TABLE 59: The Ions Observed in the Isoprene Ion-Molecule Reaction at Low, Medium and High Pressures (% Total Ion Signal)

of a hydrogen transfer from the primary ion to the collision molecule (a reaction observed in all the unsaturated systems studied). The second "low mass" ion is $C_4H_5^+$ (m/z = 53), which does not behave as a secondary ion, since it does not appear until medium-to-high pressures. This ion corresponds to the methyl radical loss process (CAD of the primary ion) found in all the previous systems in varying degrees, but in view of the skeletal structure of isoprene, its low abundance and tertiary nature are rather surprising. One possible reason for this could be that $C_5H_8^{+\cdot}$ undergoes isomerisation to a structure without the "isolated" methyl of isoprene. This will

be discussed more fully in the comparisons with other systems. The nine "high mass" ions, all of which display apparent secondary behaviour, and their probable derivations are listed in Table 60 below.

ion	m/z	derivations
$C_5H_9^+$	69	Proton transfer: $C_5H_8^{+\cdot} + C_5H_8 \longrightarrow C_5H_9^+ + C_5H_7\cdot$
$C_6H_8^{+\cdot}$	80	Breakdown of reaction complex: $C_{10}H_{16}^{+\cdot} \longrightarrow C_6H_8^{+\cdot} + C_4H_8$
$C_6H_9^+$	81	" $C_{10}H_{16}^{+\cdot} \longrightarrow C_6H_9^+ + C_4H_7\cdot$
$C_7H_9^+$	93	" $C_{10}H_{16}^{+\cdot} \longrightarrow C_7H_9^+ + C_3H_7\cdot$
$C_7H_{10}^+$	94	" $C_{10}H_{16}^{+\cdot} \longrightarrow C_7H_{10}^{+\cdot} + C_3H_6$
$C_7H_{11}^+$	95	" $C_{10}H_{16}^{+\cdot} \longrightarrow C_7H_9^+ + C_3H_5\cdot$
$C_8H_{11}^+$	107	" $C_{10}H_{16}^{+\cdot} \longrightarrow C_8H_{11}^+ + C_2H_5\cdot$
$C_8H_{12}^{+\cdot}$	108	" $C_{10}H_{16}^{+\cdot} \longrightarrow C_8H_{12}^{+\cdot} + C_2H_4$
$C_9H_{13}^+$	121	" $C_{10}H_{16}^{+\cdot} \longrightarrow C_9H_{13}^+ + CH_3\cdot$

TABLE 60: The "High Mass" Ions Found in the Isoprene Ion-Molecule Reaction and their Probable Derivations

The comparison of the isoprene ion-molecule reaction with that of butadiene shows a number of similarities in the products observed (Table 61), as does the comparison with pentyne (Table 62).

m/z	39	53	54	55	66	67	68	69	79
Reaction ion	$C_3H_3^+$	$C_4H_5^+$	$C_4H_6^{+\cdot}$	C_4H_7	$C_5H_6^{+\cdot}$	$C_5H_7^+$	$C_5H_8^{+\cdot}$	$C_5H_9^+$	$C_6H_7^+$
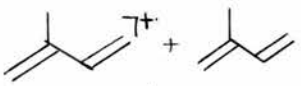	-	3	-	-	-	7	P	6	-
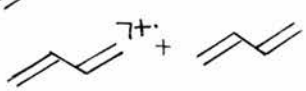	10	1	P	1	2	26	-	-	6

TABLE 61: A Comparison of the Major Ions Found in the Isoprene and 1,3-butadiene Ion-Molecule Reactions (% Total Secondary Ion Signal)

m/z	80	81	93	94	95	107	108	121
Reaction ion	$C_6H_8^{+\cdot}$	$C_6H_9^+$	$C_7H_9^+$	$C_7H_{10}^{+\cdot}$	$C_7H_{11}^+$	$C_8H_{11}^+$	$C_8H_{12}^{+\cdot}$	$C_9H_{13}^+$
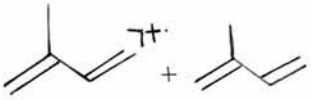	2	46	7	5	8	7	4	2
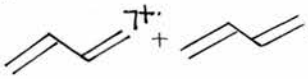	12	3	24	-	-	-	-	4

TABIE 61: Continued

Looking first at Table 61;both systems show two fragmentation ions, corresponding to hydrogen loss and methyl loss, but the relative abundances of these differ markedly. As mentioned directly above, the low abundance of the methyl radical loss product in isoprene (m/z = 53) is surprising, especially in view of the methyl group present in the neutral structure (conversely, the high abundance of the anal gous product ion in butadiene (m/z = 39) is equally unlikely when the 1,3-butadiene structure is considered), and this low abundance can be attributed to the isomerisation of the $C_5H_8^{+\cdot}$ radical cation. No references could be found to the structure of this ion (unlike $C_4H_6^{+\cdot}$ which is well documented[119,126,127], and it is suggested that this ion adopts the cyclopentene structure (T) before fragmentation. This would account for the low abundance of m/z = 53, and also the higher abundance of both m/z = 67 and 69, when compared with the analogous products in butadiene (m/z = 53, 55).

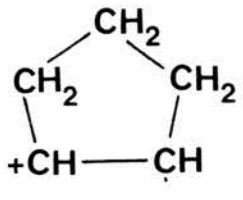

T

The ions at masses above that of the primary ion show the influence of the collision molecule upon the observed spectra. Both systems involve a conjugated 1,3-diene, and allowing for the extra methyl group in isoprene, we can cross-relate all these higher mass ions. By adding 14 mass units (for the methyl substituent on the primary ion) to each of the ions in the butadiene ion-molecule spectrum, we obtain the ions observed in the isoprene ion-molecule reaction (eg 79, 80 and 81 become 93, 94 and 95). There are two exceptions to this rule; at m/z = 108 and 121. The first of these, $C_8H_{12}^{+\cdot}$, is due to ethene loss from the $C_{10}H_{16}^{+\cdot}$ reaction complex, which has a direct equivalent in the butadiene ion-molecule reaction at m/z = 80. (This latter ion is also equivalent to m/z = 94 - propene loss - in the isoprene system.). Similarly, $C_9H_{13}^{+}$ (m/z = 121) arises from the loss of methyl radical from the transition complex, and is directly equivalent to the methyl loss product in butadiene at m/z = 93 ($C_7H_9^{+}$). $C_9H_{13}^{+}$ also appears in the butadiene ion-molecule reaction where it is a tertiary product (reaction 1·16). No equivalent tertiary ion is found in the isoprene system.

m/z	40	41	53	67	68	69	79	80
Reaction ion	$C_3H_4^{+\cdot}$	$C_3H_5^{+}$	$C_4H_5^{+}$	$C_5H_7^{+}$	$C_5H_8^{+\cdot}$	$C_5H_9^{+}$	$C_6H_7^{+}$	$C_6H_8^{+\cdot}$
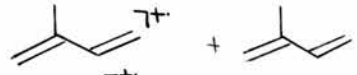	-	-	3	7	P	6	-	2
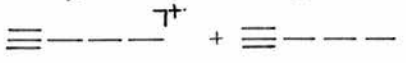	2	3	6	30	P	7	6	2

TABLE 62: A Comparison of the Major Ions Found in the Isoprene and pent-1-yne ion-molecule Reactions (% Total Secondary Ion Current) at Approximately Equal Pressures

m/z	81	83	93	94	95	107	108	121
Reaction ion	$C_6H_9^+$	$C_6H_{11}^+$	$C_7H_9^+$	$C_7H_{10}^{+\cdot}$	$C_7H_{11}^+$	$C_8H_{11}^+$	$C_8H_{12}^{+\cdot}$	$C_9H_{13}^+$
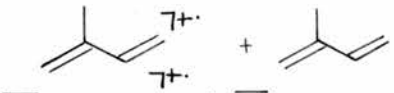	46	-	7	5	8	7	4	2
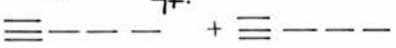	11	2	6	3	7	7	-	-

TABLE 62: Continued

The pentyne ion-molecule reaction, when compared with that of isoprene (Table 62), shows several differences in the important low mass area, which we have shown to be indicative of the primary ion structure. Additional ions are observed at m/z = 40 and 41 with pentyne, as well as enhanced abundances of the two important low-mass ions at m/z = 53 and 67 (similar enhancements were found when butyne and butadiene were compared - Table 58), indicating that isoprene and pent-1-yne radical cations have distinct structures. In the "high-mass" part of the spectrum, the differences are less obvious than those in the $C_4H_6^{+\cdot}$ spectra. Pentyne displays two extra ions at m/z = 79 and 83, whilst the isoprene spectrum contains two ions (m/z = 108 and 121) not observed with pentyne. Isoprene also produces a much stronger signal at m/z = 81, probably as a result of differences in structure in the reaction complexes.

The cross reactions between the two C_5H_8 isomers were also investigated, with the results displayed in Table 63, but these show the major reaction in both cases is charge-exchange - the spectrum for the pentyne ion-molecule reaction being very like the pentyne radical cation/isoprene reaction, and the isoprene ion-molecule reaction similar to the reverse cross reaction. As such we can

m/z	40	41	53	67	68	69	79	80	81
Reaction ion	$C_3H_4^{+\cdot}$	$C_3H_5^+$	$C_4H_5^+$	$C_5H_7^+$	$C_5H_8^+$	$C_5H_9^+$	$C_6H_7^+$	$C_6H_8^{+\cdot}$	$C_6H_9^+$
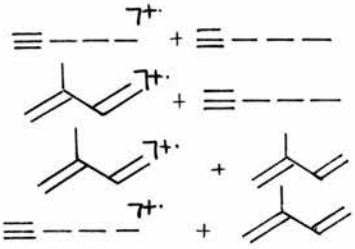	2	3	6	30	P	7	6	2	11
	2	3	5	28	P	7	6	1	11
	-	-	3	7	P	6	-	2	46
	-	-	2	8	P	6	-	2	39

TABLE 63: The Ions Observed in the Cross Reaction Between the Two C_5H_8 Isomers; Isoprene and Pentyne (% Total Secondary Ion Signal)

m/z	83	93	94	95	107	108	121
ion	$C_6H_{11}^+$	$C_7H_9^+$	$C_7H_{10}^{+\cdot}$	$C_7H_{11}^+$	$C_8H_{11}^+$	$C_8H_{12}^{+\cdot}$	$C_9H_{13}^+$
	2	6	3	7	7	-	-
	2	7	4	6	8	-	-
	-	7	5	8	7	4	2
	-	8	6	8	8	4	4

TABLE 63: Continued

say nothing further about the two $C_5H_8^{+\cdot}$ ions.

The cross reactions between isoprene and ethene display the expected behaviour (see Table 64 below); with charge-exchange the result using ethene radical cation, and complex formation/breakdown with isoprene radical cation.

m/z	28	41	53	54	55	66	67	68	69
Reaction ion	$C_2H_4^{+\cdot}$	$C_3H_5^+$	$C_4H_5^+$	$C_4H_6^{+\cdot}$	$C_4H_7^+$	$C_5H_6^+$	$C_5H_7^+$	$C_5H_8^{+\cdot}$	$C_5H_9^+$
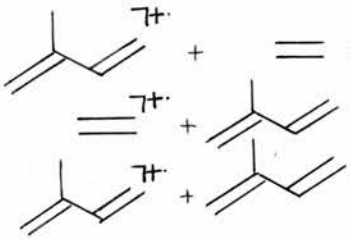	-	2	4	1	1	2	32	P	-
	P	1	7	-	1	-	10	6	7
	-	-	3	-	-	-	7	P	6

TABLE 64: The Ions Observed in the Cross Reaction Between Isoprene and Ethene Radical Cations and Ethene and Isoprene (% Total Secondary Ion Signal)

m/z	80	81	83	93	94	95	107	108	121
ion	$C_6H_8^{+\cdot}$	$C_6H_9^+$	$C_6H_{11}^+$	$C_7H_9^+$	$C_7H_{10}^{+\cdot}$	$C_7H_{11}^+$	$C_8H_{11}^+$	$C_8H_{12}^{+\cdot}$	$C_9H_{13}^+$
	2	55	1	-	-	-	-	-	-
	2	33	-	5	4	6	6	4	3
	2	46	-	7	5	8	7	4	2

TABLE 64: Continued

The close similarity of the ethene radical cation/isoprene and the isoprene ion-molecule spectra, again shows how the ionisation potential of the impacting ion promotes the charge-exchange process if it is greater than that of the collision molecule. The reverse cross reaction between isoprene radical cation and ethene shows some similarities with the butadiene radical cation/ethene system (Table 54). In both cases two very strong secondary ions are observed (one at "low mass" and the other at "high mass"), which together constitute over 80% of the secondary signal. The "high mass" ion in both cases is due to methyl loss from the reaction complex, but the "low mass" ions are different. In the case currently under discussion (isoprene$^{+\cdot}$/ethene), the major "low mass" ion is associated with the collisionally induced hydrogen loss process (with a much smaller

contribution from the methyl loss process - see Scheme 66). However, this situation is reversed in the butadiene$^{+\cdot}$/ethene system, where

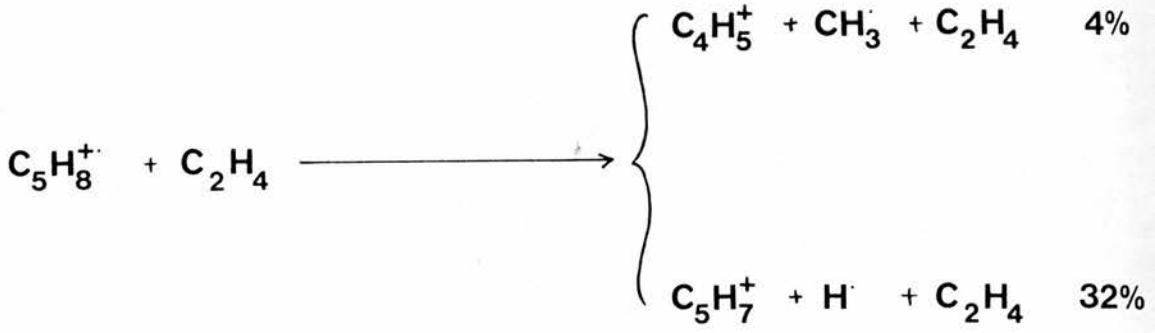

SCHEME 66

methyl loss is the major process (Scheme 67).

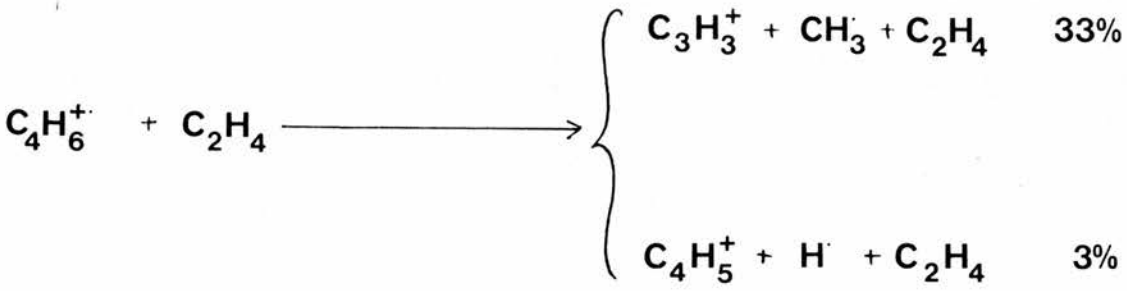

SCHEME 67

These differences in the fragmentation region of the spectra confirm that 1,3-butadiene and isoprene adopt dissimilar structures on ionisation (using 70V electrons). That $C_4H_6^{+\cdot}$ (from 1,3-butadiene) adopts the 3-methylcyclopropene structure has been widely discussed[119, 120,126,127], and the ease with which methyl is lost from this ion in this series of experiments endorses this opinion. $C_5H_8^{+\cdot}$ (from isoprene) on the other hand shows reluctance to eliminate methyl radical, preferring instead to lose hydrogen, behaviour which leads us to believe that this ion also isomerises on ionisation, but to the

cyclopentene radical cation (T), rather than the analogous dimethylcyclopropene radical cation (U and/or V).

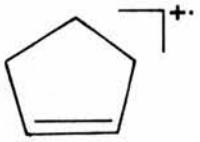

T

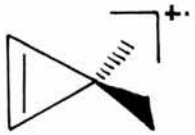

U

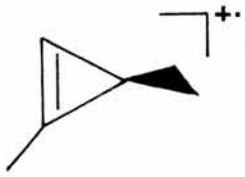

V

These results again illustrate the use of reactive collisions as a means of differentiating between primary ionic structures; although since the fragmentation region of the spectrum is of most use in this process, we are in effect using small unsaturated hydrocarbon molecules for CAD.

The last experiment in our investigation of the ion-molecule reactions of unsaturated hydrocarbons involves the cross reactions between butadiene and isoprene. These results, summarised in Table 65, show clearly that charge-exchange, followed by the isoprene ion-molecule reaction is the only important pathway in the reaction between 1,3-butadiene radical cations and isoprene. The reverse reaction also gives a spectrum which is similar in many ways to the collision molecule's ion-molecule reaction, but there is no evidence that this occurs as a major process. In particular, the abundance of the charge-exchange product (m/z = 54) fails to

m/z	39	53	54	55	67	68	69	79	80
Reaction ion	$C_3H_3^+$	$C_4H_5^+$	$C_4H_6^{+\cdot}$	$C_4H_7^+$	$C_5H_7^+$	$C_5H_8^{+\cdot}$	$C_5H_9^+$	$C_6H_7^+$	$C_6H_8^{+\cdot}$
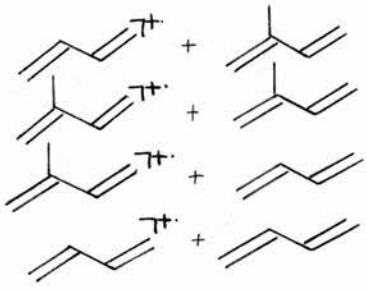	3	2	P	-	3	4	10	1	2
	-	3	-	-	7	P	6	1	2
	1	2	2	4	27	P	-	3	9
	10	1	P	1	26	-	-	6	12

TABLE 65: The Ions Observed in the Cross Reaction Between Butadiene and Isoprene Radical Cations and Isoprene and Butadiene (% Total Secondary Ion Current)

m/z	81	93	94	95	107	108	109	121
ion	$C_6H_9^+$	$C_7H_9^+$	$C_7H_{10}^{\pm}$	$C_7H_{11}^+$	$C_8H_{11}^+$	$C_8H_{12}^{+\cdot}$	$C_8H_{13}^+$	$C_9H_{13}^+$
	35	4	5	6	6	3	1	3
	46	7	5	8	7	4	-	2
	7	25	-	-	7	-	2	1
	3	24	-	-	-	-	4	5

TABLE 65: Continued

rise above 3% of the total ion signal, compared with over 22% in the reverse reaction.

The significance of the five peaks in the "low mass" region of this spectrum is difficult to interpret due to the overlap between the isoprene "low mass" and butadiene "high mass" regions. $C_4H_6^{+\cdot}$ is likely to be due to charge-exchange occurring as a minor process, probably via a loosely bound transition state. This would also account for the presence of $C_3H_3^+$ (m/z = 39) in this spectrum. The ions at m/z = 53 and 67 are characteristic of the isoprene radical cation, and although they also appear in the butadiene ion-

molecule reaction, both ions show an enhanced abundance over this latter reaction. $C_4H_7^+$ (m/z = 55) on the other hand, is characteristic of the butadiene ion-molecule reaction, but again this shows an enhanced abundance, and is due to the transfer of a proton from the primary ion to butadiene.

The "high mass" ions are also similar to the ions found in the butadiene ion-molecule reaction, with m/z = 93 ($C_7H_{11}^+$) the largest ion. This is associated with the co-production of the $C_2H_3\cdot$ radical species, probably as a result of simple bond scission in the butadiene part of the transition complex. Of the other ions, $C_6H_9^+$ (m/z = 81) and $C_8H_{11}^+$ (m/z = 107) are the most significant. Again both show enhanced abundances, and are associated with the co-production of stable radicals ($C_3H_5\cdot$ and $CH_3\cdot$) in the breakdown of the reaction complex ($C_9H_{14}^{+\cdot}$). All these factors imply that the expected associative reaction is observed in this system (with a minor charge-exchange channel also observed - the ionisation potentials are in fact relatively close: 9·07 eV butadiene; 8·85 eV isoprene), but as in the case of the butene reactions, it is increasingly difficult to interpret these results, and it seems likely that systems involving larger molecules will prove even more difficult to fully understand.

RESULTS (Tabulated)

TABLE 1: $CH_4^{+\cdot}$ REACTING WITH THE N-ALKANES (NORMALISED SECONDARY SIGNAL)

m/z	28	29	41	42	43	55	56	57	58	69	70	71	72	83	84	85	86	98	99	100	112	113	114	127	128	142
Collision Molecule																										
n- butane	5.6	8.8	1.7	15.5	100	-	3.3	12.1	39.8																	
n- pentane	-	1.9	1.9	85.1	100	-	4.6	18.3	-	-	13.9	8.4	33.1													
n- hexane	-	2.2	5.0	25.5	42.4	1.7	72.5	100	1.0	2.2	2.1	8.5	0.7	-	6.4	8.5	31.8									
n- heptane	-	1.9	4.0	15.2	67.5	1.9	46.5	83.4	-	-	53.7	100	-	-	-	3.5	-	1.9	2.1	37.1						
n- octane	-	1.1	2.4	5.5	59.5	2.2	27.5	65.9	-	2.2	27.1	66.7	0.5	-	26.8	100	-	-	-	-	1.3	1.9	15.5			
n- nonane	-	0.7	0.9	2.1	27.2	1.1	13.4	100	-	2.1	14.8	37.3	-	2.1	14.3	41.3	0.8	6.2	12.5	-	-	-	-	0.7	0.5	
n- decane	-	0.9	1.2	2.3	25.0	1.1	11.4	100	3.5	2.1	11.5	50.2	-	0.9	13.3	33.2	-	6.8	10.0	-	2.8	4.5	-	-	-	51.6

TABLE 2: CH_3^+ REACTING WITH THE N-ALKANES (NORMALSED SECONDARY SIGNAL)

m/z	27	29	41	42	43	44	55	57	69	71	72	83	85	86	97	98	99	100	113	114	128	142
Collision Molecule																						
n- butane	4.9	53.1	59.9	-	32.0	-	2.5	100														
n- pentane	1.6	9.0	4.7	0.9	100	-	1.8	3.2	-	19.7	0.7											
n- hexane	2.1	4.7	7.3	0.8	100	-	3.1	19.9	-	1.0	-	1.0	17.1	1.5								
n- heptane	1.5	4.2	5.3	-	31.0	-	1.3	100	-	2.3	-	-	-	-	-	-	-	1.5				
n- octane	1.8	4.5	5.6	-	40.5	-	1.4	100	-	70.3	-	-	2.0	-	-	-	-	-	0.9	1.9		
n- nonane	2.2	6.7	6.9	0.6	62.1	1.1	6.4	100	2.5	92.5	-	-	37.8	-	1.7	1.7	0.9	-	-	-	3.0	
n- decane	2.1	6.2	5.2	-	51.4	2.4	2.1	100	0.9	64.5	-	-	43.2	-	-	-	6.0	-	-	-	-	3.7

TABLE 3: $N_2O^{+\cdot}$, $SO_2^{+\cdot}$, $CD_4^{+\cdot}$ and CD_3^+ IN REACTION WITH N-DECANE (NORMALISED SECONDARY SIGNAL)

m/z	29	30	31	32	41	42	43	44	45	46	54	55	56	57	58	59	60	69	70	71	72	74	82	83	84	85	86	98	99	100	112	113	114	142
Primary Ion																																		
$NO_2^{+\cdot}$	1.4	0.8	-	-	3.9	7.9	100	-	-	-	1.1	4.5	13.8	99.3	1.0	-	-	3.4	6.1	31.7	0.7	-	-	1.1	1.1	5.9	-	0.6	1.1	-	-	-	-	-
$SO_2^{+\cdot}$	-	-	-	-	0.6	4.2	41.4	1.2	-	-	-	2.5	17.7	100	-	-	-	2.8	11.5	43.0	-	-	-	14.6	3.3	14.6	0.7	1.3	1.4	-	-	-	-	-
$CD_4^{+\cdot}$	-	-	-	-	-	6.4	22.9	1.8	-	-	-	4.3	25.1	100	4.6	-	-	2.8	23.6	68.7	0.9	-	0.9	2.1	16.3	32.5	1.6	10.9	10.3	6.9	3.6	3.8	2.9	2.8
CD_3^+	1.3	0.6	0.8	27	1.0	0.8	24.1	2.5	2.2	3.1	-	1.6	1.5	100	1.9	1.3	3.3	2.0	1.1	47.8	0.7	1.0	-	-	-	29.0	-	-	3.1	-	-	-	-	-

TABLE 4: $CH_4^{+\cdot}$ IN REACTION WITH CYCLO-ALKANES (NORMALISED SECONDARY SIGNAL)

m/z	29	41	42	43	54	55	56	57	67	68	69	70	71	72	82	83	84	85	96	97	98	99
Collision Molecule																						
Cyclopentane	1.0	2.0	100	12.4	4.2	72.4	4.4	5.1	-	12.0	7.0	83.0	4.5	0.7								
Methylcyclopentane	1.7	1.2	10.1	8.2	2.1	7.4	100	6.1	-	4.4	39.5	-	-	-	4.6	3.4	17.8	0.8				
Cyclohexane	0.8	1.0	7.7	7.5	1.7	7.6	61.5	1.4	-	2.9	28.2	-	-	-	1.7	6.6	100	-				
Methylcyclohexane	1.3	2.2	4.5	2.7	1.1	18.3	19.3	5.5	1.1	9.3	12.6	18.9	-	-	24.5	100	-	-	-	6.7	71.1	-

TABLE 5: CH_3^+ IN REACTION WITH CYCLOALKANES (NORMALISED SECONDARY SIGNAL)

M/Z	27	29	30	39	41	42	43	44	53	55	56	57	67	68	69	70	71	82	83	84	85	97	98
Collision Molecule																							
Cyclopentane	4.2	1.3	-	1.1	60.0	3.0	34.6	0.4	0.8	15.3	0.9	3.1	1.3	0.7	100	0.8	1.2						
Methyl-cyclopentane	2.4	11.8	-	0.9	27.7	1.2	18.2	-	-	100	3.5	4.4	-	-	5.6	-	-	-	41.2	3.2	0.5	-	-
Cyclohexane	1.2	12.5	0.5	0.8	32.2	0.5	16.0	-	-	87.4	2.9	3.7	-	-	1.5	-	-	-	100	26.7	-	-	-
Methyl-cycloclohexane	0.6	5.1	-	-	13.3	0.6	15.9	-	-	100	0.6	3.3	0.6	-	13.6	-	-	0.6	4.8	-	-	36.3	45.0

TABLE 6: THE REACTION OF $CH_4^{+\cdot}$ WITH ISOBUTANE (2-METHYLPROPANE) AT DIFFERENT COLLISION PRESSURES (NORMALISED SECONDARY SIGNAL)

Pressure (Torr)	M/Z	29	41	42	43	44	56	57	58
6.1×10^{-5}		-	-	77.6	100	-	-	7.0	17.4
1.1×10^{-4}		1.8	1.5	71.6	100	-	2.4	6.6	15.2
4.2×10^{-4}		-	1.5	62.3	100	-	4.8	11.3	16.1
8.4×10^{-4}		1.0	1.4	57.4	100	0.9	8.1	20.1	17.3
2.0×10^{-3}		0.9	1.9	40.8	100	0.7	16.2	49.7	18.0

TABLE 7: THE REACTION OF CH_3^+ WITH ISOBUTANE (2-METHYLPROPANE) AT VARIOUS COLLISION GAS PRESSURES (NORMALISED SECONDARY SIGNAL

Pressure (Torr)	m/z	27	29	30	39	41	42	43	55	56	57	58
5.1×10^{-5}		-	100	-	-	83.1	-	67.5	-	-	88.3	-
1.5×10^{-4}		-	68.1	-	-	100	5.5	61.3	-	-	83.5	-
4.4×10^{-4}		2.2	52.4	0.7	0.7	70.0	2.2	50.9	2.0	-	100	0.7
1.9×10^{-3}		1.0	14.2	-	-	19.6	0.5	18.8	1.4	-	100	-

TABLE 8: THE REACTION OF $CH_4^{+\cdot}$ WITH ISOPENTANE (2-METHYLBUTANE) AT VARIOUS COLLISION GAS PRESSURES (NORMALISED SECONDARY SIGNAL)

Pressure (Torr)	m/z	29	41	42	43	44	55	56	57	58	70	71	72
6.3×10^{-5}		-	-	100	52.8	-	-	38.9	54.4	-	-	13.3	42.6
1.1×10^{-4}		-	2.2	100	57.7	0.5	-	39.7	53.8	0.9	5.0	7.4	31.8
4.4×10^{-4}		1.9	2.3	100	59.4	1.0	-	40.6	52.3	0.6	12.0	20.3	32.8
7.3×10^{-4}		1.2	3.0	100	68.6	-	0.6	43.7	57.7	-	19.7	28.4	32.9
1.4×10^{-3}		1.9	3.5	100	87.6	-	0.6	60.5	75.9	-	39.3	64.2	44.5
2.5×10^{-3}		1.6	3.3	52.1	65.6	0.5	-	52.5	62.5	-	49.1	100	40.1

TABLE 9: THE REACTION OF CH_3^+ WITH ISOPENTANE (2-METHYLBUTANE) AT VARIOUS COLLISION GAS PRESSURES (NORMALISED SECONDARY SIGNAL)

Pressure (Torr) m/z	27	29	41	42	43	44	55	56	57	58	70	71	72
7.0×10^{-5}	-	9.2	3.9	2.9	100	1.3	2.8	-	8.8	-	-	14.8	1.5
1.0×10^{-4}	0.9	6.8	2.4	2.0	100	-	2.7	0.9	9.3	0.9	-	15.9	1.3
4.4×10^{-4}	1.1	6.1	3.4	1.4	100	-	2.6	0.8	9.6	-	-	22.7	1.0
9.1×10^{-4}	0.7	5.3	3.7	1.3	100	-	2.1	0.8	9.6	-	-	28.3	1.4
2.3×10^{-3}	1.1	5.5	5.0	0.9	100	0.5	3.4	1.1	13.4	-	-	72.3	1.9
5.4×10^{-3}	0.8	2.9	2.7	-	43.5	-	2.3	0.9	10.9	-	0.6	100	2.0

TABLE 10: THE EFFECT OF VARYING THE BIAS VOLTAGE ON THE REACTION BETWEEN $CH_4^{+\cdot}$ AND ISOPENTANE (2-METHYLBUTANE) AT CONSTANT PRESSURE (NORMALISED SECONDARY SIGNAL)

Bias Setting m/z	29	41	42	43	44	56	57	58	70	71	72	73
-0.25	16.1	10.8	31.9	100	7.8	11.8	64.0	-	-	-	7.0	-
0.0	2.7	4.6	100	74.5	-	31.4	58.4	2.0	6.8	13.2	14.8	-
+0.25	1.8	2.3	100	59.4	1.0	40.6	52.3	0.5	12.1	20.3	32.8	-
+0.50	1.8	2.3	100	59.2	0.7	43.5	53.7	1.0	14.7	20.6	38.8	-
+0.75	2.7	3.6	100	62.6	1.4	44.5	53.0	1.4	12.2	19.3	33.0	0.8
+1.0	4.2	4.2	100	68.4	0.8	45.9	57.0	0.8	16.9	21.2	30.4	-
+1.25	4.8	4.6	100	70.5	3.2	43.5	51.6	2.0	11.3	24.6	33.0	0.7

TABLE 11: THE EFFECT OF VARYING THE BIAS VOLTAGE ON THE REACTION BETWEEN CH_3^+ AND ISOPENTANE (2-METHYLBUTANE) AT CONSTANT PRESSURE (NORMALISED SECONDARY SIGNAL)

Bias Setting m/z	27	29	41	42	43	44	55	56	57	71	72
-0.25	11.4	35.5	23.9	-	100	-	-	-	22.7		
0.0	1.5	9.7	5.8	1.5	100	-	2.7	-	9.2	14.0	0.7
+0.25	1.1	6.1	3.4	1.4	100	-	2.6	0.8	9.6	26.7	1.0
+0.50	1.3	5.4	4.7	1.5	100	0.7	2.7	0.6	9.3	23.3	1.7
+1.0	2.3	9.7	5.3	3.8	100	1.4	2.7	0.8	13.3	20.7	3.5

TABLE 12: THE EFFECT OF VARYING THE BIAS VOLTAGE ON THE ETHENE ION-MOLECULE REACTION (TOTAL ION CURRENT)

Bias Setting m/z	26	27	28	39	40	41	55
-0.25	6	1	988	1	-	3	-
-0.10	5	1	985	2	-	6	1
0.0	5	2	980	2	-	10	1
+0.10	5	2	973	2	-	16	2
+0.25	3	1	969	1	1	23	2
+0.50	2	1	966	1	1	26	2
+0.75	2	1	974	1	-	21	1
+1.00	1	1	982	1	-	14	1
+1.25	1	-	991	-	-	7	1
+1.50	-	-	994	-	-	5	-

TABLE 13: THE EFFECT OF VARYING THE COLLISION GAS PRESSURE ON THE ETHENE ION-MOLECULE REACTION (TOTAL ION CURRENT)

Bias Setting m/z	26	27	28	29	39	40	41	42	43	53	54	55	56	57	67	68	69	70	71	83	97
5.0×10^{-5}	1	-	992	-	1	-	6	-	-	-	-	1									
1.2×10^{-4}	2	1	976	-	1	1	18	-	-	-	-	2									
4.3×10^{-4}	6	2	870	-	4	3	101	-	-	1	1	9	-	-	2	-	2				
7.2×10^{-4}	8	3	775	-	6	4	168	-	-	1	1	17	-	-	6	-	10				
1.1×10^{-3}	10	4	644	2	9	5	256	-	-	2	2	27	-	-	13	-	25				
1.5×10^{-3}	8	4	537	5	10	6	314	-	-	3	2	32	1	-	22	-	56	1			
2.0×10^{-3}	8	5	365	10	13	7	368	-	2	4	3	50	1	-	46	-	117	-	-	2	
2.5×10^{-3}	8	4	298	12	17	5	344	-	2	6	3	52	1	-	57	-	187	-	-	4	
3.4×10^{-3}	5	5	163	13	21	5	298	-	3	8	4	55	3	-	82	1	327	-	-	8	
4.9×10^{-3}	3	4	82	13	28	3	201	1	2	10	5	52	4	2	105	1	487	-	3	20	
7.8×10^{-3}	-	4	28	8	35	1	103	1	-	13	4	35	7	4	114	-	605	1	3	26	3

TABLE 14: THE EFFECT OF VARYING THE PRESSURE OF THE COLLISION GAS ON THE REACTION BETWEEN $C_2H_2^{+\cdot}$ (DERIVED FROM C_2H_4) & C_2H_4 (TOTAL ION CURRENT)

Pressure (Torr) m/z	26	27	28	29	39	40	41	43	51	52	53	54	55	56	67	69	71	79	83
4.8×10^{-5}	973	-	22	1	2	-	1	-	-	-	1								
1.2×10^{-4}	933	-	52	1	4	-	5	-	1	1	4	-	1						
3.8×10^{-4}	775	-	137	3	12	1	52	-	2	1	10	-	4	-	1	1			
8.8×10^{-4}	513	6	180	11	22	3	188	-	4	3	18	1	19	-	10	20			
2.6×10^{-3}	115	16	90	16	46	5	285	2	5	4	39	3	55	1	76	260			
5.1×10^{-3}	16	8	18	11	64	2	104	-	2	6	48	4	40	4	112	526	2	14	20

TABLE 15: THE EFFECT OF VARYING THE PRESSURE OF THE COLLISION GAS ON THE REACTION BETWEEN $C_2H_3^+$ (DERIVED FROM C_2H_4) AND C_2H_4 (TOTAL ION CURRENT)

Pressure (Torr) m/z	27	29	39	40	41	42	43	51	53	54	55	57	65	67	68	69	71	74	81	83
4.6×10^{-5}	988	9	1	1	-	-	-	-	1											
9.7×10^{-5}	974	21	2	1	1	-	-	-	1											
3.8×10^{-4}	882	92	6	1	13	-	-	-	5	1	1									
7.5×10^{-4}	795	135	10	1	45	-	-	1	9	1	2	-	-	1	-	1				
2.2×10^{-3}	471	201	14	1	205	-	2	1	22	1	8	2	1	18	-	53	-	2		
5.0×10^{-3}	189	161	17	-	235	1	3	-	33	-	13	9	-	56	2	268	1	7	1	5

TABLE 16: THE EFFECT OF VARYING THE PRESSURE OF THE COLLISION GAS ON THE REACTION BETWEEN $C_2H_5^+$ (DERIVED FROM C_2H_6) AND C_2H_4 (TOTAL ION CURRENT)

Pressure (Torr) m/z	27	28	29	39	40	41	42	43	53	54	55	56	57	67	68	69	70	71	83
1.2×10^{-4}	7	2	984	1	-	5	1	-	-	-	1								
6.2×10^{-4}	25	16	878	3	1	58	7	-	1	-	5	1	-	1	-	3			
2.6×10^{-3}	32	18	458	7	5	222	16	2	4	1	20	5	2	39	3	16	5	1	4

TABLE 17: THE EFFECT OF VARYING THE COLLISION GAS PRESSURE ON THE REACTION BETWEEN $C_3H_3^+$ (PROPENE DERIVED) AND C_2H_4 (TOTAL ION CURRENT)

Pressure (Torr) m/z	27	28	29	37	38	39	41	43	51	52	53	65	66	67	68	69	71	77	78	79
8.5×10^{-5}	-	-	-	1	2	988	9	-	-	-	-	1								
5.5×10^{-4}	2	1	1	1	2	924	62	-	2	1	-	4	1							
3.8×10^{-3}	2	5	3	-	2	726	121	3	3	2	3	7	3	19	2	95	1	1	1	6

TABLE 18: THE EFFECT OF VARYING THE COLLISION GAS PRESSURE ON THE REACTION BETWEEN $C_3H_5^+$ (PROPENE DERIVED) AND C_2H_4 (TOTAL ION CURRENT)

Pressure (Torr) m/z	29	39	40	41	43	53	54	55	65	67	68	69	71	79	83	97
4.7×10^{-5}	-	5	-	995												
1.2×10^{-4}	-	8	-	992	-	-	-	-	-	1						
4.3×10^{-4}	2	8	-	984	1	1	-	-	-	2	-	3				
9.9×10^{-4}	5	12	-	950	2	3	-	1	-	7	-	18				
2.9×10^{-3}	7	23	-	700	5	5	-	2	1	48	2	202	2	2		
5.0×10^{-3}	7	29	2	381	8	8	1	3	1	81	3	459	5	6	2	4

TABLE 19: THE EFFECT OF VARYING THE COLLISION GAS PRESSURE ON THE REACTION BETWEEN $C_3H_5^+$ (CIS BUT-2-ENE DERIVED) AND C_2H_4 (TOTAL ION CURRENT)

Pressure (Torr) m/z	29	39	41	43	53	55	67	69	70	71	79
4.0×10^{-5}	1	6	993								
1.0×10^{-4}	1	7	992								
3.8×10^{-4}	3	8	983	1	1	-	1	1			
9.3×10^{-4}	7	14	964	2	2	-	4	7			
2.7×10^{-3}	4	10	919	4	3	-	15	44	1		
4.8×10^{-3}	7	22	672	7	11	2	51	217	-	5	6

TABLE 20: THE EFFECT OF VARYING THE COLLISION GAS PRESSURE ON THE REACTION BETWEEN $C_4H_7^+$ (CIS BUT-2-ENE) AND C_2H_4 (TOTAL ION CURRENT)

Pressure (Torr) m/z	27	29	39	40	41	43	53	54	55	67	68	69	71	79	83	85
9.0×10^{-5}	-	3	3	-	1	-	4	1	989							
6.5×10^{-4}	1	15	4	1	6	1	5	3	965							
2.2×10^{-3}	2	49	8	1	48	4	6	2	814	6	1	14	1	2	43	1

TABLE 21: THE EFFECT OF VARYING THE COLLISION GAS PRESSURE ON THE REACTION BETWEEN $C_5H_9^+$ (DERIVED FROM CYCLOHEXANE) AND C_2H_4 (TOTAL ION CURRENT)

Pressure (Torr) m/z	29	41	55	67	68	69	83	97
9.0×10^{-5}	-	20	2	9	5	964		
5.5×10^{-4}	-	55	4	8	5	928		
3.0×10^{-3}	5	192	43	27	7	701	5	19

TABLE 22: THE EFFECT OF VARYING THE COLLISION GAS PRESSURE ON THE PROPENE ION-MOLECULE REACTION (TOTAL ION CURRENT)

Pressure (Torr) m/z	27	29	39	40	41	42	43	54	55	56	57	67	68	69	70	71	81	83	84	85	97	98	99	111
4.4×10^{-4}	-	-	-	2	8	985	-	-	2	2	-	-	-	1										
9.9×10^{-5}	-	-	-	2	9	974	-	-	5	7	-	-	-	3										
3.6×10^{-4}	-	-	-	2	11	901	11	1	19	30	4	-	-	18	1									
6.7×10^{-4}	1	1	1	2	13	758	47	3	39	63	20	-	1	43	5	-	1	1	-	1	2			
1.2×10^{-3}	1	1	-	2	17	567	87	3	55	88	65	1	2	79	14	1	2	2	-	7	6	-	-	1
2.0×10^{-3}	1	1	1	3	18	333	100	3	62	104	155	2	1	122	33	1	3	4	1	21	18	2	3	6
3.0×10^{-3}	2	2	1	3	16	181	88	2	55	86	218	4	3	134	63	2	6	8	3	47	39	9	13	17
4.0×10^{-3}	2	1	1	4	18	123		1	50	69	244	5	2	119	83	4	7	8	3	66	56	12	24	26

TABLE 23: THE EFFECT OF VARYING THE PRESSURE OF THE COLLISION GAS ON THE REACTION BETWEEN $C_3H_5^+$ (METHYLCYCLOHEXANE DERIVED) AND C_3H_6 (TOTAL ION CURRENT)

Pressure(Torr)	m/z	27	29	39	40	41	43	53	55	57	67	68	69	81	83	85	97	99	111
9.1×10^{-5}		-	-	6	1	982	2	-	8										
5.8×10^{-4}		1	3	14	2	877	19	1	79	2	1	-	2						
3.0×10^{-3}		1	5	27	2	441	60	4	229	61	7	1	47	3	1	17	84	2	7

TABLE 24: THE EFFECT OF VARYING THE PRESSURE OF THE COLLISION GAS ON THE REACTION BETWEEN $C_3H_7^+$ (DERIVED FROM N-BUTANE) AND C_3H_6 (TOTAL ION CURRENT)

Pressure(Torr)	m/z	27	29	39	41	42	43	55	56	57	69	70	71	81	83	85
9.0×10^{-5}		-	-	-	5	3	991	-	-	1						
5.0×10^{-4}		3	1	-	13	4	963	3	2	10	1					
4.0×10^{-3}		4	1	1	16	7	558	19	9	305	17	9	5	1	1	68

TABLE 25: THE EFFECT OF VARYING THE PRESSURE OF THE COLLISION GAS ON THE REACTION BETWEEN $C_4H_7^+$ (METHYLCYCLOHEXANE DERIVED) AND C_3H_6 (TOTAL ION CURRENT)

Pressure(Torr)	m/z	29	39	41	43	53	54	55	57	58	67	69	83	85	97	99	111
1.1×10^{-4}		3	2	-	1	2	2	989									
5.5×10^{-4}		9	3	2	5	3	1	972	1	-	-	4					
3.0×10^{-3}		18	4	6	29	5	1	740	27	1	6	57	1	8	91	1	8

TABLE 26: THE EFFECT OF VARYING THE COLLISION GAS PRESSURE ON THE REACTION OF $C_4H_8^{+\cdot}$ (TRANS HEX-3-ENE DERIVED) WITH C_3H_6 (TOTAL ION CURRENT)

Pressure(Torr)	m/z	29	30	40	41	42	43	54	55	56	57	68	69	70	83	85	97	98	99	111	112
9.1×10^{-5}		-	1	3	5	1	1	1	6	983											
6.6×10^{-4}		1	1	4	17	1	4	1	13	952	-	-	3	2							
3.3×10^{-3}		6	-	4	45	1	13	2	42	685	64	3	18	66	7	5	15	15	5	2	1

TABLE 27: THE EFFECT OF COLLISION GAS PRESSURE VARIATION ON THE REACTION BETWEEN $C_4H_9^+$ (BROMOBUTANE DERIVED) AND C_3H_6 (TOTAL ION CURRENT)

Pressure (Torr) m/z	29	41	43	55	56	57	69	70	71	85	97	99
1.2×10^{-4}	-	5	-	-	1	994						
6.6×10^{-4}	6	26	10	3	4	949						
3.2×10^{-3}	12	28	37	15	1	876	4	1	3	9	4	10

TABLE 28: THE EFFECT OF VARYING THE COLLISION GAS PRESSURE ON THE REACTION BETWEEN $C_5H_9^+$ (TRANS HEX-3-ENE DERIVED) AND C_3H_6 (TOTAL ION CURRENT)

Pressure (Torr) m/z	29	41	43	55	57	67	68	69	81	85	97	111
1.1×10^{-4}	-	32	-	2	-	10	1	956				
5.9×10^{-4}	-	64	1	12	-	11	2	911				
3.2×10^{-3}	4	89	4	79	6	16	1	761	1	2	21	17

TABLE 29: THE EFFECT OF VARYING THE COLLISION GAS PRESSURE ON THE REACTION BETWEEN $C_5H_{10}^{+\cdot}$ (CYCLOPENTANE DERIVED) AND C_3H_6 (TOTAL ION CURRENT)

Pressure (Torr) m/z	41	42	43	54	55	56	57	58	66	67	68	69	70	81	82	83	85	97	98	99	111
$9.2 \times 10^{-}$	-	32	-	10	80	-	-	-	-	-	2	7	869								
6.1×10^{-4}	1	99	11	11	125	5	3	-	-	1	10	29	704	-	-	-	-	1			
3.7×10^{-3}	4	53	27	6	240	28	83	2	7	8	6	97	340	10	3	3	12	57	1	4	11

TABLE 30: THE EFFECT OF VARYING THE COLLISION GAS PRESSURE ON THE REACTION BETWEEN $C_6H_{11}^+$ (METHYLCYCLOHEXANE DERIVED) AND C_3H_6 (TOTAL ION CURRENT)

Pressure (Torr) m/z	41	43	55	57	67	68	69	81	82	83	85	97	98	99	111	125
8.9×10^{-5}	-	-	27	-	-	-	2	-	1	970						
5.2×10^{-4}	2	-	52	4	-	-	7	-	3	931						
3.0×10^{-3}	6	3	112	9	3	2	27	4	2	788	2	29	1	2	4	6

TABLE 31: THE EFFECT OF VARYING THE COLLISION GAS PRESSURE ON THE REACTION BETWEEN $C_6H_{12}^{+\cdot}$ (DERIVED FROM TRANS HEX-3-ENE) AND C_3H_6 (TOTAL ION CURRENT)

Pressure (Torr) m/z	41	42	43	55	56	57	58	66	67	68	69	70	80	81	82	83	84	85	97	98	99	111	125
8.0×10^{-5}	-	37	3	2	18	-	-	-	3	2	12	-	-	-	9	23	891						
6.0×10^{-4}	-	166	25	22	65	7	1	-	13	2	40	1	-	-	42	139	475						
3.5×10^{-3}	9	48	40	76	95	138	2	4	27	3	114	50	10	6	24	247	191	24	31	5	9	11	3

TABLE 32: THE EFFECT OF COLLISION GAS PRESSURE VARIATION ON THE BUT-1-ENE ION-MOLECULE REACTION (TOTAL ION CURRENT)

Pressure (Torr) m/z	29	40	41	43	54	55	56	57	67	68	69	70	71	80	81	82	83	84	85	96	97	98	112	127
5.0×10^{-5}	-	4	1	-	1	7	985	-	-	-	-	2												
1.2×10^{-4}	-	3	2	-	1	7	980	-	-	-	1	4	-	-	-	-	2	1						
4.7×10^{-4}	-	2	3	-	1	6	967	-	-	1	2	11	1	-	-	-	4	2	-	-	1			
1.1×10^{-3}	-	2	8	-	2	10	933	-	1	1	4	18	4	-	-	1	9	6	-	-	1			
3.4×10^{-3}	1	2	17	1	2	17	786	27	1	3	17	33	33	-	1	4	21	19	3	1	7	3		
6.2×10^{-3}	1	2	24	1	2	26	655	54	2	3	29	41	60	1	3	6	31	34	4	4	11	3	3	2

TABLE 33: THE EFFECT OF COLLISION GAS PRESSURE VARIATION ON THE CIS BUT-2-ENE ION-MOLECULE REACTION (TOTAL ION CURRENT)

Pressure (Torr) m/z	29	40	41	43	54	55	56	57	68	69	70	71	82	83	84	97	112
4.8×10^{-5}	-	7	2	-	-	9	983										
1.0×10^{-4}	-	6	2	-	1	11	978										
4.6×10^{-4}	-	4	4	-	1	8	981	-	-	1	-	-	-	1	1		
9.9×10^{-4}	-	3	5	-	1	12	971	-	-	1	1	1	-	3	2		
2.9×10^{-3}	1	1	7	1	1	11	898	-	-	7	9	5	2	29	25	1	1
4.5×10^{-3}	1	1	9	1	1	13	772	18	1	13	18	12	4	73	57	1	5

TABLE 34: THE EFFECT OF COLLISION GAS PRESSURE VARIATION ON THE ISOBUTENE (2-METHYPROPENE) ION-MOLECULE REACTION (TOTAL ION CURRENT)

Pressure (Torr) m/z	29	40	41	43	54	55	56	57	67	68	69	70	71	72	81	82	83	84
2.2×10^{-4}	-	7	3	-	-	9	982											
4.8×10^{-4}	-	5	5	-	-	11	979											
7.6×10^{-4}	-	4	8	-	-	12	912	58	-	-	2	2	-	-	-	-	1	
1.2×10^{-3}	-	3	11	-	1	12	805	156	-	-	3	4	3	-	-	-	1	1
1.8×10^{-3}	-	1	12	2	1	10	607	340	1	-	5	7	8	-	1	-	2	3
2.3×10^{-3}	1	1	14	1	-	13	480	447	1	1	7	10	17	1	1	1	2	3
2.8×10^{-3}	2	1	26	2	-	10	374	529	1	1	8	13	25	1	1	1	3	3
3.5×10^{-3}	1	-	13	3	-	10	292	616	1	-	9	11	38	-	1	1	3	3

TABLE 35: THE EFFECT OF VARYING THE COLLISION GAS PRESSURE ON THE REACTION BETWEEN THE BUT-1-ENE RADICAL CATION AND CIS BUT-2-ENE (TOTAL ION CURRENT)

Pressure (Torr) m/z	29	40	41	43	54	55	56	57	67	68	69	70	71	82	83	84	97	112
4.9×10^{-5}	-	5	1	-	-	7	986											
1.1×10^{-4}	-	5	3	-	1	10	982											
4.7×10^{-4}	-	4	4	-	1	10	979	-	-	-	1	1	-	-	1			
9.7×10^{-4}	1	3	6	1	1	10	969	-	-	-	1	1	1	-	4	3		
2.8×10^{-3}	1	1	10	1	1	10	895	-	-	-	5	9	5	2	34	24	1	1
4.6×10^{-3}	1	-	7	1	-	11	757	20	1	1	13	22	14	4	82	75	1	7

TABLE 36: THE EFFECT OF COLLISION GAS PRESSURE VARIATION ON THE REACTION OF CIS BUT-2-ENE RADICAL CATION WITH BUT-1-ENE (TOTAL ION CURRENT)

Pressure (Torr) m/z	29	40	41	43	54	55	56	57	67	68	69	70	71	80	81	82	83	84	85	95	96	97	98	111	112	113	125	126	127
4.4×10^{-5}	+	6	2	-	1	11	980																						
1.3×10^{-4}	-	5	4	-	1	11	978	-	-	-	-	1	-	-	-	-	1												
4.7×10^{-4}	-	7	10	-	2	17	935	-	-	1	3	15	1	-	1	1	7	2											
1.2×10^{-3}	1	3	10	-	1	11	925	-	-	1	5	19	6	-	1	1	8	6	-	-	1	2	1						
3.1×10^{-3}	1	1	17	1	2	19	717	37	1	3	19	41	49	1	2	5	29	29	5	1	4	12	3	-	1				
6.0×10^{-3}	1	-	17	2	1	20	471	75	1	3	32	61	97	2	4	12	54	71	15	3	7	26	9	1	5	2	2	1	3

TABLE 37: THE EFFECT OF VARYING THE COLLISION GAS PRESSURE ON THE REACTION BETWEEN ISOBUTENE (2-METHYLPROPENE) RADICAL CATIONS AND BUT-1-ENE (TOTAL ION CURRENT)

Pressure (Torr) m/z	29	40	41	43	55	56	57	68	69	70	71	81	82	83	84	85	96	97
2.0×10^{-4}	-	6	3	-	11	979	-	-	-	1								
4.1×10^{-4}	-	4	6	-	11	973	-	-	2	3								
7.2×10^{-4}	-	6	11	-	10	957	-	-	3	7	1	-		3	4			
1.1×10^{-3}	1	5	15	-	15	913	21	-	4	11	6	-	-	5	4			
1.8×10^{-3}	2	2	18	1	17	820	75	-	11	18	17	-	-	9	10			
2.5×10^{-3}	-	-	20	2	23	696	122	4	19	28	43	-	3	16	17	3	-	4
3.2×10^{-3}	-	-	22	2	24	588	166	2	23	39	70	2	5	16	25	8	2	5

TABLE 38: THE EFFECT OF VARYING THE COLLISION GAS PRESSURE ON THE REACTION BETWEEN ISOBUTENE (2-METHYLPROPENE) RADICAL CATIONS AND CIS BUT-2-ENE (TOTAL ION CURRENT)

Pressure (Torr) m/z	40	41	55	56	57	69	70	71	82	83	84
2.4×10^{-4}	6	2	9	983							
4.1×10^{-4}	4	4	9	982							
7.0×10^{-4}	3	6	10	977	-	1	1	1	-	1	1
1.2×10^{-3}	3	9	12	955	4	-	4	3	1	5	4
1.9×10^{-3}	3	9	12	906	27	4	7	7	-	16	9
3.0×10^{-3}	-	10	10	797	63	11	15	17	2	40	37

TABLE 39: THE EFFECT OF VARYING THE COLLISION GAS PRESSURE ON THE REACTION BETWEEN $C_2H_4^{+\cdot}$ AND PROPENE (TOTAL ION CURRENT)

Pressure (Torr) m/z	26	27	28	29	39	40	41	42	43	44	53	54	55	56	57	58	66	67	68	69	70	71	72	81	82	83	84	85	97	98	99	111	112
6.3×10^{-5}	1	1	877	-	1	-	3	100	5	-	-	-	4	5	-	-	-	-	-	2													
2.0×10^{-4}	3	3	811	-	-	-	8	159	6	-	-	-	4	5	-	-	-	-	-	2													
6.4×10^{-4}	2	2	682	-	2	1	8	182	33	1	-	2	20	35	8	-	-	-	-	22	2												
2.2×10^{-3}	3	4	243	1	3	2	17	156	100	1	2	4	65	114	116	1	-	2	1	107	28	1	-	2	-	3	1	9	8	1	1	2	
5.3×10^{-3}	4	6	72	4	8	3	19	49	80	1	4	2	53	80	266	-	1	7	5	129	70	5	1	6	2	12	3	40	33	8	15	11	1

TABLE 40: THE EFFECT OF COLLISION GAS PRESSURE VARIATION ON THE REACTION OF $C_3H_6^{+\cdot}$ AND C_2H_4 (TOTAL ION CURRENT)

Pressure (Torr) m/z	27	29	39	40	41	42	53	54	55	67	68	69	70	83
6.4×10^{-5}	-	-	-	2	4	991	-	-	3					
2.4×10^{-4}	-	1	-	1	9	981	-	-	8					
6.3×10^{-4}	1	1	-	2	16	949	-	1	29	-	-	-	1	
2.1×10^{-3}	-	5	-	3	36	770	-	4	163	2	-	4	7	7
6.1×10^{-3}	-	6	2	10	42	470	3	14	262	11	2	32	62	85

TABLE 41: THE EFFECT OF COLLISION GAS PRESSURE VARIATION ON THE REACTION OF $C_2H_4^{+-}$ WITH BUT-1-ENE (TOTAL ION CURRENT)

Pressure (Torr) m/z	26	27	28	29	39	41	42	43	54	55	56	57	67	68	69	70	71	72	81	82	83	84	85	86	95	96	97	98
4.6×10^{-5}	-	-	993	-	-	1	-	-	-	-	6																	
1.0×10^{-4}	1	1	964	-	-	2	1	-	-	1	29	1																
4.9×10^{-4}	1	1	851	-	-	8	1	1	-	7	115	5	-	-	1	5	1	-	-	-	2	2						
9.4×10^{-4}	2	1	735	-	-	13	1	3	1	14	189	9	-	1	4	9	3	-	-	1	6	5	1	-	-	-	1	
2.7×10^{-3}	3	3	451	-	2	26	2	4	2	36	300	43	2	3	19	26	24	1	2	4	20	19	2	-	-	1	5	2
5.5×10^{-3}	3	2	249	2	3	32	6	11	3	60	289	78	4	5	40	40	51	4	3	12	43	27	5	2	2	2	11	11

TABLE 42: THE EFFECT OF VARYING THE COLLISION GAS PRESSURE ON THE REACTION BETWEEN BUT-1-ENE RADICAL CATIONS AND C_2H_4 (TOTAL ION CURRENT)

Pressure (Torr) m/z	40	41	42	43	54	55	56	67	69	70	71	83	84
8.5×10^{-5}	3	2	1	1	-	7	985	-	2				
4.0×10^{-4}	3	5	5	4	2	13	960	-	8				
9.5×10^{-4}	4	14	11	5	4	23	925	-	15				
2.8×10^{-3}	-	26	10	9	5	42	864	5	27	4	-	4	5
5.2×10^{-3}	-	27	-	7	4	31	850	9	43	7	3	14	7

TABLE 43: THE EFFECT OF VARYING THE COLLISION GAS PRESSURE ON THE REACTION BETWEEN $C_2H_4^{+\cdot}$ AND CIS BUT-2-ENE (TOTAL ION CURRENT)

Pressure (Torr) m/z	26	27	28	39	41	43	55	56	57	58	67	69	70	71	72	82	83	84	85	97	112	125
5.0×10^{-5}	-	1	976	-	1	-	1	22														
1.2×10^{-4}	1	-	936	-	2	-	2	58	1													
3.6×10^{-4}	2	1	812	-	5	-	5	173	2	-	-	-	-	-	-	-	1					
7.0×10^{-4}	1	1	662	-	7	-	9	309	3	-	-	2	-	-	-	-	2	2				
1.3×10^{-3}	-	-	418	-	10	-	16	514	10	-	-	8	3	3	-	-	12	8				
3.6×10^{-3}	-	-	89	-	10	4	20	595	43	-	-	33	15	18	-	5	86	69	2	-	5	
6.0×10^{-3}	-	-	26	2	7	3	22	365	97	1	3	47	30	30	1	7	169	156	-	4	15	6

TABLE 44: THE EFFECT OF VARYING THE COLLISION GAS PRESSURE ON THE REACTION BETWEEN CIS BUT-2-ENE RADICAL CATION AND C_2H_4 (TOTAL ION CURRENT)

Pressure (Torr) m/z	29	39	40	41	42	43	53	54	55	56	67	69	70	71	83	84	85
5.8×10^{-5}	-	-	5	4	-	-	-	-	13	979							
1.4×10^{-4}	-	-	8	4	-	-	-	1	11	975							
4.5×10^{-4}	-	-	8	10	-	-	-	-	12	970	-	1					
1.1×10^{-3}	-	-	4	16	1	-	-	-	11	964	1	2					
2.6×10^{-3}	2	-	5	25	1	1	-	1	11	935	5	9	-	-	-	4	
4.6×10^{-3}	2	-	2	25	-	-	1	1	10	921	6	21	3	-	2	8	
6.5×10^{-3}	-	1	2	18	2	2	1	1	12	877	13	43	1	1	4	22	1

TABLE 45: THE EFFECT OF COLLISION GAS PRESSURE VARIATION ON THE REACTION BETWEEN $C_2H_4^{+\cdot}$ AND ISOBUTENE (2-METHYLPROPANE) (TOTAL ION CURRENT)

Pressure (Torr) m/z	26	27	28	41	42	43	55	56	57	58	69	70	71	82	83	84
5.0×10^{-5}	1	1	987	1	-	-	1	9	1							
9.5×10^{-5}	-	1	977	1	-	-	1	19	1							
2.9×10^{-4}	1	1	916	4	1	1	2	60	14							
5.9×10^{-4}	1	1	855	9	1	1	4	91	36	1	1	1				
8.0×10^{-4}	2	2	747	12	2	2	7	120	97	1	3	2	1	-	1	1
1.3×10^{-3}	3	1	663	16	1	3	11	126	161	1	5	4	4	-	1	2
1.8×10^{-3}	2	2	508	17	1	4	13	129	295	-	10	7	9	-	1	3
2.3×10^{-3}	2	2	368	18	-	5	16	122	418	-	14	10	18	-	4	3
3.2×10^{-3}	-	-	242	19	-	4	17	92	552	1	15	13	37	-	4	3
4.1×10^{-3}	1	1	175	18	-	6	16	67	624	-	16	19	45	2	6	3

TABLE 46: THE EFFECT OF COLLISION GAS PRESSURE VARIATION ON THE VINYL FLUORIDE ION-MOLECULE REACTION (TOTAL ION CURRENT)

Pressure (Torr) m/z	26	27	31	39	41	45	46	47	53	59	65	66	67*	68	72	73	77	85*	86	91	103
4.8×10^{-5}	5	-	-	-	-	2	994														
9.1×10^{-5}	4	-	-	-	-	2	993	-	-	1	-	-	-	-	-	-	1				
3.9×10^{-4}	3	1	-	-	3	1	977	-	-	5	-	-	1	-	-	-	8				
7.3×10^{-4}	3	2	-	1	9	3	920	-	-	15	-	-	4	-	1	1	39	1			
1.4×10^{-3}	4	3	-	-	15	3	782	-	1	36	1	-	19	-	4	1	125	6			
1.7×10^{-3}	2	2	-	-	14	2	717	-	1	37	1	-	32	1	4	2	175	10			
2.8×10^{-3}	1	5	-	1	18	4	442	-	3	48	2	1	78	-	10	6	352	27	-	-	2
3.5×10^{-3}	-	5	2	4	13	4	319	-	4	42	2	-	127	-	18	9	407	39	-	3	2
5.2×10^{-3}	-	7	7	-	11	-	174	5	9	35	9	3	185	3	27	27	424	63	1	7	5

TABLE 47: THE EFFECT OF PRESSURE VARIATION ON THE REACTION BETWEEN $C_2H_4^{+\cdot}$ AND VINYL FLUORIDE (TOTAL ION CURRENT)

Pressure (Torr) m/z	26	27	28	39	41	46	47	53	54	56	59	65	67	72	73	74	77	79	85
4.9×10^{-5}	2	1	981	-	-	15	1	-	-	-	1								
9.9×10^{-5}	3	1	960	-	1	32	1	-	-	-	2								
4.0×10^{-4}	11	3	815	1	5	140	4	-	-	-	12								
9.0×10^{-4}	18	5	611	2	14	240	6	-	-	-	35	-	8	1	2	-	57	-	2
1.4×10^{-3}	18	8	454	3	19	256	12	3	3	-	52	1	23	4	6	-	131	-	7
2.2×10^{-3}	16	10	292	5	20	208	20	6	5	2	64	6	55	8	17	-	248	-	18
3.1×10^{-3}	12	12	213	6	18	152	20	12	9	3	58	9	85	12	35	-	306	3	34
4.1×10^{-3}	11	18	116	9	11	85	22	16	16	2	44	13	135	20	61	8	360	2	51

TABLE 48: THE EFFECT OF VARYING THE COLLISION GAS PRESSURE ON THE REACTION BETWEEN VINYL FLUORIDE RADICAL CATION AND ETHENE (TOTAL ION CURRENT)

Pressure (Torr) m/z	26	27	28	29	39	40	41	42	45	46	47	53	54	55	56	59	67	69	70	73	83	87
6.0×10^{-5}	7	-	11	-	-	-	-	-		963	-	-	-	-	-	6						
1.5×10^{-4}	6	-	30	-	-	-	5	-	6	939	-	-	-	-	-	14						
4.8×10^{-4}	6	1	80	2	-	-	36	1	7	821	-	-	3	2	-	38	2	-	-	3		
9.1×10^{-4}	3	1	106	3	1	2	96	-	4	693	-	2	5	7	-	64	5	5	-	3		
1.6×10^{-3}	3	2	114	3	2	3	166	-	2	556	-	1	9	14	-	87	12	15	3	6	-	1
2.3×10^{-3}	2	3	112	8	4	3	249	3	-	344	-	3	20	25	-	108	42	61	3	9	-	1
3.1×10^{-3}	-	4	98	8	6	5	227	-	2	287	-	5	19	35	2	103	66	109	6	7	2	5
4.4×10^{-3}	-	5	61	9	8	4	199	2	2	199	-	8	28	39	3	92	120	197	11	10	3	7
5.5×10^{-3}	-	4	50	14	9	-	192	-	-	133	3	12	18	33	5	81	121	278	17	10	6	16

TABLE 49: THE EFFECT OF COLLISION GAS PRESSURE VARIATION ON THE 1,1-DIFLUOROETHENE ION-MOLECULE REACTION (TOTAL ION CURRENT)

Pressure (Torr) m/z	27	31	33	39	40	44	45	59	60	63	64	65	66	77	95	108	128
4.8×10^{-5}	-	-	-	-	-	2	-	-	-	1	997						
9.4×10^{-5}	-	-	-	-	-	1	-	-	-	5	994						
3.6×10^{-4}	-	-	-	-	-	2	-	-	-	4	994						
7.8×10^{-4}	-	-	1	-	-	2	-	1	-	4	992						
1.4×10^{-3}	-	-	2	1	-	1	1	1	1	2	988	-	-	1	1	-	-
2.3×10^{-3}	1	1	3	2	2	1	1	2	4	2	953	9	-	4	9	1	3
2.9×10^{-3}	-	4	4	3	4	-	1	3	11	-	906	34	1	11	13	1	3
3.9×10^{-3}	-	2	7	3	1	-	4	5	15	-	842	67	2	15	33	2	3

TABLE 50: THE EFFECT OF VARYING THE COLLISION GAS PRESSURE ON THE REACTION BETWEEN $C_2H_4^{+\cdot}$ AND 1,1-DIFLUOROETHENE (TOTAL ION CURRENT)

Pressure (Torr) m/z	26	27	28	33	39	40	41	42	45	51	59	60	64	65	71	77	95
4.2×10^{-5}	4	1	979	-	-	-	-	-	-	-	-	-	15	1			
9.0×10^{-5}	4	1	973	-	-	-	-	-	-	-	-	-	20	1			
2.9×10^{-4}	10	1	886	-	-	-	1	-	-	1	-	-	98	2	-	1	
7.0×10^{-4}	18	4	719	1	-	1	1	1	1	2	-	-	244	8	-	2	
1.5×10^{-3}	22	6	565	1	1	-	2	1	2	2	-	-	383	13	-	3	
1.7×10^{-3}	22	9	443	1	2	1	2	1	1	2	1	1	486	20	1	5	2
2.2×10^{-3}	21	10	335	2	4	-	4	3	3	2	1	4	549	47	2	10	5
2.9×10^{-3}	24	15	254	-	5	3	4	-	-	3	4	9	528	121	4	12	16

TABLE 51: THE EFFECT OF COLLISION GAS PRESSURE ON THE REACTION OF 1,1-DIFLUOROETHENE RADICAL CATIONS WITH C_2H_4
(TOTAL ION CURRENT)

Pressure (Torr) m/z	28	29	33	39	40	41	42	51	53	54	55	56	59	63	64	67	69	70	72	73	77	83	84	85	87	91	92	105	106
4.1×10^{-5}	6	-	-	-	-	-	-	-	-	-	-	-	-	5	986	-	-	-	-	-	1								
9.3×10^{-4}	16	-	-	-	-	1	-	-	-	-	-	-	-	3	977	-	-	-	-	-	3								
2.7×10^{-4}	40	1	-	-	-	11	-	-	-	-	1	-	-	2	935	-	-	-	-	-	9								
5.0×10^{-4}	56	-	-	-	1	32	-	1	-	-	3	1	1	2	879	2	2	-	-	-	20								
8.6×10^{-4}	64	1	-	-	2	59	1	1	-	-	8	2	1	-	792	6	10	-	1	-	50	-	-	2					
1.3×10^{-3}	68	-	-	-	3	94	1	-	-	-	13	4	2	-	690	16	29	-	-	-	74	-	-	4	-	-	-	3	
1.8×10^{-3}	54	1	1	-	3	104	1	2	1	-	17	4	3	-	593	22	66	1	2	1	109	1	-	6	-	-	-	10	
2.6×10^{-3}	43	-	1	2	2	97	1	1	3	2	24	5	2	-	462	34	128	1	2	1	149	4	1	12	2	2	2	16	1

TABLE 52: THE EFFECT OF VARYING THE COLLISION GAS PRESSURE ON THE TRIFLUOROETHENE ION-MOLECULE REACTION
(TOTAL ION CURRENT)

Pressure (Torr) m/z	31	32	42	43	51	58	59	64	69	77	81	82	84	95	98	99	100	113	116	118
1.0×10^{-4}	-	-	-	-	1	1	-	-	-	-	6	993								
5.0×10^{-4}	-	-	-	-	5	2	-	-	-	-	5	978	-	5	-	-	-	-	4	1
9.0×10^{-4}	-	1	-	1	9	3	-	-	1	1	3	946	1	23	1	-	-	-	9	4
1.5×10^{-3}	1	1	1	1	14	8	1	1	2	3	3	881	1	55	2	-	-	3	17	6
2.0×10^{-3}	-	-	-	3	15	17	-	1	4	4	1	781	3	112	4	-	-	9	36	10
2.6×10^{-3}	-	-	-	4	19	27	1	-	7	7	2	675	4	173	7	-	-	17	43	15
3.4×10^{-3}	-	-	-	7	23	34	4	-	10	12	2	498	7	269	10	-	2	32	67	21
4.6×10^{-3}	3	-	-	16	18	50	8	-	11	23	12	351	15	309	16	2	2	64	73	26

TABLE 53: THE EFFECT OF VARYING THE COLLISION GAS PRESSURE ON THE REACTION BETWEEN $C_2H_4^{+\cdot}$ AND TRIFLUOROETHENE (TOTAL ION CURRENT)

Pressure (Torr) m/z	26	27	28	33	39	40	41	46	57	58	59	60	64	69	77	82	83	95	96	98	100	113	116	118
6.6×10^{-5}	3	1	977	-	-	-	-	-	-	-	-	-	-	-	-	18								
1.7×10^{-4}	7	1	925	-	-	-	-	-	1	-	-	-	1	-	-	63	-	1	-	-	-	-	1	
5.0×10^{-4}	17	3	757	1	1	-	-	1	2	1	1	1	1	1	1	193	-	12	-	1	-	1	6	2
7.7×10^{-4}	13	5	614	1	1	-	1	-	4	1	2	1	1	-	2	291	2	37	-	1	1	2	15	5
1.5×10^{-3}	18	9	406	1	1	1	1	-	7	2	5	4	-	4	9	348	1	124	-	3	1	10	37	11
2.1×10^{-3}	20	9	264	-	4	2	-	-	7	5	5	6	-	9	12	275	8	250	2	2	-	30	69	23
3.2×10^{-3}	19	22	135	-	11	6	-	-	17	5	9	-	-	17	31	165	9	363	-	-	-	61	107	25

TABLE 54: THE EFFECT OF VARYING THE COLLISION GAS PRESSURE ON THE REACTION BETWEEN $C_2HF_3^{+\cdot}$ AND C_2H_4 (TOTAL ION CURRENT)

Pressure (Torr) m/z	28	29	39	40	41	42	46	51	53	54	55	56	59	60	64	65	67	69	70	72	73	77	81	82	85	87	90	91	95	105
5.2×10^{-5}	3	-	-	-	-	-	1	-	-	-	-	-	-	-	4	-	-	-	-	-	-	-	3	988						
1.3×10^{-4}	8	-	-	-	2	-	3	1	-	-	-	-	-	-	8	-	-	-	-	-	-	1	3	974	-	-	-	-	1	
4.0×10^{-4}	20	-	-	1	11	-	6	2	-	1	1	-	4	1	20	-	1	1	-	-	-	3	3	926	-	-	-	-	2	
8.6×10^{-4}	31	-	-	1	32	-	10	4	-	1	3	-	8	2	31	-	3	4	-	-	1	13	3	845	-	-	1	-	5	
1.3×10^{-3}	31	1	1	2	49	1	10	4	-	2	6	-	12	3	35	-	8	13	-	-	2	26	3	783	1	1	1	-	6	1
1.8×10^{-3}	38	-	1	1	67	-	12	5	1	3	8	-	19	3	47	-	14	30	1	-	2	49	3	697	1	3	1	-	9	3
2.2×10^{-3}	36	1	1	2	75	1	13	4	1	5	12	1	25	4	48	1	28	65	1	1	4	71	4	566	3	6	1	1	12	10
3.2×10^{-3}	29	1	1	2	68	-	11	6	2	7	15	2	29	4	47	1	48	113	4	1	7	91	2	448	6	13	1	1	18	22

TABLE 55: THE EFFECT OF VARYING THE COLLISION GAS PRESSURE ON THE TETRAFLUOROETHENE ION-MOLECULE REACTION (TOTAL ION CURRENT)

Pressure (Torr) m/z	31	43	56	58	69	99	100	131
5.1×10^{-5}	-	-	-	-	2	5	993	
1.6×10^{-4}	-	-	-	-	7	3	990	
5.6×10^{-4}	4	-	-	-	13	6	977	
1.1×10^{-3}	12	-	-	2	21	2	962	
2.2×10^{-3}	13	-	6	11	83	-	894	6
4.0×10^{-3}	-	29	22	44	152	-	754	

TABLE 56: THE EFFECT OF VARYING THE COLLISION GAS PRESSURE ON THE REACTION OF $C_2H_4^{+\cdot}$ WITH C_2F_4 (TOTAL ION CURRENT)

Pressure (Torr) m/z	26	27	28	31	50	51	58	59	64	69	77	78	100	107	131
6.0×10^{-5}	2	1	994	-	-	-	-	-	-	-	-	-	3		
1.2×10^{-4}	4	1	987	-	-	-	-	-	-	-	-	-	8		
4.5×10^{-4}	13	2	945	-	-	-	-	-	-	1	1	-	36		
9.1×10^{-4}	22	5	881	1	1	1	1	-	1	3	3	1	82		
1.5×10^{-3}	28	9	794	1	1	1	2	1	2	4	5	1	151		
2.0×10^{-3}	31	18	694	1	1	3	3	2	2	12	8	3	218	1	2
2.5×10^{-3}	40	19	569	4	5	3	6	4	-	20	14	2	310	-	6
3.1×10^{-3}	31	25	508	9	-	5	4	-	-	33	15	7	362	2	-

TABLE 57: THE EFFECT OF VARYING THE COLLISION GAS PRESSURE ON THE ACETYLENE (ETHYNE) ION-MOLECULE REACTION (TOTAL ION CURRENT)

Pressure (Torr) m/z	26	27	50	51	52	53	74	75	76	77	78	100	101	102	103	126	128
4.1×10^{-5}	972	-	10	18													
8.8×10^{-5}	893	-	34	73													
1.9×10^{-4}	775	-	77	146	-	-	-	1	1								
4.2×10^{-4}	530	6	139	304	-	-	-	3	11	7							
8.0×10^{-4}	267	19	160	444	-	-	-	8	53	48	-	-	-	2			
1.4×10^{-3}	121	20	125	439	-	5	3	12	121	136	-	-	1	11	6		
2.2×10^{-3}	43	17	73	325	2	13	3	13	195	250	-	-	3	36	26		
3.1×10^{-3}	15	12	40	203	3	23	3	13	234	322	-	4	4	71	55		
4.0×10^{-3}	6	8	23	114	5	32	3	11	241	359	2	6	5	97	86	3	
5.4×10^{-3}	1	6	10	55	7	42	2	8	251	374	2	6	4	120	106	3	2

TABLE 58: THE EFFECT OF VARYING THE PRESSURE OF ACETYLENE ON THE REACTION BETWEEN $C_2H_4^{+\cdot}$ AND ACETYLENE (ETHYNE)

Pressure (Torr) m/z	26	27	28	29	38	39	50	51	52	53	63	65	76	77
4.7×10^{-5}	5	3	989	-	-	2	-	-	-	1				
1.1×10^{-4}	11	5	972	-	-	8	-	1	-	3				
4.0×10^{-4}	37	25	888	-	1	28	3	4	2	12				
7.6×10^{-4}	40	36	810	-	2	62	5	14	3	28	-	-	-	1
1.3×10^{-3}	37	55	675	-	1	132	9	29	6	50	1	-	1	5
2.4×10^{-3}	27	56	446	1	-	294	6	42	6	100	2	3	9	10
3.1×10^{-3}	26	54	365	7	-	338	6	38	4	134	3	5	6	15
4.8×10^{-3}	12	74	198	16	-	418	9	26	5	186	2	12	19	22

TABLE 59: THE EFFECT OF VARYING THE PRESSURE OF ETHENE ON THE REACTION BETWEEN $C_2H_2^{+\cdot}$ AND C_2H_4 (TOTAL ION CURRENT)

Pressure (Torr) m/z	26	27	28	29	38	39	40	41	42	43	51	52	53	54	55	56	65	67	68	69	70	79	83
4.7×10^{-5}	972	-	23	-	-	2	-	1	-	-	1	-	1										
9.3×10^{-5}	927	-	58	1	-	5	-	4	-	-	1	-	4										
4.1×10^{-4}	713	-	181	4	1	17	2	59	1	-	2	2	13	-	5	-	-	1	-	1			
9.0×10^{-4}	474	8	226	12	1	28	4	193	-	-	3	3	20	1	16	-	-	6	-	7			
1.4×10^{-3}	367	9	206	14	1	32	5	276	-	-	4	3	25	1	24	-	-	12	-	22			
1.8×10^{-3}	216	13	184	17	1	40	6	259	1	1	4	3	26	2	35	1	-	27	5	59	2		
3.0×10^{-3}	95	15	102	20	-	54	5	341	1	3	5	5	38	3	54	1	-	59	-	193	-	4	3
4.6×10^{-3}	31	12	40	15	-	75	4	213	-	5	3	6	46	3	51	3	2	90	-	388	-	7	8

TABLE 60: THE EFFECT OF VARYING THE PRESSURE OF ACETYLENE ON THE REACTION BETWEEN $C_3H_3^+$ (DERIVED FROM BUT-1-ENE) AND C_2H_2 (TOTAL ION CURRENT)

Pressure (Torr) m/z	37	38	39	63	64	65
1.1×10^{-4}	1	1	999			
3.6×10^{-4}	1	2	997			
1.2×10^{-3}	1	2	995	2		
2.0×10^{-3}	1	3	986	5	1	4

TABLE 61: The Effect of Varying the Acetylene Pressure on the Reaction Between $C_3H_5^+$ and C_2H_2 (Total Ion Current)

Pressure (Torr) m/z	15	27	39	40	41	43	65	67
2.2×10^{-4}	-	-	10	1	988	-	1	
3.6×10^{-4}	-	2	15	1	980	-	2	
4.0×10^{-4}	-	2	19	1	975	-	3	
5.0×10^{-4}	-	2	20	1	973	-	4	
5.2×10^{-4}	1	2	22	1	972	-	4	
7.5×10^{-4}	1	3	35	1	950	-	10	
9.0×10^{-4}	1	3	44	2	941	-	8	1
1.2×10^{-3}	2	4	53	2	922	-	15	2
1.8×10^{-3}	3	7	85	-	868	3	29	6
2.5×10^{-3}	-	6	165	3	750	12	40	23

TABLE 62: The Effect of Varying the Pressure of Acetylene on the Reaction Between $C_4H_3^+$ and C_2H_2 (Total Ion Current)

Pressure (Torr) m/z	26	27	50	51	53	79
1.9×10^{-4}	3	5	12	980		
5.3×10^{-4}	-	17	25	957		
2.0×10^{-3}	-	52	35	872	18	23

TABLE 63: The Effect of Varying the Pressure of Acetylene on the Reaction Between $C_4H_5^+$ and C_2H_2 (Total Ion Current)

Pressure (Torr) m/z	27	29	51	52	53	77
3.0×10^{-4}	14	1	19	2	964	
9.5×10^{-4}	41	6	21	8	921	3
2.3×10^{-3}	57	20	33	6	872	11

TABLE 66: THE EFFECT OF VARYING THE ETHENE PRESSURE ON THE REACTION BETWEEN BUTADIENE RADICAL CATION AND ETHENE (TOTAL ION CURRENT)

Pressure (Torr) m/z	28	29	39	41	53	54	65	67	69	79	80	81	82	93
5.2×10^{-5}	-	-	13	-	2	985								
1.0×10^{-4}	-	-	18	-	2	980								
3.7×10^{-4}	-	-	27	1	2	969	-	1						
7.8×10^{-4}	-	-	33	1	5	958	-	4						
1.4×10^{-3}	1	-	40	2	4	949	-	8						
1.9×10^{-3}	1	1	52	3	5	915	-	20	-	1	1	1	1	
2.4×10^{-3}	1	1	61	3	5	888	-	38	1	1	1	1	1	
3.4×10^{-3}	-	-	66	5	4	852	-	65	1	1	1	2	2	
4.1×10^{-3}	1	1	78	3	5	803	-	92	3	1	1	3	6	
5.0×10^{-3}	-	-	85	3	7	740	1	139	4	2	2	3	12	1

TABLE 67: THE EFFECT OF VARYING THE PRESSURE OF ACETYLENE ON THE REACTION BETWEEN BUTADIENE RADICAL CATION AND ACETYLENE (TOTAL ION CURRENT)

Pressure (Torr) m/z	27	28	39	41	52	53	54	65	77	79
8.0×10^{-5}	-	-	34	-	1	2	964			
1.9×10^{-4}	-	1	38	-	1	4	956	-	-	1
5.0×10^{-4}	1	2	51	-	2	5	937	-	-	2
1.1×10^{-3}	2	4	83	2	3	5	892	1	1	7
2.0×10^{-3}	2	4	137	2	3	9	818	1	3	23
2.9×10^{-3}	4	4	175	2	4	15	756	3	3	34
4.0×10^{-3}	1	5	249	3	-	15	674	3	3	48
4.8×10^{-3}	2	-	371	-	-	27	528	2	-	70

TABLE 64: THE EFFECT OF VARYING THE COLLISION GAS PRESSURE ON THE BUTADIENE ION-MOLECULE REACTION (TOTAL ION CURRENT)

Pressure (Torr) m/z	28	39	41	52	53	54	55	56	66	67	68	78	79	80	81	91	92	93	95	104	105	106	107	109	117	119	120	121	129	133	134	145
5.2×10^{-5}	-	17	-	1	3	977	-	-	-	1	-	-	1	-	-	-	-	1														
1.2×10^{-4}	-	18	-	-	3	970	-	1	-	1	-	-	3	2	-	-	-	2														
4.5×10^{-4}	-	20	-	1	2	927	-	-	6	8	-	1	14	11	-	-	-	11														
1.2×10^{-3}	1	27	1	-	4	746	-	-	23	42	-	2	51	47	1	1	2	50	-	-	1	-	1	1								
1.9×10^{-3}	-	29	1	-	3	560	15	1	33	89	-	2	75	81	3	3	3	93	-	-	2	-	1	3	-	1	1	1				
2.5×10^{-3}	1	34	1	-	3	454	18	-	36	119	-	2	77	101	8	3	6	119	-	1	2	-	1	6	-	2	1	2	-	-	1	
3.4×10^{-3}	-	46	1	-	4	328	18	-	30	176	-	1	73	117	13	4	8	150	-	2	3	-	2	12	-	3	3	6	-	-	2	
4.6×10^{-3}	-	66	2	-	5	226	18	1	23	208	1	1	62	107	18	5	10	174	1	3	5	1	3	24	2	5	5	17	1	-	5	2
5.8×10^{-3}	-	79	2	-	8	199	11	1	17	206	2	-	46	95	21	7	9	195	2	3	6	-	3	35	1	3	7	28	2	2	9	2

TABLE 65: THE EFFECT OF VARYING THE PRESSURE OF BUTADIENE ON THE REACTION BETWEEN $C_2H_4^{+\cdot}$ AND BUTADIENE (TOTAL ION CURRENT)

Pressure (Torr) m/z	26	27	28	39	40	41	42	53	54	55	56	65	66	67	68	78	79	80	81	91	92	93	95	104	105	107	109	119	120	121	128	132	133	134
5.4×10^{-5}	-	1	972	1	-	1	-	-	22	1	-	-	-	-	-	-	1																	
9.5×10^{-5}	1	1	955	1	-	1	-	-	37	1	-	-	1	1	-	-	1	1	-	-	-	1												
2.2×10^{-4}	1	1	890	3	-	2	-	1	87	4	-	-	2	2	-	-	3	2	-	-	-	3												
4.0×10^{-4}	2	1	819	5	-	4	-	3	125	7	-	-	4	6	-	1	10	7	-	-	-	7												
6.4×10^{-4}	3	1	720	8	-	5	-	3	163	11	-	-	10	17	-	1	21	19	1	-	-	17												
9.5×10^{-4}	3	2	597	13	-	7	1	3	181	24	-	2	17	37	1	1	36	37	2	1	1	34												
1.6×10^{-3}	2	1	468	23	-	10	1	4	167	29	2	1	22	80	-	2	51	59	4	2	3	61	-	1	1	1	4	1	-	1				
2.0×10^{-3}	2	2	388	28	1	10	1	7	129	31	1	2	22	127	-	2	49	77	7	4	3	91	-	1	2	1	6	1	2	3	-	-	2
2.5×10^{-3}	2	2	299	38	-	12	1	9	114	39	1	2	21	162	1	1	54	85	14	4	4	110	-	1	2	2	9	2	2	6	-	-	2
2.9×10^{-3}	2	4	237	47	2	12	2	9	100	39	-	1	25	189	-	-	53	89	18	4	7	120	1	2	5	3	13	3	2	8	-	-	4
3.6×10^{-3}	1	4	187	55	2	12	4	13	78	33	1	3	18	204	4	1	53	85	22	8	7	142	3	2	4	4	19	2	5	17	1	1	5
4.3×10^{-3}	-	3	161	79	1	12	2	15	60	32	1	3	14	228	1	1	50	80	26	7	6	132	3	3	5	3	29	3	5	20	2	2	8	2

TABLE 68: THE EFFECT OF VARYING THE PRESSURE OF BUTADIENE ON THE REACTION BETWEEN $C_2H_2^{+\cdot}$ AND BUTADIENE (TOTAL ION CURRENT)

Pressure (Torr) m/z	26	27	28	29	39	40	41	51	52	53	54	55	63	65	66	67	68	77	78	79	80	81	91	92	93	94	105	107	109	116	117	119	120	121	129	133	134	145
5.4×10^{-5}	969	-	2	1	12	-	-	-	-	2	14	1																										
9.2×10^{-5}	921	-	5	1	29	1	1	1	1	3	34	2	-	-	-	1	-	1																				
4.1×10^{-4}	613	-	11	2	136	1	3	2	1	15	158	10	-	1	3	8	1	4	1	11	8	-	2	-	8													
9.0×10^{-4}	407	-	9	2	250	-	3	2	2	20	159	16	-	2	10	26	2	4	1	24	22	1	4	-	22													
1.3×10^{-3}	219	-	8	2	282	1	5	2	1	32	165	29	-	3	17	64	-	5	2	47	51	4	9	1	51	-	-	1									
2.1×10^{-3}	100	3	5	1	352	1	5	2	1	45	114	31	-	4	21	140	1	6	2	56	79	10	13	5	86	1	2	2	7	2	-	2	2	4	-	-	2
3.3×10^{-3}	38	2	4	-	348	-	4	1	-	48	40	25	-	4	13	157	-	4	-	40	60	17	13	4	90	-	3	2	14	2	1	3	3	12	-	-	4
5.2×10^{-3}	10	2	-	-	391	-	2	-	-	72	10	11	2	5	5	158	1	3	-	24	45	24	15	5	103	2	4	3	31	5	1	3	5	39	3	2	8	7

TABLE 69: THE EFFECT OF VARYING THE COLLISION GAS PRESSURE ON THE ISOPRENE ION-MOLECULE REACTION (TOTAL ION CURRENT)

Pressure (Torr) m/z	29	39	40	41	42	53	55	57	66	67	68	69	70	71	79	80	81	82	83	92	93	94	95	106	107	108	109	121
7.0×10^{-5}	-	-	-	1	-	-	-	-	2	15	981	-	-	-	-	-	-	-	-	-	1							
2.0×10^{-4}	-	-	-	-	-	-	-	-	1	14	978	-	-	-	-	1	-	-	-	-	3	2	1					
4.7×10^{-4}	-	-	-	1	-	-	-	-	2	13	949	-	1	-	1	3	2	1	-	3	12	4	1	1	3	2	-	2
9.6×10^{-4}	-	-	1	1	-	-	-	-	3	16	908	-	2	-	1	8	9	1	-	3	24	9	4	-	8	2	-	2
1.7×10^{-3}	-	-	+	1	-	2	1	1	2	22	856	-	4	1	2	15	32	3	1	5	48	19	9	-	15	6	-	4
2.2×10^{-3}	1	1	1	1	1	3	1	1	2	28	692	25	3	1	3	17	67	2	-	4	54	29	18	1	25	11	1	6
3.2×10^{-3}	1	1	1	2	1	5	1	4	3	32	547	40	5	1	3	22	135	3	-	4	58	37	27	2	38	16	1	11
4.0×10^{-3}	-	-	-	3	1	7	2	2	4	37	431	58	4	2	3	23	198	3	1	4	65	38	35	3	41	23	-	12
5.0×10^{-3}	-	-	-	2	2	10	3	5	3	45	372	44	3	2	3	17	247	4	1	3	61	37	44	3	49	24	-	17
6.4×10^{-3}	-	-	-	3	1	20	2	2	2	46	314	41	3	2	4	14	315	2	1	2	45	34	57	3	46	26	2	13

TABLE 70: THE EFFECT OF VARYING THE PRESSURE OF ISOPRENE ON THE REACTION OF $C_2H_4^{+\cdot}$ WITH ISOPRENE (TOTAL ION CURRENT)

Pressure (Torr) m/z	26	27	28	39	40	41	42	43	53	54	55	56	57	66	67	68	69	70	71	79	80	81	82	92	93	94	95	96	106	107	108	109	119	121	135	137
5.2×10^{-4}	-	3	982	-	-	-	-	-	1	-	-	-	-	-	-	15																				
1.2×10^{-4}	1	2	945	-	-	2	-	-	1	-	-	-	-	-	3	42	2	-	-	-	1	1	-	-	1											
4.4×10^{-4}	1	1	917	-	1	2	-	-	2	-	1	-	-	-	6	58	3	1	-	1	1	1	-	1	3	2	-	-	-	1	1					
9.1×10^{-4}	1	2	697	2	1	6	1	1	7	-	2	1	-	1	31	154	18	2	-	2	6	10	1	3	23	11	4	-	-	8	3	-	-	3		
1.6×10^{-3}	2	2	555	2	2	7	1	1	15	1	4	1	1	2	48	172	35	2	1	3	10	29	1	4	39	18	9	-	1	19	9	-	-	6		
2.5×10^{-3}	2	2	360	3	2	10	1	1	17	1	7	1	2	1	77	148	63	2	1	4	17	97	-	4	59	30	20	-	2	37	15	1	-	14	1	
3.5×10^{-3}	-	2	197	4	-	10	2	2	39	1	7	-	5	2	88	105	74	2	1	5	14	201	2	3	58	38	40	-	2	48	22	1	-	19	2	
4.3×10^{-3}	1	2	159	5	1	8	-	2	55	1	7	-	5	2	94	74	66	2	2	6	16	240	4	3	47	37	48	-	3	47	27	2	-	22	4	3
5.1×10^{-3}	2	3	121	5	-	9	-	2	63	2	9	-	3	2	91	53	63	2	1	7	14	287	2	3	45	36	49	1	3	48	31	2	2	26	4	4

TABLE 71: THE EFFECT OF VARYING THE PRESSURE OF ETHENE ON THE REACTION BETWEEN ISOPRENE RADICAL CATION AND C_2H_4 (TOTAL ION CURRENT)

Pressure (Torr) m/z	39	40	41	42	53	54	55	66	67	68	80	81	83
5.0×10^{-5}	-	-	-	-	-	-	-	-	17	983			
1.6×10^{-3}	-	-	-	-	-	-	-	2	17	981			
3.1×10^{-4}	2	-	1	-	-	-	-	2	16	979	-	2	
7.0×10^{-4}	-	-	-	-	1	-	-	2	21	973	-	3	
1.3×10^{-3}	1	2	1	2	2	2	1	2	19	961	-	8	
2.1×10^{-3}	-	2	1	3	3	-	-	3	35	922	3	27	
3.3×10^{-3}	-	-	8	-	6	3	3	3	43	872	2	61	
4.8×10^{-3}	-	-	5	-	11	3	3	4	82	746	5	140	2

TABLE 72: THE EFFECT OF VARYING THE PRESSURE OF ISOPRENE ON THE REACTION OF BUTADIENE RADICAL CATION WITH ISOPRENE (TOTAL ION CURRENT)

Pressure (Torr) m/z	26	27	28	29	39	41	43	52	53	54	56	57	67	68	69	70	71	78	79	80	81	82	91	92	93	94	95	96	105	106	107	108	109	117	118	121	137
9.0×10^{-5}	-	-	-	-	10	-	-	-	3	956	-	-	-	29																							
4.5×10^{-4}	-	-	-	-	20	-	-	2	3	733	-	-	3	199	4	3	-	1	3	5	3	-	-	2	17	8	3	-	-	-	7	2	-	-	-	2	
9.2×10^{-4}	-	-	-	-	23	1	-	-	5	581	-	-	7	230	19	4	-	-	3	12	12	2	-	4	41	21	7	-	-	-	19	6	-	-	-	7	
1.6×10^{-3}	-	3	3	-	22	2	-	-	3	481	-	2	9	203	44	2	-	-	4	17	39	2	-	5	59	26	12	-	-	1	33	10	-	-	-	14	
2.5×10^{-3}	-	4	3	-	18	2	2	1	5	457	1	2	14	110	59	4	2	2	4	19	88	5	-	5	51	39	21	1	1	2	40	20	1	-	-	17	
3.4×10^{-3}	-	6	4	1	17	5	2	2	6	488	2	3	18	60	55	1	-	2	8	16	133	3	-	5	41	22	32	-	2	4	32	20	1	-	-	19	
3.9×10^{-3}	1	8	5	-	18	3	2	2	3	509	3	1	15	41	56	-	-	2	3	15	139	5	2	5	32	29	28	-	2	3	31	17	2	-	2	15	
5.0×10^{-3}	1	8	2	1	14	4	-	2	8	568	2	3	14	19	44	1	3	3	2	8	152	2	3	4	17	22	27	2	-	1	27	13	3	3	3	11	2

TABLE 73: THE EFFECT OF VARYING THE PRESSURE OF BUTADIENE ON THE REACTION OF ISOPRENE RADICAL CATION WITH BUTADIENE (TOTAL ION CURRENT)

Pressure (Torr) m/z	39	41	53	54	55	66	67	68	79	80	81	92	93	94	105	107	109	119	120	121	122
5.0×10^{-5}	-	-	-	1	-	2	16	977	1	-	-	-	2	1							
9.8×10^{-5}	-	-	-	2	-	2	15	973	-	3	1	2	1	-	-	1					
4.0×10^{-4}	-	-	-	8	2	3	16	941	4	4	2	1	13	4	-	3					
9.1×10^{-4}	-	-	1	15	3	7	17	875	7	15	5	1	34	8	-	9					
1.8×10^{-3}	2	1	3	18	11	13	43	756	16	26	11	4	61	19	-	12					
2.6×10^{-3}	-	2	4	20	14	13	74	662	17	30	20	7	83	24	-	27	3				
3.5×10^{-3}	-	-	7	16	21	11	112	548	20	44	19	5	16	35	3	31	6				
4.1×10^{-3}	-	-	11	17	15	14	141	464	14	57	25	4	148	49	-	32	10				
5.0×10^{-3}	3	-	12	13	23	10	170	369	21	55	42	6	157	51	7	44	11	3	2	7	3

TABLE 74: THE EFFECT OF VARYING THE COLLISION GAS PRESSURE ON THE PENT-1-YNE ION-MOLECULE REACTION (TOTAL ION CURRENT)

Pressure (Torr) m/z	29	39	40	41	42	43	52	53	55	57	65	66	67	68	69	71	73	77	78	79	80	81	82	83	85	91	92	93	94	95	105	107	109	117
6.0×10^{-5}	-	-	2	2	1	2	-	-	-	-	-	2	32	955	-	-	-	-	-	3	-	-	-	-	-	1	-	1					
1.4×10^{-4}	-	-	5	7	-	1	-	-	2	-	-	4	44	924	-	-	-	-	-	5	-	-	-	-	-	3	-	-	-	-	3		
4.0×10^{-4}	4	-	9	11	3	2	-	3	3	1	-	4	84	840	-	-	-	-	-	12	1	2	-	2	-	3	-	4	-	-	2	8		
9.0×10^{-4}	11	1	18	19	3	5	1	6	10	2	2	4	145	660	38	-	-	2	-	25	1	3	-	4	-	8	-	8	1	2	1	18		
1.6×10^{-3}	8	1	21	33	6	7	1	12	12	4	3	5	207	549	78	2	1	3	-	44	2	13	1	6	-	8	-	11	3	7	2	29		
2.3×10^{-3}	6	1	20	27	4	9	2	14	12	7	3	7	214	411	103	1	1	2	-	43	4	20	1	8	1	10	1	17	5	11	3	33		
2.9×10^{-3}	8	2	16	24	3	7	1	15	11	7	5	7	239	355	96	2	1	2	1	45	8	34	1	10	2	6	1	22	9	16	5	35	1	1
3.9×10^{-3}	4	3	18	26	4	4	-	24	13	9	7	6	297	297	79	3	2	2	1	52	9	59	2	10	1	10	1	32	17	28	4	46	1	1
5.3×10^{-3}	2	3	15	19	5	5	-	43	7	11	6	6	219	266	48	2	2	2	1	43	12	82	4	14	2	7	4	44	21	48	4	49	1	5

TABLE 75: THE EFFECT OF VARYING THE PRESSURE OF PENT-1-YNE ON THE REACTION BETWEEN ISOPRENE RADICAL CATION AND PENT-1-YNE (TOTAL ION CURRENT)

Pressure (Torr) m/z	29	39	40	41	42	43	53	55	57	65	66	67	68	69	71	73	77	78	79	80	81	82	83	85	87	91	92	93	94	95	105	107	109	117	118	119	121
5.7×10^{-5}	-	-	-	-	-	-	-	-	-	-	1	1	983	-	-	-	-	-	1	1	-	-	-	-	-	-	1										
1.4×10^{-4}	-	-	1	1	-	1	-	-	-	-	1	18	971	-	-	-	-	-	3	-	-	-	-	-	-	-	1	-	-	-	2					
4.4×10^{-4}	1	-	3	3	1	-	1	2	1	-	3	36	921	-	-	-	-	-	7	1	1	1	-	-	-	2	-	4	3	-	1	6					
9.1×10^{-4}	3	-	9	10	3	4	3	5	2	1	3	81	808	-	-	-	1	-	3	2	3	-	5	-	-	4	-	10	5	1	1	14					
1.5×10^{-3}	4	-	14	13	4	4	6	5	3	1	3	130	680	24	1	-	1	1	35	2	8	2	5	-	-	5	1	17	6	3	2	22					
2.2×10^{-3}	7	1	15	17	4	5	11	9	6	2	6	178	525	52	1	-	2	2	46	3	17	1	11	1	-	5	1	22	10	8	3	28	-	2			
3.0×10^{-3}	4	1	13	18	3	4	16	8	8	4	6	203	428	70	3	1	2	1	42	9	28	-	11	1	-	5	2	29	16	14	3	42	1	2	-	-	2
4.2×10^{-3}	3	1	13	17	2	5	23	8	11	3	6	218	354	62	3	2	2	1	42	11	49	2	14	2	1	6	2	40	18	28	3	42	1	2	-	1	1
5.0×10^{-3}	5	4	15	28	5	6	41	12	11	5	4	248	125	62	4	3	2	2	51	10	97	2	17	3	3	8	4	63	32	49	3	66	1	3	3	2	1

TABLE 76: THE EFFECT OF VARYING THE PRESSURE OF ISOPRENE ON THE REACTION OF PENT-1-YNE RADICAL CATION WITH ISOPRENE (TOTAL ION CURRENT)

Pressure (Torr)	m/z 29	39	40	41	42	43	53	55	57	66	67	68	69	70	79	80	81	82	83	92	93	94	95	106	107	108	121	135	136
6.0×10^{-5}	-	-	-	-	-	-	-	-	-	2	25	973																	
1.9×10^{-4}	-	-	-	-	-	-	-	-	-	2	22	969	-	1	2	1	-	-	-	-	5								
6.4×10^{-4}	-	-	1	1	-	1	-	-	-	2	20	920	-	2	2	5	4	1	-	2	19	8	3	-	6	3	3		
1.4×10^{-3}	-	1	-	1	1	-	1	1	1	2	23	833	-	1	2	12	17	2	-	5	47	15	7	-	16	6	4		
2.4×10^{-3}	1	1	1	2	1	1	3	1	3	3	30	622	30	3	3	21	81	3	-	6	66	31	22	1	40	14	9		
3.0×10^{-3}	-	-	1	2	1	-	6	2	3	3	38	522	48	2	3	24	127	1	1	5	69	43	27	2	37	19	15		
4.0×10^{-3}	-	-	-	3	2	-	8	2	3	3	40	440	47	3	2	21	188	2	1	3	60	40	39	2	50	23	17		
5.5×10^{-3}	-	-	-	3	1	-	11	2	2	3	50	347	41	2	3	15	254	3	1	3	53	43	50	4	53	27	24	2	2

TABLE 77: THE EFFECT OF VARYING THE PRESSURE OF BUTADIENE ON THE REACTION BETWEEN ISOBUTENE (2-METHYLPROPENE) RADICAL CATION AND BUTADIENE (TIC)

Pressure (Torr)	m/z 28	29	39	40	41	43	54	55	56	66	67	68	69	78	79	80	81	82	92	93	95	107	109
1.9×10^{-4}	-	-	-	5	3	-	27	12	952														
3.0×10^{-4}	-	-	-	4	5	-	77	13	889	2	2	1	-	-	3	2	1	-	-	2	1		
4.0×10^{-4}	-	-	-	4	5	-	105	16	846	3	3	1	1	-	5	5	1	-	-	4	1		
5.0×10^{-4}	1	-	-	4	8	-	127	17	807	4	5	1	-	1	10	7	1	-	-	7	2		
5.9×10^{-4}	-	-	-	4	8	1	148	20	766	6	8	1	1	1	12	10	1	-	-	11	2		
7.1×10^{-4}	1	1	1	3	11	1	166	22	721	8	12	1	1	1	19	15	2	-	-	14	2		
8.0×10^{-4}	1	1	1	3	11	1	175	27	687	12	17	2	1	1	23	17	3	-	-	17	2		
9.1×10^{-4}	1	1	-	3	12	1	170	26	674	13	20	2	1	1	27	20	3	-	1	21	2		
1.2×10^{-3}	-	1	1	3	15	1	184	30	612	17	33	2	1	1	34	30	4	-	1	29	3		
2.0×10^{-3}	1	1	2	2	21	2	174	46	391	29	106	3	2	2	60	66	10	1	4	68	4	2	3

TABLE 78: THE EFFECT OF VARYING THE PRESSURE OF ISOBUTENE (2-METHYLPROPENE) ON THE REACTION BETWEEN BUTADIENE RADICAL CATION AND ISOBUTENE (TIC)

Pressure (Torr) m/z	27	28	39	41	43	52	53	54	56	57	58	66	67	68	69	70	71	80	81	82	83	84	95	107	109	113
2.0×10^{-4}	-	-	25	-	-	1	3	954	14	1	-	-	-	1	-	-	-	-	-	-	-	-	1			
3.0×10^{-4}	-	-	26	1	-	1	4	927	32	5	-	-	1	1	1	-	-	-	1	1	-	-	1			
4.0×10^{-4}	-	-	27	1	-	-	2	914	39	9	-	-	1	1	1	-	-	-	1	1	-	-	1			
5.1×10^{-4}	-	-	28	1	-	1	3	886	54	16	-	-	1	2	1	1	-	-	2	1	-	1	2			
6.0×10^{-4}	-	1	28	1	1	1	4	867	61	24	-	-	1	2	1	1	-	-	3	1	-	1	3			
6.9×10^{-4}	-	1	28	1	1	-	3	845	68	34	-	-	1	2	2	1	1	-	4	2	-	1	4			
8.0×10^{-4}	-	1	29	1	1	-	3	823	77	42	-	-	2	4	2	1	1	-	4	2	-	1	5			
9.1×10^{-4}	1	1	32	2	1	1	3	795	83	56	-	-	2	4	2	2	1	-	6	2	1	1	5			
1.2×10^{-3}	1	1	31	1	1	-	5	741	92	89	-	1	3	5	4	3	2	1	9	3	1	2	7			
2.1×10^{-3}	1	1	33	2	1	-	4	561	103	205	1	1	6	7	10	6	10	4	14	6	2	3	16	-	1	
2.9×10^{-3}	1	1	43	4	2	-	5	432	112	249	4	3	11	10	12	11	21	7	25	7	5	5	26	1	1	2

TABLE 79: THE EFFECT OF COLLISION GAS PRESSURE ON THE BUT-2-YNE ION-MOLECULE REACTION (TIC)

Pressure (Torr) m/z	27	28	29	39	41	43	52	53	54	55	66	67	77	79	81	91	93	94	107
4.6×10^{-4}	-	-	-	6	-	-	-	3	979	-	-	-	3	-	-	3	7		
6.2×10^{-4}	-	-	-	7	-	-	-	5	966	-	-	-	4	1	-	4	11	-	2
7.9×10^{-4}	1	1	-	10	-	2	-	6	947	-	-	-	6	2	-	5	16	-	4
1.0×10^{-3}	1	-	-	15	-	1	-	5	925	1	-	4	8	2	1	8	23	-	3
1.5×10^{-3}	2	2	3	23	1	2	2	5	859	31	1	8	8	4	2	11	31	-	5
2.2×10^{-3}	2	2	3	36	2	4	1	12	757	61	-	21	12	4	7	17	48	1	6
3.0×10^{-3}	3	-	8	78	5	7	-	12	580	119	5	34	15	10	17	21	71	1	13

TABLE 80: THE EFFECT OF COLLISION GAS PRESSURE VARIATION ON THE REACTION BETWEEN CH_3^+ AND ACETYLENE (TIC)

Pressure (Torr) m/z	15	26	27	38	39	40	51	63	65
5.0×10^{-5}	972	-	-	-	28	1			
1.0×10^{-4}	941	1	1	-	57				
2.0×10^{-4}	862	1	2	1	131	2	1		
4.0×10^{-4}	747	1	4	2	245	1	-		
6.0×10^{-4}	657	1	4	4	326	-	3	2	4
8.4×10^{-4}	628	-	4	3	353	-	3	2	8
1.0×10^{-3}	520	-	4	4	460	-	2	2	9

TABLE 81: THE EFFECT OF VARYING THE PRESSURE OF ACETYLENE ON THE REACTION BETWEEN CD_3^+ AND ACETYLENE (TIC)

Pressure (Torr) m/z	15	16	17	18	26	27	28	38	39	40	41	42	43	50	51	53	63	64	65
1.2×10^{-4}	-	5	9	931	5	4	1	-	2	14	25	5	-	-	2				
2.0×10^{-4}	-	10	18	844	12	4	2	-	6	34	51	12	2	2	4				
4.2×10^{-4}	2	13	22	730	15	9	2	-	23	61	88	12	5	5	13				
6.0×10^{-4}	2	15	27	657	11	11	3	1	41	90	100	14	6	5	17				
8.0×10^{-4}	1	20	29	567	11	11	4	1	74	122	99	18	6	6	23	-	2	-	3
1.0×10^{-3}	4	23	28	482	7	10	3	1	112	142	118	17	10	5	21	-	1	1	7
1.6×10^{-3}	2	21	22	355	8	12	3	3	184	164	123	27	13	5	15	3	2	5	20
2.0×10^{-3}	3	19	19	198	4	11	4	3	275	202	126	25	20	3	14	5	5	4	37
3.0×10^{-3}	-	12	12	115	-	9	-	-	325	237	121	20	22	-	6	12	5	7	54
4.1×10^{-3}	-	4	3	52	-	7	-	-	392	221	126	22	18	-	8	13	12	11	76

TABLE 82: THE EFFECT OF VARYING THE PRESSURE OF ACETYLENE ON THE REACTION BETWEEN CH_2F^+ and C_2H_2 (TIC)

Pressure (Torr) m/z	27	31	33	38	39	40	41	51	53	57	58	65	66	67	77	83	91
9.5×10^{-5}	-	14	986														
2.0×10^{-4}	2	10	979	-	6	-	-	-	-	3							
4.0×10^{-4}	14	13	941	-	26	-	-	-	-	7							
6.7×10^{-4}	16	15	914	3	42	-	-	-	-	11							
7.9×10^{-4}	17	14	846	-	97	1	2	2	-	16	-	5					
1.0×10^{-3}	20	18	791	-	130	-	4	6	-	20	2	9					
1.4×10^{-3}	24	24	676	-	221	-	6	4	4	15	2	24					
1.9×10^{-3}	20	17	528	2	337	-	7	6	6	28	1	42	1	-	4	2	
2.8×10^{-3}	8	17	365	3	441	4	5	4	8	46	2	83	2	3	2	5	4

TABLE 83: THE EFFECT OF VARYING THE COLLISION GAS PRESSURE ON THE REACTION OF CH_3^+ (DERIVED FROM CH_4) WITH C_2H_4 (TIC)

Pressure (Torr) m/z	15	27	28	29	30	39	40	41	43	53	55	67	69
9.8×10^{-5}	959	29	2	2	-	4	-	6					
2.1×10^{-4}	890	68	5	12	2	8	-	15					
5.1×10^{-4}	709	148	10	54	1	21	-	55	-	3	1		
7.5×10^{-4}	558	185	11	95	-	34	-	107	-	5	2	1	2
1.1×10^{-3}	458	185	12	126	-	38	1	160	1	8	4	3	6

TABLE 84: THE EFFECT OF VARYING THE PRESSURE OF ETHENE ON THE REACTION BETWEEN CH_3^+ (DERIVED FROM CH_3Cl) AND C_2H_4 (TIC)

Pressure (Torr) m/z	15	27	28	29	30	39	40	41	53	55	65	67	69
1.0×10^{-4}	965	22	2	1	-	5	-	5					
2.0×10^{-4}	910	53	6	6	-	13	-	13					
5.0×10^{-4}	749	115	13	39	1	29	-	50	2	1	1	1	1
7.8×10^{-4}	608	149	16	75	-	40	1	98	4	3	1	2	3
1.0×10^{-3}	529	151	13	95	-	47	1	142	6	3	1	4	8

TABLE 85: THE EFFECT OF VARYING THE PRESSURE OF ETHENE ON THE REACTION BETWEEN CH_3^+ (CH_3NO_2 DERIVED) AND ETHENE (TIC)

Pressure (Torr) m/z	15	26	27	28	29	30	39	40	41	42	53	55	65	67	69
1.8×10^{-4}	921	2	41	13	5	-	12	-	7						
3.0×10^{-4}	816	3	86	25	18	1	27	1	23	1	1	1			
5.0×10^{-4}	676	3	128	34	49	-	41	2	58	1	2	4	-	1	2
1.0×10^{-3}	439	4	151	41	109	1	57	2	169	1	7	6	1	4	8

TABLE 86: THE EFFECT OF VARYING THE PRESSURE OF PROPENE ON THE REACTION BETWEEN CH_3^+ (DERIVED FROM CH_4) AND PROPENE (TIC)

Pressure (Torr) m/z	15	27	29	39	40	41	42	43	53	54	55	56	57	67	69	70
1.0×10^{-4}	940	3	12	3	-	13	25	1	-	-	1	1	-	-	1	
2.0×10^{-4}	863	6	27	7	-	27	51	7	-	-	4	5	1	-	2	
5.1×10^{-4}	607	16	57	19	1	74	97	42	3	1	27	32	8	-	14	1
7.4×10^{-4}	479	20	63	21	1	85	109	74	3	1	49	49	19	1	23	3
1.2×10^{-3}	353	19	60	28	1	97	93	109	5	2	76	60	49	1	41	6

TABLE 87: THE EFFECT OF VARYING THE PRESSURE OF PROPENE ON THE REACTION BETWEEN CH_3^+ (CH_3Cl DERIVED) AND PROPENE (TIC)

Pressure (Torr) m/z	15	27	29	39	40	41	42	43	53	54	55	56	57	67	69	70	85
1.1×10^{-4}	956	3	7	3	-	9	18	1	-	-	1	1	-	-	1		
2.0×10^{-4}	893	8	14	7	-	17	46	5	1	-	2	4	1	-	2		
5.0×10^{-4}	708	17	34	17	1	47	82	29	2	1	17	23	7	-	14	1	
7.5×10^{-4}	580	24	43	20	1	63	91	52	3	2	37	39	18	-	25	3	
1.0×10^{-3}	482	27	37	27	2	71	92	75	5	2	53	50	36	1	36	5	1

TABLE 88: THE EFFECT OF VARYING THE PRESSURE OF PROPENE ON THE REACTION BETWEEN CH_3^+ (CH_3NO_2 DERIVED) AND PROPENE (TIC)

Pressure (Torr) m/z	15	27	28	29	39	40	41	42	43	53	54	55	56	57	67	69	70	81	85
1.8×10^{-4}	870	12	1	12	8	1	22	59	5	-	-	2	5	-	-	2			
3.0×10^{-4}	726	20	-	26	19	2	46	104	19	2	1	11	15	-	-	8	1		
5.0×10^{-4}	570	25	-	30	25	2	70	127	48	4	2	32	32	11	1	21	2		
1.0×10^{-3}	285	30	1	33	30	3	88	118	116	6	3	20	79	50	3	54	7	1	2

TABLE 89: THE EFFECT OF VARYING THE PRESSURE OF BUT-1-ENE ON THE REACTION BETWEEN CH_3 (CH_4 DERIVED) AND BUT-1-ENE (TIC)

Pressure (Torr) m/z	15	27	28	29	39	41	42	43	53	54	55	56	57	67	68	69	70	71	82	83	84
1.1×10^{-4}	947	3	-	12	2	8	11	1	-	-	4	12									
2.0×10^{-4}	883	6	-	23	4	17	22	4	1	-	8	27	2	-	-	1	1				
5.0×10^{-4}	689	14	1	52	10	43	36	17	2	2	31	72	15	-	1	7	6	1	-	2	1
7.6×10^{-4}	563	16	1	63	13	54	37	27	4	2	53	95	35	1	2	14	11	3	-	3	2
1.1×10^{-3}	462	18	-	61	15	61	35	35	4	2	66	121	58	2	3	24	16	7	1	5	2

TABLE 90: THE EFFECT OF VARYING THE PRESSURE OF BUT-1-ENE ON THE REACTION BETWEEN CH_3 (CH_3Cl DERIVED) AND BUT-1-ENE (TIC)

Pressure (Torr) m/z	15	27	28	29	39	41	42	43	53	54	55	56	57	67	68	69	70	71	82	83	84
9.5×10^{-5}	962	3	-	7	2	6	7	1	-	-	2	9	1								
2.1×10^{-4}	909	7	-	15	4	12	16	3	1	-	7	23	1	-	-	1	1				
5.0×10^{-4}	758	21	-	33	9	29	29	10	2	1	22	59	10	-	1	6	5	2	-	2	1
7.5×10^{-4}	658	20	-	42	13	36	31	18	4	2	36	80	25	1	3	14	9	3	-	4	2
1.0×10^{-3}	568	24	1	54	16	52	36	29	5	1	55	113	42	2	3	23	14	7	1	7	4

TABLE 91: THE EFFECT OF VARYING THE PRESSURE OF BUT-1-ENE ON THE REACTION BETWEEN CH_3^+ (CH_3NO_2 DERIVED) AND BUT-1-ENE (TIC)

Pressure (Torr) m/z	15	27	28	29	39	41	42	43	53	54	55	56	57	67	68	69	70	71	82	83	84
1.8×10^{-4}	896	8	1	15	4	12	6	1	2	-	10	41	3	-	-	1	2				
3.0×10^{-4}	767	15	1	33	8	27	8	6	2	-	27	87	8	-	-	2	6	1	-	2	1
6.0×10^{-4}	601	24	3	42	12	40	9	13	4	2	54	135	26	1	1	9	13	4	-	5	3
1.0×10^{-3}	402	26	1	50	14	48	6	22	7	2	87	189	67	2	2	27	20	12	1	10	8

TABLE 92: THE EFFECT OF VARYING THE PRESSURE OF ETHENE ON THE REACTION BETWEEN CH_3^+ AND $C_2H_4^+$ (TIC)

Pressure (Torr) m/z	15	26	27	28	29	39	40	41	42	43	53	55	56	65	67	69	79
9.6×10^{-5}	975	-	14	4	1	4	-	2									
1.9×10^{-4}	918	1	45	9	6	11	-	9									
3.0×10^{-4}	840	1	79	17	18	21	-	22	-	-	1	1					
4.1×10^{-4}	786	1	107	20	29	26	-	34	-	-	1	1	-	-	-	1	
5.1×10^{-4}	721	2	126	22	43	30	-	51	-	-	2	1	-	-	1	1	
6.5×10^{-4}	630	2	144	24	69	38	1	81	1	1	4	3	-	1	1	3	
7.0×10^{-4}	604	2	148	24	77	40	1	90	-	1	4	3	-	1	2	4	
8.1×10^{-4}	557	2	159	24	87	41	1	111	1	1	5	4	-	1	3	5	
9.0×10^{-4}	505	2	154	25	96	44	1	143	-	1	6	5	1	1	4	8	
1.3×10^{-4}	358	2	148	22	121	48	1	215	-	2	9	9	-	1	10	25	1

TABLE 93: THE EFFECT OF VARYING THE PRESSURE OF PROPENE ON THE REACTION BETWEEN CH_3^+ AND C_3H_6 (TIC)

Pressure (Torr) m/z	15	27	29	39	40	41	42	43	53	54	55	56	57	66	67	69	70	71	79	81	83	85	97
1.0×10^{-4}	956	3	5	4	-	8	21	1	-	-	1	1											
2.0×10^{-4}	859	9	15	9	1	25	60	6	1	-	4	7	1	-	-	3							
3.0×10^{-4}	763	15	22	14	1	40	86	18	1	1	11	17	3	-	-	8	1						
4.1×10^{-4}	660	19	26	19	2	62	115	29	2	1	19	26	7	-	-	14	1						
5.0×10^{-4}	602	21	30	22	1	67	119	39	3	2	27	35	11	-	1	19	2						
6.1×10^{-4}	532	24	34	23	2	77	121	52	3	1	38	45	16	-	1	26	3	-	-	-	1		
7.0×10^{-4}	471	25	32	26	2	82	122	72	4	2	47	48	24	1	2	32	4	-	-	-	1	1	
8.0×10^{-4}	421	26	33	26	2	87	118	82	4	2	58	60	32	1	1	37	7	-	-	-	1	1	
9.0×10^{-4}	407	24	33	26	2	76	104	84	5	2	66	67	44	1	2	44	7	1	-	1	1	1	
1.3×10^{-3}	269	26	35	29	2	81	82	110	7	2	94	83	86	1	4	67	13	2	1	1	2	3	3

TABLE 94: THE EFFECT OF VARYING THE PRESSURE OF BUT-1-ENE ON THE REACTION BETWEEN CH_3^+ AND BUT-1-ENE (TIC)

Pressure (Torr) m/z	15	27	28	29	39	40	41	43	53	54	55	56	57	67	68	69	70	71	82	83	84	85	97
9.8×10^{-5}	968	2	-	6	1	-	4	-	-	-	3	15											
2.0×10^{-4}	900	7	1	17	3	-	10	2	1	-	11	42	3	-	-	1	2	-	-	1			
3.1×10^{-4}	809	13	1	29	5	-	19	4	2	1	23	77	7	-	-	3	4	1	-	2	1		
4.1×10^{-4}	760	15	1	36	5	-	24	6	2	1	29	93	11	1	1	4	7	2	-	3	2		
5.0×10^{-4}	688	16	1	39	7	-	29	9	3	1	42	123	17	1	1	5	9	4	1	4	2		
6.0×10^{-4}	632	19	1	44	7	1	31	10	3	1	48	140	26	1	1	8	11	5	1	6	4	1	1
7.1×10^{-4}	567	20	1	48	8	1	35	13	3	1	57	158	34	2	2	12	13	8	2	8	4	1	1
8.0×10^{-4}	548	20	1	49	8	1	38	14	4	1	64	152	40	2	2	16	15	9	2	9	6	-	1
9.1×10^{-4}	468	21	1	49	9	-	43	16	4	1	77	182	50	3	2	23	17	13	2	10	6	1	1
1.2×10^{-3}	381	20	1	48	10	-	39	19	5	1	79	183	90	4	3	37	21	26	3	17	8	2	2

TABLE 95: THE EFFECT OF VARYING THE PRESSURE OF CIS BUT-2-ENE ON THE REACTION BETWEEN CH_3^+ AND CIS BUT-2-ENE (TIC)

Pressure (Torr) m/z	15	27	28	29	39	41	43	53	55	56	57	67	69	70	71	83	84
1.1×10^{-4}	965	2	-	5	1	4	1	-	5	18							
2.0×10^{-4}	903	5	-	12	2	9	2	1	14	49	1	-	1				
3.0×10^{-4}	819	9	1	10	3	15	4	1	27	97	3	-	2				
4.2×10^{-4}	748	11	1	24	5	19	5	1	37	141	4	-	3				
5.0×10^{-4}	693	12	1	27	5	21	6	2	42	176	7	-	6	-	1	1	
6.1×10^{-4}	636	13	1	29	6	24	7	2	48	211	10	-	9	-	1	1	1
7.0×10^{-4}	585	13	1	32	5	24	9	2	65	232	14	-	12	1	1	2	1
8.1×10^{-4}	537	15	1	32	6	27	9	2	70	258	19	1	16	1	3	2	2
9.1×10^{-4}	499	15	1	31	6	27	9	3	76	280	20	1	21	1	3	3	2
1.3×10^{-3}	384	14	1	32	8	28	13	3	85	330	41	2	39	2	6	9	5

TABLE 96: THE EFFECT OF VARYING THE PRESSURE OF ISOBUTENE (2-METHYLPROPENE) ON THE REACTION BETWEEN CH_3^+ AND ISOBUTENE (TIC)

Pressure (Torr) m/z	15	27	28	29	39	41	43	53	54	55	56	57	67	68	69	70	71	83	84
1.0×10^{-4}	975	1	-	5	1	3	1	-	-	3	11	1							
2.0×10^{-4}	926	5	-	12	2	7	2	-	-	9	31	5							
3.1×10^{-4}	866	6	-	17	2	12	4	1	-	16	55	18	-	-	2				
4.1×10^{-4}	822	8	1	21	3	15	5	1	-	20	71	29	-	-	3	1			
5.0×10^{-4}	787	9	1	24	4	17	6	2	-	24	81	38	-	-	4	1	-	-	1
6.2×10^{-4}	721	11	1	29	4	20	8	2	-	30	93	70	1	-	6	1	1	1	1
6.8×10^{-4}	710	12	1	29	5	22	8	2	-	32	89	79	1	1	7	2	1	1	1
8.0×10^{-4}	628	15	1	36	5	26	10	2	1	40	101	115	1	1	11	3	2	1	1
9.1×10^{-4}	615	15	1	37	6	28	11	3	1	45	106	153	1	1	14	3	3	2	1
1.3×10^{-3}	492	15	1	36	6	29	14	3	1	50	104	212	2	1	21	4	5	3	2

TABLE 97: THE EFFECT OF VARYING THE PRESSURE OF ETHENE ON THE REACTION BETWEEN CH_2F^+ AND C_2H_4 (TIC)

Pressure (Torr) m/z	15	27	28	29	31	33	39	41	45	46	47	53	55	59	67	69
1.1×10^{-4}	1	1	1	-	6	990	-	1	-	-	-	-	-	1		
2.0×10^{-4}	2	4	2	2	6	977	1	3	1	-	-	-	-	3		
2.9×10^{-4}	4	7	4	4	6	957	2	9	2	1	-	-	-	5		
4.1×10^{-4}	4	9	4	6	6	946	3	13	2	1	-	-	-	6		
5.1×10^{-4}	4	14	6	10	6	924	5	20	3	1	-	-	-	8		
6.0×10^{-4}	5	15	6	11	7	907	5	27	3	1	-	-	1	11		
7.1×10^{-4}	5	16	7	13	6	891	6	36	4	1	-	-	1	12	1	1
8.1×10^{-4}	6	18	7	14	7	871	7	45	4	1	-	1	1	14	1	1
9.1×10^{-4}	6	19	7	18	6	853	7	56	3	1	-	1	1	16	2	3
1.3×10^{-3}	7	23	7	25	7	801	10	78	5	2	1	1	2	22	3	5

TABLE 98: THE EFFECT OF VARYING THE PRESSURE OF PROPENE ON THE REACTION BETWEEN CH_2F^+ AND C_3H_6 (TIC)

Pressure (Torr) m/z	27	29	31	33	39	41	42	43	47	53	55	56	57	59	69	70	85
1.1×10^{-4}	1	3	5	988	-	1	1	-	1								
2.0×10^{-4}	3	14	5	959	1	6	6	2	3	-	1						
3.0×10^{-4}	5	26	5	923	2	13	10	6	5	1	3	1					
4.1×10^{-4}	7	34	5	905	2	16	12	10	7	1	4	2	1	-	1		
5.0×10^{-4}	7	42	6	869	2	21	13	16	9	1	7	3	1	1	2		
6.0×10^{-4}	10	50	6	841	2	25	16	21	9	1	10	4	2	1	2		
7.1×10^{-4}	9	54	4	820	3	26	17	29	12	1	13	5	3	1	3		
8.0×10^{-4}	11	57	5	796	3	30	17	33	13	2	16	4	5	1	4	1	
9.3×10^{-4}	12	65	5	764	4	33	18	45	13	2	20	6	7	1	5	-	
1.4×10^{-3}	14	75	4	688	5	42	15	65	17	2	33	9	19	2	8	1	1

TABLE 99: THE EFFECT OF VARYING THE PRESSURE OF BUT-1-ENE ON THE REACTION BETWEEN CH_2F^+ AND BUT-1-ENE (TIC)

Pressure (Torr) m/z	27	28	29	31	33	39	41	43	47	53	55	56	57	59	61	67	69	70	71	83	84
2.1×10^{-4}	2	-	7	5	958	1	9	4	2	-	6	6	1								
3.0×10^{-4}	5	-	12	5	928	1	13	6	4	-	13	9	2	-	-	-	1				
4.0×10^{-4}	7	-	14	5	904	1	19	9	4	1	19	12	4	-	-	-	1	1			
5.0×10^{-4}	6	1	17	5	882	2	21	10	5	1	23	15	5	1	1	-	2	1	1	1	
6.1×10^{-4}	8	-	19	5	856	2	27	13	7	1	28	17	9	1	1	-	3	1	1	1	
7.0×10^{-4}	8	1	23	5	827	3	30	15	8	1	35	21	13	1	1	-	5	1	1	1	
8.1×10^{-4}	9	1	26	5	797	3	33	18	9	2	43	22	16	1	1	1	7	2	2	1	
9.2×10^{-4}	10	1	27	5	780	2	35	20	8	2	44	25	20	2	1	1	10	2	3	2	1
1.2×10^{-3}	11	1	29	4	737	4	40	24	11	2	54	29	26	2	1	1	14	2	5	2	1

TABLE 100: THE EFFECT OF VARYING THE PRESSURE OF CIS BUT-2-ENE ON THE REACTION OF CH_2F^+ AND CIS BUT-2-ENE (TIC)

Pressure (Torr) m/z	27	28	29	31	33	39	41	43	47	53	55	56	57	59	61	69	70	71	83	84
9.6×10^{-5}	-	-	2	6	982	-	1	1	1	-	2	6								
2.0×10^{-4}	2	-	6	5	947	1	5	2	3	-	8	21	1							
2.9×10^{-4}	2	1	9	5	906	1	9	4	5	-	15	40	2	1	1	1				
4.0×10^{-4}	4	-	13	5	861	1	13	6	7	1	23	59	4	1	1	2				
5.0×10^{-4}	4	1	15	4	825	1	14	8	8	1	29	76	5	1	1	3	1	1	1	
6.0×10^{-4}	5	1	19	4	787	1	17	9	11	1	36	91	8	1	2	5	1	1	1	1
7.2×10^{-4}	6	1	22	4	742	2	20	11	10	1	44	114	10	2	2	8	1	2	1	1
8.0×10^{-4}	7	1	22	4	724	2	22	13	12	1	48	130	14	2	2	11	1	2	2	1
9.0×10^{-4}	7	1	23	4	673	2	21	14	12	2	50	152	15	2	2	13	2	3	2	2
1.2×10^{-3}	7	1	25	3	596	2	25	18	14	2	59	185	23	2	3	20	2	4	4	3

TABLE 101: THE EFFECT OF VARYING THE PRESSURE OF ISOBUTENE (2-METHYLPROPENE) ON THE REACTION OF CH_2F^+ WITH ISOBUTENE (TIC)

Pressure (Torr) m/z	27	28	29	31	33	39	41	43	47	53	55	56	57	59	61	67	69	70	71	83	84
1.1×10^{-4}	1	-	2	6	979	-	3	2	1	-	2	5	1								
2.0×10^{-4}	2	-	5	5	947	1	7	4	3	1	7	15	3	-	-	-	1				
3.1×10^{-4}	4	1	9	5	908	1	12	7	4	1	13	25	9	1	-	-	1				
4.0×10^{-4}	4	-	11	5	873	1	16	10	6	1	19	32	17	1	1	-	2				
5.0×10^{-4}	5	1	14	5	838	2	19	13	7	2	23	38	26	1	1	-	4	1			
6.1×10^{-4}	6	1	16	5	801	2	22	15	8	2	27	45	41	1	1	-	6	1	1	1	1
7.1×10^{-4}	7	1	19	4	764	2	26	17	9	2	33	50	52	1	1	1	8	1	1	1	1
8.1×10^{-4}	7	1	20	5	733	2	28	19	9	2	36	49	70	1	1	-	11	2	1	1	1
9.5×10^{-4}	8	1	22	5	678	2	32	24	9	2	43	56	92	1	2	1	14	2	2	2	1
1.3×10^{-3}	9	1	24	4	619	3	34	26	11	3	50	61	121	1	3	1	21	3	3	2	1

TABLE 102: THE EFFECT OF VARYING THE PRESSURE OF ETHENE ON THE REACTION BETWEEN CHF_2^+ AND ETHENE (TIC)

Pressure (Torr) m/z	27	28	29	31	33	39	41	51	55	59	67	69	77
2.0×10^{-4}	1	-	2	1	1	-	-	994	-	1			
3.0×10^{-4}	3	-	4	-	3	-	1	984	-	4			
3.9×10^{-4}	4	-	6	1	4	-	1	978	-	6			
5.0×10^{-4}	5	1	8	1	7	-	2	964	-	11			
6.0×10^{-4}	6	1	10	1	7	-	4	958	-	13	-	-	1
7.0×10^{-4}	7	1	11	1	9	1	5	947	-	18	1	-	-
8.0×10^{-4}	7	1	14	1	9	1	8	935	-	24	1	-	1
9.0×10^{-4}	9	1	17	1	10	1	12	916	-	31	2	1	1
1.0×10^{-3}	9	1	18	1	10	1	14	907	-	35	-	1	1

TABLE 103: THE EFFECT OF COLLISION GAS PRESSURE VARIATION ON THE REACTION BETWEEN CHF_2^+ AND PROPENE (TIC)

Pressure (Torr) m/z	27	29	31	33	39	41	42	43	47	51	53	55	56	57	61	65	67	69	73	85	97
2.0×10^{-4}	1	3	-	-	-	4	1	2	14	971	3	-	-	-	-	1	-	-	1		
3.0×10^{-4}	1	7	-	-	-	8	2	6	28	938	5	1	-	-	-	3	-	1	2		
4.1×10^{-4}	1	9	-	-	-	12	2	10	40	904	9	3	1	-	-	4	-	1	3		
4.9×10^{-4}	2	12	1	-	-	15	3	17	50	869	12	6	1	1	-	6	1	2	4		
6.2×10^{-4}	2	14	1	1	-	18	3	22	52	848	13	9	1	2	1	7	1	3	4		
7.0×10^{-4}	3	13	-	1	-	22	3	26	60	825	15	11	1	3	1	9	1	4	4		
8.1×10^{-4}	3	16	-	1	-	25	4	33	70	791	17	15	1	5	1	7	2	5	4		
9.1×10^{-4}	3	17	-	1	1	26	3	41	69	770	18	19	1	7	1	9	2	6	5		
1.0×10^{-3}	4	17	-	1	1	28	4	48	72	746	20	23	1	9	1	10	2	7	5	1	1

TABLE 104: THE EFFECT OF VARYING THE PRESSURE OF THE COLLISION GAS ON THE REACTION BETWEEN CHF_2^+ AND BUT-1-ENE (TIC)

Pressure (Torr) m/z	27	29	39	41	43	47	51	53	55	56	57	59	61	65	67	69	71	73	79	83	93	95
2.0×10^{-4}	-	4	-	5	1	4	974	-	4	1	1	5	2	1								
3.1×10^{-4}	1	6	-	9	2	6	946	-	9	2	2	8	4	2	1	1						
4.1×10^{-4}	1	8	-	12	3	8	932	1	12	2	3	9	4	3	1	1	-	1				
5.0×10^{-4}	1	11	1	16	4	11	899	1	19	3	5	14	6	4	2	2	1	1				
6.2×10^{-4}	1	13	1	17	6	12	875	1	26	3	8	17	7	4	2	4	1	1				
7.2×10^{-4}	1	13	1	21	6	13	857	1	29	4	10	16	8	5	3	5	1	1	1	1		
8.5×10^{-4}	1	16	1	23	8	14	831	1	36	4	13	19	10	4	4	8	2	1	1	1	1	
9.0×10^{-4}	1	17	1	23	8	15	819	1	40	5	15	19	10	5	3	9	3	2	1	1	-	
1.2×10^{-3}	1	17	1	26	10	16	783	1	47	5	21	22	12	6	4	15	4	2	1	1	1	1

TABLE 105: THE EFFECT OF VARYING THE PRESSURE OF CIS BUT-2-ENE ON THE REACTION BETWEEN CHF_2^+ AND CIS BUT-2-ENE (TIC)

Pressure (Torr) m/z	27	29	39	41	43	47	51	55	56	57	59	61	65	67	69	71	73	77	79	83	87
2.0×10^{-4}	-	3	-	3	1	5	971	6	4	1	3	1	2								
3.0×10^{-4}	-	5	-	6	1	8	943	11	9	2	6	3	3	1	1						
4.0×10^{-4}	1	9	-	9	3	12	916	17	11	4	8	3	5	1	2	1	1	-	1		
5.1×10^{-4}	1	10	-	11	3	14	887	24	17	6	10	5	6	1	3	1	1	-	1		
6.0×10^{-4}	1	24	1	11	4	16	870	26	19	7	11	5	6	1	5	1	1	-	1		
7.1×10^{-4}	1	14	1	14	5	19	839	34	25	9	12	7	8	2	6	1	2	-	1		
8.0×10^{-4}	1	15	1	15	7	20	820	37	27	12	14	8	8	2	8	2	2	-	1	1	
8.9×10^{-4}	1	16	1	16	7	21	801	41	31	15	14	8	8	2	11	2	3	-	1	1	
1.1×10^{-3}	1	18	1	18	8	24	765	48	35	19	15	10	10	3	16	3	3	1	2	1	1

TABLE 106: THE EFFECT OF ISOBUTENE (2-METHYLPROPENE) PRESSURE VARIATION ON THE REACTION OF CHF_2^+ WITH ISOBUTENE (TIC)

Pressure (Torr) m/z	27	29	39	41	43	47	51	55	56	57	59	61	65	67	69	71	73	79	83	87
2.0×10^{-4}	-	2	-	4	1	2	975	4	3	2	3	3	1							
3.2×10^{-4}	-	4	1	9	2	5	944	9	5	5	6	8	2	1	1					
4.0×10^{-4}	-	5	-	11	2	6	924	12	7	7	9	10	2	1	1					
5.0×10^{-4}	-	7	-	14	3	8	877	17	9	13	11	12	3	2	3	1	1			
6.0×10^{-4}	1	9	-	15	4	9	869	20	9	17	12	15	3	2	4	1	1	1		
7.4×10^{-4}	1	11	1	17	5	10	850	25	10	24	14	18	4	2	6	1	1	-		
8.0×10^{-4}	1	10	1	20	6	11	832	29	10	28	16	20	4	2	8	1	1	-		
9.0×10^{-4}	1	11	1	21	6	12	808	30	12	35	16	23	5	2	11	2	2	1	1	
1.2×10^{-3}	1	13	1	27	8	13	747	38	14	57	20	29	5	4	16	2	2	1	1	1

TABLE 107: THE EFFECT OF VARYING THE PRESSURE OF ETHENE ON THE REACTION BETWEEN CF_3^+ AND ETHENE (TIC)

Pressure (Torr) m/z	27	28	29	33	39	41	45	47	51	53	55	59	67	69	77
1.9×10^{-4}	4	5	-	6	-	1	-	7	6	-	-	-	-	970	1
3.0×10^{-4}	8	10	2	13	-	5	1	17	12	-	1	1	-	928	4
4.1×10^{-4}	10	12	4	18	-	10	1	26	17	-	1	1	-	895	6
5.2×10^{-4}	11	13	4	22	-	14	1	32	22	-	2	2	1	869	7
5.9×10^{-4}	13	14	6	24	-	19	2	36	24	1	2	2	1	847	10
7.0×10^{-4}	15	17	9	29	-	27	2	47	30	1	4	4	2	803	11
8.0×10^{-4}	15	15	10	29	-	29	2	53	31	1	4	5	2	792	13
9.0×10^{-4}	17	13	12	30	1	36	3	54	36	1	6	6	3	768	14
1.3×10^{-3}	20	13	18	34	1	50	3	75	43	2	13	11	5	687	25

TABLE 108: THE EFFECT OF VARYING THE PRESSURE OF PROPENE ON THE REACTION OF CF_3^+ WITH PROPENE (TIC)

Pressure (Torr) m/z	27	28	29	33	39	41	42	43	47	51	53	54	55	56	57	59	61	65	67	69	71	77	83	85	89	91	97
1.9×10^{-4}	1	1	-	1	-	3	14	1	11	2	-	-	-	1	-	-	-	1	-	964	1						
3.0×10^{-4}	2	1	1	2	-	8	32	4	27	5	-	-	2	3	-	1	1	1	-	908	2	1	-	-	-	1	
4.1×10^{-4}	3	1	1	2	1	11	40	8	37	7	-	-	5	6	1	1	1	2	-	866	4	-	-	-	-	1	
5.1×10^{-4}	4	1	1	3	1	14	50	13	49	9	-	1	8	10	2	1	2	2	-	823	5	1	-	-	-	1	
6.0×10^{-4}	4	2	2	3	1	18	52	17	57	10	-	1	11	12	4	1	2	3	-	795	6	1	-	-	-	1	
7.0×10^{-4}	4	1	2	3	1	31	56	25	64	10	1	1	15	15	7	1	2	3	-	756	7	1	-	-	-	1	
8.0×10^{-4}	5	1	3	4	1	22	57	30	68	12	1	1	19	19	8	1	2	3	1	730	8	2	1	-	-	1	1
9.1×10^{-4}	5	1	3	4	1	28	58	38	76	13	1	1	24	24	14	2	3	4	1	682	10	2	1	1	1	2	1
1.3×10^{-3}	6	2	4	4	2	33	55	56	91	14	1	1	35	26	25	2	4	6	1	611	11	2	1	2	1	3	2

TABLE 109: THE EFFECT OF VARYING THE PRESSURE OF BUT-1-ENE ON THE REACTION OF CF_3^+ WITH BUT-1-ENE (TIC)

Pressure (Torr) m/z	27	29	33	39	41	43	47	51	53	54	55	56	57	59	61	65	67	69	71	73	77	82	83	84	85	89	97
2.0×10^{-4}	1	5	-	-	5	-	1	-	-	-	3	16	-	1	2	1	-	964	-	-	1						
3.0×10^{-4}	1	11	1	1	11	1	3	1	-	-	10	42	2	3	5	1	-	902	-	-	4	-	1				
3.9×10^{-4}	2	16	1	1	15	2	4	1	-	-	13	55	4	4	6	1	-	866	1	-	4	-	2	1			
5.2×10^{-4}	3	20	1	2	19	3	4	2	-	1	19	74	7	5	7	2	1	819	1	1	7	1	2	2	-	1	
6.0×10^{-4}	3	21	1	2	21	4	5	2	-	-	24	83	10	5	9	2	1	793	2	1	7	1	3	2	-	1	
6.9×10^{-4}	4	25	1	3	24	6	6	3	1	1	31	92	15	7	9	2	1	754	3	1	7	1	4	2	1	1	1
8.1×10^{-4}	4	26	1	2	24	6	6	3	1	1	35	114	19	6	11	3	1	708	5	1	9	1	6	4	1	1	1
9.1×10^{-4}	4	31	1	3	29	8	7	3	1	1	44	126	23	8	13	2	1	658	7	1	9	1	7	4	1	1	1
1.3×10^{-3}	4	29	2	3	29	11	7	3	1	1	52	136	36	9	15	3	2	603	13	1	11	2	10	6	2	1	2

TABLE 110: THE EFFECT OF VARYING THE PRESSURE OF CIS BUT-2-ENE ON THE REACTION OF CF_3^+ WITH CIS BUT-2-ENE (TIC)

Pressure (Torr) m/z	27	29	33	39	41	43	47	51	55	56	57	59	61	65	69	71	73	77	83	84	91
1.9×10^{-4}	-	4	-	-	2	-	2	-	3	23	-	-	1	1	964	-	-	1			
3.0×10^{-4}	1	10	-	-	4	1	7	1	9	70	1	2	2	1	891	-	-	2			
4.2×10^{-4}	2	13	-	1	6	2	10	1	14	109	1	2	3	2	832	-	-	3			
5.0×10^{-4}	2	17	-	1	7	3	12	1	17	149	2	3	3	2	776	1	-	4	1	1	
6.0×10^{-4}	2	21	1	1	8	3	13	1	23	177	3	4	4	3	731	1	-	4	1	1	
7.1×10^{-4}	3	20	-	1	9	4	15	1	25	213	7	4	5	3	680	1	1	5	2	1	
8.2×10^{-4}	3	22	-	1	11	5	18	2	30	254	8	4	6	3	623	2	1	4	2	2	
9.1×10^{-4}	3	22	1	1	11	5	16	1	33	270	10	4	7	3	598	2	1	5	3	3	
1.3×10^{-3}	3	25	-	2	15	8	22	2	45	338	20	5	8	4	475	6	1	7	7	6	1

TABLE 111: THE EFFECT OF VARYING THE PRESSURE OF ISOBUTENE (2-METHYLPROPENE) ON THE REACTION BETWEEN CF_3^+ AND ISOBUTENE (TIC)

Pressure (Torr) m/z	27	29	33	39	41	43	47	51	55	56	57	59	61	65	69	71	73	77	83	84	85	89
2.1×10^{-4}	-	2	-	-	3	-	1	-	2	17	1	1	2	-	969	-	-	1				
3.0×10^{-4}	1	6	-	-	7	1	2	1	6	39	8	2	4	1	923	-	-	2				
4.1×10^{-4}	1	8	1	1	11	1	3	1	11	67	19	4	8	1	860	-	-	3				
5.0×10^{-4}	2	12	-	1	13	2	4	1	13	80	32	4	10	1	832	-	-	4	-	1		
6.0×10^{-4}	2	13	1	1	16	3	5	1	20	94	57	5	12	2	759	1	-	5	1	1	-	1
7.0×10^{-4}	2	14	1	2	18	4	8	1	21	98	74	6	15	2	726	1	-	6	1	1	1	1
8.0×10^{-4}	2	16	1	2	19	4	6	2	25	105	97	6	16	2	686	2	-	6	1	1	-	1
9.2×10^{-4}	3	19	1	2	22	6	6	2	30	103	129	7	20	2	640	2	1	7	2	1	1	1
1.2×10^{-3}	3	19	1	3	26	6	7	2	35	79	225	8	24	4	536	5	1	9	2	2	1	1

APPENDIX 1

a) The "degradation" schemes for the straight-chain $C_nH_{2n+2}^{+\cdot}$ radical cations, initiated by the $CH_4^{+\cdot}$ primary ion; where the figures below the individual ions indicate the relative abundances (expressed as % secondary ion signal).

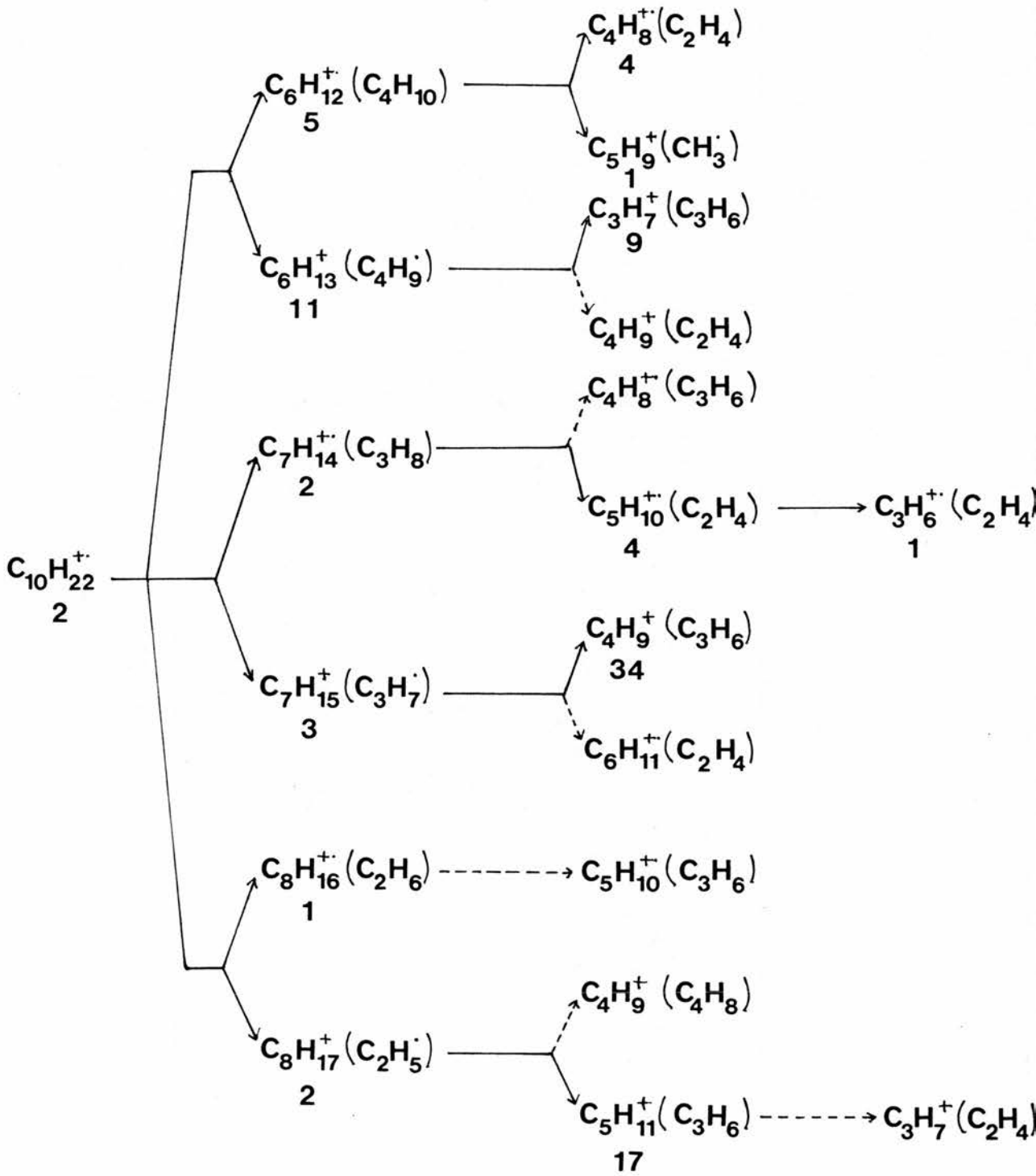

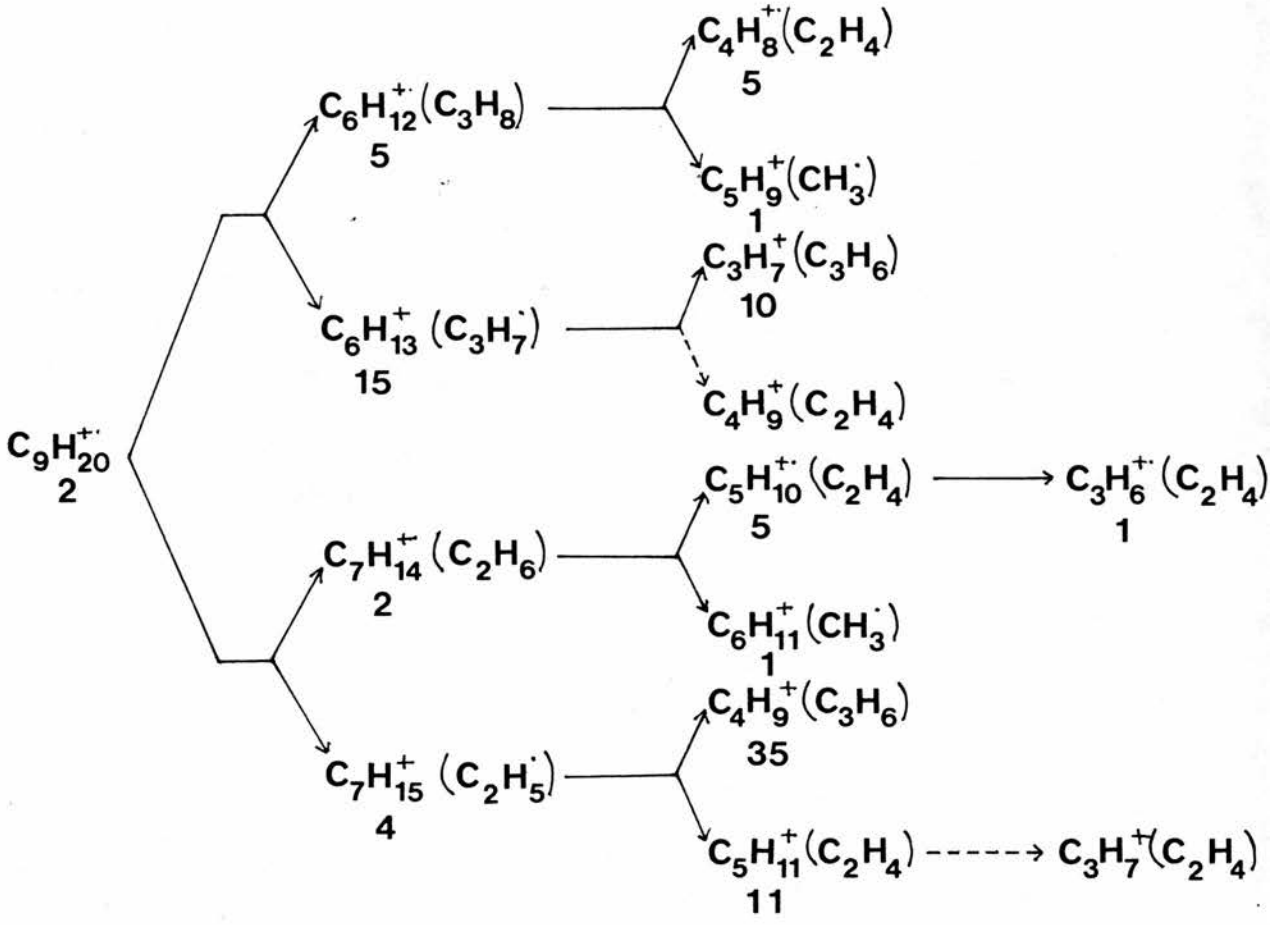
C9H20+· 2
C6H12+· (C3H8) 5
C6H13+ (C3H7·) 15
C7H14+· (C2H6) 2
C7H15+ (C2H5·) 4
C4H8+· (C2H4) 5
C5H9+ (CH3·) 1
C3H7+ (C3H6) 10
C4H9+ (C2H4)
C5H10+· (C2H4) 5
C6H11+ (CH3·) 1
C4H9+ (C3H6) 35
C5H11+ (C2H4) 11
C3H6+· (C2H4) 1
C3H7+ (C2H4)

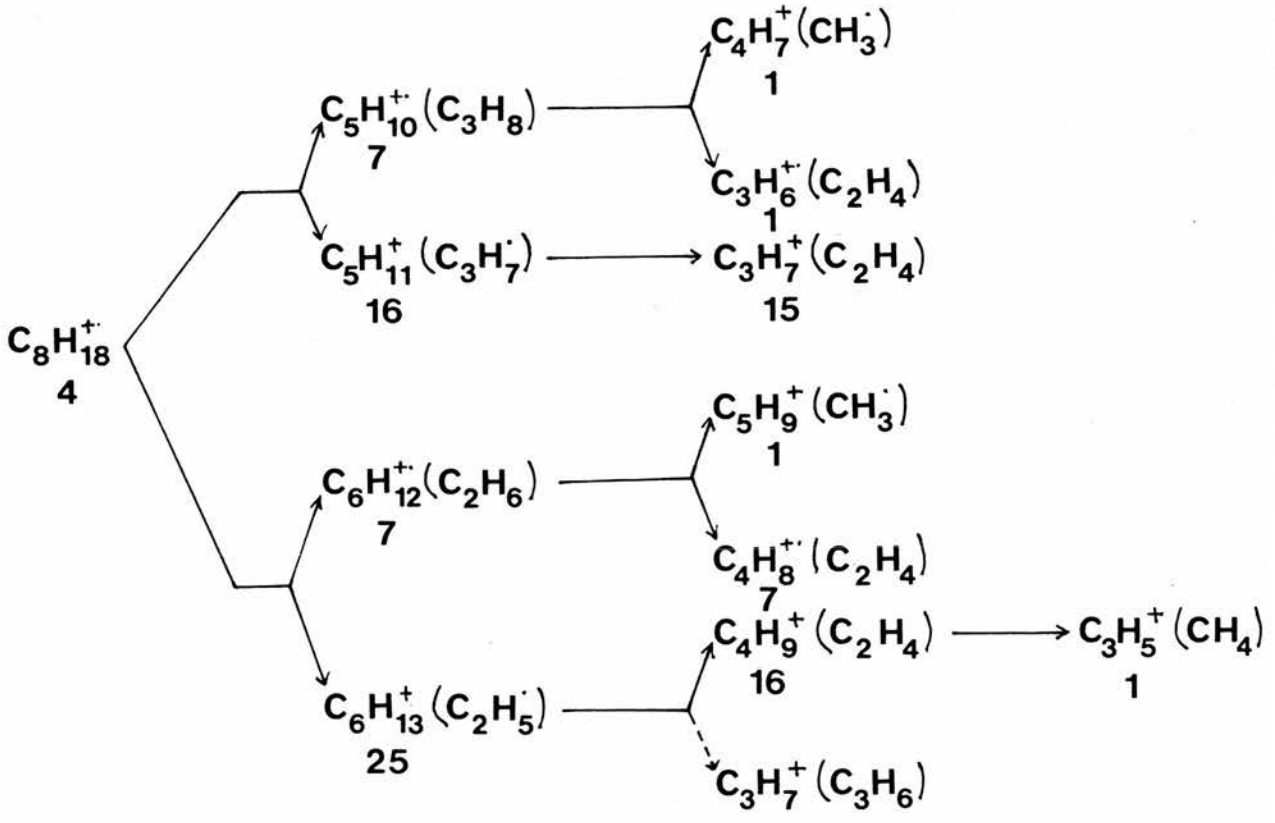
C8H18+· 4
C5H10+· (C3H8) 7
C5H11+ (C3H7·) 16
C6H12+· (C2H6) 7
C6H13+ (C2H5·) 25
C4H7+ (CH3·) 1
C3H6+· (C2H4) 1
C3H7+ (C2H4) 15
C5H9+ (CH3·) 1
C4H8+· (C2H4) 7
C4H9+ (C2H4) 16
C3H7+ (C3H6)
C3H5+ (CH4) 1

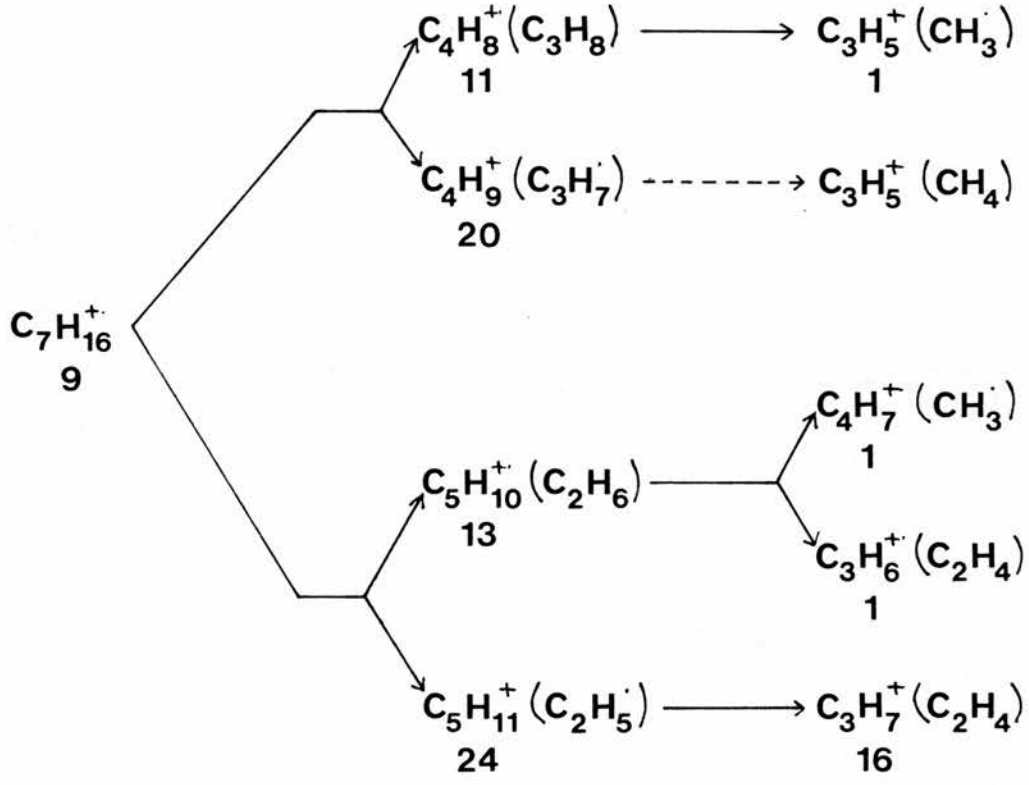
$C_7H_{16}^{+\cdot}$
9
$C_4H_8^{+\cdot}(C_3H_8)$
11
$C_3H_5^{+}(CH_3^{\cdot})$
1
$C_4H_9^{+}(C_3H_7^{\cdot})$
20
$C_3H_5^{+}(CH_4)$
$C_5H_{10}^{+\cdot}(C_2H_6)$
13
$C_4H_7^{+}(CH_3^{\cdot})$
1
$C_3H_6^{+\cdot}(C_2H_4)$
1
$C_5H_{11}^{+}(C_2H_5^{\cdot})$
24
$C_3H_7^{+}(C_2H_4)$
16

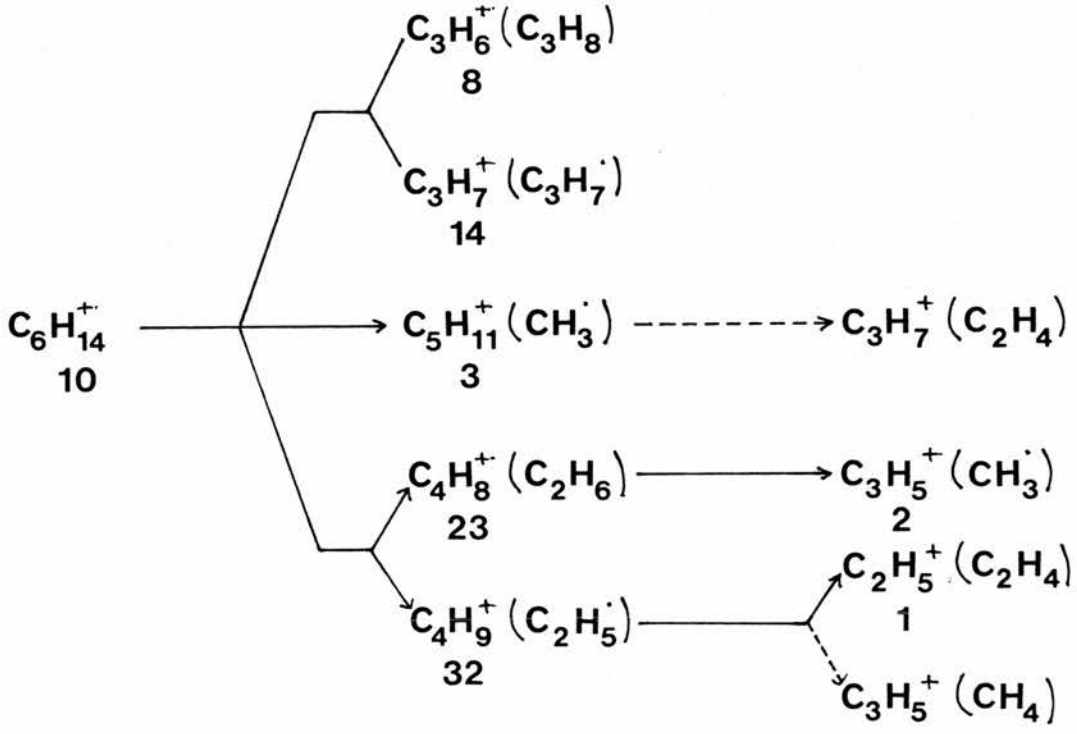
$C_6H_{14}^{+\cdot}$
10
$C_3H_6^{+\cdot}(C_3H_8)$
8
$C_3H_7^{+}(C_3H_7^{\cdot})$
14
$C_5H_{11}^{+}(CH_3^{\cdot})$
3
$C_3H_7^{+}(C_2H_4)$
$C_4H_8^{+\cdot}(C_2H_6)$
23
$C_3H_5^{+}(CH_3^{\cdot})$
2
$C_4H_9^{+}(C_2H_5^{\cdot})$
32
$C_2H_5^{+}(C_2H_4)$
1
$C_3H_5^{+}(CH_4)$

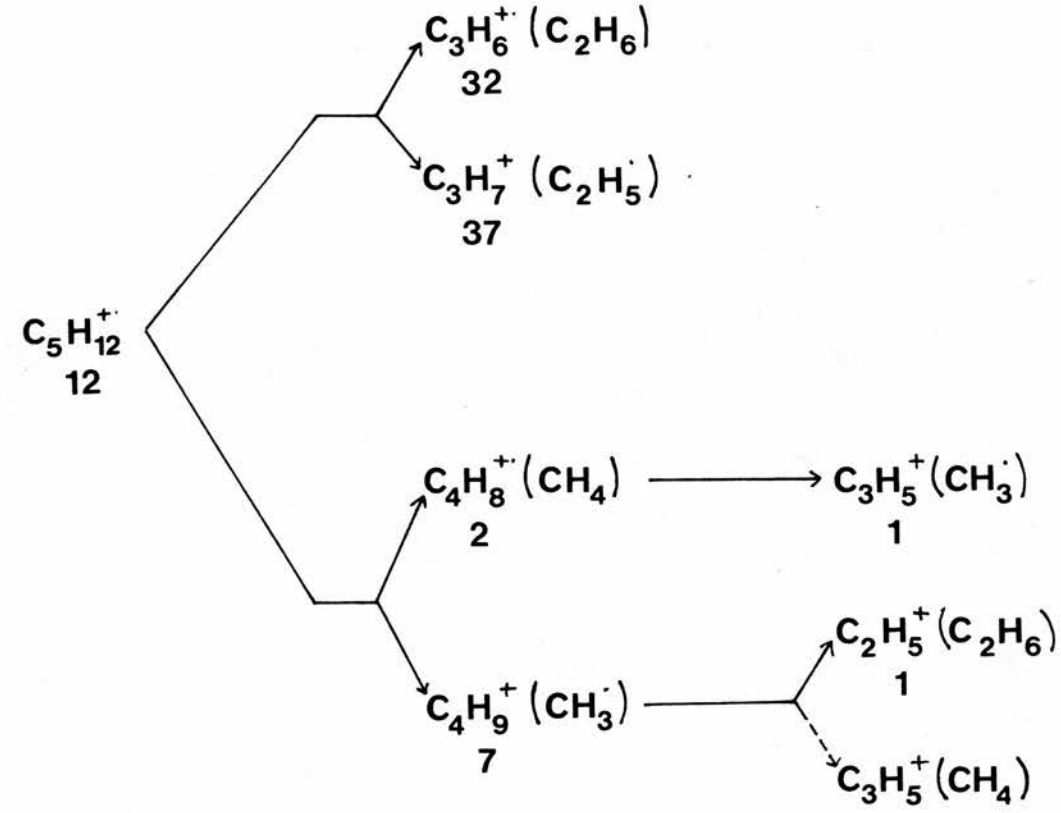
$C_3H_6^{+\cdot}$ (C_2H_6)
32
$C_3H_7^{+}$ $(C_2H_5^{\cdot})$
37
$C_5H_{12}^{+\cdot}$
12
$C_4H_8^{+\cdot}$ (CH_4)
2
$C_3H_5^{+}$ $(CH_3^{\cdot})$
1
$C_4H_9^{+}$ $(CH_3^{\cdot})$
7
$C_2H_5^{+}$ (C_2H_6)
1
$C_3H_5^{+}$ (CH_4)

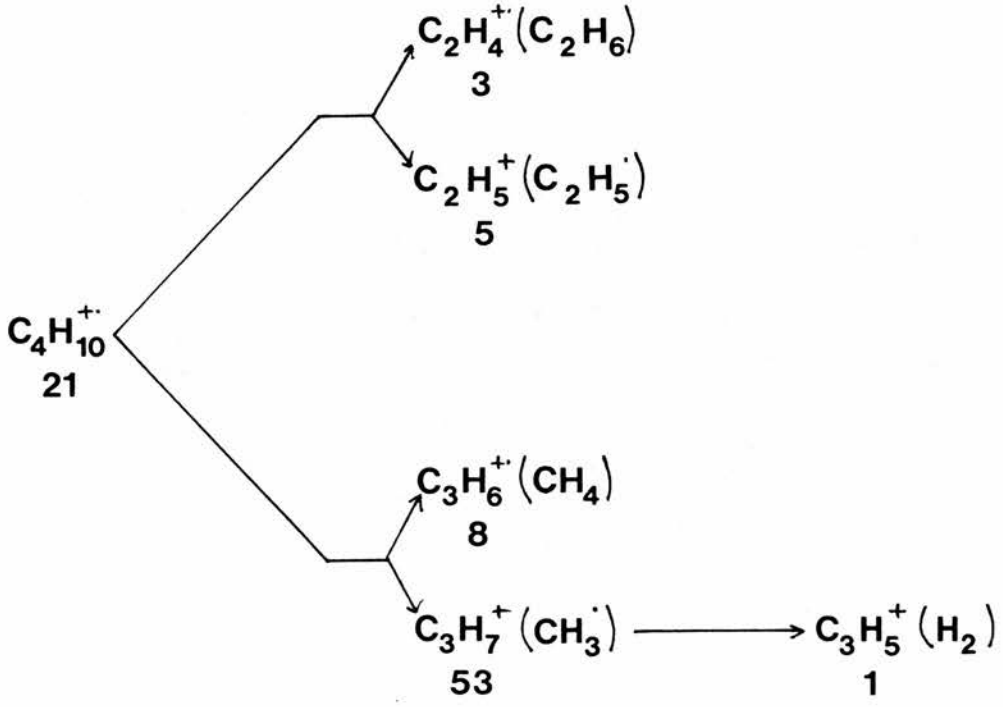
$C_2H_4^{+\cdot}$ (C_2H_6)
3
$C_2H_5^{+}$ $(C_2H_5^{\cdot})$
5
$C_4H_{10}^{+\cdot}$
21
$C_3H_6^{+\cdot}$ (CH_4)
8
$C_3H_7^{+}$ $(CH_3^{\cdot})$
53
$C_3H_5^{+}$ (H_2)
1

NB. There are alternative routes to many of the smaller ions depicted in the foregoing fragmentation schemes (ie four-carbon ions or less), but these are not included for reasons of simplicity & readability. We have included what we consider to be the most routes to these ions.

b) The "degradation" schemes for the straight-chain $C_nH_{2n+1}^+$ cations, initiated by the CH_3^+ primary ion; where the figures below the individual ions indicate the relative abundances (expressed as % secondary ion signal).

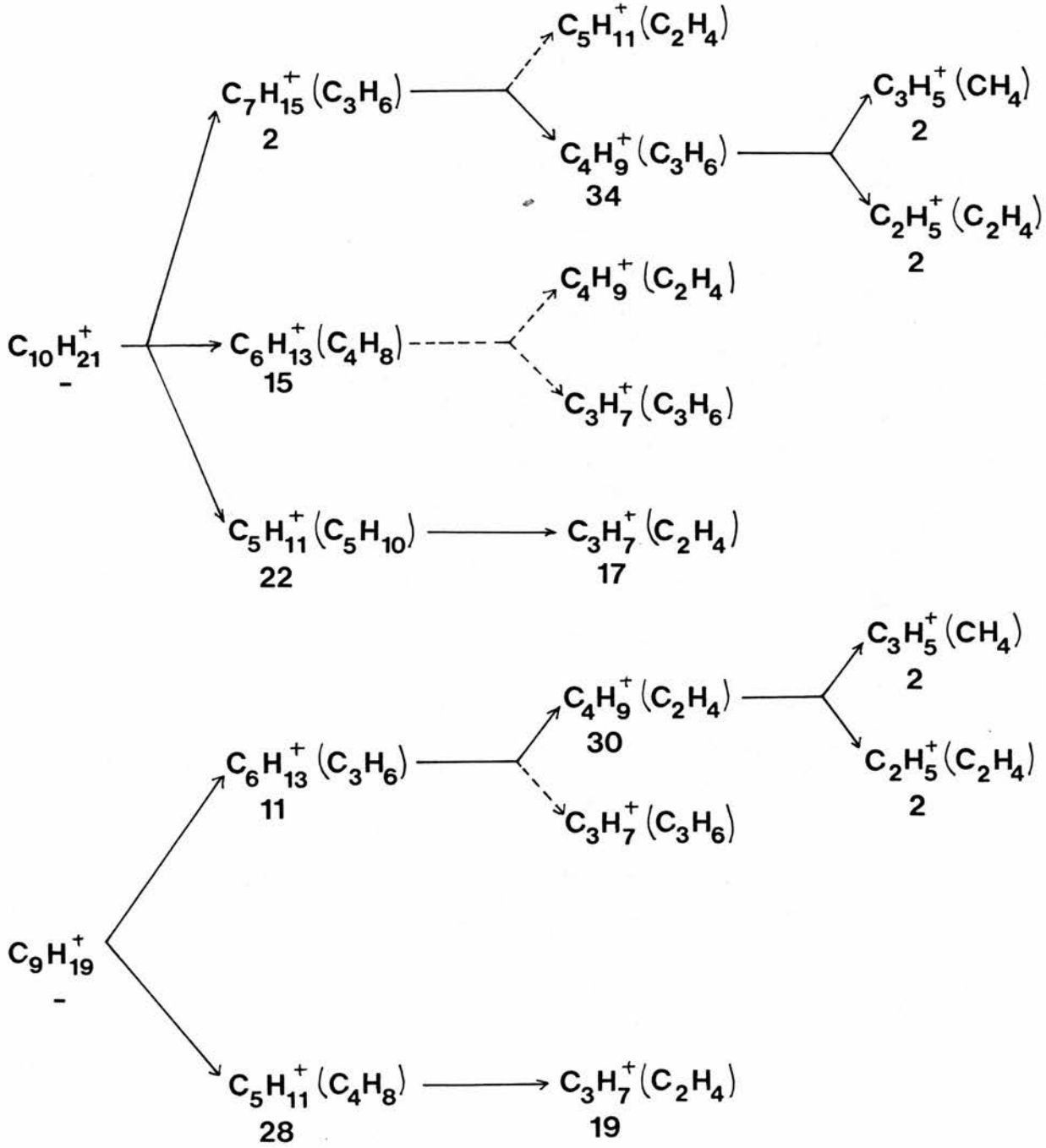

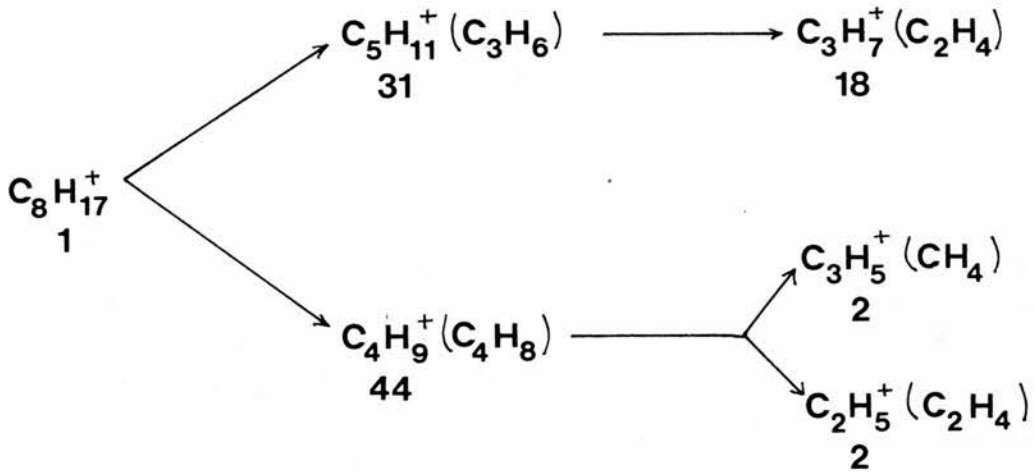
$C_8H_{17}^+$
1
$C_5H_{11}^+(C_3H_6)$
31
$C_3H_7^+(C_2H_4)$
18
$C_4H_9^+(C_4H_8)$
44
$C_3H_5^+(CH_4)$
2
$C_2H_5^+(C_2H_4)$
2

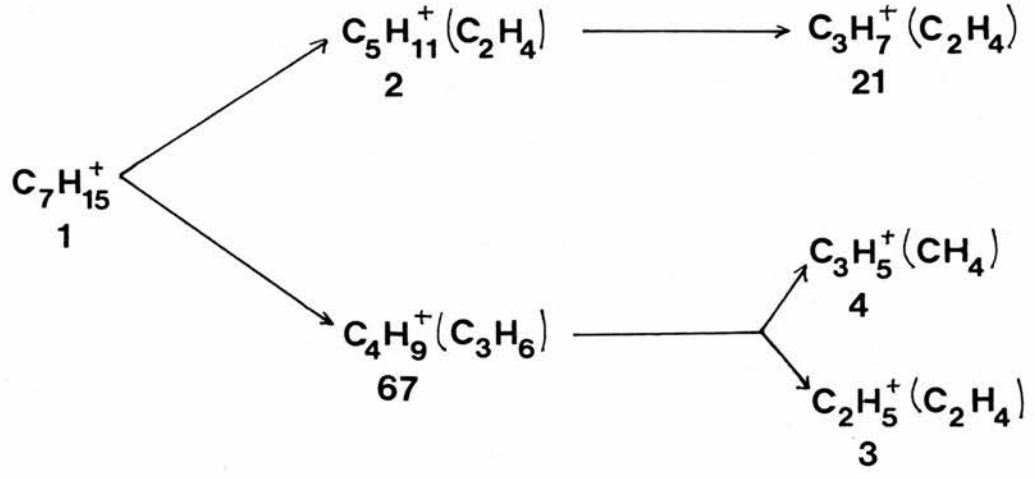
$C_7H_{15}^+$
1
$C_5H_{11}^+(C_2H_4)$
2
$C_3H_7^+(C_2H_4)$
21
$C_4H_9^+(C_3H_6)$
67
$C_3H_5^+(CH_4)$
4
$C_2H_5^+(C_2H_4)$
3

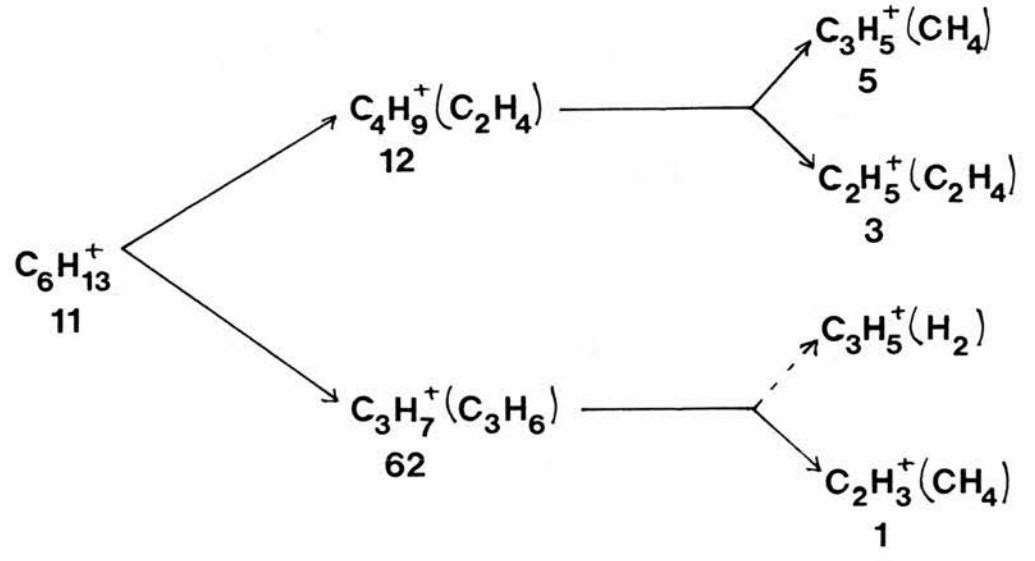
$C_6H_{13}^+$
11
$C_4H_9^+(C_2H_4)$
12
$C_3H_5^+(CH_4)$
5
$C_2H_5^+(C_2H_4)$
3
$C_3H_7^+(C_3H_6)$
62
$C_3H_5^+(H_2)$
$C_2H_3^+(CH_4)$
1

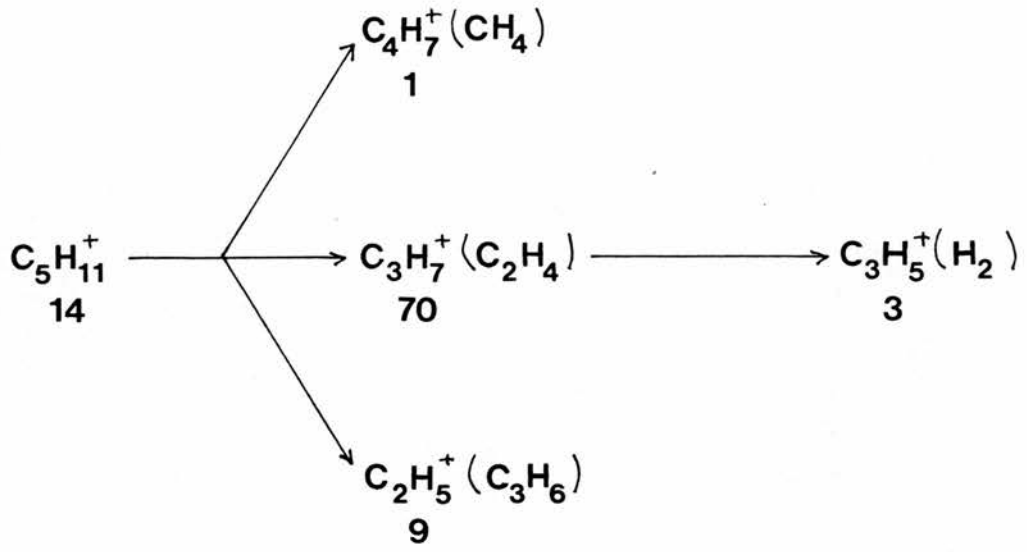

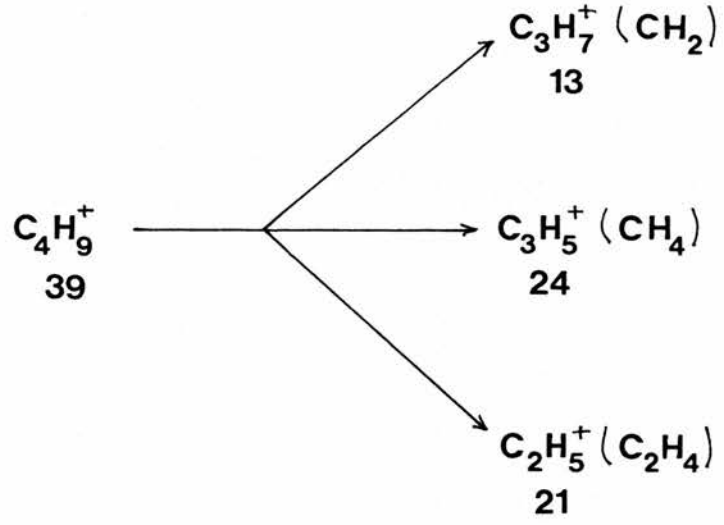

NB. In all cases a peak corresponding to the <u>alkane</u> molecular ion is observed, indicating that a secondary (very minor) ionisation process also takes place. The presence of this charge-exchange product probably accounts for the presence of some of the very minor daughter ions. In particular $C_3H_7^+$ indicated as arising from the elimination of the carbene, CH_2, from $C_4H_9^+$, is probably due to methyl elimination from the $C_4H_{10}^{+\cdot}$ charge-exchange product.

APPENDIX 2

CAD Spectra

The following tables show the collisionally activated dissociation spectra for many of the major ions involved in the systems studied throughout this research.

The ion subjected to CAD is listed first, followed by the breakdown products & their relative abundance (% total secondary ion signal).

Where more than one source molecule has been used to derive the primary ion, these results are arranged in columns, with the source molecule listed at the top of the relevant column.

		i-C_4	i-C_5	
$C_3H_6^{+\cdot}$ →	$C_3H_5^+$ (41)	85.6	75.7	84.9
	$C_3H_4^{+\cdot}$ (40)	14.4	13.8	15.1
	$C_2H_3^+$ (27)	-	10.5	-

		i-C_4	
$C_3H_5^+$ →	$C_3H_3^+$ (39)	100	100

		n-C_4	n-C_7	n-C_8	n-C_{10}		i-C_4	i-C_5
$C_3H_7^+$ →	$C_3H_5^+$ (41)	91.6	91.5	84.6	89.9	100	84.1	82.7
	$C_2H_3^+$ (27)	8.4	8.5	15.4	10.1	-	15.9	17.3

		n-C_9	n-C_{10}		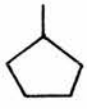		
$C_4H_7^+$ →	$C_4H_5^+$ (53)	23.0	22.6	32.7	29.8	30.9	32.2
	$C_3H_3^+$ (39)	26.4	27.1	25.0	33.3	26.6	32.2
	$C_2H_5^+$ (29)	50.6	50.3	42.3	36.8	42.5	35.6

$C_4H_8^{+\cdot}$ →		n-C_9	n-C_{10}				i-C_5	1-C_4H_8
	$C_4H_7^+$ (55)	-	-	35.5	42.3	42.7	14.2	10.9
	$C_4H_6^{+\cdot}$ (54)	-	-	-	-	-	-	3.2
	$C_3H_5^+$ (41)	74.5	74.9	42.0	35.6	33.0	67.8	67.2
	$C_3H_4^{+\cdot}$ (40)	21.9	17.0	21.0	21.0	24.3	18.0	6.7
	$C_3H_3^+$ (39)	-	-	-	-	-	-	4.0
	$C_2H_6^{+\cdot}$ (30)	-	-	-	-	-	-	2.1
	$C_2H_5^+$ (29)	2.2	1.7	-	-	-	-	2.6
	$C_2H_4^{+\cdot}$ (28)	1.4	3.4	1.5	1.1	-	-	3.4
	$C_2H_3^+$ (27)	-	3.1	-	-	-	-	-

$C_4H_9^+$ →		n-C_6	n-C_7	n-C_8	n-C_9	n-C_{10}	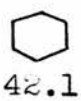	i-C_4	i-C_5
	$C_3H_6^+$ (42)	-	-	-	-	-	42.1	-	-
	$C_3H_5^+$ (41)	78.7	83.2	75.8	87.1	84.4	57.9	80.3	77.8
	$C_2H_5^+$ (29)	21.3	16.8	24.2	12.9	15.6	-	19.7	22.2

$C_4H_{10}^+$ →		n-C_4	i-C_4
	$C_4H_9^+$ (57)	-	2.5
	$C_3H_7^+$ (43)	71.6	13.1
	$C_3H_6^+$ (42)	25.6	84.4
	$C_2H_5^+$ (29)	1.8	-
	$C_2H_4^+$ (28)	1.0	

$C_5H_9^+$ →		n-C_{10}			
	$C_5H_7^+$ (67)	11.4	24.6	28.3	24.0
	$C_4H_7^+$ (55)	12.1	-	-	-
	$C_3H_5^+$ (41)	76.5	75.4	71.7	76.0

		n-C_9	n-C_{10}	
$C_5H_{10}^+$ → $C_4H_7^+$	(55)	62.0	64.0	53.8
$C_4H_6^+$	(54)	8.6	4.9	3.2
$C_3H_6^+$	(42)	29.4	31.1	40.0
$C_3H_5^+$	(41)	-	-	3.0

		n-C_7	n-C_8	n-C_9	n-C_{10}	i-C_5
$C_5H_{11}^+$ → $C_4H_8^+$	(56)	-	-	1.1	1.8	-
$C_4H_7^+$	(55)	-	-	0.4	-	-
$C_3H_7^+$	(43)	100	100	98.5	98.2	100

		n-C_5	i-C_5
$C_5H_{12}^+$ → $C_5H_{10}^+$	(70)	2.5	-
$C_4H_9^+$	(57)	3.5	5.2
$C_4H_8^+$	(56)	3.7	37.4
$C_3H_7^+$	(43)	22.1	8.2
$C_3H_6^+$	(42)	68.1	49.2

		
$C_6H_{11}^+$ → $C_4H_7^+$	(55)	100

		n-C_{10}	n-C_9		
$C_6H_{12}^+$ → $C_5H_9^+$	(69)	30.3	30.1	33.0	27.5
$C_5H_8^+$	(68)	-	-	0.8	2.8
$C_4H_8^+$	(56)	60.9	64.0	64.9	54.6
$C_4H_7^+$	(55)	3.4	2.5	0.6	5.4
$C_3H_7^+$	(43)	1.0	3.4	-	3.8
$C_3H_6^+$	(42)	4.4	-	0.7	4.6
$C_3H_5^+$	(41)	-	-	-	0.8
$C_2H_3^+$	(27)	-	-	-	0.6

		n-C_9	n-C_{10}	n-C_8
$C_6H_{13}^+$ →	$C_5H_{10}^+$ (70)	-	1.0	-
	$C_4H_9^+$ (57)	47.1	42.1	31.0
	$C_4H_8^+$ (56)	0.8	-	-
	$C_3H_7^+$ (43)	52.1	56.9	69.0

		n-C_6
$C_6H_{14}^+$ →	$C_5H_{11}^+$ (71)	1.6
	$C_5H_{10}^+$ (70)	1.3
	$C_4H_9^+$ (57)	33.7
	$C_4H_8^+$ (56)	53.3
	$C_3H_7^+$ (43)	3.2
	$C_3H_6^+$ (42)	6.9

		n-C_9	n-C_{10}	
$C_7H_{14}^+$ →	$C_6H_{11}^+$ (83)	10.2	8.2	31.8
	$C_6H_{10}^+$ (82)	4.3	-	24.7
	$C_5H_{10}^+$ (70)	46.9	47.0	28.3
	$C_5H_9^+$ (69)	5.7	9.0	-
	$C_5H_8^+$ (68)	3.0	2.2	-
	$C_5H_7^+$ (67)	-	0.9	-
	$C_4H_9^+$ (57)	7.3	8.0	6.9
	$C_4H_8^+$ (56)	22.6	22.7	8.3
	$C_4H_7^+$ (55)	-	1.9	-

		n-C_9	n-C_{10}
$C_7H_{15}^+$ →	$C_6H_{12}^+$ (84)	-	7.8
	$C_5H_{11}^+$ (71)	-	1.3
	$C_5H_{10}^+$ (70)	1.0	0.9
	$C_4H_9^+$ (57)	99.0	90.0

		n-C_7
$C_7H_{16}^+$ →	$C_6H_{13}^+$ (85)	0.7
	$C_6H_{12}^+$ (84)	0.5
	$C_5H_{11}^+$ (71)	34.8
	$C_5H_{10}^+$ (70)	40.0
	$C_4H_9^+$ (57)	5.3
	$C_4H_8^+$ (56)	16.1
	$C_3H_7^+$ (43)	0.4
	$C_3H_6^+$ (42)	2.1

		n-C_{10}
$C_8H_{16}^+$ →	$C_7H_{13}^+$ (97)	4.7
	$C_6H_{12}^+$ (84)	8.4
	$C_6H_{11}^+$ (83)	23.5
	$C_6H_{10}^+$ (82)	22.4
	$C_5H_{10}^+$ (70)	24.6
	$C_5H_9^+$ (69)	1.2
	$C_4H_9^+$ (57)	6.8
	$C_4H_8^+$ (56)	7.0
	$C_4H_7^+$ (55)	1.5

		n-C_{10}
$C_8H_{17}^+$ →	$C_6H_{13}^+$ (85)	0.6
	$C_6H_{12}^+$ (84)	0.7
	$C_5H_{11}^+$ (71)	70.1
	$C_4H_9^+$ (57)	28.6

			n-C_8
$C_8H_{18}^+$	$C_6H_{13}^+$	(85)	53.8
	$C_6H_{12}^+$	(84)	34.3
	$C_5H_{11}^+$	(71)	3.5
	$C_5H_{10}^+$	(70)	3.8
	$C_4H_9^+$	(57)	1.4
	$C_4H_8^+$	(56)	2.0
	$C_3H_7^+$	(43)	1.1

			n-C_9
$C_9H_{20}^+$	$C_7H_{15}^+$	(99)	33.3
	$C_7H_{14}^+$	(98)	18.6
	$C_6H_{13}^+$	(85)	11.4
	$C_6H_{12}^+$	(84)	26.3
	$C_5H_{11}^+$	(71)	1.4
	$C_5H_{10}^+$	(70)	4.3
	$C_4H_9^+$	(57)	4.6

			n-C_{10}
$C_{10}H_{22}^+$	$C_8H_{17}^+$	(113)	18.5
	$C_8H_{16}^+$	(112)	9.1
	$C_7H_{15}^+$	(99)	21.0
	$C_7H_{14}^+$	(98)	18.2
	$C_6H_{13}^+$	(85)	9.4
	$C_6H_{12}^+$	(84)	16.4
	$C_5H_{11}^+$	(71)	1.9
	$C_5H_{10}^+$	(70)	0.9
	$C_4H_9^+$	(57)	3.3
	$C_4H_8^+$	(56)	0.9
	$C_3H_7^+$	(43)	0.4

REFERENCES

REFERENCES

1. J.J. Thomson, Chem. News, 1911, 103, 265.

2. J.J. Thomson, Phil. Mag., 1912, 24, 209.

3. F.W. Aston, Proc. Chem. Phil. Soc., 1919, 19, 317.

4. F.W. Aston, Phil. Mag., 1919, 38, 707.

5. W.F. Haddon & F.W. McLafferty, J. Am. Chem. Soc., 1968, 90, 4745.

6. W.F. Haddon and F.W. McLafferty, Anal. Chem., 1969, 41, 31.

7. K.R. Jennings, Int. J. Mass Spectrom. Ion Phys., 1968, 1, 227.

8. F.W. McLafferty, P.F. Bente III, R. Kornfeld, S.-C. Tsai & I. Howe, J. Am. Chem. Soc., 1973, 95, 2120.

9. F.W. McLafferty, P.F. Bente III, R. Kornfeld, S.-C. Tsai, W.F. Haddon, K. Levsen, I. Sakai & H.D.R. Schuddemage, ibid, 1973, 95, 3886.

10. K. Levsen & H.D. Beckey, Org. Mass Spectrom., 1974, 9, 570.

11. M. Barber & R.M. Elliot, 12th Annual Conf. on Mass Spectrometry, Montreal (1964) p. 150.

12. M.L. Gross & D.H. Russell in "Tandem Mass Spectrometry", F.W. McLafferty, Ed., Wiley, New York (1983), pp 255-270.

13. P.J. Todd, D.C. McGilvery, M.A. Baldwin & F.W. McLafferty, in "Tandem Mass Spectrometry", F.W. McLafferty, Ed., Wiley, New York (1983), pp 271-288.

14. E. Lindholm, Ion-Molecule Reactions, Vol. 2, J.L. Franklin, Ed., Butterworths, London (1970), p 457.

15. J.M. Tedder & P.H. Vidaud, J. Phys. D., Appl. Phys., 1980, 13, 1949.

16. R.E. Ferguson, K.E. McCulloch & H.M. Rosenstock, J. Chem. Phys., 1965, 42, 100.

17. W.W. Hunt, Jr., R.E. Huffman, J. Saari, G. Wassel, J.F. Betts, E.H. Paufre, W. Wyess & R.A. Fluegge, Rev. Sci. Inst., 1964, 35, 88.

18. M.T. Bowers, D.D. Elleman & J.L. Beauchamp, J. Phys. Chem., 1968, 72, 3599.

19. M.B. Comisarow & A.G. Marshall, Chem. Phys. Lett., 1974, 25, 282.

20. S. Wexler & R. Marshall, J. Am. Chem. Soc., 1964, 86, 781.

21. I. Koyano, I. Omura & I. Tanaka, J. Chem. Phys., 1966, 44, 3850.

22. C.E. Melton & P.S. Rudolph, ibid, 1960, 32, 1128.

23. D.C. McGilvery & J.D. Morrison, Int. J. Mass Spectrom. Ion Phys., 1978, 28, 81.

24. M.L. Vestal & J.H. Futrell, Chem. Phys. Lett., 1974, 28, 559.

25. T.-Y. Yu, M.H. Cheng, V. Kempter & F.W. Lampe, J. Phys. Chem., 1972, 76, 3321.

26. R.A. Yost & C.G. Enke, J. Am. Chem. Soc., 1978, 100,2274.

27. R.A. Yost & C.G. Enke, Org. Mass Spectrom., 1981, 16, 171.

28. R.A. Yost & C.G. Enke, Anal. Chem., 1979, 51, 1251A.

29. D.F. Hunt, A.B. Giordani & J. Shabanowitz, ibid, 1980, 52, 386.

30. D. Zakett, R.G. Cooks & W.J. Fies, Anal. Chim. Acta, 1980, 119, 129.

31. P.H. Dawson, J.B. French, J.A. Buckley, D.J. Douglas, D. Simmons, Org. Mass Spectrom., 1982, 17, 205.

32. P.H. Dawson, J.B. French, J.A. Buckley, D.J. Douglas & D. Simmons, ibid, 1982, 17, 212.

33. I.J. Amster, M.A. Baldwin, M.T. Cheng, C.J. Proctor & F.W. McLafferty, J. Am. Chem. Soc., 1983, 105, 1654.

34. M.T. Cheng, M.P. Barbalas, F.R. Pegues & F.W. McLafferty, ibid, 1983, 105, 1510.

35. M.T. Cheng, G.H. Kruppa, F.W. McLafferty & D.A. Cooper, Anal. Chem., 1982, 54, 2204.

36. At the time of writing a "penta" - quadrupole device was under construction in this laboratory.

37. D.J. Burinsky, R.G. Cooks, E.K. Chess & M.L. Gross, Anal. Chem., 1982, 54, 295.

38. G. Lawson & J.F.J. Todd, Chemistry in Britain, 1972, 8, 373.

39. J.F.J. Todd & G. Lawson, MTP International Review of Science; Physical Chemistry, Series Two, Vol 5, A. Maccoll, Ed., Butterworths, London (1975), p 289.

40. P.H. Dawson, "Quadrupole Mass Spectrometry and its Applications", Elsevier, Amsterdam (1976).

41. A.J. Lorquet & W.H. Hamill, J. Phys. Chem., 1963, 67, 1709.

42. J.V. Dugan & J.L. Magee, J. Chem. Phys., 1967, 47, 3103,

43, J.C. Light, ibid, 1965, 43, 3209.

44. F.A. Wolf, ibid, 1966, 44, 1619.

45. R.A. Yost, C.G. Enke, D. McGilvery & J.D. Morrison, Int. J. Mass Spectrom. Ion Phys., 1979, 30, 127.

46. J.H. Batey & J.M. Tedder, J. Chem. Soc. Perkin Trans. II, 1983, 1263.

47. L. Bretherick, Ed., "The Handbook of Reactive Chemical Hazards", 3rd Edition, Butterworths, London (1985), p. 226.

48. N. Irving Sax, Ed., "Dangerous Properties of Industrial Materials", 6th Edition, Van Nostrand Reinhold, New York (1984), p 107.

49. D.D. Perrin,W.L.F. Armarego & D.R. Perrin, Eds, "Purification of Laboratory Chemicals", 2nd Edition, Pergammon Press, Oxford (1980), p 83.

50. P.H. Dawson & D.J. Douglas in "Tandem Mass Spectrometry", F.W. McLafferty, Ed., Wiley, New York (1983) p 127.

51. P.H. Dawson & Wing-Fung Sun, Int. J. Mass Spectrom. Ion Phys., 1984, 55, 155.

52. M.S.B. Munson & F.H. Field, J. Am. Chem. Soc., 1966, 88, 2621.

53. F.H. Field, Acc. Chem. Res., 1968, 1, 42.

54. R.P. Clow & J.H. Futrell, J. Am. Chem. Soc., 1972, 94, 3748.

55. R. Houriet, G. Parisod & T. Gaumann, ibid, 1977, 99, 3599.

56. P. Tecon, D. Stahl & T. Gaumann, Int. J. Mass Spectrom. Ion Physics, 1978, 27, 83.

57. J.K. Kim, V.G. Anicich & W.T. Huntress, J. Phys. Chem., 1977, 81, 1798.

58. J.H. Beynon, R.A. Saunders & A.E. Williams, "The Mass Spectra of Organic Molecules", 1st Edition, Elsevier, London (1968), p 93.

59. R.D. Bowen & D.H. Williams; J. Chem. Soc. Perkin Trans. II, 1976, 1479.

60. B.J. Stapleton, R.D. Bowen & D.H. Williams, Tetrahedron, 1978, 34, 259.

61. M.E. Rose & R.A.W. Johnstone, "Mass Spectrometry for Chemists & Biochemists", 1st Edition, Cambridge University Press, Cambridge (1982), p 204.

62. R. Liardon & T. Gaumann, Helv. Chim. Acta, 1969, 52, 1042 (French).

63. P. Wolkoff & J.L. Holmes, J. Am. Chem. Soc., 1978, 100, 7346.

64. B.W. Davis, D.H. Williams & A.N.H. Yeo, J. Chem. Soc. Series B, 1970, 81.

65. S. Mayerson & P.N. Rylander, J. Am. Chem. Soc., 1956, 78, 5799.

66. R. Liardon & T. Gaumann, Helv. Chim. Acta, 1971, 54, 1968 (French).

67. A. Fiaux, B. Wirz & T. Gaumann, ibid, 1974, 57, 525.

68. A. Fiaux, B. Wirz & T. Gaumann, ibid, 1974, 57, 708.

69. R. Liardon & T. Gaumann, ibid, 1969, 52, 528.

70. J.L. Holmes, P. Wolkoff & R.T.B. Rye, J. Chem. Soc. Chem. Commun., 1979, 544.

71. R.D.Bowen, M.P. Barbalas, F.P. Pagano, P.J. Todd & F.W. McLafferty, Org. Mass Spectrom., 1980, 15, 51.

72. J.F. Wendelboe, R.D. Bowen & D.H. Williams, J. Am. Chem. Soc., 1981, 103, 2333.

73. J.L. Holmes, P.C. Burgess, M. Yousuf, A. Mollah & P. Wolkoff, ibid, 1982, 104, 2879.

74. A. Maquestiau, Y. Van Haverbeke, Nouv. J. Chim., 1979, 3, 517.

75. C. Wesdemiotis, R. Wolfschitz & H. Schwarz, Tetrahedron, 1980, 36, 275 (German).

76. C.N. McEwan & M.A. Rudat, "Tandem Mass Spectrometry", F.W. McLafferty, Ed., Wiley, New York (1983) p 396.

77. H. Schwarz, Angew. Chem. Int. Ed. Eng., 1981, 20, 991.

78. W. Franke, H. Schwarz, H. Thies, J. Chandrasekhar, P. Von Ragué Schleyer, W.J. Hehre, M. Saunders & G. Walker, Chem. Berr., 1981, 114, 2808.

79. W. Franke, G. Frenking, H. Schwarz & R. Wolfschitz, ibid, 1981, 114, 3878.

80. L. Radom, P.C. Hariharan, J.A. Pople & P. Von Ragué Schleyer, J. Am. Chem. Soc., 1976, 98, 10.

81. R. Kebabcioglu & V. Dyczmons, Z. Naturforsch, 1975, 30a, 1680.

82. F.P. Lossing, Can. J. Chem., 1972, 50, 3973.

83. D.D. Fetterolf, R.A. Yost & J.R. Eyler, Org. Mass Spectrom., 1984, 19, 104.

84. P.J. Ausloos & S.G. Lias, J. Am. Chem. Soc., 1981, 103, 6506.

85. J.C. Conner, Senior Honours Project, University of St. Andrews, 1984.

86. K.A. Stanney & J.M. Tedder, J. Chem. Soc. Perkin Trans. II, 1986, 1383.

87. T.D. Tiernan & J.H. Futrell, J. Phys. Chem., 1968, 72, 3080.

88. F.H. Field, J. Am. Chem. Soc., 1961, 83, 236.

89. F.P. Abramson & J.H. Futrell, J. Phys. Chem., 1968, 72, 1994.

90. I. Koyano, I. Omura & I. Tanaka, J. Chem. Phys., 1966, 44, 3850.

91. A.G. Harrison, Can. J. Chem., 1962, 41, 236.

92. A. MacKenzie Peers & P. Vigny, J. Chim. Phys., 1968, 65, 805.

93. A.A. Herod & A.G. Harrison, J. Phys. Chem., 1969, 73, 3189.

94. M.T. Bowers, D.H. Aue & D.D. Elleman, J. Am. Chem. Soc., 1972, 94, 4255.

95. F.P. Abramson & J.H. Futrell, J. Phys. Chem., 1968, 72, 1826.

96. A. MacKenzie Peers, ibid, 1969, 73, 4141.

97. J.L. Franklin & H.E. Lumpkin, J. Chem. Phys., 1952, 20, 745.

98. I. Hanazaki, H. Hosoya & S. Nagakura, Bull. Chem. Soc. Japan, 1963, 36, 1673.

99. Z. Luczynski & J.A. Herman, Int. J. Mass Spectrom. Ion Phys., 1979, 31, 237.

100. I. Koyano, J. Chem. Phys., 1966, 45, 706.

101. J. Jalonen, paper no. 35 at the 14th meeting of the British Mass Spectrometry Society.

102. F.S. Cohen & P. Kraft, Encycl. Polymer Sci. Technol., 1971, 14, 522.

103. F. Swartz, Bull. Soc. Chim. Fr., 1919, 25, 163.

104. F. Swartz, Bull. Acad. Royale Belg., 1901, 383 and ibid 1909, 728.

105. A.E. Newkirk, J. Am. Chem. Soc., 1946, 68, 2467.

106. P.R. LeBreton, A.D. Williamson, J.L. Beauchamp & W.T. Huntress, J. Chem. Phys., 1975, 62, 1623.

107. V.G. Anicich & M.T. Bowers, Int. J. Mass Spectrom. Ion. Phys., 1973, 12, 231.

108. V.G. Anicich & M.T. Bowers, ibid, 1974, 13, 359.

109. V.G. Anicich & M.T. Bowers, J. Am. Chem. Soc., 1974, 96, 1279.

110. V.G. Anicich, M.T. Bowers, R.M. O'Malley & K.R. Jennings, Int. J. Mass Spectrom. Ion Phys., 1973, 11, 99.

111. A.J. Ferrer-Correia & K.R. Jennings, ibid, 1973, 11, 111.

112. F.H. Field, J.L. Franklin & F.W. Lampe, J. Am. Chem. Soc., 1957, 79, 2665.

113. P.S. Rudolph & C.E. Melton, J. Phys. Chem., 1959, 63, 916.

114. R. Fuchs, Z. Naturforsch, 1961, 16a, 1026.

115. E. Lindholm, I. Szabo & P. Wilmenius, Arkiv Fysik, 1963, 25, 417.

116. M.S.B. Munson, J. Phys. Chem., 1965, 69, 572.

117. J.H. Futrell & T.O. Tiernan, ibid, 1968, 72, 158.

118. W.J. Chesnavich, L.M. Bass, T. Su & M.T. Bowers, J. Chem. Phys., 1981, 74, 2228.

119. M.F. Jarrold, L.M. Bass, P.R. Kemper, P.A.M. van Koppen and M.T. Bowers, ibid, 1983, 78, 3756.

120. F.N. Preuninger & J.M. Farrar, ibid, 1982, 77, 263.

121. S.E. Buttrill Jr, ibid, 1970, 52, 6174.

122. F.P. Lossing & J.C. Traeger, Int. J. Mass Spectrom. Ion Phys., 1976, 19, 9.

123. M.L. Gross, D.H. Russell, R. Phongbetchara & P.-H. Lin, Adv. Mass Spec., 1978, 7A, 129.

124. P.J. Derrick, A.M. Falick & A.L. Burlingame, J. Am. Chem. Soc., 1972, 94, 6794.

125. R. van Doorn, N.M.M. Nibbering, A.J.V. Ferrer-Corriea and K.R. Jennings, Org. Mass Spectrom., 1978, 13, 729.

126. A.S. Werner & T. Baer, J. Chem. Phys., 1975, 62, 2900.

127. D.H. Russell, M.L. Gross, J. van der Greef & N.M.M. Nibbering, J. Am. Chem. Soc., 1979, 101, 2086.